UNIVERSITA' DEGLI STUDI DI PAVIA

Dipartimento di Genetica e Microbiologia

"A. Buzzati Traverso"

Silencing of cellular prion protein (PrPC) induces autophagy-dependent cell death in glioma cells

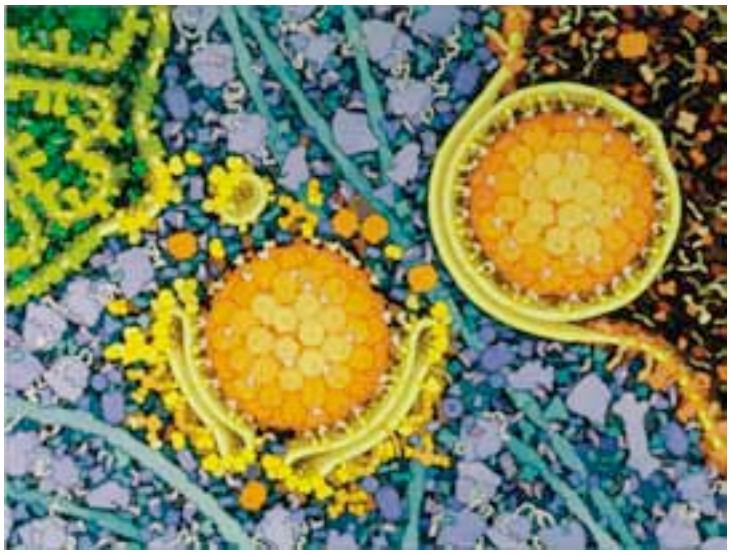

Giulia Barbieri

Dottorato di Ricerca in
Scienze Genetiche e Biomolecolari
XXIII Ciclo (2007-2010)

UNIVERSITA' DEGLI STUDI DI PAVIA

Dipartimento di Genetica e Microbiologia

"A. Buzzati Traverso"

Silencing of cellular prion protein (PrPC) induces autophagy-dependent cell death in glioma cells

Giulia Barbieri

Supervised by Dr. Sergio Comincini

Dottorato di Ricerca in

Scienze Genetiche e Biomolecolari

XXIII Ciclo – A.A. 2007-2010

Abstract

The cellular prion protein (PrPC) is a glycosylphosphatidylinositol (GPI) - anchored membrane protein that is highly conserved in mammalian species. Although the pathogenic isoform of PrPC, PrPSc, has attracted worldwide attention due to its involvement in the pathogenesis of transmissible spongiform encephalopathies, the biological role of normal PrPC is not defined yet. A variety of functions have been proposed for mammalian PrPC, including cell adhesion, transmembrane signaling, metal ion trafficking, immunomodulation, differentiation. Several intriguing lines of evidence have recently emerged indicating that the cellular prion protein may exert a neuro- and cyto-protective role against different pro-apoptotic stimuli. In addition, PrPC ectopic over-expression in breast and gastric cancer has been associated to the development of resistance to cell death by tumor cells.

The ability to resist to apoptosis is one of the main mechanisms by which cancer cells can escape conventional therapies. Indeed, the poor prognosis of patients affected by malignant gliomas, the most common and lethal primary central nervous system neoplasm, is mainly due to the intrinsic resistance of glial tumor cells to apoptosis, a feature that renders them elusive targets for pro-apoptotic chemotherapy and radiotherapy.

In order to determine whether PrPC is involved in the resistance of glial tumors to cell death, the effects of cellular prion protein down-regulation were investigated in different human malignant glioma cell lines. PrPC silencing by antisense approach induced profound morphological changes and a significant decrease in cell viability. To investigate the cell death pathway induced by PrPC down-regulation, autophagic as well as typical apoptotic markers (nuclear morphology, caspase-3/7 and PARP-1 cleavage) were analyzed in T98G human glioma cells. The results indicated that apoptosis was not induced by PrPC down-regulation. On the contrary, electron microscopy analysis, acridine orange staining, and an accumulation of GFP-LC3-II in autophagosomal membranes of GFP-LC3 transfected cells, indicated a predominant activation of autophagy. Induction of type II programmed cell death was also confirmed by the increase in LC3-I to LC3-II conversion and in p62 degradation, as well as by the inhibition of PI3K/Akt/mTOR pathway and the concomitant increase of Beclin-1 expression. Inhibition of autophagy by siRNA mediated Beclin-1 or Atg7 silencing, partially restored cell viability after PrPC knockdown. Since PrPC silencing was shown to down-regulate Bcl-2 expression, the possible functional link between PrPC and Bcl-2 was investigated: Bcl-2 silencing led to decreased T98G cellular viability, down-regulation of PrPC, and induction of apoptosis.

The results here presented show for the first time that down-regulation of PrPC induces autophagy dependent cell death in glioma cells, thus suggesting a cytoprotective role of the cellular prion protein in the context of glial tumors.

Acknowledgements

I'm very grateful to Dr. Sergio Comincini for having given me the opportunity to work in his laboratory and for the trust, support and freedom he gave me during the realization of this research project.

Thank you to all the past and present members of the laboratory of functional oncogenomics for their help and support during the realization of this work.

I thank Professor Biggioggera for the electron microscopy analysis and Dr. Mazzini for the FACS analysis.

Abbreviations

aa	aminoacid
ADR	Adriamycin
AVO	Acidic Vesicular Organelle
BafA1	Bafilomycin A1
Bcl-2	B-cell leukemia/lymphoma 2
BH	Bcl-2 Homology Domain
bp	Base pair
CNS	Central nervous system
CRC	Colorectal Cancer
Dpl	Doppel protein
ER	Endoplasmic reticulum
FLNA	Filamin A
GBM	Glioblastoma multiforme
GFP	Green Fluorescent Protein
GPI	Glycosylphosphatidylinositol
GPI-PSS	GPI peptide signal sequence
IAP	inhibitor of apoptosis protein
kb	kilobase
kDa	kilodalton
MDR	Multi Drug Resistance
MGMT	methyl-guanine methyl transferase
MTT	3-[4,5-dimethylthiazol-2-yl]-2,5-diphenyltetrazolium bromide
nt	nucleotide
PDAC	Pancreatic Ductal Adenocarcinoma
PRND/Prnd	Human / murine Doppel gene
PRNP/Prnp	Human / murine prion gene
PrPC	Cellular prion protein
Pro-PrPC	Unglycosilated PrPC retaining its GPI-PSS
PrPSc	Scrapie prion protein
^{Ctm}PrPC	COOH-terminal transmembrane form of PrPC
^{Cyt}PrPC	Cytoplasmic PrPC
^{Ntm}PrPC	NH_2-terminal transmembrane form of PrPC
p.t.	Post transfection
RTK	Receptor tyrosine kinase
s-ODN	Antisense phosphorothioate oligodeoxynucleotide
siRNA	Small interfering RNA
TSE	Transmissible Spongiform Encephalopathies
WHO	World Health Organization

Contents

1. Introduction

The word prion was coined twenty years ago by Stanley Prusiner to describe the "proteinaceous infectious particle" that causes a family of fatal neurodegenerative diseases known as transmissible spongiform encephalopathies (TSEs). For each of them, the 'protein-only' hypothesis proposes that the actual infectious agent is merely a modified form of the cellular prion protein that, differently from all other known infectious pathogens, is capable of replicating and transmitting infection in the absence of a nucleic acid genome, by conversion of its normal isoform to a pathological one (PrPSc) (Aguzzi and Polymenidou, 2004).

The cellular prion protein (PrPC), encoded by the *PRNP* gene, is a highly conserved glycoprotein bound to the outer leaflet of the plasma membrane by a GPI anchor. Like other membrane proteins, PrPC is synthesized in the rough endoplasmic reticulum (ER) and travels through the Golgi apparatus to the plasma membrane. During its biosynthesis, PrPC undergoes several posttranslational modifications, including cleavage of the amino (N)-terminal signal peptide, addition of N-linked oligosaccharide chains, formation of a disulfide bond and attachment of the GPI anchor, which facilitates its association with specific lipid membrane domains called 'rafts' (Campana et al., 2005). The mature PrPC protein contains a well-defined carboxy-terminal globular domain, consisting of three alpha helices and two beta sheets (Riek et al., 1996), and a structurally less-defined amino proximal region containing a stretch of several (five in human PrPC) octapeptide repeats that confer copper binding ability (Aguzzi et al., 2008b).

PrPC is evolutionary conserved and is expressed in all vertebrates, at all stages and in almost all tissues, especially in the brain. Although such ubiquity suggests that PrPC might perform some essential cellular function (Le Pichon et al., 2009), its physiological role is still unknown since genetic ablation of PrPC expression in mice, either prenatally or postnatally, produces relatively little phenotypic effect other than an inability to propagate prions (Büeler et al., 1993). Nevertheless, it is unlikely that the PrPC protein would have evolved simply to enable a rare fatal disease. Indeed, since the initial knockout mouse study, many subtle behavioral changes and electrophysiological and biochemical alterations have been reported (Steele et al., 2007). They include altered circadian rhythm (Tobler et al., 1996), modified sleep patterns (Tobler et al., 1997), impaired spatial learning behavior and increased sensitivity to seizure (Walz et al., 1999). In addition, PrPC has been reported to be

involved in the regulation of intracellular calcium (Colling et al., 1996) and copper concentrations (Vassallo and Herms, 2003), signal transduction (Mouillet-Richard et al., 2000), activation of immune cells (Mabbott and Turner, 2005) and in anti-apoptotic or anti-oxidant protective functions (Anantharam et al., 2008). More recently, Arantes and collaborators reported that PrPC expression is essential for the astrocyte cellular development (Arantes et al., 2009).

Several intriguing lines of evidence have recently emerged indicating that PrPC may function to protect cells from various kinds of internal or environmental stresses. PrPC over-expression rescued not only cultured neurons but also tumor cell lines from pro-apoptotic stimuli, including Bax expression, serum withdrawal, DNA damage, cytokine and anti-cancer drug treatment (Kuwahara et al., 1999; Roucou and LeBlanc, 2005; Senator et al., 2004). Worthy of note is the fact that this cytoprotective activity of PrPC has also been reported to be involved the ability of the protein to confer resistance to cell death to tumor cells. PrPC ectopic over-expression in breast and gastric cancer confers resistance to apoptotic cell death and to chemotherapy, a phenotype that can be reverted through *PRNP* silencing by siRNA or antisense strategy (Diarra-Mehrpour et al., 2004; Du et al., 2005; Meslin et al., 2007b).

Resistance to cell death is one of the main mechanisms by which cancer cells can escape conventional therapies. The extremely unfavourable prognosis for patients suffering of glioblastoma, the most common and life-threatening primary central nervous system malignant tumor, is strongly correlated to the intrinsic apoptosis resistance of GBM cells.

In this work of thesis, the potential involvement of PrPC in the development of resistance to cell death by malignant glioma tumor cells was investigated. Antisense oligonucleotide mediated silencing of PrPC was demonstrated to induce autophagy dependent cell death in T98G glioma cell line. These results therefore suggest a possible role for PrPC in modulating cell survival. Since induction of autophagic cell death is an alternative and emerging strategy to trigger glioma cell death, the action of anti-prion antisense molecules may represent a relatively selective strategy to sensitize cancer cells to therapy.

2. Review of the literature

2.1 The Prion protein

2.1.1 The human *PRNP* locus

The human *PRNP* locus is localized in the p12/p13 region of chromosome 20 and comprises the gene encoding for the cellular prion protein (*PRNP*), together with two other genes (*PRND* and *PRNT*). These three genes are located within a 55 kb region and show low sequence homology, implying that, although they may be evolutionarily related, they are functionally distinct (Fig. 1) (Makrinou et al., 2002).

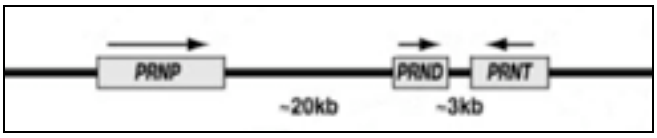

Figure 1. Human *PRNP* locus. Schematic representation of the human *PRNP* locus, located in the p12/p13 region of chromosome 20 and comprising the *PRNP, PRND* and *PRNT* genes. Arrows indicate gene orientation; numbers indicate intercistronic distances in kilobases (Kb). Adapted from (Makrinou et al., 2002)

PRNP is a single-copy gene that spans 16 kb and is comprised of 2 exons (Kretzschmar et al., 1986), the second of which encodes a 253-amino acid protein of 32–35 kDa (PrPC). The cellular prion protein is expressed by all mammals in a developmentally regulated manner, predominantly in the brain, and at variable levels in different tissues as breast myoepithelial cells, lymphocytes and stromal cells of lymphoid organs (Aguzzi and Polymenidou, 2004; Lee et al., 1998; Puckett et al., 1991).

PRND also harbors two exons and encodes a 179-amino acid protein, Doppel, which shares approximately 25% identity and 50% similarity of amino acid sequence with the C-terminal globular domain of PrPC. It is expressed in various tissues during

fetal development and is testis-specific in adults (Makrinou et al., 2002). However, in astrocytomas, a particular kind of glial tumor, *PRND* is over-expressed and Doppel is localized in the cytoplasm of the tumor cells (Comincini et al., 2007; Sbalchiero et al., 2008).

The third gene at this locus, *PRNT*, has only recently been identified in humans (Makrinou et al., 2002). *PRNT* encodes three alternative splicing transcripts, and is expressed exclusively in the adult testis. It is now thought that this gene does not encode a protein (Mehrpour and Codogno, 2010).

During a search of publicly-available databases for nucleotide sequences with similarities to the *PRNP* sequence, a fourth member of the prion gene family was identified. The protein and gene have been designated Shadoo and *SPRN*, respectively. *SPRN* is not part of the Prion genomic locus, but is located on chromosomes 7 and 10 in mice and humans, respectively. Like *PRNP* and *PRND*, the entire open reading frame of *SPRN* is contained within a single exon. Analysis of expression patterns implies that *SPRN* expression is restricted to the brain, suggesting that unlike Doppel, the Shadoo protein may be pertinent to prion-associated CNS phenomena (Watts and Westaway, 2007).

2.1.2 Structure and regulation of the *PRNP* gene

The human prion protein gene (*PRNP*) has been mapped to human chromosome 20 p12-pterminus and to the syntenic region on mouse chromosome 2 (Sparkes et al., 1986). *PRNP* contains a 358 bp exon I separated from the 2378 bp coding exon II by a 12700 bp intron I (Lee et al., 1998) (Fig. 2). Mouse *Prnp* contains three exons the third of which is analogous to exon 2 of the human gene and contains the protein coding sequence (Sakaguchi, 2007) (Fig. 2).

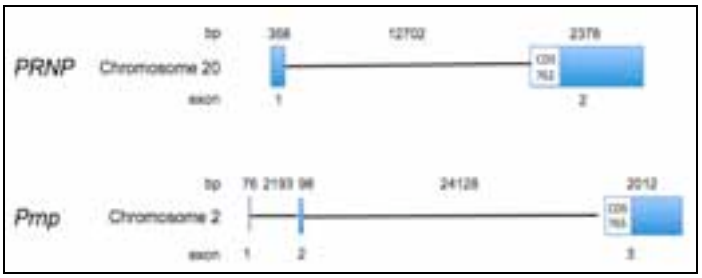

Figure 2: Schematic representation of the human (*PRNP*) and mouse (*Prnp*) prion genes. Numbers above the structure indicate sizes in bp. Exons are represented as blue boxes and introns as black lines. CDS are shown as white boxes with their size in bp. Exon numbers are reported below the structure.

The coding and promoter regions of the prion gene are highly conserved between human and mouse, with the exception of the first exon and the beginning of intron 1 that are poorly conserved. Among the apparently conserved regions there is a 99-bp region in human DNA which starts 2303 bp after exon 1 and corresponds to exon 2 in mouse. This region is not present in human *PRNP* mature transcripts analyzed to date. It does not contain a translation start codon (ATG) in the proper translational reading frame with the human *PRNP* coding exon, and forms part of the 5'UTR of *PRNP* mRNA. The human exon 2-like sequence shares 81% sequence identity with mouse exon 2 and, like this one, it is flanked by consensus splice donor and acceptor sites. In addition to this putative human exon 2 sequence, human e mouse prion genes share three other conserved regions: one 500 bp upstream of human "exon 2'', one at the 3'end of the transcripts, and one 3–4 kb downstream of the polyadenylation site (Lee et al., 1998).

The analysis of the *PRNP* promoter sequence revealed that, like a housekeeping gene, it is highly G+C-rich, lacks a canonical TATA box and has a number of putative binding sites for the transcription factor Sp1. However, evidence that transcription of *PRNP* is modulated by chromatin structure (Cabral et al., 2002) as well as the identification of potential binding sites for many transcription factors, indicate that *PRNP* expression likely depends on a variety of cellular factors (Linden et al., 2008).

The *PRNP* promoter region presents two G+C-rich (>50% GC) regions (-2461 to -1961 and -257 into intron I), a CpG island extending from -235 to 167 bp into intron I, and Alu repeat elements of the Alu-Sx and Alu-Jo subfamilies located in reverse orientation with respect to *PRNP* transcription at -2560 to -2352 and -1155 to -834, respectively (Mahal et al., 2001). Four conserved motifs of as yet unknown significance were also detected upstream of the prion gene in mouse, human, and sheep (Westaway et al., 1994) (Fig. 3).

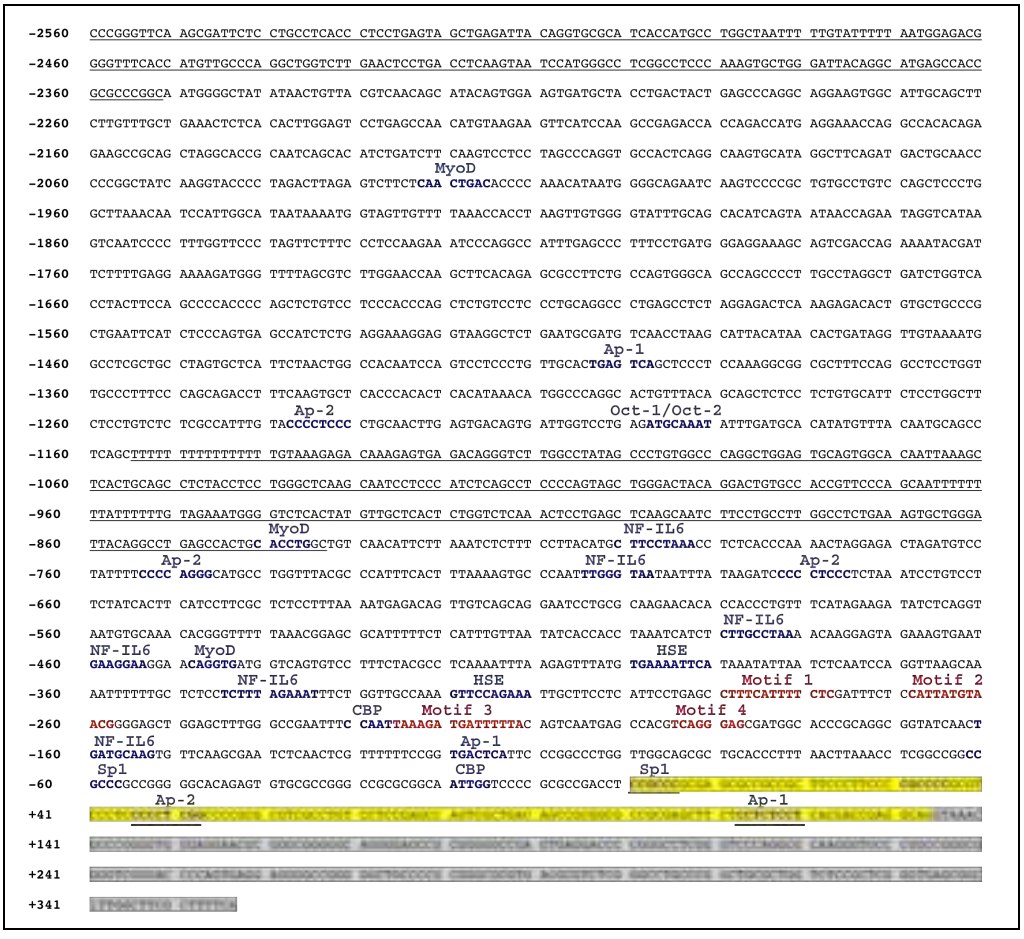

Figure 3. *PRNP* promoter region and non coding exon 1. Nucleotide sequence of the 2916 bp genomic DNA fragment containing the promoter and exon 1 (+1 to +134, highlighted in yellow) sequence of *PRNP* (EMBL Accession no. AJ289875). Numbers -2560 to +341 on the left represent the nucleotide position relative to the reported transcriptional start site at +1 (Puckett et al., 1991). Two Alu sequences (in reverse orientation to transcription of *PRNP*): Alu-Sx (-2560 to -2352) and Alu-Jo (-1155 to -834) are underlined. The first 222 bp of the 13 kb intron (+135 to +356) are highlighted in grey. Putative transcription factor binding sites are in blue. The four sequence motives that are highly conserved among mammalian species are indicated in bold red. Adapted from (Mahal et al., 2001).

A number of factor binding sites in the *PRNP* promoter are completely conserved between mammalian species and large regions of homology are evident especially between bovine and human sequences. Putative transcription factor binding sites occur mainly in two clusters between -800 to -670 and -490 to +127 (Mahal et al., 2001) (Fig. 3).

Binding sites for the transcriptional activator nuclear-factor IL-6 (NF-IL6), muscle-specific factor MyoD, the transcriptional activator Sp1 and the heat shock factor (HSF), are completely conserved between the human and bovine *PRNP* sequences. Functional analysis using transient transfection assays, interestingly revealed that deletion of the region from -148 to -114 resulted in an approximately 62% drop in the level of reporter gene expression in 911 cells (i.e. human embryonic retinoblasts) (Fallaux et al., 1996) but not in HeLa cells suggesting the presence in this region of an activator that contributes to the higher levels of *PRNP* expression in neurons. This region contains a putative AP-1 site at -120 (Fig.3). AP-1 may regulate *PRNP* expression through the influence of AP-1-inducible agents such as phorbol esters (Cabral et al., 2002) and DNA-damaging agents (Devary et al., 1992).

PRNP is constitutively expressed in various tissues, with highest expression in brain, particularly in neurons, and, to a lesser extent, in spleen, kidney, lung, and heart (Oesch et al., 1985).

Expression of both prion transcript and protein are developmentally regulated, increasing postnatally with distinct time courses for various regions of the hamster, rat, and mouse brains. Injections of NGF into the brains of neonatal hamsters upregulated *Prnp* mRNA together with activity of choline acetyltransferase in regions that contain NGF-responsive cholinergic neurons (Mobley et al., 1988); neuronal-like differentiation of PC12 cells induced by either interleukin (IL)-6 or NGF was accompanied by increased expression of *Prnp* mRNA (Lazarini et al., 1994). Many evidences suggest that *PRNP* expression can also be modulated by stress and by copper concentration. In neuroblastoma cells, heat shock increased both prion mRNA and protein, together with Hsp70 (Shyu et al., 2002). In addition inflammation both in skin and in gastrointestinal epithelium led to upregulation of PrPC (Pammer et al., 2000; Pammer et al., 1998). Chronic copper overload resulted in upregulation of *Prnp* in two lines of fibroblasts from mutant mice which accumulate abnormally high levels of copper in normal culture medium (Armendariz et al., 2004).

2.1.3 PrPC structure

At present, about 50 nuclear magnetic resonance (NMR) structures and about 20 X-ray crystallographic structures of PrPC are available from the Protein Data Bank (PDB) (Sakudo et al., 2010). The secondary and a proposed tertiary structure for human PrPC are shown in figure 4.

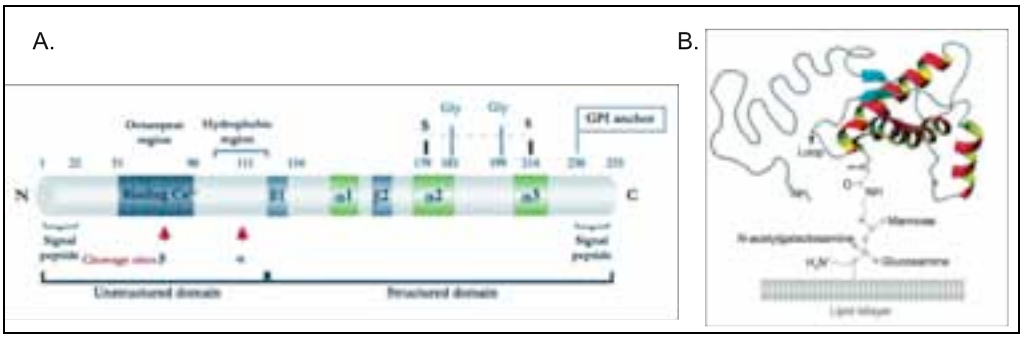

Figure 4. Structural features and biochemical properties of the human cellular prion protein. (A) Scheme of the secondary structure of PrPC and its post-translational modifications. Human PrPC contains a N-terminal signal peptide (1–22), five octapeptide repeats (51–91), a highly-conserved hydrophobic domain (106–126), three peptide sequences implicated in the α-helix structure (α1–α2–α3), two peptide sequences implicated in the β-helix structure, and a signal sequence for the GPI anchor (231–254). Disulfide bridges are indicated above the proteins (–S–S–) and N-glycosylation sites (Gly) are denoted. Red arrows indicate sites of endoproteolitic cleavage (see 2.1.4). Adapted from (Mehrpour and Codogno, 2010). (B) Tertiary structure of the cellular prion protein, as deduced from NMR spectroscopy, inserted into a lipid bilayer, including the unstructured N-terminal tail (gray) and the GPI anchor. The α-helices are indicated in red; the antiparallel β-sheets are shown in turquoise. Sugar residues are shown as colored small circles. Adapted from (Aguzzi et al., 2008b)

Early low-resolution structural studies indicated that PrPC had a high α-helix content (40% of the protein) and relatively low β-sheet content (3% of the protein) (Pan et al., 1993). These findings were further refined by Wüthrich and colleagues who determined the fine structure of PrPC by nuclear magnetic resonance spectroscopy (Riek et al., 1996), and later also by crystallographic studies (Knaus et al., 2001).

Human PrPC is composed of a highly structured C-terminal region (residues 121–232) (roughly 110 residues) and an unstructured N-terminal tail (spanning the

first 120 residues approximately). The NMR structure of the N-terminal domain was not determined due to its high flexibility and to its unfolded predicted structure (Sakudo et al., 2010). The COOH-proximal half of the protein is arranged in three α-helices corresponding, for human PrPC, to the residues 144 –154, 173–194, and 200 – 228, interspersed with an antiparallel β-pleated sheet formed by β-strands at residues 128 –131 and 161–164. A single disulfide bond is found between cysteine residues 179 and 214 (Riek et al., 1996; Zahn et al., 2000) (Fig.4).

PrPC is synthesized with N- and C- terminal signal sequences, the former targeting it to the endoplasmic reticulum and the secretory pathway, and the latter directing the removal of a C- terminal signal peptide followed by the addition of a GPI anchor, which tethers PrPC to the outer leaflet of the plasma membrane. As is common with GPI-anchored proteins, PrPC is found in cholesterol-rich lipid raft domains within the membrane (Watts and Westaway, 2007).

The PrPC N-terminal domain is characterized by two notable regions: the octapeptide repeat and the hydrophobic tract prior to the beginning of the structured domain. The former consists, in the case of human PrPC, of five repeats of the PHGGGWGQ sequence and is characterized by the presence of four copper binding sites (Viles et al., 1999). The latter is well conserved among PrPC sequences from a variety of species and mutations within this sequence can increase the formation of a transmembrane topological variant of PrPC (^{Ctm}PrPC) which has been linked to neurodegeneration (Hegde et al., 1998). Furthermore, as N-terminal deletions in PrPC invade the hydrophobic tract, the truncated proteins become increasingly toxic to transgenic mice (Shmerling et al., 1998).

PrPC contains two consensus sequences for N- linked glycosylation and un-, mono-, and di-glycosylated versions of PrPC are simultaneously present in the cell (Fig. 4A).

2.1.4 Cellular localization and trafficking of the prion protein

The precise localization of PrPC in neurons – exclusively synaptic or in neuronal cell bodies - remains enigmatic and several discrepancies can be noted among published reports owing to conflicting data obtained by different techniques. For example, although anti-PrPC antibodies usually cross-react among mammalian PrPC, it is possible that, due to either subtle differences in protein structure or glycosylation patterns, low protein levels may not be detected in certain cell types (Aguzzi and Polymenidou, 2004; Beringue et al., 2003).

PrPC is a cell-surface glycosylphosphatidylinositol (GPI)-anchored protein that, like other membrane proteins, is synthesized in the rough endoplasmic reticulum (ER) and travels through the Golgi apparatus to the plasma membrane (Aguzzi and Polymenidou, 2004). During its biosynthesis, PrPC undergoes several posttranslational modifications, including cleavage of the amino-terminal signal peptide, addition of N-linked oligosaccharide chains, formation of a disulfide bond and attachment of a GPI anchor, which facilitates its association with specific lipid membrane domains called 'rafts'. These are defined as small (10–200 nm), heterogeneous, highly dynamic, sterol- and sphingolipid-enriched domains that compartmentalize cellular processes and can sometimes be stabilized to form larger platforms through protein-protein and protein-lipid interactions (Pike, 2006). Membrane rafts are involved in pathogen invasion, regulation of protein and lipid sorting, as well as in cellular signaling (Linden et al., 2008). Association of PrPC with lipid rafts starts early within the ER, and maturation of PrPC along the ER-Golgi-plasma membrane pathway is associated with a changing association with distinct membrane rafts. Raft association is required for the correct folding of PrPC, for the export of the protein to the Golgi, and appears to control the distribution of mature PrPC among very distinct regions of the plasma membrane (Sarnataro et al., 2004).

PrPC can be synthesized with at least three topologies in the endoplasmic reticulum: a secreted form, which fully translocates into the ER and from which the major GPI-anchored form derives, and two COOH- or NH_2-terminal transmembrane forms (^{Ctm}PrPC and ^{Ntm}PrPC respectively) derived as the result of the transmembrane insertion of the hydrophobic pocket between aa 110 –134 in the ER membrane (Hegde et al., 1998). The physiological roles of the transmembrane forms of PrPC are not clear to date. The ^{Ctm}PrPC was suggested to be toxic and cause degeneration since transgenic mice expressing ^{Ctm}PrPC develop neurological illness and neuronal death that resembles certain prion diseases (see 2.1.5). However, since ^{Ctm}PrPC accumulates in the Golgi apparatus of transgenic ^{Ctm}PrPC expressing mice, the observed neuropathology may be due to a Golgi dysfuntion (Stewart et al., 2005). In addition, it is noteworthy that the transmembrane domain in membrane inserted PrPC is similar to the region that binds certain PrPC ligands: it is therefore possible that the membrane occlusion of this site may influence cell physiology (Linden et al., 2008).

PrPC has also been detected in a cytosolic soluble form. It is not clear why PrPC is occasionally retained in the cytosol, nor whether it serves any physiological function or, alternatively, may be associated with neuronal pathogenesis. Initially, ^{Cyt}PrPC was thought to be formed by misfolded chains that retrotranslocated through the endoplasmic reticulum-associated protein degradation-proteasome pathway (Ma and Lindquist, 2002). However, it was later shown that cytosolic PrPC contains the N-

terminal signal peptide, indicating that this subcellular location may be exclusively related to abortive translocation into the ER (Drisaldi et al., 2003). Recently, using signal sequence mutants, ^{Cyt}PrPC was found to be translated from a downstream AUG (coding for Met-8 in human): shortening of the signal sequence dictates the spillage of this isoform into the cytosol, from where it accesses the nucleus or forms insoluble cytosolic aggregates if the proteasome is inhibited (Juanes et al., 2009). Regarding the role of ^{Cyt}PrPC, most knowledge has been provided by models consisting of mutant polypeptides (PrP(23–230)) lacking both the N-terminal signal sequence and the GPI anchor that are inappropriately expressed and folded in the cytosol. These PrP(23–230) chains exhibit a widespread intracellular distribution and an alleged role that varies from cytotoxic (Ma et al., 2002) to innocuous or even protective (Roucou et al., 2003).

PrPC is constitutively internalized and recycles back to the surface (Campana et al., 2005). The biological role of PrPC internalization is unknown, but it has been shown to be inducible by copper and zinc ions and thus could have a physiological function in chelating extracellular copper ions (Pauly and Harris, 1998; Watt and Hooper, 2003) or in modulating the signaling activity of the protein (Mouillet-Richard et al., 2000). It is not clear, however, whether the mechanism involved in copper-stimulated PrPC endocytosis is identical to that responsible for constitutive endocytosis of PrPC (Campana et al., 2005).

The mechanism of PrPC internalization is currently debated but mounting evidence supports a major role of clathrin-coated vesicles in the internalization of raft associated PrPC. To undergo endocytosis by clathrin-coated pits, PrPC needs to leave the lipid rafts before being internalized because the rigid structure of rafts lipids is unlikely to be able to accommodate the tight curvature of coated pits. Through its N-terminal domain, GPI-anchored PrPC may interact with an integral membrane protein containing a localization signal for coated pits, and therefore enter the clathrin-dependent internalization pathway (Sunyach et al., 2003). PrPC binds to several proteins present at the cell surface including STI1, N-CAM, 37-kDa/67-kDa laminin receptor. Of these proteins, only the 37-kDa/67-kDa laminin receptor has been implicated directly in the internalization of PrPC; however, it was shown to be responsible for the internalization of only 25–50% of membrane-bound recombinant PrPC (Gauczynski et al., 2001). Low-density lipoprotein receptor-related protein 1 (LRP1) was subsequently shown to control both biosynthetic and endocytic, trafficking of PrPC (Parkyn et al., 2008). It is likely that cytosolic factors that participate in clathrin-mediated endocytosis, such as the small GTP binding Rab proteins, may also have a key role in controlling PrPC trafficking.

Like many cell surface proteins PrPC, can undergo two distinct endoproteolytic cleavages. The 'normal' constitutive cleavage of PrPC occurs in the brain and in neuronal cultured cells between residues 110 and 111 and leads to the formation of a 9-kDa, soluble, N-terminal fragment (N1; residues 23–110), and a 17 kDa C-terminal fragment (C1 or PrP-II) that is still attached to the membrane via the GPI anchor. This 'normal' cleavage of PrPC has been designated α-cleavage (Mangé et al., 2004), and may be mediated by two members of the ADAM family (ADAM 10 and ADAM 17) (Vincent et al., 2001). PrPC can also be cleaved within or adjacent to the octapeptide repeats to generate a 19-kDa, GPI-anchored C-terminal fragment C2, and the corresponding 7-kDa, N- terminal fragment N2 (residues 23–90). This cleavage event is mediated by reactive oxygen species (ROS), and is termed β-cleavage (see Fig. 4A) (Watt et al., 2005).

2.1.5 History

The word prion was coined twenty years ago by Stanley Prusiner to describe the "proteinaceous infectious particle" that causes a family of fatal neurodegenerative diseases known as transmissible spongiform encephalopathies (TSEs). These include scrapie in sheeps and goats, bovine spongiform encephalopathies in cattle, chronic wasting disease in deer and elk, and Creutzfeldt–Jakob disease, Gerstmann-Sträussler syndrome (GSS), kuru, and fatal familial insomnia (FFI) in humans (Prusiner, 1998). The etiology of these pathologies can be infectious, sporadic or genetic. For each of them, the 'protein-only' hypothesis proposes that the actual infectious agent is merely a modified form of the cellular prion protein that, differently from all other known infectious pathogens, is capable of replicating and transmitting infection in the absence of a nucleic acid genome, by conversion of its normal isoform to a pathological one (PrPSc) that has abnormal conformation and an unusual resistance to proteolytic degradation. While almost 45% of the PrPC protein is α-helical with two very short stretches of β-sheet (Riek et al., 1996) (Fig. 4), conversion to PrPSc results in a protein comprised of 30% α-helix and 45% β-sheet.

PrPSc accumulates in cells and plaque-like extracellular deposits, propagating itself by converting more PrPC into the pathogenic form and triggering neurodegeneration by mechanisms that are still not fully understood.

Although the "protein only hypothesis" is currently the most widely accepted model, data and scientific opinion do not absolutely conform to this idea and other hypothesis are still discussed such as the "virino hypothesis" that postulates that the

infectious agent responsible for transmissible spongiform encephalopathies consists of an essential scrapie-specific nucleic acid associated or coated with a host-encoded protein, for which PrPC is the most likely candidate. However, despite considerable efforts and the high sensitivity of the tools of modern molecular biology, no evidence for TSE-specific nucleic acids has yet been adduced. On the contrary a large body of epidemiological and experimental evidence is in line with the "protein only hypothesis", and very stringently designed experiments have failed to disprove it (Aguzzi and Polymenidou, 2004).

In particular it has been proved that the expression of membrane-anchored PrPC is necessary to initiate prion diseases. Knockout mice carrying a homozygous deletion of *Prnp* don't present any particular phenotype (Büeler et al., 1992), fail to develop disease upon inoculation with infectious brain homogenate (Büeler et al., 1993) and do not carry prion infectivity in the brain (Sailer et al., 1994). PrPC expression is required for neurodegeneration in host neurons, the presence of PrPSc alone does not cause disease: when neurografts propagating PrPSc were implanted into *Prnp* knockout mice, no pathological changes were seen in PrPC-deficient tissue, even in the immediate vicinity of the grafts (Brandner et al., 1996). Additionally, transgenic mice expressing only a secreted form of PrPC lacking a GPI anchor do not develop clinical signs of prion disease, although prion inoculation induces PrPSc formation and aggregation of amyloid plaques (Chesebro et al., 2005). Finally, neuron-specific ablation of PrPC in transgenic mice (Mallucci et al., 2003) or RNAi knockdown of PrPC expression in mice with established prion disease (White et al., 2008) rescues early neuronal dysfunction and prolongs the survival of mice despite the accumulation of extraneuronal PrPSc. These results, and the observation that all familial cases of human TSEs are characterized by *PRNP* mutations that result in the formation of a mutant protein that more readily undergoes spontaneous mutations to PrPSc (Hsiao et al., 1992), clearly suggests that PrPC expression is necessary for the development of prion disease. Conversion of PrPC can be the result of inherited mutations, infection of the host with a prion-infected tissue or rare sporadic events causing PrPC to PrPSc conversion.

According to the "protein only" hypothesis, there are two models to explain the conformational conversion of PrPC into PrPSc: the template directed refolding model and the seeded nucleation model. The template-directed refolding model proposes that upon infection of an appropriate host cell, the incoming conformationally altered PrPC (PrPSc) starts a catalytic cascade using PrPC as a substrate, converting it by a conformational change into a new β-sheet-rich protein. The newly formed PrPSc will in turn convert a new PrPC molecule into a new PK-resistant entity (Fig. 5A). Alternatively, the seeded nucleation hypothesis suggests that

PrPSc exists in equilibrium with PrPC. In a non-disease state, such an equilibrium would be heavily shifted toward the PrPC conformation, such that only minute amounts of PrPSc would coexist with PrPC. Converted PrPSc would be stabilized only when it adds onto a crystal like seed or aggregate of PrPSc (Fig. 5B). Once a seed is present, further monomer addition is accelerated. The infectious agent would therefore not be represented by monomeric PrPSc but would consist of a highly ordered aggregate of PrPSc molecules: the aggregated state would be an intrinsic property of infectivity. Monomeric PrPSc would be harmless, but it might be prone to incorporation into nascent PrPSc aggregates (Aguzzi et al., 2008b).

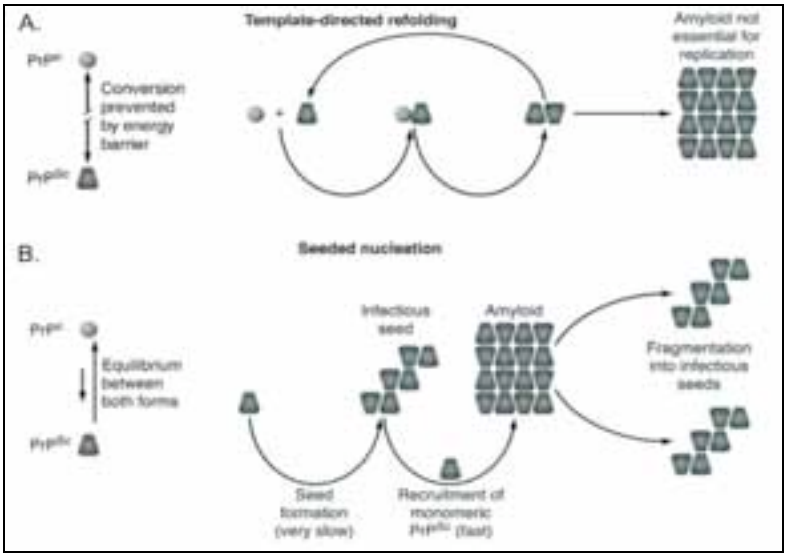

Figure 5. Models for the conformational conversion of PrPC into PrPSc. (A) The template-directed refolding model postulates that, upon interaction between exogenously introduced PrPSc and endogenous PrPC, the latter is induced to transform itself into further PrPSc. (B) The "seeding" nucleation model proposes that PrPC and PrPSc are in a reversible thermodynamic equilibrium. Only if several monomeric PrPSc molecules are mounted into a highly ordered seed, further monomeric PrPSc can be recruited and eventually aggregate to amyloid. Fragmentation of PrPSc aggregates increases the number of nuclei, which can recruit further PrPSc and thus results in apparent replication of the agent. Adapted from (Aguzzi and Calella, 2009).

Although the demonstration by Büeler and colleagues that *Prnp*$^{0/0}$mice do not develop disease following exposure to PrPSc has sometimes been defined as the "final

proof" of the protein-only hypothesis, this is certainly not the case: the supporters of the viral hypothesis suggested that PrPC may be a receptor for a hitherto unidentified virus, whose ablation would confer antiviral resistance (Aguzzi and Polymenidou, 2004).

The final proof for the protein only hypothesis would be the conversion of noninfectious PrPC into infectious material by biochemical and/or physicochemical interventions. *In vitro* conversion of radioactively labeled PrPC into partially PK-resistant (PrPSc) material was performed (Bessen et al., 1997; Kocisko et al., 1994), and highlighted that PrPSc can induce its own formation. However, the large amounts of the infectious agent used in this assay currently preclude attempts to search for an increase in infectivity (*de novo* infectivity) in the *in vitro* conversion products. Two later studies provided strong evidence that prions may be synthesized in cell-free systems, however the molecular mechanisms of the conversion process—for example, how this is accomplished under physiological conditions (e.g., pH conditions, cofactors) and exactly where it takes place in an *in vivo* setting (e.g., on the cell surface, in endosomes, in the extracellular space)—remain elusive (Aguzzi et al., 2008b)

One of the major challenges to the protein only hypothesis is the discovery of the existence of multiple prion strains defined as infectious isolates that, when transmitted to identical hosts, exhibit distinct prion-disease phenotypes. The phenotypic traits may include distinct patterns of protein aggregate deposition, incubation times, histopathological lesion profiles, and specific neuronal target areas (Aguzzi and Calella, 2009).

While the existence of different scrapie strains could be easily explained by the virino hypothesis – postulating the existence of a TSE specific-infectious agent nucleic acid - the protein only hypothesis has difficulty in explaining the propagation of different scrapie strains in mice that are homozygous in regard to their *Prnp* gene. However PrPSc itself is the molecule in which prion "strain"-specific information is encrypted. Epigenetic and posttranslational characteristics of prion strains appear to dominate over the primary prion protein sequence of the infected host. Indeed, preliminary immunochemical evidence suggests that PrPSc of different strains expose different epitopes (Safar et al., 1993) and display different degrees of stability to chaotropic salts (Peretz et al., 2002). Infrared spectroscopy measurements have shown that types of PrPSc associated with distinct hamster TSE strains can possess different conformations, even though they are derived from PrPC with the same amino acid sequence (Caughey et al., 1998). It suggests that an incoming PrPSc strain can convert the same PrPC precursor into a likeness of itself, and that this alone can create distinct

disease phenotypes, varying in clinical signs, organtropism, and regions of prion accumulation in the brain: a single protein with varying three-dimensional structures could confer prion strain diversity (Aguzzi et al., 2008b; Bessen and Marsh, 1994).

Although a lot of progress has been accomplished in the understanding of the neurotoxic mechanisms of prions, the molecular basis for neurodegenerative processes observed in prion diseases is poorly understood and many issues - such as the mechanism of prion conversion, how strain information is maintained and transmitted and the mechanisms that define the tropisms of prion – remain to be elucidated.

2.2 Physiological functions of PrPC

Although a great deal is known about the role of PrPSc in the disease process, the normal physiological function of PrPC has remained enigmatic (Westergard et al., 2007).

Different independent lines of mice lacking PrPC have been generated by homologous recombination in embryonic stem cells in many laboratories. Mice with disruptive modifications restricted to the open reading frame are known as *Prnp*$^{0/0}$ [Zurich I] (Büeler et al., 1992) or *Prnp*$^{-/-}$ [Edinburgh] (Manson et al., 1994) (Fig. 6). They developed normally, no severe pathologies were observed later in life and, as predicted by the protein-only hypothesis, these mice were entirely resistant to prion infections (Büeler et al., 1993). In contrast with these earliest lines, three lines generated afterwards by deletion of large portions of the ORF flanking regions, i.e. *Prnp*$^{-/-}$ [Nagasaki], Rcm0, and *Prnp*$^{-/-}$ [ZurichII] (Moore et al., 1999; Rossi et al., 2001; Sakaguchi et al., 1996), developed ataxia and Purkinje cell loss later in life. The remarkably distinct phenotypes of Nagasaki, Rcm0, and ZurichII mice, when compared with ZurichI and Edinburgh, were associated with the deletion approach employed for their generation. In fact, it was demonstrated that ataxia in these animals was caused by over-expression of Doppel protein: *Prnd* promoter is weak in the brain but when a splice acceptor site to the third exon of *Prnp* is deleted, exon skipping creates a chimeric mRNA containing the first two noncoding *Prnp* exons plus the Dpl-encoding *Prnd* exon (Fig. 6). Thus Dpl becomes controlled by the *Prnp* promoter and therefore is highly expressed in brain. The ectopic expression of Dpl in ZurichI mice caused ataxia and degeneration of cerebellar granule and Purkinje cells, and its levels were inversely correlated with the onset of disease (Moore et al., 1999). It is therefore possible to conclude that the ectopic expression of Dpl, rather than the absence of PrPC, caused neurodegeneration. Notably, the reintroduction of *Prnp* gene in mice over-expressing Dpl in the brain rescued the phenotype (Nishida et al., 1999). Thus Dpl neurotoxicity is counteracted by PrPC, but the mechanisms underlying this antagonism remain elusive.

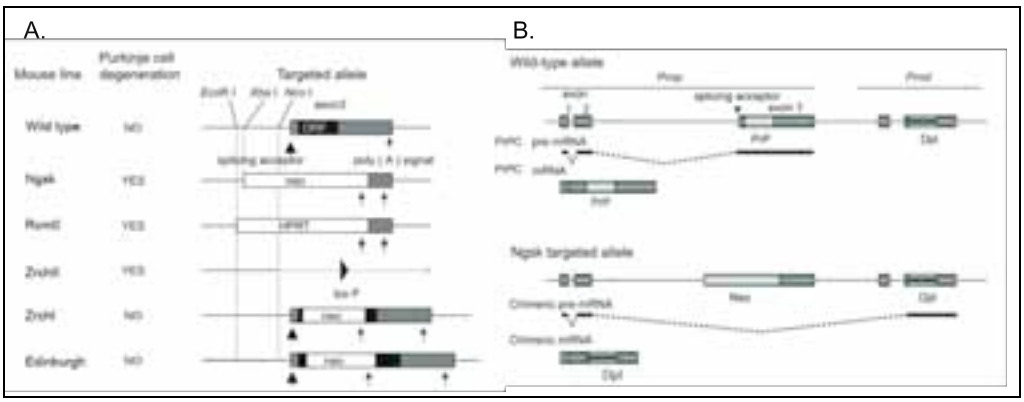

Figure 6. Purkinje cell degeneration among different lines of mice devoid of PrPC is associated with the ectopic expression of Dpl (A) Targeted *Prnp* alleles among different lines of *Prnp*$^{-/-}$ mice. In Nagasaki (Ngsk) *Prnp*$^{-/-}$ mice, a 2.1-kb genomic DNA segment including 0.9-kb of intron 2, 10-bp of 5' untranslated region (UTR) of exon 3, the entire PrPC ORF, and 0.45-kb of 3' UTR is replaced by the *neo* gene under the control of the mouse phosphoglycerate kinase (PGK) promoter. Rcm0 *Prnp*$^{-/-}$ mice were generated by a similar strategy but using the hypoxanthine phosphoribosyltransferase gene as a selectable marker. In Zrch II *Prnp*$^{-/-}$ mice, 0.27-kb of intron 2, the entire exon 3, and 0.6-kb of the 3' flanking DNA segment were targeted by a specific 34-bp *loxP* sequence. In these lines of *Prnp*$^{-/-}$ mice, the entire PrPC ORF is completely deleted. In contrast, Zrch I *Prnp*$^{-/-}$ mice were generated by replacement of codons 4-187 with the *neo* gene under the control of the herpes simplex virus thymidine kinase promoter. Edinburgh mice contain the disrupted *Prnp* alleles, in which the neo gene under the control of the mouse metalothioneine promoter was simply inserted into a unique *Knp* I site in the PrPC- coding sequence. (B) Mechanism for the generation of the Dpl-encoding chimeric mRNAs in Ngsk mice. In wild-type mice, the prion pre-mRNA is normally cleaved and polyadenylated at the last exon of the *Prnp*. In Ngsk mice, due to lack of the 3' part of intron 2, the pre-mRNA transcribed from the *Prnp* promoter is further elongated until the last exon of *Prnd* , and subjected to intergenic splicing between the residual *Prnp* exons 1/2 and the Dpl-coding exon. As a result, Dpl is abnormally expressed under the control of the *Prnp* promoter, leading to the ectopic expression of Dpl in the brains of ataxic lines of *Prnp*$^{-/-}$ mice. Adapted from (Sakaguchi, 2007).

Since PrPC-null mice in which Doppel gene is not artifactually up-regulated display no major anatomical or developmental deficits, it is possible to conclude that prenatally genetic ablation of PrPC expression in mice produces relatively little phenotypic effect, other than an inability to propagate prions (Büeler et al., 1993). Even mouse lines in which the prion gene is deleted postnatally using a conditional Cre-Lox system are phenotypically relatively normal, suggesting the existence of other proteins that compensate for essential PrPC functions in the adult (Mallucci et al., 2002).

The striking lack of phenotype reported for *Prnp* knockout mice lines is

surprising in view of the fact that PrPC is present in a broad variety of species. Genes with similarities to *Prnp* exist in birds (Gabriel et al., 1992), reptiles (Simonic et al., 2000), amphibians (Strumbo et al., 2001), and possibly in fish (Favre-Krey et al., 2007) in addition to all mammals. All cellular prion proteins are glycosylated and membrane attached by a GPI anchor. Comparisons between the available structures and molecular models suggest that all cellular prion proteins share an amino-terminal tail with repetitive domains of variable numbers, linked to a globular carboxy-terminal domain whose fold is strongly conserved and stabilized by a disulfide bridge. These two domains are linked by a highly conserved hydrophobic linker which is by far the most conserved sequence motive of PrPC in all species (Aguzzi et al., 2008a).

The strong evolutionary conservation of PrPC suggests important biological roles for the protein.

Although PrPC knockout mice display no major anatomical or developmental defects, a bewildering variety of subtle abnormalities have been described in these mice. These include altered circadian rhythms (Tobler et al., 1996) and olfaction (Le Pichon et al., 2009), abnormalities in neuronal transmission and electrical activity (Collinge et al., 1994), defective proliferation and differentiation of neural precursor cells (Steele et al., 2006) and hematopoietic stem cells (Zhang et al., 2006), and increased sensitivity to hypoxia, ischemia, and seizures (Spudich et al., 2005). Although intriguing, none of these reported abnormalities has provided a definitive clue to the physiological role of PrPC. A variety of functions have been proposed for mammalian prion protein, including involvement in cell death and survival, oxidative stress, immunomodulation, differentiation, metal ion trafficking, cell adhesion, and transmembrane signaling (Linden et al., 2008).

2.2.1 Looking for prion function: interaction partners of PrPC

A powerful strategy for elucidating the physiological function of cellular prion protein would be to identify other cellular proteins with which PrPC interacts. At least some of these interactors are likely to be components of the physiological pathways in which PrPC plays a role. Over the years, a number of candidates have been identified as potential prion-binding partners using conventional yeast two-hybrid screenings, co-immunoprecipitation, cross-linking and other methods (Westergard et al., 2007). Some of the PrPC interactors identified so far are represented in Figure 7.

All PrPC interaction partners identified so far include membrane proteins, cytoplasmic proteins, and even the nuclear protein CBP70. Unfortunately, the

physiological relevance of most of the proposed interaction partners remains unconfirmed (Aguzzi et al., 2008a). Proteins that are not even localized to the outer leaflet of the cell membrane, where PrPC is located and believed to exert its function, would at least require an additional interacting cell component, meaning that their interaction with PrPC must be indirect at best. Another possible explanation for cytosolic interaction partners is the suggested presence of the transmembranous variants of PrPC. However, under normal conditions they have been described in minute amounts only (Hegde et al., 1998). Cytosolic PrPC was described in cultured cells but the origin and the role of this form is not clear yet (Ma et al., 2002) (see 2.1.4).

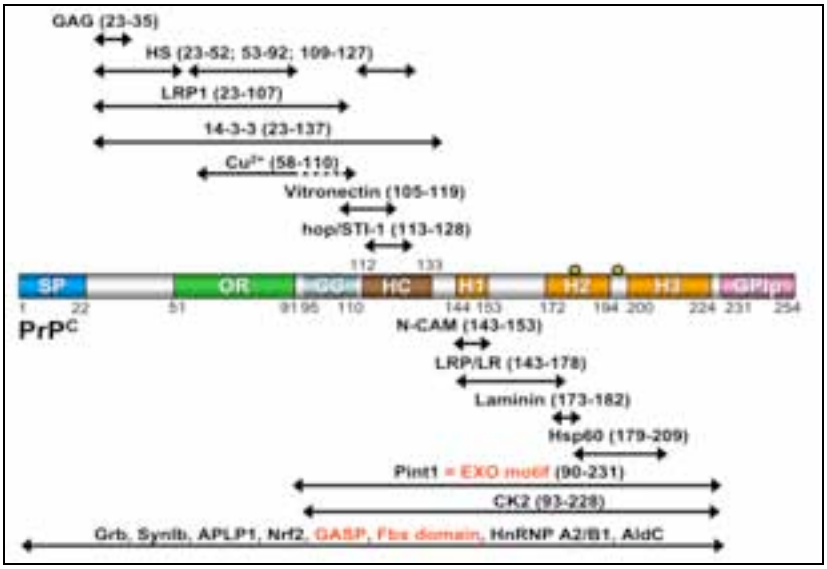

Figure 7. PrPC-binding partners. The translated sequence of the prion protein is depicted as a rodlike shape, with major domains shown in color (amino acid residue numbers as for mouse PrPC). SP, signal peptide; OR, octapeptide repeat domain; CC, charged cluster; HC, hydrophobic core; H1, H2, H3, α-helix domains; GPIp, GPI anchor-signaling peptide. Yellow stars indicate the position of the glycosylation residues. Each binding partner is indicated together with the stretch of amino acid residues that contain the binding domain in mouse PrPC. GAG, glycosaminoglycans; HS, heparan sulfate; LRP1, low-densitiy lipoprotein receptor-related protein; LRP, laminin receptor precursor protein; LR, laminin receptor; Pint1, prion protein interactor 1; EXO, exonuclease domain; CK2, casein kinase 2; Grb, growth factor receptor-bound protein; SynIb, synapsin Ib; APLP1, amyloid precursor-like protein 1; Nrf2, nuclear factor E2-related factor-2; GASP, G protein-coupled receptor-associated sorting protein; Fbx, F-box only; HnRNP, heterogeneous nuclear ribonucleoprotein; AldC, aldolase C/zebrin. Data from either human, hamster, or bovine proteins were transposed to homologous mouse sequences. From (Linden et al., 2008)

It's important to note that additional methods need to be used to confirm many of the interactions detected since the methodological approaches employed could have led to the detection of false positives. For example, because PrPC is exposed to the extracellular space, it is questionable whether a yeast two-hybrid screen that artificially exposes PrPC to the cytosolic compartment with its different biochemical composition is the most appropriate method to study PrPC interaction partners. In addition, also some of the interactions identified by immunoprecipitation may be artifactual since the choice of the detergent conditions to allow for weak and transient protein-protein interactions but destroy artificial or unspecific interactions is a critical step (Aguzzi et al., 2008a).

Copper constitutes a special case of confirmed PrPC ligand, the physiological role of which is a matter of controversy. The histidine-containing octapeptide repeats specifically bind up to four Cu^{2+} ions copper in a pH-dependent and negatively cooperative manner, with an affinity that may be as high as 0.1 nM (depending on binding site occupancy) (Walter et al., 2006). Binding involves coordination with nitrogen atoms in the imidazole side chains of histidine residues, as well as with nitrogen and oxygen atoms in main-chain amide linkages involving glycine residues. Two additional copper binding sites exist at residues 96 and 111. Copper binding has been shown to cause conformational changes in the flexible, N-terminal tail of PrPC (Jones et al., 2005a) and to alter the biochemical and cell biological properties of PrPC. Copper causes PrPC in brain homogenates to assume an aggregated and protease-resistant form that is distinct from PrPSc (Quaglio et al., 2001). In addition, micromolar concentrations of copper stimulate endocytosis of cell-surface PrPC via clathrin-coated pits (Pauly and Harris, 1998). However, a major role for PrPC in Cu^{2+} transport into the cell was ruled out, as PrPC expression levels do not seem to affect Cu^{2+} delivery. The affinity and number of Cu^{2+}-binding sites support the suggestion that PrPC could act as an anti-oxidant by binding potentially harmful Cu^{2+} ions and quenching the free radicals generated as a result of copper redox cycling (Mehrpour and Codogno, 2010). It has recently been reported that endogenous PrPC rapidly reacts to Cu^{2+} in murine neuro-2a and human HeLa cells. Specifically, the Cu^{2+}-induced elevation of PrPC is modulated through transcriptional up-regulation mediated via the ataxia-telangiectasia mutated (ATM). The elevated PrPC protects against copper-induced oxidativebstresses and cell death and plays an active role in modulation of intracellular copper concentration (Qin et al., 2009).

2.2.2 Functions of the prion protein in the nervous system

Several processes in the nervous system have been shown to be influenced by the prion protein. PrPC is expressed throughout the entire CNS, and occurs at particularly high levels in the hippocampus, striatum, and frontal cortex, with an apparently wide subcellular distribution, including synaptic sites (Mehrpour and Codogno, 2010).

Several experimental observations suggest that PrPC could play a role in synaptic structure, function or maintenance. Early pathologic changes occurring in prion diseases involve synapse loss and PrPSc deposition in synaptic terminals (Jeffrey et al., 2000). Synaptic vesicle proteins associated with exosomes and neurotransmission are reduced in brains of patients with spongiform encephalopathy (Ferrer et al., 1999). Synaptic disorganization and loss are fundamental and constant features of prion diseases, irrespective of the presence or absence of spongiform change, neuronal loss, and severe gliosis (Clinton et al., 1993). Abnormal electrophysiological recordings in scrapie-infected mouse and hamster hippocampal and cortical slices further support the synaptic dysfunction during the course of prion diseases (Barrow et al., 1999).

In hippocampal slices from *Prnp*$^{0/0}$ mice, it was initially reported that long term potentiation was impaired and receptor-mediated fast inhibition involving GABA-A receptors was decreased (Collinge et al., 1994). However, this result was subsequently disputed (Lledo et al., 1996). More recent studies have demonstrated a positive correlation between the expression level of PrPC and the overall strength of glutamatergic transmission in the hippocampus, with PrPC-over-expressing mice exhibiting supra-physiological responses (Carleton et al., 2001). At least part of this effect seemed to result from more efficient recruitment of pre-synaptic fibers as the level of PrPC increased. The suggestion of an involvment of PrPC in synapse formation originated from *in vitro* observations: incubation of cultured hippocampal neurons with recombinant PrPC induces rapid elaboration of axons and dendrites, and increases the number of synaptic contacts (Kanaani et al., 2005).

Prnp$^{0/0}$ mice have been reported to display several other neurobiological abnormalities that may also relate to the participation of PrPC in synapse formation and function. These include alterations in nerve fiber organization (Colling et al., 1997), circadian rhythm (Tobler et al., 1996), and spatial learning (Criado et al., 2005).

There is evidence that PrPC could contribute to neuronal functions in

peripheral as well as in central synapses. It was reported that PrPC is concentrated at the neuromuscular junction where it is localized in the sub-synaptic sarcoplasm, possibly associated with endosomal structures (Gohel et al., 1999). In addition, nanomolar concentrations of recombinant PrPC have been found to potentiate acetylcholine release at the neuromuscular junction (Re et al., 2006).

Several lines of evidence indicate involvement of PrPC in neuronal development, differentiation, and neurite outgrowth. Cell surface PrPC facilitates axonal outgrowth by a process that involves recruitment of N-CAM to lipid rafts and activation of Fyn kinase (Santuccione et al., 2005). Treatment of cultured neurons with recombinant PrPC also enhances neurite outgrowth and neuronal survival, concomitant with activation of several kinases, including Fyn, PKC, PKA, PI-3 kinase/Akt, and ERK (Westergard et al., 2007).

Recently, using three lines of PrPC knockouts mice on different genetic backgrounds and transgenic mice in which *Prnp* expression was driven by cell neuronal–specific promoters, Le Pichon et al. have reported that PrPC is important in the normal processing of sensory information by the olfactory system (Le Pichon et al., 2009). PrPC may be therefore important in the normal processing of sensory information by the olfactory system.

2.2.3 Functions of the prion protein in the immune system

The main thrust of research in prion biology is aimed at the CNS. However, expression of PrPC is widespread, selectively enriched, and developmentally regulated in certain cell types also outside the nervous system (Linden et al., 2008).

PrPC is expressed widely in the immune system, and in mature lymphoid and myeloid compartments (human T- and B-lymphocytes, natural killer (NK) cells, platelets, monocytes, dendritic cells (DCs) and follicular dendritic cells) (Mehrpour and Codogno, 2010). However, the expression of PrPC is non-homogeneous both across species and among subsets and states of maturation of immune cells: the expression of PrPC is down-regulated with maturation of granulocytes and upregulated with maturation of myeloid antigen-presenting cells (APC) (Linden et al., 2008; Zhang et al., 2006) .

PrPC may play important roles in the development and maintenance of the immune system, as well as in specific cellular immunological responses. Although *Prnp*$^{-/-}$ mice have been reported to display only minor alterations in immune function,

recent work has suggested that cellular prion protein affects the ability of long-term hematopoietic stem cells (HSC) to sustain self-renewal under stressful conditions (Zhang et al., 2006). Recently, the contribution of PrPC in alloantigen and major histocompatibility complex (MHC)-driven DC-T cell interaction was reported. An absence of PrPC on DCs results in a reduced allogenic T-cell response. Moreover, PrPC is responsible for the phagocytic capacity of macrophages by activating ERK1/2 and Akt kinase. Finally PrPC plays a functional role in T-cell development, activation and proliferation. In human T-lymphocytes, PrPC interacts with zeta-chain associated protein (ZAP)-70, a transduction signal responsible for T-cell activation and proliferation. Furthermore the expression of interleukin-2 by T cells is enhanced in the presence of PrPC (Mehrpour and Codogno, 2010).

2.2.4 PrPC and cell adhesion

Several reports are consistent with a possible function of PrPC as a cell adhesion or recognition molecule. In association with cell adhesion, distinct functions of PrPC were observed, depending on the cell type.

Some interaction partners of PrPC identified so far have include laminin (Graner et al., 2000), laminin-receptor precursor (Rieger et al., 1997), and N-CAM (Schmitt-Ulms et al., 2001). These molecules are involved in adhesion and in a diversity of signal transduction pathways leading to differentiation and neurite outgrowth (Aguzzi et al., 2008a). Laminin, a major structural component of basement membranes, plays a significant role in neuronal proliferation, supports neurite outgrowth, and aids in cellular migration. It was shown that PrPC binding to laminin promotes neurite outgrowth in PC12 cells and hippocampal neurons and that laser ablation of cell-surface PrPC caused retraction of neurites (Graner et al., 2000). Both cis and trans interactions at the neuronal surface between N-CAM and PrPC promote neurite outgrowth by recruitment of N-CAM to lipid rafts and subsequent activation of Fyn kinase, an enzyme involved in N-CAM- mediated signaling (Santuccione et al., 2005).

A preferential localization of PrPC at the level of intercellular junctions has recently been observed in brain endothelial cells that form the blood–brain barrier (Viegas et al., 2006). Moreover, anti-PrPC antibodies unexpectedly inhibited the transmigration of U937 human monocytic cells as well as that of freshly isolated monocytes through human brain endothelial cells. These observations suggest that PrPC is expressed by brain endothelium as a junctional protein that is involved in the trans-endothelial migration of monocytes (Mehrpour and Codogno, 2010).

2.2.5 PrPC and cell signaling

Like other GPI-anchored proteins, PrPC resides in lipid raft domains on the plasma membrane, which are known to serve as molecular scaffolds for signal transduction (Taylor and Hooper, 2006). Since its polypeptide chain is entirely extracellular, PrPC would presumably need to interact with transmembrane adaptor proteins in order to transmit signals into the cytoplasm. There are now a number of studies suggesting that PrPC can activate transmembrane signaling pathways involved in several different phenomena, including neuronal survival, neurite outgrowth, and neurotoxicity. In some of these cases, signal transduction is initiated by interaction of PrPC with specific protein or peptide ligands. In other cases, PrPC appears to act constitutively (Westergard et al., 2007). Several signaling pathways or signaling components, such as Akt, Fyn, cAMP, and Erk1/2, are modulated by PrPC expression, its cross-linking, or its interaction with another protein (Aguzzi et al., 2008a).

Antibody-induced cross-linking of GPI-anchored proteins on the cell surface is a technique commonly used to activate phosphorylation-dependent signaling cascades in lymphocytes (Westergard et al., 2007). Antibody-mediated cross-linking of PrPC on a neuroectodermal cell line (1C11) was found to stimulate the activity of the non-receptor tyrosine kinase Fyn (Mouillet-Richard et al., 2000), leading to downstream stimulation of NADPH oxidase and extracellular-regulated kinases (ERKs) (Schneider et al., 2003). Because Fyn is an intracellular protein, this signaling pathway was reported to require interaction of PrPC with the raft protein caveolin to activate Fyn. The activities of several G protein-coupled serotonin receptors found on the surface of these cells were also altered by PrPC cross-linking (Mouillet-Richard et al., 2005). The signaling pathways engaged by anti-PrPC antibodies in 1C11 cells are postulated to have pro-survival effects (Schneider et al., 2003).

Another kind of pro-survival signaling pathway that has been characterized involves an interaction between PrPC and stress-inducible protein 1 (STI-1). Although STI-1 lacks a signal sequence and is primarily localized in the cytoplasm and nucleus, some molecules have been reported to reside on the plasma membrane and to co-immunoprecipitate with PrPC. Interaction with cell surface STI-1 has been proposed to mediate PrPC-dependent protection of retinal explants from anisomycin-mediated cell death (Zanata et al., 2002). This effect was found to depend on activation of a cAMP/protein kinase A pathway (Chiarini et al., 2002). A recent study also demonstrated that incubation of cultured hippocampal neurons with recombinant STI-1 stimulated neurite outgrowth in a PrPC-dependent manner, an effect requiring signaling through a mitogen-activated protein kinase (MAPK) pathway (Lopes et al.,

2005).

Chen et al. reported increased neuronal survival and neurite outgrowth from neurons when cultured on Chinese hamster ovary (CHO) cells transfected to express mouse PrPC. Although p59Fyn kinase activity in this context was involved mainly in neurite outgrowth, the PI3 kinase/Akt pathway as well as regulation of Bcl-2 and Bax expression contributed to the survival effect elicited by PrPC. Cyclic AMP/protein kinase A (PKA) and Erk signaling pathways contributed to both neurite outgrowth and neuronal survival (Chen et al., 2003; Santuccione et al., 2005).

PrPC is rapidly internalized from the cell membrane. Endocytosis of membrane receptors does not necessarily down-regulate receptor activity. While being internalized, both tyrosine kinase and G protein–coupled receptors may remain activated and produce intracellular responses along the endosome-lysosome pathway (Prado et al., 2004). TrkA receptors, for example, mediate nerve growth factor (NGF)-dependent cell survival while they are located at the cell membrane, whereas internalization is required for induction of neurite outgrowth.

PrPC is involved in a number of cellular functions and how endocytosis influences them *in vivo* remains widely unknown; internalization of PrPC could contribute to down-regulation of a signaling event or could be necessary for signaling (Aguzzi et al., 2008a).

2.2.6 PrPC cytoprotective activity

Some intriguing evidence has emerged recently indicating that PrPC may exert a cytoprotective activity against various kinds of internal or environmental stresses. The original suggestion that PrPC could possibly be involved in modulating cell sensitivity to programmed cell death arose from the identification of a significant similarity between PrPC octapeptide repeat and the Bcl-2 homology domain 2 (BH2), and from the ability of PrPC to bind Bcl-2 in a yeast double-hybrid approach (Kurschner and Morgan, 1996). Anti-apoptotic activity of PrPC was then demonstrated in a variety of experimental systems, including mice, cultured mammalian cells, and yeast (Westergard et al., 2007).

Early evidence that expression of PrPC modulates sensitivity to cell death was obtained in cell lines established from hippocampal neurons derived from either wild type (HW8, HW9, HW18 cells) or Nagasaki *Prnp*-null (HpL2-1 and HpL3-4 cells) mice. *Prnp*$^{-/-}$ cells died quickly upon serum deprivation while PrPC expressing cells

survived. In PrPC-null cells, serum deprivation led to p53 and Bax upregulation, cleavage of both caspase-3 and poly(ADP-ribose) polymerase (PARP), decreased Bcl-2, increased levels of mitochondrial calcium, and lower mitochondrial membrane potential. Transfection of knockout cells with a *Prnp* expression vector prevented all these typical apoptotic changes (Kuwahara et al., 1999). However, since the neuronal cells employed in this study had been derived from from mice over-expressing Doppel (Nagasaki line), their increased sensitivity to serum deprivation might have been a consequence of Doppel over-expression rather than an effect of the absence of PrPC. To investigate whether PrPC inhibits apoptotic neuronal cell death without Doppel contribution, an immortalized cell line was established (NpL2) from the brain of Zürich I $Prnp^{0/0}$ mice, which do not display any ectopic expression of Doppel. The results showed that PrPC potently inhibited serum-induced apoptotic cell death, indicating that Doppel expression is not involved in the anti-apoptotic function of PrPC (Nishimura et al., 2007).

Several studies indicate that PrPC has a cytoprotective function against apoptotic stimuli. One of the clearest examples of PrPC cytoprotective activity is the protein's ability to protect cultured human fetal neurons against Bax induced apoptosis. When human fetal neurons in culture were microinjected with a plasmid encoding Bax, ~90% of the neurons underwent apoptosis; but when the neurons were co-injected with both Bax- and PrPC-encoding plasmids, the percentage of apoptotic cells fell to ~10% (Bounhar et al., 2001). The octapeptide repeat domain that displays some similarity with the BH2 domain of Bcl-2 is essential for the neuroprotective function of PrPC against Bax. PrPC needs to achieve some form of maturity for its anti-Bax function since treatment of cells with Brefeldin A, a specific inhibitor of endoplasmic reticulum to Golgi transport, and with monensin, an inhibitor of protein transport beyond trans-Golgi vesicles, prevent its antiapoptotic function against Bax. However, the GPI anchor of PrPC is not required for the anti-Bax function, indicating that the presence of PrPC at the plasma membrane is not essential (Bounhar et al., 2001). Furthermore, PrPC expressed uniquely in the cytosol is also able to inhibit Bax mediated cell death induction (Roucou et al., 2003). The cytoprotective effect of PrPC against Bax is specific since PrPC does not prevent apoptosis induced by caspase, Bak, t-Bid, staurosporine, or thapsigargin. PrPC does not colocalize with Bax in normal or apoptotic primary neurons, and does not prevent Bax-mediated cytochrome c release in a mitochondrial cell-free system. PrPC could therefore protect against Bax-mediated cell death by preventing the Bax proapoptotic conformational change that is the first step in Bax activation (Roucou et al., 2005).

Ectopic expression of mouse *Prnp* in yeast also prevented Bax-induced cell death (Li and Harris, 2005). However, whereas deletion of the octapeptide repeats

abrogated the protective effects of of PrPC in human neurons (Bounhar et al., 2001), it did not affect yeast. Also contrary to human neurons, cytosolic PrPC failed to provide protection against Bax induced cell death in yeast (Li and Harris, 2005).

PrPC has also been found to rescue cultured cerebellar granule neurons (Drisaldi et al., 2004) and N2a neuroblastoma cells (Qin et al., 2006) from apoptosis induced by its paralog Doppel.

PrPC cytoprotective activity seems to be involved also in other contests.

In a screening approach for proteins protecting cancer cells from apoptosis, researchers investigated the gene-expression profile in an established cell clone of MCF-7 breast cancer cell line resistant to TNFα-induced apoptosis. PrPC was reported to be over-expressed 17-fold in the resistant clone. Conversely, over-expression of PrPC converted MCF-7 cells sensitive to TNFα-induced apoptosis into resistant cells (Diarra-Mehrpour et al., 2004) (see 2.3.1).

In a recently published study, it was reported that PrPC promoted self-renewal of hematopoietic stem cells during serial transplantation (Zhang et al., 2006). This phenomenon could also relate to the cytoprotective activities of PrPC, since serial transplantation is likely to subject cells to apoptotic stress. In what could be a related effect, it was recently reported that PrPC positively regulates proliferation and differentiation of neural precursor cells *in vitro* and *in vivo* (Steele et al., 2006).

PrPC cytoprotective activity has been exemplified also *in vivo*. PrPC was reported to have a role in the neuroprotective adaptive cellular response to ischemic lesions in rodent brain: levels of PrPC after ischemia were increased compared with controls and adenovirus-mediated over-expression of PrPC improved neurological behavior and reduced the volume of cerebral infarction (Shyu et al., 2005). Conversely, in a mouse model of ischemic brain injury, PrPC accumulated in neuronal soma within the penumbra of ischemic lesions. Furthermore, the infarct size in *Prnp*-null mice was significantly greater than in the wild type, supporting the proposed role for PrPC in the neuroprotective adaptive cellular response to hypoxic injury. $Prnp^{0/0}$ mice displayed significantly increased infarct volumes when compared with wild-type mice (McLennan et al., 2004).

2.2.6.1. Domains involved in PrPC cytoprotective activity

The comparison of the PrPC sequence domains that are essential for its cytoprotective activity in yeast, cultured mammalian cells, and mice, highlights a number of similarities between these three systems, as well as a few differences. Thus, the cytoprotective function of PrPC appears to be partially but not completely conserved in evolution (Westergard et al., 2007).

The first region of importance (residues 23-31; KKRPKPGGW in mouse) lies at the extreme N-terminus of the protein and includes four positively charged residues. This segment is known to play a role in endocytic trafficking of PrPC (Taylor et al., 2005) and in localization of the protein to lipid rafts (Walmsley et al., 2003). This region has been found to be essential for PrPC protection against Bax in yeast (Li and Harris, 2005) and Dpl in cerebellar granule neurons (Drisaldi et al., 2004). In transgenic mice, deletions beginning at residue 32 (PrPΔ32-80 and PrPΔ32-93) do not affect the ability of PrPC to suppress neurodegeneration induced by PrPΔN (Shmerling et al., 1998). In contrast, deletion of residues 23-88 obliterates the ability of PrPC to rescue mice from Dpl-induced toxicity (Atarashi et al., 2003). These two results together suggest that residues 23–31 are implicated in protecting against PrPΔN and Doppel, although it will be necessary to generate Tg(PrPΔ23–31) mice to confirm this inference. The requirement for residues 23–31 suggests that PrPC cytoprotective activity may depend on its relocation to the cell surface, lipid rafts, or endosomal compartments (Mehrpour and Codogno, 2010).

The C-terminal GPI anchor signal has also been tested for its potential involvement in PrPC cytoprotective activity. In both yeast (Li and Harris, 2005) and human neurons (Bounhar et al., 2001), deletion of this region does not impair the ability of PrPC to suppress Bax-mediated apoptosis, implying that PrPC cytoprotective activity does not require tethering to the plasma membrane. Similarly, PrPC-mediated rescue of granule neurons from Dpl-induced apoptosis does not require the GPI anchor (Drisaldi et al., 2004).

A related issue concerns the necessity for expression of PrPC in the secretory pathway. The PrPC mutant lacking the N- and C- terminal peptides (PrP23-231) fails to rescue yeast from Bax-induced cell death (Li and Harris, 2005) but retains full rescue activity against Bax in cultured human neurons (Roucou et al., 2003). Whether this discrepancy implies a fundamental difference in the cytoprotective pathways operative in yeast and mammalian cells remains to be determined. The protective activity of cytoplasmic PrPC in human neurons is surprising, since in other cultured cell types and in transgenic mice cytoplasmic PrPC is toxic (Ma et al., 2002; Rambold

et al., 2006).

The role of the PrPC octapeptide repeats has also been analyzed in several systems: deletion of this repetitive region has been reported to abolish the ability of PrPC to protect cortical neurons from Bax (Bounhar et al., 2001), granule neurons from Doppel (Drisaldi et al., 2004), and immortalized hippocampal neurons from serum deprivation (Sakudo et al., 2005). In contrast, removal of the repeats does not affect the ability of PrPC to protect yeast from Bax (Li and Harris, 2005) or transgenic mice from PrPΔN (Shmerling et al., 1998). These observations are difficult to reconcile, perhaps because the octapeptide repeats perform distinct functions in different cell types or in the context of different toxic insults.

2.2.7 PrPC and protection against oxidative stress

Several lines of evidence suggest that, besides its possible antiapoptotic function, PrPC may play a role in protecting cells from oxidative stress. Cell culture experiments reveal that neurons (cerebellar granular and neocortical) cultured from *Prnp*$^{0/0}$ mice are more susceptible than neurons from wild-type mice to treatments with agents that induce oxidative stress, including hydrogen peroxide, xanthine oxidase and copper ions. These results are consistent with the reduced Cu/Zn superoxide dismutase activity and the increase in the levels of oxidative damage to proteins and lipids observed in the brain lysates of *Prnp*$^{0/0}$ mice (Brown et al., 2002; Brown et al., 1997; Wong et al., 2001).

How PrPC protects cells against oxidative stress remains unclear. One possibility is that PrPC could itself have SOD activity, and thereby mediate the anti-oxidant function (Brown et al., 1999). However, there is significant controversy about the reality of this alleged SOD activity *in vitro* (Jones et al., 2005b) and *in vivo* (Hutter et al., 2003). A second hypothesis is that PrPC may act indirectly to protect cells against oxidative stress by upregulating the activities of other proteins, such as Cu–Zn SOD or glutathione reductase, that detoxify ROS (Brown et al., 1997).

It is also possible that PrPC acts either upstream or downstream of ROS to protect cells from oxidative stress. In some situations, for example, oxidative stress may activate apoptotic pathways (Halliwell, 2006). In such cases, the anti-apoptotic effects of PrPC may account for its ability to protect cells against oxidative stress.

2.3 PrPC and Cancer

2.3.1 PrPC and Breast cancer

Immunohistochemistry analysis of PrPC expression in normal breast has shown that PrPC is expressed in the cytoplasm and plasma membrane of normal myoepithelial cells, but not of the luminal cells. Moreover, PrPC was found in lymphocytes and fibroblasts in breast tissue (Mehrpour and Codogno, 2010).

Breast cancer is a major cause of morbidity and mortality in women world wide (Key, 2001). Anthracyclines-based chemotherapy administered either before surgery (neoadjuvant) or after surgery (adjuvant) in patients with stage I–III breast cancers improves survival rates. Nevertheless, the 10-year absolute benefit of adjuvant anthracyclines-based chemotherapy is limited, ranging between 2% and 11%, indicating that most patients do not in fact benefit from this treatment (Meslin et al., 2007a). Several studies have been conducted with the aim to identify predictive factors of chemotherapy efficacy. To this regard, estrogen receptor expression has been reported to split breast neoplasms in two highly distinct entities regarding gene expression profile (Sotiriou et al., 2003). As a consequence, biomarkers associated with efficacy of adjuvant chemotherapy could differ according to estrogen receptor expression and cell lineage (Andre and Pusztai, 2006). A role for PrPC in modulating breast cancer sensitivity to chemotherapy has emerged in a study where PrPC expression was analyzed by immunohistochemistry in a series of 756 patients included in two randomized trials comparing anthracycline-based chemotherapy to no chemotherapy: PrPC expression was reported to be associated with estrogen receptor - negative breast cancer ($P < 0{,}001$) and with a lower sensitivity to adjuvant chemotherapy (Meslin et al., 2007a).

This ability of PrPC to confer tumor resistance is also supported by previous *in vitro* data reporting the association between PrPC expression and resistance to TNF-induced apoptosis in breast carcinoma MCF7 cell line (Diarra-Mehrpour et al., 2004) . In this study, the gene expression profile of TNF-resistant and TNF-sensitive human breast carcinoma cell lines were compared by cDNA microarray. Among the multitude of differentially expressed genes identified, a great number was implicated in the PI3K/ Akt signaling pathway. Unexpectedly, endogenous PrPC was found to be over-expressed at both the mRNA (17-fold) and protein levels (10-fold) in TNF-resistant derivative cells as compared to the TNF-sensitive MCF7 cell line. Examining

a panel of human breast carcinoma cell lines for their sensitivity to TNF and their PrPC expression, revealed a close correlation between susceptibility to the cytotoxic action of TNF and expression of PrPC. Furthermore, the ectopic expression of human PrPC conferred TNF resistance on previously TNF-sensitive MCF7 cells, by a mechanism involving alteration of cytochrome c release from mitochondria and nuclear condensation. These data showed for the first time that PrPC is involved in tumor resistance and that the ectopic expression of PrPC can protect a breast cancer cell line from TNF-mediated cell death by interfering with the mitochondrial pathway (Diarra-Mehrpour et al., 2004).

In order to investigate whether down-regulation of PrPC sensitizes resistant breast carcinoma cell lines to apoptosis, in a follow-on study by the same group, PrPC expression was transiently silenced by siRNA in two tumor necrosis factor–related apoptosis inducing ligand (TRAIL) resistant MCF-7 human breast adenocarcinoma cell lines (2101 and MCF-7/ADR). PrPC knockdown partly restored the sensitivity of MCF-7/ADR and 2101 cells to the cytotoxic action of TRAIL by down-regulating Bcl-2 expression and therefore facilitating the activation of proapoptotic Bax. TRAIL-mediated apoptosis in PrPC knocked down cells was associated with caspase processing, Bid cleavage and Mcl-1 degradation. However, this increased susceptibility to apoptosis was not associated with any increase in the recruitment of TRAIL receptors or intracellular signaling molecule to DISC (Meslin et al., 2007b).

2.3.2 PrPC and Gastric cancer

A modified subtractive hybridization method used to identify upregulated genes in Adriamycin (ADR)-resistant human gastric adenocarcinoma cell lines, led for the first time to the discovery that PrPC is over-expressed in the ADR-resistant gastric cancer cell line SGC7901/ADR as compared to the parental ADR sensitive SGC7901 (Zhao et al., 2002). Although SGC7901/ADR was selected with a single anti-cancer drug, it also displayed cross-resistance to other anti-tumoral compounds such as cisplatin, VP-16, mitomycin C and 5-fluorouracil, indicating that PrPC over-expression relates to the occurrence and development of multidrug-resistant phenotype in gastric carcinoma (Zhao et al., 2002). PrPC was later found to be upregulated in several gastric carcinoma cell lines AGS, SGC7901, MGC803 and KATOIII (Du et al., 2005).

PrPC is predominantly located in the cytoplasm and plasma membrane of gastric cancer cells and PrPC expression is higher in gastric cancer tissues than in

adjacent non-tumoral tissues or normal gastric mucosa. No significant difference in PrPC expression was found between the primary site and the metastatic site of lymph node in metastatic gastric cancer. However, PrPC was found to be highly expressed in metastatic gastric cancers compared to non-metastatic ones suggesting that alteration of PrPC expression is one of the early determinant events of metastasis, and that PrPC may be used as a prognostic factor for metastasis of gastric cancer (Pan et al., 2006).

PrPC was reported to significantly promote the adhesive, invasive, and *in vivo* metastatic capacities of the gastric cancer cell line SGC7901 by activating the MEK/ERK pathway (Pan et al., 2006; Reddy et al., 2003). ERK1/2 are targets of PrPC-mediated signal in neuronal and non-neuronal cells. As downstream effectors of oncogene Ras, the MEK/ ERKs pathway has been demonstrated to be an important mediator of tumor progression and invasion (Reddy et al., 2003). PrPC expressing gastric cancer cells had necessary to be cultured on Matrigel to increase the expression level of phosphorylated ERK1/2. No significant alteration of phospho-ERK1/2 was found in PrPC transfectants when no Matrigel existed in cell culture system. Since Matrigel component include laminin and heparan sulfate proteoglycans, i.e two PrPC interactants, they could be the initiators of the PrPC signal in gastric cancer cells. The invasion promoting effects of PrPC can be inhibited by pharmacological blockade of MEK by PD98059, indicating that MEK/ERK pathway plays an important role in transducing invasion-promoting signal of PrPC in gastric cancer cells (Pan et al., 2006).

Subsequent studies have indicated that over-expression of PrPC might also promote the proliferation of gastric cancer cells at least partially by activating the PI3K/Akt pathway and the transcription of CyclinD1, thus accelerating the G1/S-phase transition. The octapeptide repeat region might be indispensable for this function (Liang et al., 2007). Interestingly, one octapeptide repeat deletion was found in several gastric cancer cell lines, and its mutation frequency was higher in gastric cancer (Liang et al., 2006b). Over-expression of PrPC containing one octapeptide repeat deletion might promote the proliferation of gastric cancer cells, at least partially through transcriptional activation of CyclinD3 in addition to CyclinD1 to accelerate G1/S-phase transition. The effect of PrPC with one octapeptide repeat deletion in promoting proliferation was greater than that of wild-type PrPC (Liang et al., 2009a).

PI3K/Akt signal transduction pathway is one of the critical steps in cell survival and MDR. PrPC and Akt are co-expressed in gastric carcinoma. PrPC-transfected cell lines showed increased expression of phosphorylated Akt, indicating that PrPC may serve as a positive upstream regulator of PI3K/Akt in gastric cancer cells. By inhibiting the PI3K/Akt pathway using LY294002 or co-transfection with

Akt siRNA, the drug sensitivity and accumulation in SGC7901/PrPC cells were significantly increased. The results indicate that inhibition of the PI3K/Akt signaling pathway may lead to inhibition of the MDR induced by PrPC in gastric cancer cells. The observation that PrPC-transfected cells treated with an inhibitor of Akt exhibit down-regulation of P-glicoprotein at both the mRNA and protein levels suggest that PrPC activated PI3K/Akt pathway may be involved in transcriptional activation of P-glicoprotein in PrPC-transfected gastric cancer (Liang et al., 2009b).

2.3.4 PrPC and Pancreatic cancer

Pancreatic ductal adenocarcinoma (PDAC) is the fourth leading cause of cancer deaths in the US and is one of the cancers with the poorest prognosis (Jemal et al., 2007). The overall median survival for all PDAC is 6 months and the 5-year survival rate is < 5%. This bleak outcome reflects the aggressiveness and highly metastatic nature of the tumor, the lack of an early diagnostic marker, as well as the inefficacy of the treatment regimens.

PRNP is one of the twenty-five genes that were found to be over-expressed in a panel of PDAC cell lines (Han et al., 2002). Surprisingly, further biochemical studies revealed that, in contrast to normal cells, the prion protein expressed by PDAC cell lines is unglycosylated and exists as pro-PrPC, retaining its normally cleaved GPI peptide signal sequence (GPI-PSS). Pro-PrPC is detected on the cell surface of PDAC cell line, using GPI-PSS as a surrogate transmembrane domain (Li et al., 2010) (Fig. 8).

Pro-PrPC is undetectable in cells with normal GPI-anchored PrPC, indicating that the transit from pro-PrPC to PrPC is either very rapid or that the removal of the GPI-PSS is very efficient in these cells. The reason why the GPI-PSS is not removed in PDAC cell lines is not to be addressed to a global defect in the GPI anchor modification machinery, nor to mutations in *PRNP*. Worthy of note is that the GPI-PSS of PrPC is intrinsically inefficient in accepting the lipid anchor: in an *in vitro* GPI anchor modification assay comparing the efficiency of nine different GPI-PSSs, the GPI-PSS of PrPC is by far the least efficient in accepting the GPI anchor (Chen et al., 2001). Hence, a slight defect in the GPI assembly pathway will have a more dramatic effect on PrPC than other GPI-anchored protein.

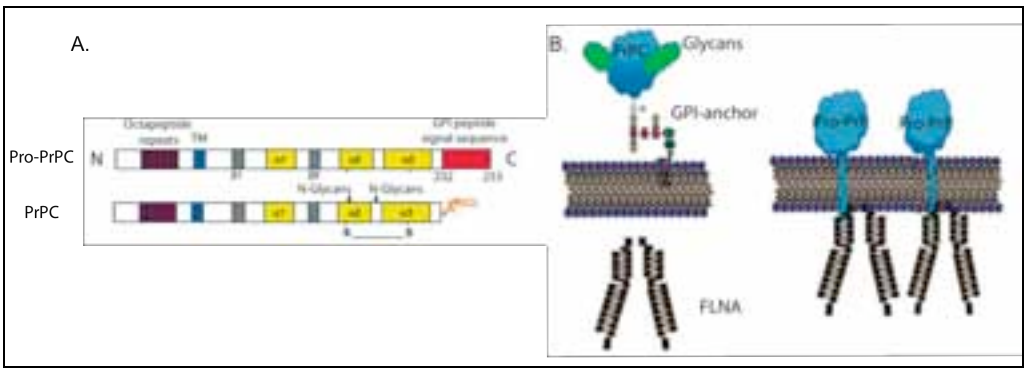

Figure 8. Pro-PrPC structure and localization. (A) Diagrammatic drawings of pro-PrPC and of mature, N-glycosylated and GPI-anchored PrPC. (B) Left panel: Normal glycosylated and GPI anchored PrPC on the cell surface; Right panel: pro-PrPC uses the GPI-PSS as a surrogate transmembrane domain to anchor itself to the cell surface and binds to FLNA just underneath the inner membrane leaflet. The sizes of PrPC and FLNA are not proportional. From (Li et al., 2010)

Despite the fact that the GPI-PSS is discarded after the attachment of the GPI anchor, this 22 aminoacids sequence comprises a highly conserved filamin A (FLNA) binding motif (Li et al., 2010). Binding of FLNA to pro-PrPC has been demonstrated by different approaches. *In vitro* pull-down assays have shown that FLNA only binds recombinant pro-PrPC, but not mature PrPC that lacks the GPI-PSS (Fig. 8). Co-immunoprecipitation experiments demonstrated that PrPC copurifies with FLNA and vice versa in the PDAC cell lysates. Finally, by immuno-fluorescent staining and confocal microscopic analysis, it was observed that PrPC and FLNA colocalize in the PDAC cell lines.

Filamin A is a cytolinker that connects cell surface receptors to the cytoskeleton. It interacts with a plethora of proteins with diverse functions including cell surface receptors, cytoplasmic adapter proteins, signal transducing molecules and transcription factors (Robertson, 2005).

Whether FLNA anomaly contributes to tumorigenesis has not been studied in detail. The immunohistochemical analysis of the expression pattern of FLNA in different cancer tissues as compared to their corresponding normal tissues highlighted some noticeable differences (Uhlén et al., 2005). While in normal pancreas exocrine ductal cells had low to moderate levels of FLNA, the expression of FLNA was increased in pancreatic cancer.

FLNA is an integrator of mechanical and chemical signaling events. Binding of pro-PrPC to FLNA is likely to have widespread effects on the PDAC cells: it may physically relocate FLNA from its normal environment thus rendering it unable to interact with its regular binding partners, or, alternatively, binding of pro-PrPC may also compete for binding sites on FLNA that are normally reserved for other molecules. Down-regulation of PrPC expression by small hairpin RNA in PDAC cell lines does not alter the expression levels of FLNA but it does alter the spatial distribution of FLNA in these cells. In control cells, FLNA is present just underneath the inner membrane leaflets, in PrPC down-regulated cells, FLNA is disconnected from the inner membrane leaflets and is more concentrated in the cytosol. Down-regulation of PrPC in the PDAC cell lines also drastically alters the organization of actin filaments. These biochemical modifications result in changes in the behavior of the PDAC cells. Compared with control cells, PrPC down-regulated PDAC cell lines have reduced *in vitro* proliferation and invasiveness. When the level of PrPC is reduced, the growth of the PDAC cell lines as xenograft in nude mice is also greatly reduced. Collectively, these results suggest that the expression of pro-PrPC modulates the functions of FLNA, and provides the PDAC cells with a growth advantage.

Analysis of PrPC expression in normal human pancreas, in pancreas with pancreatitis, in pancreas with pre-neoplastic lesions, such as PanIN-1, -2, and -3, or in pancreas with PDAC evidenced that in normal human pancreas, only islet cells show PrPC immunoreactivity. Neither acinar nor ductal epithelial cells stain for PrPC. PrPC is also undetectable in the duct cells in chronic pancreatitis, PanIN-1, and PanIN-2. About 13% PanIN-3 specimens show weak PrPC staining. Among the 83 PDAC cases examined, 34 show strong PrPC staining. The PDAC tumor cells also react with the anti-GPI-PSS antiserum indicating the presence of the GPI-PSS. Thus, as in the PDAC cell lines, PrPC exists as pro-PrPC in human PDAC lesions (Li et al., 2009). Interestingly, in the 34 PrPC positive tumor samples, 22 of the tumors (65%) also had detectable p53 levels. On the other hand, in PrPC negative tumors, only 12 out of the 49 (24%) PrPC negative tumors showed p53 expression. These results suggested that tumor cells with TP53 mutations preferentially expressed PrPC or, alternatively, expression of PrPC might favor the accumulation of p53 (Li et al., 2010).

Most importantly, the expression of PrPC is associated with poorer clinical outcome. Patients with intra-tumoral PrPC have a median survival time of ~1 year days, whereas patients without PrPC expression in their tumors have a mean survival time of more than 2,5 years. This association is independent of other factors, such as age and gender of the patient, as well as the size or differentiation stage of the tumor. Therefore, expression of PrPC divides the PDAC patients into two groups with drastic difference in their survival rates. PrPC expression is not essential for PDAC initiation

because only 41% of the PDAC cases have detectable PrPC. However, the presence of PrPC is associated with poorer clinical outcome. Therefore, similar to PDAC cell lines, PDAC tumors with PrPC have a growth advantage and are more aggressive.

Although all PDAC cell lines express PrPC, only 41% of the tumor biopsies have detectable levels of PrPC. One possibility is that during *in vitro* culture PrPC bearing tumor cells are preferentially expanded.

2.3.5 PrPC and human melanoma

The progression from melanocyte to melanoma is complex and not completely understood (Herlyn, 2006). By immunohistochemical staining, normal human melanocytes do not react with either anti-PrPC antibodies or anti-PrPC GPI-PSS specific antibodies, indicating that normal melanocytes do not express PrPC. In contrast, both the anti-PrPC and the anti-GPI-PSS antibodies react with melanoma *in situ* and invasive melanoma in the dermal component express the highest levels of PrPC. These results suggest that expression of PrPC may be important in the neoplastic transformation of melanocyte and invasion of human melanoma. However, whether expression of pro-PrPC has diagnostic or prognostic value will require studying a much larger cohort of melanoma patients (Li et al., 2010).

2.3.6 PrPC and Colorectal cancer

Colorectal cancer is the second leading cause of cancer death in the western world.

Publicly available microarray data have identified *PRNP* as one of the 139 genes differentially expressed between relapsed and non relapsed colorectal cancer. In particular, *PRNP* was found to be over-expressed in carcinoma from relapsed patients. In accordance with these data, cellular prion protein expression was later reported to significantly correlate with disease recurrence: patients with high PrPC levels relapsed earlier than those with low expression levels (Antonacopoulou et al., 2008). Although PrPC is expressed during embryogenesis in the central and peripheral nervous system and in non-neuronal cells, it is expressed at low levels in the colon during development. However, expression increases in CRC and follows the same pattern of expression as genes involved in cell-cycle progression, tissue disruption and angiogenesis, including VEGF, LIF, FOXO3A, and RB1 (Kaiser et al., 2007).

Analysis of *PRNP* mRNA expression in carcinoma specimens and normal tissue samples highlighted higher transcript levels in cancerous as compared to normal tissue suggesting a role for PrPC in colorectal cancer (Antonacopoulou et al., 2008). In a later study by the same group also prion protein expression was demonstrated to increase in neoplastic compared to normal tissue sample. Additionally, expression levels of PrPC were higher in the more aggressive cell lines (Antonacopoulou et al., 2010).

Recently it was shown that antibodies against PrPC are effective in reducing apoptosis in colon cancer cells as well as enhancing their sensitivity to antineoplastic agents such as irinotecan, 5-fluorouracyl and cisplatin (McEwan et al., 2009).

All the evidences here reported suggest the involvment of PrPC in cancer progression. To fully elucidate the contributions of PrPC to tumor biology some additional questions, such as the mechanism that causes the upregulation of PrPC in some, but not all, tumor cells remain to be answered.

The current concept divides genes involved in tumorigenesis into driver genes and passenger genes (Li et al., 2010; Liu, 2008). PrPC is clearly not a driver, but more likely a passenger with deadly potential (Li et al., 2010)

2.4 Malignant glioma

2.4.1 Histological classification

Malignant gliomas are the most common and lethal primary central nervous system tumor in adults. Primary brain tumours consist of a diverse group of neoplasms that are derived from various different cell lineages. Much like those arising from other anatomic sites, tumors of the CNS have historically been classified on the basis of morphological and, more recently, immunohistochemical features with less emphasis on their underlying molecular pathogenesis. (Huse and Holland, 2010).

The World Health Organization (WHO) classification, which was first formalized in 1979 and updated in 2007 (Louis et al., 2007), defines four grades of glioma tumors on the basis of their histogenesis and histological characteristics. Although the WHO classification does remain firmly grounded in morphological criteria, relevant molecular information regarding the different tumour classes has been integrated over time (Huse and Holland, 2010). Most gliomas diffusely infiltrate surrounding brain tissue and together represent a broad diagnostic group, which the WHO classifies into astrocytic, oligodendro-glial and mixed (oligoastrocytic) (Louis et al., 2007). In addition to a morphological grouping of brain tumours on the basis of presumed histogenesis, the WHO schemes have been notable for their grading of individual tumour classes (I, II, III and IV) as a means of reflecting anticipated biological behaviour (Huse and Holland, 2010).

Grade I tumors typically have a good prognosis and more frequently occur in children (Wen and Kesari, 2008). Grade II astrocytic tumors are histologically characterized by hypercellularity and have a 5–8-year median survival. Grade III astrocytoma tumors (anaplastic astrocytoma tumors) are characterized by hypercellularity, as well as nuclear atypia and mitotic figures; patients have a 3-year median survival. Grade IV gliomas, also known as glioblastomas (GBMs), are characterized on histologic examination by hypercellularity, nuclear atypia, mitotic figures, and evidence of angiogenesis and/or necrosis. The median survival for patients with GBM tumors is 12–18 months, older patients (>60 years of age) typically have a survival that is somewhat shorter than the median (Gladson et al., 2010). Glioblastoma is the most malignant variant of diffuse glioma and, although the generally reliable expression of protein markers such as glial fibrillary acid protein

(GFAP) has historically placed it in the confines of the astrocytic class, its precise histogenesis remains unclear despite considerable advances in the understanding of its basic biology. It has long been known that glioblastomas may evolve from lower grade astrocytic neoplasms over time (secondary glioblastoma), although most of these tumours seem to arise *de novo* (primary glioblastoma) (Ohgaki and Kleihues, 2005).

Oligodendroglioma tumors are histologically separated into Grades II and III according to the WHO criteria. Grade II tumors exhibit hypercellularity and bland nuclei on histologic examination, Grade III tumors (anaplastic oligodendrogliomas) exhibit the additional histologic features of prominent mitotic figures and evidence of angiogenesis (Wen and Kesari, 2008).

2.4.2 Major genetics alterations of gliomas

The ongoing characterization of the genetic alterations in glioma tumor cells is revealing considerable variability among tumors of the same type and grade. This heterogeneity may contribute to the current limitations in predicting patient survival on the basis of histologic analysis of glioma type and grade alone and suggests that classification of certain types and grades of gliomas according to their genetic phenotype will lead to a more accurate prediction of survival and response to therapy (Mason and Cairncross, 2008).

Numerous molecular abnormalities have been linked with the underlying biology of diffuse glioma.

Mutations in the *TP53* tumour suppressor gene were first implicated in gliomagenesis almost 20 years ago and are a frequent characteristic of sporadic low-grade astrocytic tumours and secondary glioblastomas (Louis, 1994). By contrast, primary glioblastomas were initially associated with genomic amplifications and activating mutations of the gene encoding the epidermal growth factor receptor (*EGFR*), found on chromosome 7. The most common mutation is a gain-of-function mutation due to an in-frame deletion of exons 2–7; this mutation - found in 20–30% of all primary glioblastomas and 50-60% of those also exhibiting *EGFR* amplification (Frederick et al., 2000) - results in the constitutive activation of EGFR, which can promote glioma cell proliferation and invasion (Soni et al., 2005).

A substantial number of oligodendroglial tumours (60–90%) were found to exhibit loss of heterozygosity (LOH) on chromosomes 1p and 19q, a genomic

abnormality that interestingly predicts less aggressive biological behaviour and a relatively robust response to chemotherapy (Nutt, 2005). Despite the fact that 1p/19q deletion analysis is frequently used in the diagnosis and management of oligodendroglial neoplasms, the precise identity of the presumed tumour suppressors resident in these genomic loci remains elusive (Barbashina et al., 2005).

In more recent years, additional cancer-related genes and signaling networks have been directly implicated in glioma pathogenesis. The retinoblastoma (Rb) tumour suppressor pathway has been shown to be defective in a significant number of high-grade gliomas of both astrocytic and oligodendroglial lineage, whether by inactivating mutations in *RB1* itself or amplification of its negative regulators cyclin-dependent kinase 4 (*CDK4*) and, less frequently, *CDK6* (Henson et al., 1994) (Fig. 9). Analogously, amplification of the p53 antagonists *MDM2* and *MDM4* have also been found in distinct subsets of *TP53*-intact glioblastomas, as have mutations and/or deletions in the *CDKN2A* locus that encodes both INK4A and ARF, which are crucial positive regulators of RB and p53, respectively (Fig. 9). These findings emphasize the importance of perturbed cell cycle regulation through the disruption of the p53 and Rb pathways in glioma pathogenesis (Huse and Holland, 2010).

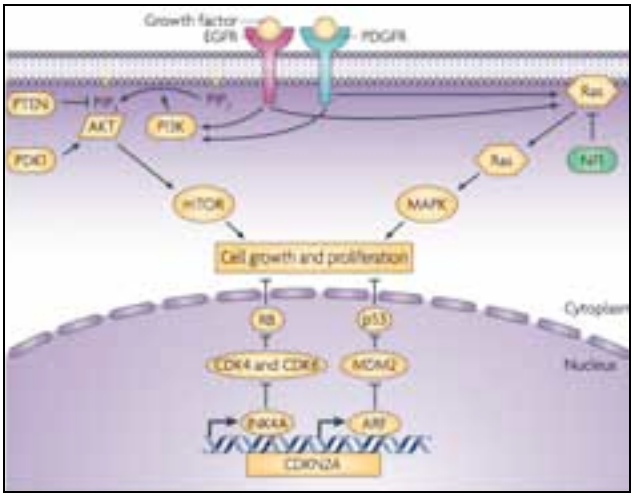

Figure 9. Molecular pathways implicated in the pathogenesis of glioma. Downstream oncogenic signalling through receptor tyrosine kinases such as epithelial growth factor receptor (EGFR) and platelet-derived growth factor receptor (PDGFR) is mediated by the PI3K–AKT–mTOR and Ras–MAPK networks. Defects in the p53 and RB tumour suppressor pathways are also common. Targeted deletions of the neurofibromatosis type 1-associated tumour suppressor neurofibromin 1 (*NF1*), a negative regulator of Ras signalling, have also been shown to drive gliomagenesis in mice. From (Huse and Holland, 2010).

The involvement of receptor tyrosine kinases (RTKs) in addition to EGFR in gliomagenesis has also been repeatedly demonstrated. Most notably, enhanced signaling through platelet-derived growth factor receptor-α (PDGFRα) has been found to be a common feature of low-grade astrocytic and oligodendroglial tumours along with a significant subset of glioblastoma (Westermark et al., 1995). Although activating mutations in *PDGFRA* are uncommon, frequent co-expression of both the receptor and its ligand, most commonly PDGFB, indicates the potential for autocrine or paracrine loops boosting oncogenic signaling through the PDGF network. Similar findings regarding hepatocyte growth factor (HGF) and its RTK MET (also known as HGFR) have also been reported for glioma (Abounader and Laterra, 2005). Therefore, enhanced RTK signaling seems to be a fundamental oncogenic event in the plurality of malignant gliomas, the effects of which are probably mediated in large part through oncogenic PI3K–Akt–mTOR and Ras–MAPK signaling that promote cell survival, proliferation and invasion (Fig. 9). Underscoring this fact is the not infrequent dysregulation in malignant gliomas of molecular components in these downstream networks, the most common of which is functional loss of the tumour suppressor *PTEN*, the primary negative regulator of PI3K–Akt–mTOR signaling (Wang et al., 2004) (see 2.4.3).

The widespread implementation of comparative genomic hybridization (CGH) has resulted in more comprehensive analyses of the molecular aberrations underlying gliomagenesis, as well as insights into their biological heterogeneity (Huse and Holland, 2010). CGH profiling of primary and secondary glioblastomas, for instance, has shown strikingly distinct patterns of copy number alteration (CNA), while also demonstrating that secondary glioblastomas themselves consist of two subgroups in which the clinical progression times differ significantly (Maher et al., 2006). Coupling array CGH with additional genomic techniques, has allowed for queries into the identities and functional characteristics of glioma relevant genes (Parsons et al., 2008). These studies have confirmed the importance of the many glioma-associated genes previously identified and have led to the development of more effective prognostic stratification algorithms (Bredel et al., 2009). Integrated genomic analysis has also facilitated the identification and characterization of additional genes involved in glioma pathogenesis. Recently, missense mutations in isocitrate dehydrogenase 1 (*IDH1*) were found in a significant number of glioblastomas that tend to occur mostly in younger patients with more protracted clinical courses (Parsons et al., 2008). These point mutations are restricted exclusively to the R132 residue in the active site region of the protein in which they disrupt hydrogen bonding with its substrate. Interestingly, a separate group of gliomas harbour mutations in the *IDH1* homologue *IDH2* at the analogous residue (R172). Further investigations have shown that mutations in *IDH1*

and *IDH2* are present in high proportions of grade II and III astrocytic and oligo dendroglial tumours (72–100%) along with secondary glioblastomas (85%), but are largely absent in primary glioblastomas (5%) (Yan et al., 2009). Additionally, *IDH* mutations are associated with other genomic abnormalities that are typically seen in lower grade diffuse gliomas, such as *TP53* mutation and 1p/19q deletion; they are also mutually exclusive with *EGFR* amplification and chromosome 10 loss, and multivariate analysis suggests that they are independent favourable prognostic markers (Sanson et al., 2009). These findings suggest that, although *IDH* mutations probably contribute to the early evolution of low-grade gliomas (including those that subsequently progress to higher grade lesions), they seem to have no role in the underlying biology of *de novo* glioblastoma, further emphasizing the fundamental differences in pathogenesis between these two broad diagnostic categories (Huse and Holland, 2010).

Genomics has also revealed connections between gliomagenesis and microRNA (miRNA) biology. It has recently been shown that amplification of *miR-26a-2* leads to the over-expression of miR-26a in ~12% of glioblastomas, promoting gliomagenesis through direct repression of PTEN, RB and MAP3K2 (Huse and Holland, 2010; Kim et al., 2010). Several other miRNAs have also been implicated in glioma formation, including miR-21, miR-7, miR-124a, miR-137, miR-221, miR-222 and the miR-181 family (Novakova et al., 2009). miRNA-based regulation of the numerous molecular pathways involved in gliomagenesis is undoubtedly complex and this active area of research should produce numerous additional candidates for therapeutic targeting in the near future (Huse and Holland, 2010).

2.4.3 Proliferating and survival signaling in glioblastoma

Like other malignant tumors, gliomas proliferate rapidly and augment survival pathways. This phenotype is due to the loss of multiple cell-cycle inhibitors as well as to increased signaling from multiple growth factor receptors that act through downstream effectors to exert positive effects on the regulation of the cell cycle. The growth factors receptors that initiate a pro-proliferative signal in these tumors include EGFR and PDGFR, the most common receptor tyrosine kinase (RTKs) with intrinsic tyrosine kinase activity that are aberrantly expressed in GBMs. Frequently, expression of both the ligand and the receptor is increased in glioma tumors, suggesting the existence of an autocrine or paracrine loop that amplifies signaling (Gladson et al., 2010).

The class IA phosphatidylinositol-3-kinase (PI3K) translocates to the plasma membrane through binding to phosphotyrosine residues on RTK and is then activated by the receptor itself. Activated PI3K produce phosphatidylinositol-3,4,5 triphosphate (PIP_3) from phosphatidylionositol-3,4 diphosphate (PIP_2). Accumulation of PIP_3 recruits phosphoinositide-dependent kinase 1 (PDK1) and Akt to the plasma membrane. Once activated through phosphorylation at two key regulatory sites, Thr308 (by PDK1) and Ser473 (by mTOR complex 2), Akt promotes survival by facilitating nuclear translocation of nuclear factor κB (NFκB) which then transcriptionally activates multiple genes that mediate cell survival and drive proliferation (Karin et al., 2002) (Fig. 10). An immunohistochemistry study of 70 GBMs on a tissue micro-array reported that 91.3% of the GBMs samples possessed activated NFκB that was highly correlated with activated Akt levels (Wang et al., 2004).

PTEN functions as a tumour suppressor that negatively regulates PI3K activity by dephosphorylating PIP_3 to PIP_2 and thereby terminating PI3K signaling (Fig. 9). Mutations of the *PTEN* gene in GBMs result in elevated levels of PIP_3, through which PI3K hyperphosphorylates PDK1/Akt (Maehama and Dixon, 1999). This is consistent with the observation that losses on chromosome 10, i.e. loss of the *PTEN* locus, are associated with poor outcome in GBM (Chakravarti et al., 2004).

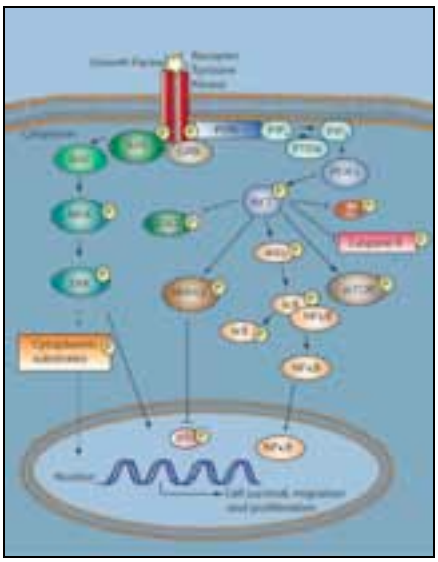

Figure 10. Survival signaling in GBM. Upon ligand binding, or because of constitutive activation, EGFR and PDGFR signal via PI3K-AKT to promote survival by facilitating nuclear translocation of nuclear factor κB (NFκB) which transcriptionally activates multiple genes that mediate cell survival and drive proliferation. In addition, constitutive RTK activation leads to activation of Ras and subsequent initiation of the MAPKs and ERK-1 signaling cascade leading to the activation of cytoplasmic targets that translocate to the nucleus to activate transcription factors involved in cell survival and proliferation. Since PTEN functions as a tumour suppressor that negatively regulates PI3K activity, loss of the *PTEN* locus is associated with poor outcome in GBM. From (Krakstad and Chekenya, 2010)

The PI3K/Akt signaling cascade crosstalks with other signaling pathways, i.e. mTOR and MEK (Fig. 11).

Activated Akt phosphorylates and inactivates tuberous sclerosis 2 (TSC2), a GTPase-activating protein for Ras homologue enriched in brain (RHEB). Inactivation of TSC2 allows RHEB to accumulate in the GTP-bound state and thus activate the serine-threonine kinase mTORC1, a complex of mTOR, Raptor and LST8. mTORC1 phosphorylates p70S6kinase and 4E-binding protein 1 (4E-BP1), 4E-BP2 and 4E-BP3, and leads to translation of mRNAs that encode many cell cycle regulators such as MYC, cyclin D1, hypoxia inducible factor alpha (HIF1α), subsequently leading to proliferation and angiogenesis (Krakstad and Chekenya, 2010).

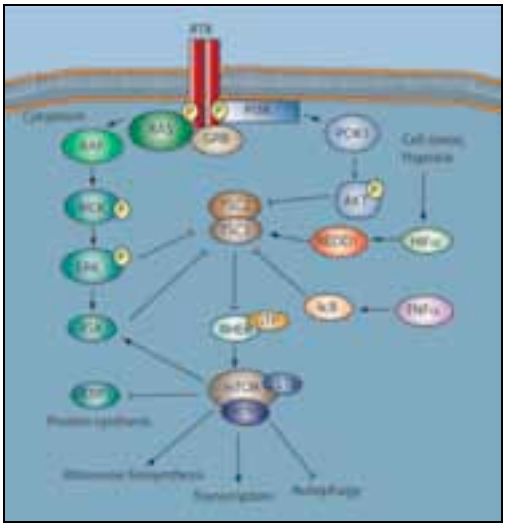

Figure 11. PI3K crosstalks with MEK and mTOR pathways. Activated AKT phosphorylates and inactivates TSC2. RHEB therefore accumulates in the GTP-bound state and activates mTORC1, a complex of mTOR, Raptor and LST8, which indirectly regulates the expression of different proteins involved in survival and proliferation. From (Krakstad and Chekenya, 2010).

The PI3K/Akt signaling cascade crosstalks with the mitogen activated protein-kinase (MAPK) via Ras, a membrane bound G-protein that initiates signaling downstream from activated RTKs. Receptor induced Ras activation is a common feature of GBMs. Constitutive activation of EGFR or PDGFR leads to auto-phosphorylation of intracellular tyrosine residues and activation of Ras via interaction with adaptor proteins. Activation of Ras recruits Raf to the cell membrane and this initiates a signaling cascade downstream via the MAPKs and ERK-1 and 2 kinases, which then activate cytoplasmic targets such as p90RSK, a serine/threonine kinase

that translocates to the nucleus where it activates transcription factors including IκB/NFκB and cyclic AMP response element binding protein (CREB) that regulate glioma cell survival and proliferation, respectively (Fig. 10 and 11).

PI3K/Akt and Ras/ MAPK are thus important cellular survival and growth signaling pathways that are constitutively activated in tumours harbouring mutations in *PTEN* and genetic aberrations in growth factor receptors (Krakstad and Chekenya, 2010).

2.4.3.1 Targeting pro-survival and proliferation signaling in glioblastoma

Two small molecule EGFR tyrosine kinase inhibitors have been developed and evaluated for GBM treatment: erlotinib (Tarceva®, OSI-774, Genentech, Inc, CA, USA) and gefitinib (Iressa®, ZD1839, AstraZeneca, DE, USA). However, monotherapy with neither drug had a clear benefit of prolonged survival. In fact, although EGFR is important for activation of PI3K/Akt, numerous other RTK are co-activated in GBM cells and treatment with single tyrosine kinase inhibitors may not be sufficient to decrease survival signaling (Krakstad and Chekenya, 2010). It has been demonstrated that PDGFR and c-MET receptors are engaged after EGFR inhibition and maintain downstream pathway activation (Stommel et al., 2007). This suggests that carefully designed inhibitor combinations with limited toxicity profiles and maximal additive or synergistic effects may provide more beneficial therapeutic effects.Worthy of note is also that EGFR inhibitors cause G1 cell cycle arrest, making cells less sensitive to the cell cycle dependent effects of radiotherapy and temozolomide, a drug causing cell cycle arrest in G2-M: by preventing cells from progressing beyond G1, erlotinib and gefitinib may therefore compromise the activity of other cell cycle-specific agents (Krakstad and Chekenya, 2010).

Several inhibitors of the PI3K/Akt pathway have been developed, and some are in the early phases of clinical trials. Perifosine (Keryx Biopharmaceuticals, NY, USA), an oral inhibitor of Akt/MAPK that has been demonstrated to effectively reduce tumour growth in a oligodendroglioma mouse model, is currently in a phase II clinical trial on recurrent or progressive malignant glioma (Trial #NCT00590954 http://clinicaltrials.gov) (Momota et al., 2005). In addition, three phase I trials are currently recruiting patients diagnosed with GBM for treatment studies of radio- and/or chemotherapy combined with nelfinavir, a protease inhibitor that interferes with Akt activity downstream of EGFR (Trial #s NCT00915694, NCT01020292, NCT00694837 http://clinicaltrials.gov) (Cuneo et al., 2007).

Several mTOR small molecule inhibitors have been developed, including rapamycin (sirolimus™ or Rapamune®, Wyeth, PA, USA), everolimus™ (RAD001, Norvatis, NJ, USA) and deforolimus™ (AP23573, produced by Ariad Pharmaceuticals, Cambridge, MA, USA). These agents are lipophilic, show good blood brain barrier penetration and have been evaluated in clinical trials for GBM (Krakstad and Chekenya, 2010). mTOR monotherapies are limited by the fact that they only abrogate the mTORC1 complex and not mTORC2, which is involved in tumour cell invasion. In addition, mTORC1 inhibition by rapamycin and its analogues often leads to negative feedback hyperactivation of PI3K/Akt, thus limiting the therapeutic effects (O'Reilly et al., 2006).

Although dual-PI3K-mTOR inhibitors such as PI-103, might mitigate these partial effects, their effect on simultaneous mTORC-1 and -2 inhibition in normal cells is uncertain (Fan et al., 2007). A phase I study is currently recruiting GBM and anaplastic glioma patients to examine the safety, toxicity, and maximum tolerated dose of XL765, dual-PI3K-mTOR capsules administered in combination with temozolomide (Trial # NCT00704080, http://clinicaltrials.gov) (Krakstad and Chekenya, 2010).

Several clinical trials are investigating combination targeting of intracellular effectors in the EGFR and PI3K/Akt pathways in an attempt to both target tumour growth and circumvent possible resistance mechanisms. A preclinical study combining a tyrosine kinase inhibitor, AEE788, (Norvartis Pharma, Basel Switzerland) with everolimus™ demonstrated reduced proliferation, cell cycle arrest and apoptosis *in vitro*, and greater tumour growth inhibition and improved median survival in subcutaneous xenograft models compared to monotherapy (Goudar et al., 2005).

Erlotinib has been combined with the dual-PI3K-mTOR inhibitor, PI-103, and demonstrated efficacy in *PTEN* mutant glioma compared to monotherapy (Fan et al., 2007).

Other combinations include a Raf inhibitor LBT613 (Norvartis, Basel, Switzerland) and everolimus in blocking proliferation and invasion of glioma cell lines (Hjelmeland et al., 2007). A phase I/II clinical trial (# NCT00335764) is currently recruiting recurrent GBM patients for combined Raf and mTOR inhibition with Sorafenib (Nexavar®, Bayer, and Onyx, Emeryville, CA, USA), and temsirolimus (CCI-779), respectively (Krakstad and Chekenya, 2010).

2.4.4 Invasive phenotype of glioblastoma

The highly invasive phenotype of malignant gliomas has been referred as a signature feature of this type of neoplasm which is denoted by diffuse invasion of the brain parenchyma by single cells *trans* corpus callosum to form the characteristic "butterfly" GBM (Demuth and Berens, 2004).

As for the proliferative phenotype, growth factor receptor signaling plays a major role in promoting the invasive phenotype in cooperation with, or in coordination with, cell-adhesion receptors and proteases (Gladson et al., 2010). Multiple growth factor receptors have been shown to promote glioma cell migration and invasion, including c-Met (Lamszus et al., 1998), EGFR (Lund-Johansen et al., 1990), and PDGFR (Assanah et al., 2006). Typically, there is increased expression of both the growth factor receptor and ligand in the tumor, again suggesting that an autocrine or paracrine loop that promotes signaling is in place (Gladson et al., 2010).

Members of several different families of cell-adhesion receptors, including members of the integrin family, the Eph/Ephrin family, and the CD44 family, have been shown to promote glioma cell migration and invasion ((Nakada et al., 2006; Natarajan et al., 2006; Radotra and McCormick, 1997).. In some instances, expression of cell-adhesion receptors, such as integrins, is increased in malignant glioma tumors.

Signaling molecules in the glioma cells act downstream of the cell-surface growth factor receptor and cell-adhesion receptor to amplify and propagate the proinvasion signal. These signaling molecules include cytoplasmic tyrosine kinases, adaptor molecules, and cytoskeletal proteins (Furnari et al., 2007). The Src family tyrosine kinases is necessary for glioma cell invasion (Stettner et al., 2005). Adaptor molecules from the Crk-associated substrate (CAS) family, such as HEF1 and p130CAS, promote glioma invasion, and members of the Crk family of adaptor molecules act downstream of HEF1 or CAS proteins in this process (Natarajan et al., 2006). Two signaling molecules that regulate glioma cell survival and proliferation, phosphatidylinositol-3-kinase (PI3K) and PTEN, also regulate glioma cell migration and invasion. PI3K positively regulates glioma cell migration and invasion. PTEN appears to negatively regulate these processes; thus, the loss of PTEN function in malignant gliomas can promote glioma cell invasion (Tamura et al., 1999).

Glioma cell invasion most likely requires protease degradation of the extracellular matrix.

Several families of proteases, including the serine proteases, cathepsins,

matrix metalloproteinases (MMPs), and the ADAMTS family of metalloproteases have been shown to play a role in glioma cell migration and invasion (Gladson et al., 2010).

2.4.4.1 Invasive phenotype: a challenge for therapy

Invading glioma cells transiently arrest from mitosis (Berens and Giese, 1999) and may thus be refractory from DNA damaging agents such as chemotherapy and radiotherapy. Nevertheless, the morbidity and mortality from GBM stems from local invasion that invariably limits complete surgical resection. Thus, in addition to achieving local control, novel therapies must act on cells disseminated into the normal brain (Krakstad and Chekenya, 2010)

Since cells invading the relatively normal parenchyma are often protected by an intact brain blood barrier, small, uncharged, lipid soluble molecules are favoured as therapeutic agents.

Although GBMs are highly vascular, the brain blood barrier of the gross tumour is variably disrupted, exhibiting breaks in tight junctions, increased pinocytosis, fenestrations, permeability (partially due to upregulated VEGF and aquaporin-4) and decreased pericyte coverage (Rascher et al., 2002). The leaky vessels give rise to stagnant blood flow, oedema, high interstitial fluid pressure gradients that result in capillary and venous collapse that further forms obstacles for drug penetration. Convection enhanced delivery emerged as the drug-delivery method of choice for effective delivery of large and small substances to the brain where the therapeutic agent is infused at high pressure and is dependent on bulk flow (Bobo et al., 1994).

2.4.5 Apoptosis resistance in glioblastoma

The extremely unfavorable prognosis for patients suffering from glioblastoma is strongly correlated to the intrinsic apoptosis resistance of GBM cells, which especially occurs in diffusely migrating tumor cells. The ultimate goal for molecular, apoptosis-based therapies is to target specific components of the two major apoptotic pathways, i.e. the extrinsic and the intrinsic pathway, to trigger tumor-selective apoptosis while, at the same time, limiting toxicity in normal tissues (Kögel et al., 2010).

Apoptosis is a process whereby cells undergo programmed death and is a counterbalance to proliferation. It is morphologically characterized by membrane blebbing, cell shrinkage and chromatin condensation and fragmentation (Leist and Jäättelä, 2001).

The biochemical activation of classical apoptosis occurs through two main pathways: the extrinsic pathway, which originates through the activation of cell-surface death receptors and results in the activation of caspase-8 or -10; and the intrinsic pathway, which originates from mitochondrial release of cytochrome c and associated activation of caspase-9 via binding of adaptor protein apoptotic protease activating factor-1 (Apaf-1) (Fig.12). Both the intrinsic and the extrinsic apoptotic pathways ultimately rely on the activation of caspases for death to ensue. Caspases are cysteine-aspartyl-specific proteases that cleave with remarkable specificity at a small subset of aspartic acid residues. There are two types of apoptotic caspase: initiators and effectors. The initiator caspases (caspase-8, 9 and 10) cleave inactive forms of effector caspases, thereby activating them; effector caspases (for example, caspase-3 and 7) in turn cleave other protein substrates in the cell, resulting in the apoptotic process. Both type of caspase are relatively inactive when first synthesized, but they differ markedly in terms of their activation. Initiator caspases exist as monomers and bind to other proteins by means of the caspase activation and recruitment domain (CARD) in caspase-9 and a death effector domain (DED) in caspase-8 and 10. This protein–protein interaction results in dimerization of the caspases, which leads to their activation. The effector caspases exist as dimers in the cell and are activated by cleavage that produces a tetramer composed by two large and two small subunits. The caspase substrates contribute to the apoptotic phenotype in various ways, such as by activation of proteolytic cascades, inactivation of repair, DNA cleavage, mitochondrial permeabilization and initiation of the process of phagocytosis to clear up the dying cells, apoptotic bodies and debris (Bredesen et al., 2006).

The extrinsic pathway is triggered by ligand binding to receptors of the tumor necrosis factor (TNF) receptor superfamily which consists of 29 transmembrane receptor proteins, organized in homotrimers. The receptors that mediate apoptosis are TNF-R1, FAS and DR4/DR5, and bind TNFα, CD95 and Tumour necrosis factor-related apoptosis-inducing ligand (TRAIL). Binding of death ligands to their agonistic cognate cell surface receptors leads to recruitment of the adaptor proteins FADD (Fas-associated death domain) or TRADD (Tumor necrosis factor receptor type 1-associated death domain), the initiator caspases procaspase-8 and procaspase-10, ensuing formation of a membrane-bound multiprotein complex called DISC (death-inducing signaling complex). DISC formation then leads to auto-proteolytic cleavage of procaspase-8 and -10 (Kögel et al., 2010) (Fig.12).

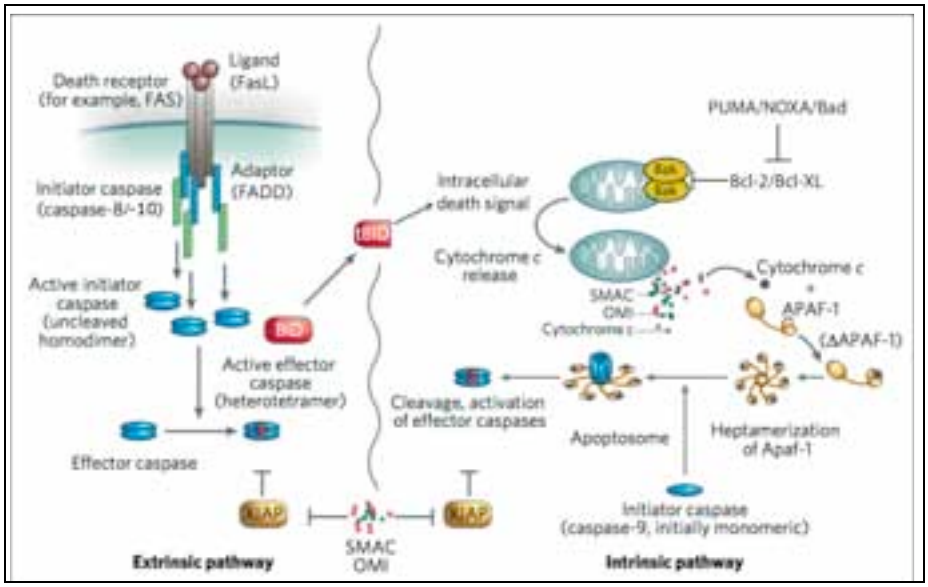

Figure 12 Schematic representation of apoptotic intrinsic and extrinsic pathways. In the extrinsic pathway (left panel) ligand (FasL) binding to receptors of the TNF receptor superfamily (Fas) leads to the recruitment of adaptor proteins (FADD) and initiator pro-caspases-8 or 10, ensuing the formation of the DISC complex and the activation of the pro-caspases by auto-proteolitic cleavage. The extrinsic pathway interacts with the intrinsic pathway via caspase-8 mediated cleavage of Bid to produce tBid (right panel). The propensity of cells to undergo apoptosis, is largely determined by the balance between anti-apoptotic and pro-apoptotic members of the Bcl-2 family: Bax and Bak (BH1–3 proteins), once activated by BH3 only proteins (such as Bim and t-Bid), can permeabilize mitochondrial outer membranes; BH3-only derepressors such as PUMA, NOXA and Bad sequester the anti-apoptotic Bcl-2 and Bcl-xL, freeing up BH1–3 proteins to permeabilize the mitochondria. This causes the release of various pro-apoptotic mitochondrial proteins, such as cytochrome c and SMAC (also known as DIABLO), into the cytosol. After release from the mitochondria, cytochrome c induces conformational change and heptamerization of the cytosolic protein APAF-1. The heptamer binds and activates caspase-9 leading to the activation of effector caspases such as caspase-3 and 7. These active caspases can still be held in check by inhibitor of apoptosis proteins (IAPs) such as XIAP. This IAP-mediated block may be released by proteins such as SMAC and OMI. Adapted from (Bredesen et al., 2006).

The intrinsic pathway is triggered by signals such as DNA damage, oxidative stress or growth factor deprivation. Upon activation by death signals, the pro-apoptotic B-cell lymphoma 2 (Bcl-2) members Bax and Bak undergo conformational changes and insert into the outer mitochondrial membrane to form a channel that allows the

release of cytochrome *c* and other pro-apoptotic factors (Brenner and Mak, 2009) (Fig. 12). In most cell types, Bax is located in the cytoplasm and translocates to mitochondria during apoptosis, while Bak is in its non-active form already associated with mitochondria. Under conditions that favour cell survival, anti-apoptotic Bcl-2 family members, such as Bcl-2 and Bcl-xL bind and inhibit pro-apoptotic Bcl-2 proteins Bax and Bak, thereby inhibiting the intrinsic apoptosis pathway. The expression level of Bcl-2 proteins is controlled by transcriptional activation by several factors, including TP53, and the level of pro- versus anti-apoptotic Bcl-2 proteins plays a critical role in regulating the apoptotic process (Lessene et al., 2008).

Up-regulation of the pro-survival proteins Bcl-2 and Bcl-xL, but down-regulation of Bax has been described in recurrent GBMs independent of treatment. This indicates that untreated GBMs are subjected to pressure for development of apoptosis resistance. Not surprisingly, in a microarray study of GBM biopsies from 20 patient, Ruano *et al* found that several apoptosis related genes were dysregulated. The authors also investigated the significance of expression-levels of the pro-apoptotic protein Bax and found that lower expression of *BAX* correlated with an adverse clinical outcome (Ruano et al., 2008). On the other hand, over-expression of Bcl-2 or Bcl-xL not only leads to resistance to apoptosis but has also been linked to increased tumor cell motility (Wick et al., 1998).

The anti-apoptotic protein Bcl-2L12 has also been reported to be over-expressed in nearly all GBMs (Stegh et al., 2007). Its over-expression leads to disregulation of apoptosis at the post-mitochondrial level through inhibition of caspase activation (Stegh et al., 2008).

Inhibitor-of-apoptosis proteins (IAPs) are endogenous inhibitors of caspase activation that may have evolved to prevent unwanted caspase activation (Fig.12). Members of this family include X-linked inhibitor of apoptosis (XIAP), cellular inhibitor of apoptosis protein 1(cIAP1), cellular inhibitor of apoptosis protein 2 (cIAP2), NRL family, apoptosis inhibiting protein (NAIP), BRUCE and Livin (Deveraux and Reed, 1999). IAPs have a dual function during apoptosis: they are able to directly inhibit initator and executioner caspases by either sequestering their pro-forms or by binding directly to the catalytic site of active caspase subunits. Moreover, due to an E3 ligase activity, IAPs trigger the ubiquitination and proteasomal degradation of active subunits and other pro-apoptotic factors. During apoptosis, two other proteins are released from mitochondria that can neutralize the anti-apoptotic activity of IAPs: the second mitochondria-derived activator of caspase/direct IAP binding protein (Smac/DIABLO) and Omi/HtrA2 (Du et al., 2000) (Fig.12).

All IAPs are highly expressed in most high-grade gliomas and significantly

contribute to the high apoptosis resistance of these neoplasms (Wagenknecht et al., 1999). These include for example XIAP - which is almost absent in CNS cells but shows a significant upregulation in neoplastic glial cells, with a steady increase over the WHO tumor grades (Kögel et al., 2010) - and survivin, which has been described as a prognostic marker for glioma. However, the anti-apoptotic function of survivin is controversial, and its tumor-promoting effects might rather be related to its role in mitosis and proliferation (Zhen et al., 2005).

Highly malignant neoplasms such as the glioblastoma often undergo a metabolic switch and mitochondrial remodeling. The transition from oxidative phosphorylation in mitochondria to cytoplasmic aerobic glycolysis is accompanied by resistance towards apoptotic stimuli (Bonnet et al., 2007). Apoptosis resistance is primarily related to a change in the mitochondrial membrane potential shifting to a hyperpolarization state in malignant tumor cells (Kögel et al., 2010).

2.4.5.1 Therapeutic exploitation of apoptosis for glioblatoma

2.4.5.1.1 Bcl-2 proteins

Bcl-2 family members can contain up to four Bcl-2 homology domains (BH1-4). The anti-apoptotic heterodimerization of Bcl-2/Bcl-xL with Bax/Bak requires a pocket formed by the BH1, BH2, and BH3 regions of Bcl-2/Bcl-xL as well as a central region in Bax/Bak where the BH3 domain is located (Kögel et al., 2010). In apoptotic cells, the transcriptional induction or posttranslational activation of Bcl-2-homology domain-3 (BH3)-only proteins triggers the activation of Bax and Bak. All members of this subgroup of the Bcl-2 family share a nine amino acid BH3-domain, but otherwise possess very little structural homology. Members of this subgroup include Bim, Bid, Bad, PUMA, Noxa, Hrk, and Bmf (Bouillet and Strasser, 2002) (Fig. 13). The role of the individual BH3-only family members is to couple specific upstream stress signals to the intrinsic pathway of apoptosis.

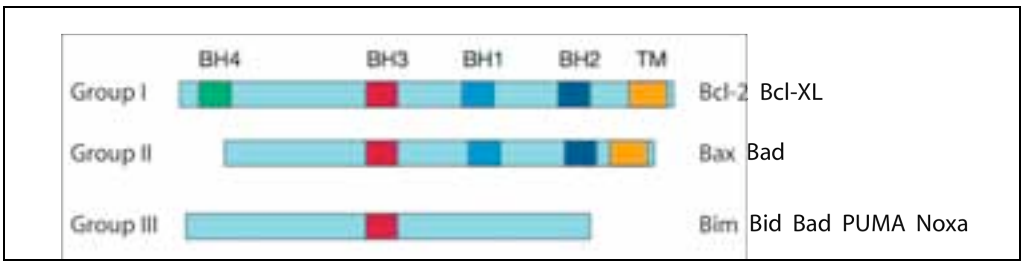

Figure 13. Bcl-2 family members classification. The Bcl-2 family members have been classified into three functional groups. Members of the first group, such as Bcl-2 and Bcl-xL, are characterized by four short, conserved Bcl-2 homology (BH) domains (BH1–BH4). They also possess a C-terminal hydrophobic tail (TM), which localizes the proteins to the outer surface of mitochondria — and occasionally of the endoplasmic reticulum — with the bulk of the protein facing the cytosol. The key feature of group I members is that they all possess anti-apoptotic activity, and protect cells from death. In contrast, group II consists of Bcl-2 family members with pro-apoptotic activity. Members of this group, which includes Bax and Bak, have a similar overall structure to group I proteins, but lack the BH4 domain. Group III consists of a large and diverse collection of proteins whose only common feature is the presence of the ~12–16-amino-acid BH3 domain. Adapted from (Hengartner, 2000)

There are two competing models for activation of Bak and Bax by BH3-only proteins (Green, 2006). In the direct activation model, BH3-only proteins termed activators (Bid, Bim) directly bind to and activate Bax and Bak. In the indirect activation model, BH3-only proteins described as sensitizers (Noxa, PUMA, Hrk, Bmf) bind to prosurvival Bcl-2 family members, thereby displacing them from Bax and Bak to trigger mitochondrial outer membrane permeability. BH3 domains bind to a hydrophobic groove of anti-apoptotic Bcl-2 family members that comprises residues of their BH1, BH2 and BH3 domains. This observation lay the foundation for the development of BH3 mimetics, a class of small-molecule inhibitors targeting the BH3-binding domain of pro-survival Bcl-2 family members (Kang and Reynolds, 2009).

There are several synthetic BH3 mimetics with different binding profiles to the major four pro-survival Bcl-2 family members (Bcl-2, Bcl-xL, myeloid cell leukemia-1 [Mcl-1], Bcl2-like-2 [Bcl-w]). Most BH3 mimetics target Bcl-2 and/or Bcl-xL. ABT-737 and its orally applicable derivative ABT-263 target Bcl-2, Bcl-xL and Bcl-w with high affinity, but not Mcl-1. Obatoclax (GX15-070, Geminx) is a pan-Bcl-2 inhibitor targeting Bcl-2, Bcl-xL, Mcl-1 and Bcl-w (Chonghaile and Letai, 2008). In contrast to the BH3 mimetics functioning as sensitizers (ABT-737/ABT-263, Obatoclax), BH3 mimetics that directly activate Bax and Bak are in the early stages of preclinical development. ABT-263 is currently evaluated in phase I/II trials for lymphoma, chronic lymphocytic leukemia and small cell lung cancer, but not yet for

gliomas (Tse et al., 2008).

Despite the partially redundant functions of Bcl-2-like proteins, there is also evidence that specific inhibition of Bcl-2 may alone be sufficient to sensitize various types of cancers to chemotherapy. Oblimersen (Genasense), a phosphorothioated Bcl-2 antisense oligonucleotide has been extensively studied in clinical trials, none of which investigated its impact on glioma. In a recent phase III study, Oblimersen combined with fludarabine/cyclophosphamide was shown to prolong survival of a subset of patients with refractory or relapsed chronic lymphocytic leukemia (CLL) (O'Brien et al., 2009).

Another alternative way to selectively target members of the Bcl-2 family is via the induction of an endoplasmic reticulum stress response. This can be achieved by a cytokine of the IL-10 family namely the melanoma differentiation-associated gene-7/interleukin-24 (mda-7/IL-24). The endoplasmic reticulum stress response leads to a translational inhibition of the antiapoptotic protein Mcl-1. Decreased Mcl-1 expression causes apoptosis via an oligomerization of the pro-apoptotic Bak protein (Dash et al., 2010). Currently, mda-7 is given via the recombinant adenovirus Ad.mda-7 and already entered clinical phase II studies for solid cancers but not yet for gliomas (Dent et al., 2008). Probably, first clinical Ad.mda-7 trials for glioma will also start soon since preclinical data are very promising displaying a prolonged survival of Ad.mda-7 treated glioma-bearing animals without showing considerable side effects (Yacoub et al., 2008).

2.4.5.1.2 Triggering apoptosis via activation of death receptors

Activation of death receptor signaling by TRAIL or by agonistic antibodies against TRAIL receptors DR4 and DR5 has been extensively studied in preclinical models as a strategy to trigger apoptosis in glioma (Kögel et al., 2010). TRAIL receptors have been shown to be expressed in glioma cell lines as well as in primary patient tumor samples. Interestingly, TRAIL is capable to induce apoptosis in many tumor cells, but not in normal tissue. This tumor-selective effects of TRAIL could also be observed in glioma cells in comparison to non-transformed astrocytes *in vitro* (Hao et al., 2001).

Despite the considerable interest raised by the therapeutic potential of TRAIL, accumulating evidence suggests that TRAIL alone may not be sufficient to efficiently activate apoptosis in many cases. Hence, a lot of effort has been put forward to establish new modalities for combined treatments with TRAIL and other

antineoplastic agents or apoptosis inducers to improve the impact of TRAIL-based therapies. A considerable proportion of neoplastic glial cells displaying resistance against TRAIL can regain TRAIL sensitivity by inhibition of protein kinase C (PKC) (Hao et al., 2001). Synergistic effects of TRAIL have also been described for temozolomide (TMZ), Akt inhibitors, proteasome inhibitors, histone deacetylase inhibitors (HDAC), mammalian target of rapamycin (mTOR) inhibitors, Bcl-2 inhibitors and IAP inhibitors (Hetschko et al., 2008; Puduvalli et al., 2005; Saito et al., 2004; Sonnemann et al., 2006). In addition, some chemotherapeutic drugs (e.g. the aureolic acid-type polyketide Mithramycin A) which act synergistically with TRAIL not only reduce XIAP levels or increase sensitivity of tumor cells to TRAIL but also exert significant anti-migratory effects in preclinical studies (Seznec et al., 2010). Mithramycin A inhibits the binding of Sp1 to its promoters leading to a down-regulation of XIAP expression (Lee et al., 2006). The reduction of the migratory potential of glioma cells after Mithramycin administration is still not fully understood, however a marked reduction of both MMP-2 and -9 protein expression and activity might be responsible for this purpose (Seznec et al., 2010). The bimodal effect of Mithramycin A is important since migrating neoplastic glial cells are highly resistant to apoptotic stimuli.

2.4.5.1.3 Targeting inhibitors of apoptosis

Smac is an endogenous antagonist of IAPs that is released from the mitochondria after mitochondrial outer membrane permeabilization, and counteracts inhibition of the caspase cascade on the post-mitochondrial level. Smac interacts with XIAP and other IAPs via its N-terminal tetrapeptide. Smac mimetics are promising new drugs for cancer therapy. Smac peptides are capable to sensitize malignant glioma cells to TRAIL-induced apoptosis *in vitro* and *in vivo*, thereby confirming the pivotal role of IAPs for apoptosis resistance of gliomas (Fulda et al., 2002).

A large number of small-molecule IAP inhibitors are in preclinical evaluation. Currently, there are several ongoing phase I clinical studies with small molecule Smac mimetics in adults with refractory advances malignancies, e.g. with TL32711 (TetraLogic Pharmaceuticals), AT-406 (Ascenta Therapeutics), GDC-0152 (Genentech) or LCL161 (Novartis). Furthermore, the XIAP antisense oligonucleotide AEG35156 to down-regulate XIAP is in phase I/II clinical trial development. Recently, AEG35156 was shown to knockdown its target and to exert antileukemic activity when combined with chemotherapy in patients with Acute myeloid leukemia refractory to a single induction regimen (Schimmer et al., 2009).

2.4.5.1.4 Modulators of mitochondria-related apoptosis

Malignant glioma often undergo a mitochondrial metabolic switch from oxidative phosphorylation to cytoplasmic aerobic glycolysis which is accompanied by resistance towards apoptotic stimuli.

There are drugs available (e.g. dichloroacetate [DCA]) being able to change cellular metabolism from glycolysis to glucose oxidation via inhibition of the mitochondrial pyruvate dehydrogenase kinase (PDK) and at the same time decreasing the mitochondrial membrane potentials. In preclinical studies, DCA induced selective tumor cell apoptosis without considerable side effects such as cytotoxicity (Bonnet et al., 2007). It quickly entered clinical trials of which the first phase II study has been currently completed. Although reliable clinical data about cancer patient out-come after DCA treatment is still lacking, single reports about severe DCA side effects are already available mainly including encephalopathy and polyneuropathy (Brandsma et al., 2010).

A very recent approach to induce apoptosis in glioma cells could be achieved by two new growth hormone-releasing hormone (GHRH) antagonists namely JMR-132 and MIA-602 (Pozsgai et al., 2010). Glioblastoma cells treated with GHRH antagonists responded by a nuclear translocation of apoptosis inducing factor (AIF) and endonuclease G (Endo G) as well as the mitochondrial release of cytochrome c. These cell culture findings were corroborated in a xenograft nude mice model displaying significantly longer survival times in the animal group treated by GHRH antagonists (Kögel et al., 2010).

2.5 Autophagy: the Trojan horse to combat glioblastoma

Induction of autophagic cell death (type II programmed cell death) by pro-autophagic drugs is an alternative and emerging strategy to trigger glioma cell death and to sensitize cancer cells to therapy (Kögel et al., 2010).

Autophagy, a process normally involved in the regulated turnover of long-lived proteins and damaged organelles, is a form of cellular self digestion in which cellular constituents are engulfed in double-membrane containing vesicles (autophagosomes), and subsequently digested by lysosomal proteases after fusion of autophagosomes with lysosomes (He and Klionsky, 2009) (Fig. 14). It is a complex, multistep process which is genetically regulated by the ~ 20 Atg genes.

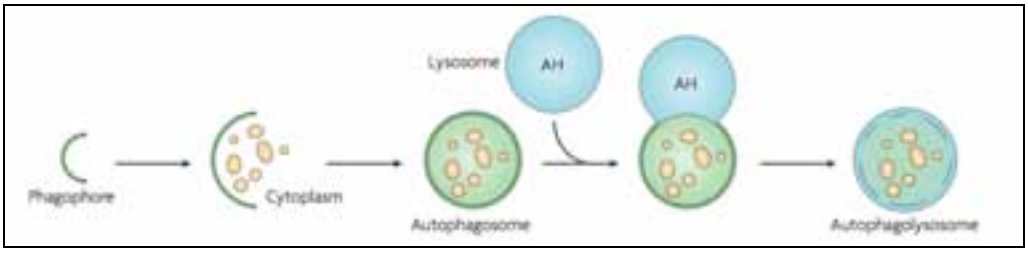

Figure 14. Schematic overview of macroautophagy. A membrane of unknown origin forms the initial phagophore or isolation membrane. The phagophore expands sequestering cytoplasm and, on completion, forms a double-membrane autophagosome. The autophagosome fuses with a lysosome thus forming the autophagolysosome (or autolysosome) where sequestered cellular components are degraded by lysosomial acid hydrolases. Following breakdown, the resulting macromolecules are released back into the cytosol through permeases for reuse in metabolic processes (during starvation). Alternatively, excessive autophagy might result in cell death. AH: acid hydrolases. From (Rubinsztein et al., 2007).

The net effect of autophagy on cell death is highly contextual: under conditions of nutrient deprivation, autophagy may constitute a primordial pro-survival stress response serving to ensure energy balance; at the same time there is also significant evidence that enforced over-activation of autophagy can lead to type II programmed cell death consisting in a massive cellular self digestion via the autophagosomal-lysosomal pathway beyond the point allowing cell survival (Gozuacik and Kimchi, 2007). Autophagy therefore represents a homeostatic cellular process which can exert both cytoprotective and death promoting effects.

Given the fact that disrupted autophagy and excess of autophagy both have detrimental consequences on cell viability, complete abrogation as well as over-activation of the autophagy pathway may represent relevant strategies for cancer therapy. Evidence from several preclinical models suggests that inhibition of autophagy can sensitize glioma cells to therapy, e.g. radiation (Lomonaco et al., 2009). In addition, in light of the high apoptosis resistance of malignant gliomas, induction of autophagic cell death by autophagy stimulators is an alternative and emerging concept to trigger glioma cell death and to exploit caspase-independent programmed cell death pathways for the development of novel glioma therapies (Lefranc et al., 2007).

2.5.1 The autophagic pathway, an overview

Autophagy is an intracellular catabolic system in which cytoplasmic components are delivered into lysosomes for degradation. Three different autophagic pathways are known: macroautophagy (hereafter referred to as autophagy), microautophagy, and chaperone-mediated autophagy (CMA) (Fig. 15). In macroautophagy, a double-membraned structure (called phagophore) elongates engulfing a portion of cytoplasm, and then fuses to form a vesicle called "autophagosome". Autophagosomes fuse with lysosomes, thereby forming autolysosomes, where the cytosolic contents are degraded by lysosomal hydrolases. In microautophagy, a portion of cytoplasm is directly engulfed into lysosomes by invagination of the lysosomal membrane. Finally, CMA involves the selective transport of cytosolic proteins containing the KFERQ pentapeptide motif across the lysosomal membrane via the chaperone hsc70 and the lysosomal membrane receptor LAMP-2A (García-Arencibia et al., 2010).

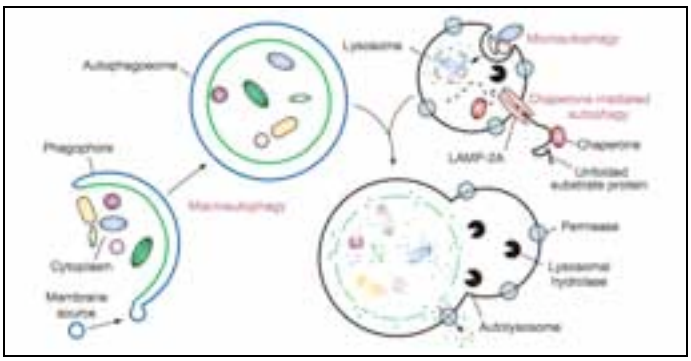

Figure 15. Different types of autophagy. Microautophagy refers to the sequestration of cytosolic components directly by lysosomes through invaginations in their limiting membrane. In macroautophagy, the cargoes are sequestered within an autophagosome which is formed by expansion of the phagophore. Fusion of the autophagosome with a lysosome leads to the lysis of the autophagosome inner membrane and contents. CMA involves direct translocation of unfolded substrate proteins across the lysosome membrane through the action of a cytosolic and lysosomal chaperone hsc70, and the integral membrane receptor LAMP-2A (lysosome-associated membrane protein type 2A). From (Mizushima et al., 2008).

Our understanding of the molecular machinery of autophagy started with the identification of the autophagy-related (*ATG*) genes in *Saccharomyces cerevisiae*. To date, more than 30 different *ATG* genes have been identified in yeast (Suzuki and Ohsumi, 2007) and many of them have mammalian orthologues.

Autophagosome formation occurs at the phagophore assembly-site(s) (PAS). The activity of Vps34, a class III phosphatidylinositol-3-kinase (PI3K), is necessary for the formation of new autophagosomes. Vps34 generates phosphatidylinositol-3-phosphate (PIP_3) at the PAS, which allows the recruitment of other Atg proteins. Vps34 is part of the autophagy-regulating macromolecular complex (PI3K complex), which contains Beclin-1/Atg6, Atg14/barkor and p150/Vps15, among other proteins (Itakura et al., 2008) (Fig. 16). The activity of Vps34 is enhanced by its binding to Beclin-1. Positive regulators of Beclin-1function include AMBRA1, UVRAG and Bif-1, whereas its negative regulators include the anti-apoptotic proteins Bcl-2 and Bcl-xL (Sinha and Levine, 2008). The other protein complex involved in the initiation of autophagosome formation is the ULK1/Atg1–Atg13–FIP200/Atg17–Atg101 complex (Mizushima, 2010) (Fig. 16). This complex plays an important role in both the recruitment of Atg proteins and the subsequent autophagosome synthesis.

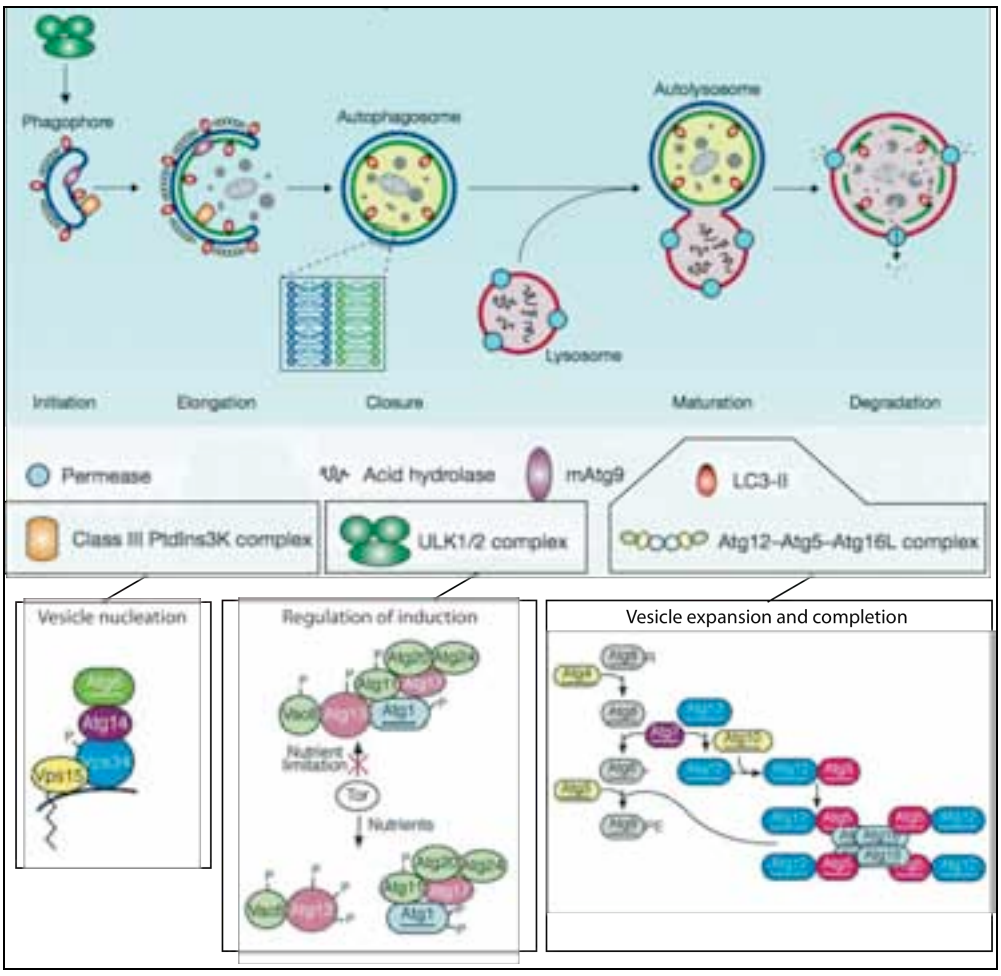

Figure 16 Schematic depiction of autophagy core molecular machinery. Mammalian autophagy is initiated by the formation of the phagophore, followed by a series of steps, including the elongation and expansion of the phagophore, closure and completion of a double-membrane autophagosome, autophagosome maturation through docking and fusion with a lysosome, breakdown and degradation of the autophagosome inner membrane and cargo through acid hydrolases inside the autolysosome, and recycling of the resulting macromolecules through permeases. The core molecular machinery is depicted: ULK1 complex is required for autophagy induction; class III PtdIns3K complexes are involved in vesicle nucleation; LC3-II and Atg12–Atg5–Atg16L complex are proposed to function during elongation and expansion of the phagophore membrane; mammalian Atg9 (mAtg9) potentially contributes to the delivery of membrane to the forming autophagosome. Adapted from (Yang and Klionsky, 2010) and (Levine and Klionsky, 2004)

Two ubiquitin-like conjugation systems are involved in the elongation and expansion of the phagophore membrane. In the first conjugation event, Atg12 is conjugated to Atg5 in a reaction that requires Atg7 (E1-like) and Atg10 (E2-like). The Atg12–Atg5 conjugate interacts non-covalently with Atg16L, which oligomerizes to form an 800-kDa complex necessary for autophagosome formation (García-Arencibia et al., 2010) (Fig.16).

The second ubiquitination-like reaction involves the conjugation of microtubule-associated protein 1 light chain 3 (MAP1-LC3/LC3/Atg8) to the lipid phosphatidylethanolamine (PE). LC3 is cleaved at its C-terminus by Atg4 to form the cytosolic LC3-I, which is conjugated with PE through the action of Atg7 (E1-like) and Atg3 (E2-like) to generate LC3-II (Tanida et al., 2004b) (Fig. 16). LC3-II is the most widely used marker to study autophagy, as it is the only known protein that specifically associates with autophagosomes and not with other vesicular structures. LC3-II is bound to both sides of the membrane, and remains membrane bound even after fusion with lysosomes, after which LC3-II on the cytosolic face of autophagosomes can be recycled to LC3-I byAtg4 (Tanida et al., 2004a), while the LC3-II on the inner face of the membrane is degraded.

Mammalian autophagosomes form randomly in the cytoplasm. They are then trafficked along microtubules in a dynein-dependent manner to lysosomes, which are clustered around the microtubule- organizing center (MTOC) located near the nucleus (Jahreiss et al., 2008). The details of the autophagosome–lysosome fusion in mammalian autophagy are still unclear, although it is thought that the fusion step involve proteins such as ESCRT, SNAREs, Rab7, UVRAG, LAMP-2 and the class C Vps proteins (Noda et al., 2009; Rusten et al., 2007).

The mammalian target of rapamycin (mTOR) kinase is a master negative regulator of autophagy (Fig. 17). It is a central sensor of energy status, growth factors and nutrient signals: under nutrient-rich conditions, mTOR suppresses autophagy through direct interaction with the ULK1-Atg13–FIP200 complex and mediates phosphorylation-dependent inhibition of the kinase activity of Atg13 and ULK1; under starvation conditions or rapamycin treatment, mTOR mediated phosphorylation of Atg13 and ULK1 is inhibited. This leads to dephosphorylation-dependent activation of ULK1 and ULK1-mediated phosphorylations of Atg13, FIP200, and ULK1 itself, which trigger autophagy (Mizushima, 2010).

As already described in 2.4.3, a major signaling cascade regulating mTOR activity is the PI3K pathway. The binding of growth factors or insulin to cell surface receptors activates the class IA PI3K. Activated PI3K catalyzes the production of phosphatidylinositol-3,4,5-triphosphate (PIP_3) at the plasma membrane which

increases the membrane recruitment of Akt and its activator PDK1, leading to the activation of Akt. The phosphorylation-dependent Akt activation results in the phosphorylation of other proteins, including the tuberous sclerosis complex1/2 (TSC1/TSC2). Phosphorylation of TSC2 by Akt, ERK, or RSK, all kinases stimulated by growth factors, leads to the disruption of the heterodimer with TSC1, resulting in loss of TSC1/TSC2 activity. Since TSC1/TSC2 acts as a GTPase-activating protein (GAP) that enhances the hydrolysis of GTP to GDP in Rheb, a Ras-family GTP binding protein which directly binds and activates mTOR, loss of TSC1/TSC2 activity allows Rheb to accumulate in the GTP-bound state and results in mTOR activation (Manning and Cantley, 2003) (Fig.17).

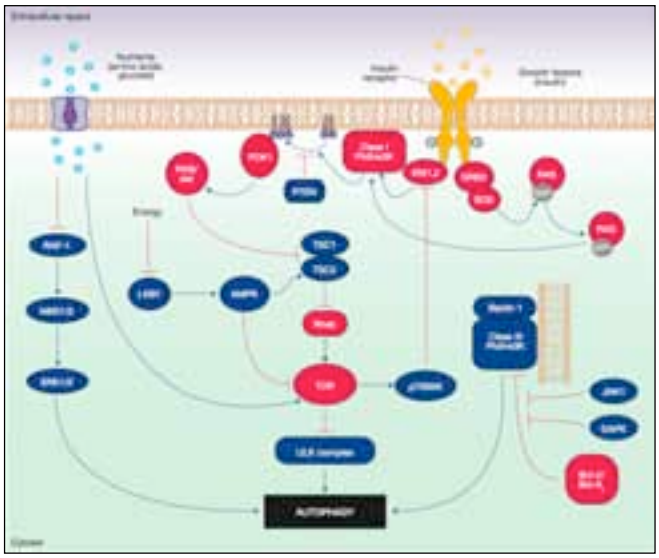

Figure 17. Signaling regulation of mammalian autophagy. Blue components represent factors that stimulate autophagy, the red ones correspond to inhibitory factors. Autophagy is regulated by a complex signalling network of various stimulatory (blue arrows) and inhibitory (red bars) inputs. mTOR plays a central role in autophagy by integrating the class I PI3K signalling and amino acid-dependent signalling pathways. Activation of insulin receptors stimulates the class I PI3K complex leading to activation of the PI3K–Akt–mTOR pathway. Amino acids inhibit the Raf-1–MEK1/2–ERK1/2 signalling cascade, leading to inhibition of autophagy. Energy depletion causes the AMP-activated protein kinase (AMPK) to be phosphorylated and activated by LKB1. AMPK phosphorylates and activates TSC1–TSC2, leading to inactivation of mTOR and autophagy induction. p70S6K kinase is a substrate of mTOR that may negatively feed back on mTOR activity, ensuring basal levels of autophagy that are important for homeostasis. JNK1 and DAPK phosphorylate and disrupt the association of anti-apoptotic proteins, Bcl-2 and Bcl-xL, with Beclin-1, leading to the activation of the Beclin-1-associated class III PI3K complex and stimulation of autophagy. From (Yang and Klionsky, 2010)

mTOR can also act as a sensor of changes in cellular energy states via AMPK: AMPK is activated under energy depletion conditions by high AMP/ATP ratios, and activates the TSC1/TSC2 complex leading to inactivation of mTOR and induction of autophagy (Inoki et al., 2006) (Fig. 17).

Recently, further insights have been provided into the mechanisms behind starvation-induced autophagy. Autophagy can be inhibited by the binding of the apoptosis-related proteins Bcl-2 or Bcl-xL to Beclin-1. Starvation induces Jun N-terminal kinase1 (Jnk1) activity, which phosphorylates Bcl-2, thereby disrupting the interaction between Beclin-1 and Bcl-2 to induce autophagy (Wei et al., 2008).

2.5.2 Autophagy as a tumor suppressor mechanism

Cancer is one of the first diseases genetically linked to autophagy malfunction (Levine and Kroemer, 2008). Cancer cells often display a reduced autophagic capacity compared to their normal counterparts: lower Beclin-1 protein expression, as compared to normal adjacent breast tissue, was confirmed in a small series of human breast tumors (Liang et al., 1999); in glioma, expression levels of Beclin-1 were reported to be inversely proportional to the tumor grade and to correlate with enhanced survival of GBM patients (Miracco et al., 2007); reduced expression of the Beclin-1 gene (*BECN1*) has been reported in human colon cancer (Koneri et al., 2007), hepatocellular carcinomas (Daniel et al., 2007), and cervical cancers (Wang et al., 2006); finally, *BECN1* is monoallelically deleted in 40–75% of cases of human breast, ovarian, and prostate cancer.

While heterozygous disruption of *BECN1* promotes tumorigenesis (Qu et al., 2003), its over-expression inhibits tumor development (Liang et al., 1999). Inhibition of autophagy in mice by heterozygous disruption of *Becn1*, increases cellular proliferation, the frequency of spontaneous malignancies (i.e., lung cancer, liver cancer, and lymphomas) and accelerates the development of carcinogen (i.e., hepatitis B virus)-induced premalignant lesions (Yue et al., 2003). Furthermore, immortalized kidney and mammary epithelial cells derived from *Becn1* heterozygous-deficient mice are more tumorigenic when transplanted *in vivo*. On the contrary, transfection of MCF-7 breast cancer cells, that express low levels of Beclin-1, with the *BECN1* gene, inhibits growth and tumor formation (Liang et al., 1999). Overall these data suggest that Beclin-1 is a haploinsufficient tumor suppressor and that a defective autophagic process is clearly linked to cancer development. Induction of autophagy may therefore help to reverse the malignant phenotype.

The mechanisms by which autophagy functions in tumour suppression remain largely undetermined. Autophagy may directly regulate cell growth, functioning as a brake to prevent cells from inappropriately dividing in the absence of appropriate trophic support (Levine and Kroemer, 2008). An additional characteristic of autophagy in tumor-suppression is the maintenance of genome integrity. Under metabolic stress, impairment of the autophagic machinery has been reported to result in genomic instability with DNA double-strand breaks, centrosome abnormalities, and increased DNA content. Gene amplification is the major mechanism of oncogene activation in cellular transformation. Enhanced chromosomal instability and gene amplification was observed in *BECN1* heterozygote cells over-expressing Bcl-2 (Mathew et al., 2007). The increased gene amplification and mutation rates enables these cells to overcome the loss of autophagy-mediated survival under metabolic stress. Similar findings were also demonstrated *in vivo* where autophagy was induced in metabolically-stressed regions of mice tumors. Allelic loss of *Becn1* resulted in enhanced genomic damage in these mice (Karantza-Wadsworth et al., 2007). Genome integrity might be maintained via autophagy-mediated elimination of damaged organelles and proteins. Depolarized mitochondria are a source for genotoxic free radicals. In the absence of autophagy as a scavenger mechanism, DNA mutations accumulate readily and may lead to cellular transformation (Eisenberg-Lerner and Kimchi, 2009).

2.5.3 Autophagy as a type-II programmed cell death mechanism

Autophagy may function as a programmed cell death-type II in cancer cells in which apoptosis is defective or hard to induce. It has been shown that apoptosis defective cells can undergo autophagy after exposure to cytotoxic signals: *BAX*$^{-/-}$ and *BAK*$^{-/-}$ knockout fibroblast cells are resistant to apoptosis and undergo autophagic cell death following starvation, growth factor withdrawal, chemotherapy (etoposide) or radiation (Shimizu et al., 2004; Xue et al., 1999). In addition, suppressing autophagy by pharmacological (e.g., 3-MA) and genetic (silencing of *ATG5*, *ATG7* and *BECN1*) approaches in apoptosis defective cancer cells, leads to a marked reduction in autophagic cell death in response to cell death stimuli with no sign of apoptosis (Dalby et al., 2010).

It is therefore reasonable to propose that induction of autophagic cell death may be used as a therapeutic strategy to treat cancer.

2.5.4 Targeting autophagy for glioma therapy

Constitutive PI3K pathway activation via EGFR-signaling and loss of function of the PI3K-antagonist PTEN, are an established hallmarks of glioblastoma leading to activation of mTOR, a serine/threonine kinase over-activated in many cancers and having multiple cellular functions: besides its role in proliferation and cell motility, it can suppress both apoptosis and autophagy (Castedo et al., 2002) (see 2.4.2-3).

mTOR is a major endogenous negative regulator of autophagy and the disassembly of the two major mTOR complexes TORC1 (containing mTOR, Raptor and mLST8) and TORC2 (containing mTOR, Rictor, mLST8, and mSin1) has been implicated in activation of autophagy, although the role of TORC2 is much less well understood in this context.

There is a large number of preclinical and clinical drugs that target mTOR and its upstream activator Akt (see 2.4.3.1). Rapamycin and its analogues (Temsirolimus/CCI-779, Everolimus/RAD001, and AP23573) inhibit TORC1 by binding the FRB (FKBP12/rapamycin-binding) domain in complex with mTOR intracellular receptor protein FKBP12 (Breuleux et al., 2009). In contrast to TORC1, the TORC2 complex is rapamycin-insensitive (Loewith et al., 2002). Inhibition of autophagy by small interfering RNA (siRNA) directed against the autophagy-related gene *BECN1,* attenuates the cytotoxicity of rapamycin in rapamycin-sensitive tumor cells, indicating that autophagy is a primary mediator of rapamycin-mediated antitumor effects rather than a protective response. Exogenous expression of an mTOR mutant lacking kinase activity, markedly enhances the incidence of rapamycin-induced autophagy. Moreover, siRNA mediated silencing of mTOR increases the inhibitory effect of rapamycin on tumor cell viability by stimulating autophagy. Importantly, not only rapamycin-sensitive, but also rapamycin-resistant malignant glioma cells with wild-type *PTEN* are sensitized to rapamycin by mTOR siRNA (Iwamaru et al., 2007). In addition, mTOR inhibitors sensitize tumor cells to DNA-damaging agents *in vitro*. Phase I and II clinical trials with mTOR inhibitors are ongoing in patients with recurrent malignant gliomas, advanced solid tumors, advanced non-small cell lung carcinoma, endometrial cancer, metastatic breast cancer, prostate cancer, and metastatic renal carcinoma (Bjornsti and Houghton, 2004; Reardon et al., 2006).

In contrast to the inhibitory effect of class I PI3K on autophagy, the class III PI3K Vps34, in complex with Beclin-1, Atg14 and p150, is required in the early stages of autophagosome formation. Recent findings show that the activity of this

autophagy activating complex is regulated by anti-apoptotic Bcl-2 family members. Indeed, Bcl-2 and Bcl-xL can bind Beclin-1 to its BH3 domain thus preventing it from forming the multiprotein complex with Vps34, Atg14 and p150 essential for vesicle nucleation during the early steps of the autophagic process, thereby inhibiting autophagy (Maiuri et al., 2007; Pattingre et al., 2005).

Consequently, BH3 mimetics are capable to activate both apoptosis and autophagy. Gossypol is a natural polyphenolic compound and BH3 mimetic derived from cottonseeds, which possesses pro-apoptotic effects in various *in vivo* and *in vitro* models. Similiar to Obatoclax (see 2.4.5.1.1), Gossypol acts as a pan-Bcl-2 inhibitor and can inactivate Bcl-2, Bcl-xL, Mcl-1 and Bcl-w. There are two enantiomers of gossypol, (+)-gossypol and (-)-gossypol, the latter being more potent as an inhibitor of tumor growth. (-)-gossypol (AT-101, Ascenta) has shown single-agent activity in various types of cancer and its potential impact for glioma therapy is currently investigated in phase I/phase II clinical trials. In cancer cells with an intact apoptotic machinery, (-)-gossypol has been reported to induce apoptotic cell death (Meng et al., 2008; Wolter et al., 2006). In contrast, cell death triggered by Gossypol largely seems to depend on induction of autophagic cell death in malignant glioma (Voss et al., 2010).

In addition to BH3 mimetics, there is a plethora of other stimuli that can trigger autophagy and may be exploited for glioma therapy.

A variety of chemical or physical treatments, including radiation (Paglin et al., 2001), arsenic trioxide (Kanzawa et al., 2005), ceramide (Daido et al., 2004), temozolomide (Kanzawa et al., 2004), tetrahydrocannabinol (THC) and resveratrol (Opipari et al., 2004), have been reported to induce autophagy in glioma cells.

There are several ongoing clinical trials investigating arsenic trioxide in combination with radiation and temozolomide (TMZ) in patients with newly diagnosed or recurrent GBM. Although being one of the first chemotherapeutic drugs used for the treatment of cancer patients, arsenic trioxide experiences a resurrection also in glioma treatment. Beside the activation of autophagy in neoplastic cells, arsenic trioxide was suggested to trigger late activation of executioner caspases caspase-3 and caspase-7, pointing to a bimodal interaction between autophagy and apoptosis (Pucer et al., 2010).

The alkylating agent Temozolomide leads to formation of O6-methylguanine in DNA, which mispairs with thymine during the following cycle of DNA replication and increases survival in patients with MGMT-negative tumors. The role of autophagy in TMZ-induced glioma cell death is currently controversial. On the one hand, there is

data suggesting that the therapeutic activity of TMZ seems to be exerted through activation of autophagy and induction of autophagic cell death (Kanzawa et al., 2004). One the other hand, it was also suggested that TMZ-induced autophagy represents a pro-survival response and TMZ may trigger late apoptosis in glioma cells (Katayama et al., 2007).

2.5.5 Pros and Cons of therapeutically targeting autophagy

The physiological function of autophagy is related to the maintenance of cellular homeostasis under cellular stress. Autophagy can be utilized as a survival mechanism in the harsh tumor microenvironment and as a protective mechanism against cancer therapies, such as radiation therapy, chemotherapy and targeted therapies (e.g., Imatinib). In these contests, inhibition of protective autophagy may break the resistance mechanism for survival and enhance efficacy of anticancer therapies leading to cell death.

On the other hand, those cancer cells that are resistant to apoptosis-inducing therapies (for exaple gliomas) can be killed by agents that induce massive autophagic response leading to programmed cell death type II. This approach may be highly useful for specifically advanced cancer and therapy-resistant cancers (Dalby et al., 2010).

In summary, autophagy possesses both tumor-promoting and tumor-suppressive properties. It is the specific intra- and extra-cellular context that determines in which cell fate induction of autophagy will culminate. Exploitation of autophagy for anti-cancerous purposes should take into account such variables including the stage in tumorigenesis, the integrity of the apoptotic machinery in the tumor, and the consequences of a necrotic inflammatory response (Eisenberg-Lerner and Kimchi, 2009).

.

3. Aims of the research

The principal aim of this work is to investigate whether the cellular prion protein (PrPC) exerts a cytoprotective function in glial tumor cells thus contributing to their resistance to cell death.

Although a great deal is known about the role of the pathogenic isoform of the cellular prion protein (PrPSc) in the etiology of a group of transmissible spongiform encephalopathies (prion diseases), several years after the generation of the first *Prnp* knockout mouse (Büeler et al., 1992) the normal function of PrPC is still elusive. A variety of functions have been proposed for mammalian PrPC, including involvement in cell death and survival, oxidative stress, immunomodulation, differentiation, metal ion trafficking, cell adhesion, and transmembrane signaling (Linden et al., 2008) (see 2.1.5 and 2.2).

Several intriguing lines of evidence have recently emerged indicating that PrPC may function to protect cells from various kinds of internal or environmental stresses: PrPC over-expression rescues not only cultured neurons (Kuwahara et al., 1999) but also tumor cell lines from pro-apoptotic stimuli, including Bax expression, serum withdrawal, DNA damage, cytokine and anti-cancer drug treatment (Roucou and LeBlanc, 2005; Senator et al., 2004). In addition, a possible role for PrPC in the acquisition of resistance to cell death by tumor cells has been demonstrated in breast and gastric cancer (Diarra-Mehrpour et al., 2004; Du et al., 2005). To this regard worthy of note is the fact that the cellular prion protein, or its unglycosylated form Pro-PrPC, have been found to be ectopically expressed in colorectal carcinoma (Antonacopoulou et al., 2010), pancreatic ductal adenocarcinoma (Li et al., 2009) and melanoma (Li et al., 2010) (see 2.3).

One of the most important advances in our understanding of cancer biology during the past decade has been the recognition that resistance to cell death, particularly to apoptotic cell death, is an important aspect of both tumorigenesis and development of resistance to drugs used to treat cancer (Green and Evan, 2002; Hanahan and Weinberg, 2000). Much recent research on new cancer therapies has therefore focused on devising ways to overcome this resistance and to trigger the death of tumor cells (Mehrpour and Codogno, 2010).

Malignant gliomas, including glioblastomas and anaplastic astrocytomas, are the most common primary brain tumors (Argyriou and Kalofonos, 2009) and are

characterized by resistance to apoptosis and high proliferation and invasiveness. These features render them elusive targets for effective surgical management, and resistant to conventional pro-apoptotic chemotherapy and radiotherapy (Lefranc et al., 2009) (see 2.4).

In order to investigate whether PrPC has a cytoprotective role in glial tumor cells and whether it is involved in their resistance to cell death, PrPC expression was silenced using an antisense strategy.

Three antisense phosphorothioate oligonucleotides, targeting different regions of the *PRNP* transcript, were designed and transfected in a set of glial tumor (T98G, IPDDC-A2, PRT-HU2, U373-MG, D384-MG, U87-MG), non glial tumor (HeLa, HL60, SHSY5Y) cell lines and in normal human primary fibroblasts (C3PV) and rat adult astrocytes (T4).

The effects of PrPC silencing were initially evaluated through the analysis of cellular viability after s-ODNs transfection.

Subsequently, with the aim to elucidate the mechanism by which PrPC is able to modulate glioma cells viability, the activation status of two biochemical pathways involved in the control of cell survival and cell death, i.e. autophagy and apoptosis, was deeply investigated in T98G cells after PrPC silencing.

Finally, first steps were moved toward the identification of a possible functional link between PrPC and Bcl-2 in controlling and regulating cell survival in glioma cells.

4. Materials and methods

4.1 Cell lines and culture conditions

Human glioma established cell lines IPDDC-A2, T98G, U87-MG, U373-MG (provided by ECACC), D384-MG (provided by Dr. M. Ceroni, University of Pavia, Italy), PRT-HU2 (provided by Dr. C. Zibera, Fondazione Maugeri, Pavia, Italy) were previously employed and extensively described (Azzalin et al., 2008; Bacciocchi et al., 1992; Comincini et al., 2006; Comincini et al., 2004; Sbalchiero et al., 2008); widely employed human non-glial tumor cells (HeLa, HL60, SHSY5Y) were purchased by ATCC. Normal human primary fibroblast cultures (C3PV) and rat adult astrocytes (T4) were provided by Dr. M. Stefanini (IGM-CNR, Pavia, Italy) and by Prof. S. Schinelli (University of Pavia, Italy), respectively. Cells were cultivated in DMEM medium supplemented with 10% FBS, 100 units/ml penicillin, 0.1 mg/ml streptomycin and 1% L-glutamine (Invitrogen), at 37°C and 5% CO_2 atmosphere.

4.2 Antisense oligonucleotides and siRNAs

PRNP targeted s-ODNs, synthesised and HPLC purified by Sigma Genosys, were designed as follows: s-ODN1 (complementary to nt 1-20 of NM_183079.2 Genebank entry, 5'-CAGCAGCCAAGGTTCGCCAT), s-ODN2 (nt 79-98 of NM_183079.2, 5'-GTGTTCCATCCTCCTCCAGGCTT) and s-ODN3 (nt 202-221 of NM_183079.2, 5'-CCCCAGCCACCACCATGAGG); as a negative control, a scrambled s-ODN3 sequence was designed (s-ODN3scr 5'-CCCCAAAGGTCAAGCCCCGC), with no significant matching with Genebank databases. An additional s-ODN3 sequence 5'-conjugated with Alexa Fluor 488, hereafter called s-ODN3 Alexa Fluor 488, was synthesized and purified as above.

s-ODN-*BCL-2* was designed based on G3139 (Oblimersen sodium/Genasense) sequence (5'-TCTCCCAGCGTGCGCCAT) and synthesised and HPLC purified by Sigma Genosys. The reverse polarity oligonucleotide (5'-TACCGCGTGCGACCCTCT), was synthesised and purified as above and was used as a control.

For siRNA mediated Beclin-1 and Atg7 silencing, Silencer Select validated siRNAs (s16537, s16538 and s16539 for Beclin-1; s20650, s20651 and s20652 for

Atg7) and a Silencer select Negative Control #1 siRNA were purchased from Ambion, CA, USA.

4.3 pGFP-LC3 plasmid construction and transfection

The pEGFP-N1 plasmid (Clontech) (Fig. 18) was mutagenized by PCR using the primers 5'-CCGGAATTCCCACCATGGTGAGCAAGGGCGAG-3' and 5'-gtcgcggccgctttcttgtacagctcgtccatg-3' to remove the stop codon at the end of *EGFP*. Human total brain RNA (Clontech) was retrotranscribed and *LC3* cDNA was amplified by PCR using LC3-U (5'-TGCGGCCGCAATGCCCTCAGACCGGCC) and LC3-L primers (5' TGCGGCCGCTTATCAGAAGCCGAAGGTTTCCTG). Purified PCR products were then cloned downstream of *EGFP* in the modified pEGFP-N1 plasmid using the *NotI* restriction site thus obtaining the pGFP-LC3 plasmid. pGFP-LC3 was then sequenced on both strands to confirm the cloning of *wild-type* LC3 coding sequence.

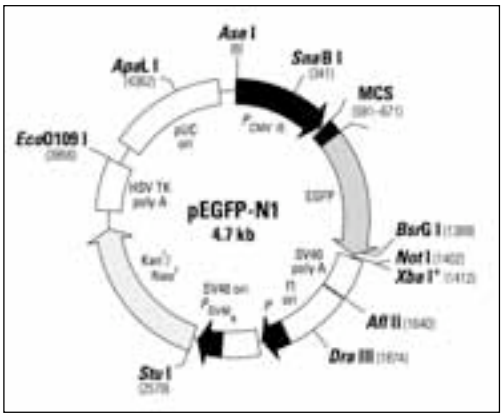

Fig. 18. pEGFP-N1 Vector (Clontech). Unique restriction sites are in bold The *NotI* site follows the *EGFP* stop codon.

4.4 Reagents

Rapamycin (R0395), Staurosporine (S5921) and Bafilomycin A1 (11711) were purchased from Sigma Aldrich and employed as indicated.

4.5 Transfection conditions

Transfections were performed in antibiotics-free medium, on a cells monolayer of about 70% confluence, using Lipofectamine 2000 reagent (Invitrogen) according to manifacturer's instructions.

For viability assays, 10^3 cells seeded onto 96-well plates were transfected with 200 ng of each s-ODNs (anti-*PRNP*, anti-*BCL-2* or the corresponding scrambled controls). To evaluate transfection efficiency, 5 x 10^4 T98G or C3PV cells were seeded on glass coverslips and transfected with 20 ng of s-ODN3 Alexa Fluor-488. For RT-PCR, immunoblotting, acridine orange experiments and analysis of nuclear morphology by DAPI staining, 5 x 10^4 cells were plated on 24-well plates or on glass coverslips (acridine orange and DAPI staining) respectively and transfected using 2 µg of s-ODNs. For electron microscopy analysis, 10^6 cells plated onto 20 cm^2 culture dishes were transfected with 8 µg of s-ODN3, or the corresponding scrambled s-ODN3scr oligonucleotide.

For the analysis of the effects of s-ODN3 treatment in Beclin-1 or Atg7 knocked down cells, 10^3 T98G cells seeded onto 96-well plates (for the analysis of cellular viability) or 5 x 10^4 cells seeded onto 24-well plates (for the analysis of the expression of autophagic markers) were transfected with 50 nM *BECN1* siRNA pool or 50 nM *Atg7* siRNA pool respectively. 48 hours later a second transfection was performed: cells were co-transfected with 50 nM *BECN1* siRNA pool or 50 nM *Atg7* siRNA pool and with 2 µg of s-ODN3 or s-ODN3scr respectively. Cellular viability and protein expression analysis were performed at 72 h after s-ODN3/s-ODN3scr transfection.

For the analysis of LC3 localization after s-ODN3 or s-ODN3scr treatment, 1 µg of pGFP-LC3 plasmid was transfected in 5 x 10^4 T98G cells seeded on a glass coverslip. The following day cells were re-transfected with 2 µg of s-ODN3 or s-ODN3scr respectively.

4.6 Viability assays

To test cell viability, the MTT-based assay "CellTiter 96 Aqueous One Solution Cell Proliferation Assay" (Promega) was employed following the manufacturer's instructions. It contains a novel tetrazolium compound [3-(4,5-dimethylthiazol-2-yl)-5-(3-carboxymethoxyphenyl)-2-(4-sulfophenyl)-2H-tetrazolium, inner salt; MTS(a)] and an electron coupling reagent (phenazine ethosulfate; PES). The MTS tetrazolium compound (Owen's reagent) is bioreduced by cells into a colored formazan product that is soluble in tissue culture medium (Figure 19). This

conversion is presumably accomplished by NADPH or NADH produced by dehydrogenase enzymes in metabolically active cells. The quantity of formazan product as measured by the absorbance at 490nm is directly proportional to the number of living cells in culture.

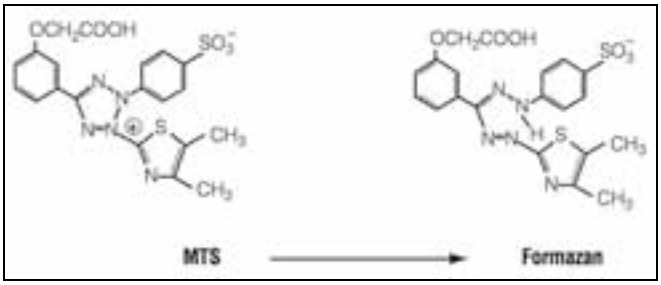

Figure 19. Structures of MTS tetrazolium and its formazan product.

Cells were plated onto 96-well flat-bottom plate in triplicate at a density of 10^3 cells per well. First readouts were measured 24 h after plating and then at 48-72 h. p.t. Absorbance were measured with a microplate reader (Titertek Multiskan) at 492 nm wavelength.

4.7 Clonogenic survival assay

For clonogenic survival assay, 2 x 10^5 T98G cells were plated on 6 well plates and transfected with 4 µg of each s-ODN using Lipofectamine 2000 reagent. At 48 h p.t., cells were trypsinized and seeded into 100 mm^2 culture dishes (10^3 cells per dish), incubated for two weeks at 37°C, and then fixed with ethanol. Cells were stained with 0,5% crystal violet (Sigma) and colonies containing more than 50 cells were counted using the densitometric software Clono Counter (Niyazi et al., 2007). Each experiment was performed in triplicate.

4.8 Real-time PCR expression analysis

Cells were harvested 48 h p.t. and their RNA was extracted using Trizol reagent (Invitrogen), following manifacturer's specifications. After RNA quantitation (Quant-it RNA Assay, Invitrogen), cDNA synthesis was performed using the High Capacity cDNA Archive kit (Applera). Gene-specific Taqman Minor Groove Binders (MGB) probes and primers were designed by means of the Primer Express, version 3.1 software (Applera). For *PRNP* expression analysis: primer forward, 5'-GCGCCGCGAGCTTCT; primer reverse, 5'-AAGGTTCGCCATAATGACTGCT;

probe 5'-6-FAM-CTCTCCTCACGACCGAG. For *BCL-2* expression analysis: primer forward, 5'-AGATCCGAAAGGAATTGGAATAAA; primer reverse, 5'-GATTCTGGTGTTTCCCCCTTG; probe, 5'-6-FAM-ATTTCCTGCATCTCATG. A β-actin (*ACTB*) Taqman probe was purchasaed from Applera and used as a reference. Real time PCR was performed on an MJ Opticon II model (MJ Research, Waltham, MA) using 1µg of cDNA. Samples were subjected to 40 amplification cycles of 95°C for 15' and 59°C for 1'. For each sample, amplifications were performed in 50 µl volume containing the primers (900 nM each) and the probe (200 nM), 1X Universal PCR Master Mix No Amperase UNG (Applera). Relative quantitation was performed using *ACTB* as an internal calibrator housekeeping gene and adopting the ΔΔCt method (Livak and Schmittgen, 2001).

4.9 Immunoblotting.

Cell pellets were resuspended in ice-cold RIPA buffer (150 mM NaCl, 50 mM Tris-HCl pH 8.0, 0.5% sodium deoxycholate, 1% Nonidet P-40, 0.1% sodium dodecylsulphate), supplemented with Complete Mini protease inhibitor cocktail (Roche). Protein samples were quantified by Qubit fluorometer (Invitrogen) following manufacturer's instructions. Before loading in SDS-PAGE, protein extracts were boiled in Laemmli sample buffer (2% SDS, 6% glycerol, 150 mM B-mercaptoethanol, 0.02% bromophenol blue and 62.5 mM Tris-HCl pH 6.8). After electrophoresis, proteins were transferred onto nitro-cellulose membrane Hybond-C Extra (GE Healthcare). Membranes were blocked with 5% non-fat milk in TBS containing 0.1% Tween 20 and incubated over-night at 4°C with primary antibodies. Primary antibodies employed were: 3F4 (Millipore, MAB1562) for PrPC; Bcl-2 (Santa Cruz Biotechnologies, sc-509); p62 (SQSTM1) (Enzo Life Sciences, PW9860), LC3B (2725), Beclin-1 (3738), Phospho-p70 S6 Kinase (Thr389, 9206), p70 S6 Kinase (49D7, 2708), Phospho-4E-BP1 (Thr70, 9451), 4E-BP1 (9452), caspase-3 (3G2, 9668), caspase-7 (C7, 9494) by Cell Signaling Technology, and PARP-1 (Santa Cruz Biotechnology, C2-10) for autophagic and apoptotic markers detection; ACTB (Cell Signaling Technology, 4967) was used as internal control. Species-specific peroxidase-labelled ECL secondary antibodies (GE Healthcare) were employed. Protein signals were revealed by the "ECL Advance Western Blotting Detection Kit" (GE Healthcare).

Densitometric quantification of the intensities in Western blot bands was carried out using Image J software (NIH) (http://rbsweb.nih:gov/ij/).

4.10 Electron microscopy analysis

For electron microscopy analysis, T98G cells (10^6) were grown in DMEM medium, treated with the autophagy inducer Rapamycin (100 nM), or transfected with s-ODN3 or s-ODN3scr as described above. At 48 h p.t., cells were harvested by centrifugation at 800 rpm for 3 min and fixed with 2% glutaraldehyde in DMEM, for 2 h at room temperature. Cells were then rinsed in PBS (pH 7.2) overnight and post-fixed in 1% aqueous OsO_4 for 2 h at room temperature. Cells were pre-embedded in 2% agarose in water, dehydrated in acetone, and finally embedded in epoxy resin (Electron Microscopy Sciences, EM-bed812). Ultrathin sections (50-60 nm) were collected on formvar-carbon-coated nickel grids and stained with uranyl acetate and lead citrate. The specimens were observed with a Zeiss EM900 electron microscope equipped with a 30 µm objective aperture and operating at 80 kV.

4.11 Acridine orange staining.

At 48h after s-ODN3 and s-ODN3scr transfection (for transfection conditions see above) cells were visualized with a fluorescent inverted microscope (Nikon Eclipse TS100) using a 488-fluorescent filter. To quantify the development of AVOs, total floating and adherent cells were removed from the plate with trypsin-EDTA (Invitrogen), washed with PBS and analyzed on a Partec PAS flow cytometer using a "Flow Max" software to acquire and elaborate the data. The intensity of autophagy was visualised as red fluorescence (FL3), which increases during autophagy.

4.12 Caspase-3/7 activity assay.

Caspase-3 and -7 activities were measured in living cells using the Apo-ONE Homogeneous Caspase-3/7 Assay (Promega) according to the manufacturer's instructions; It provides a profluorescent substrate with an optimized bifunctional cell lysis/activity buffer for caspase-3/7 (DEVDase) activity assays. The Apo-ONE®Homogeneous Caspase-3/7 Buffer rapidly and efficiently lyses/permeabilizes cultured mammalian cells and supports optimal caspase-3/7 enzymatic activity. The caspase-3/7 substrate rhodamine 110, bis-(N-CBZ- L-aspartyl-L-glutamyl-L-valyl-L-aspartic acid amide; Z-DEVD-R110), exists as a profluorescent substrate prior to the assay. Upon sequential cleavage and removal of the DEVD peptides by caspase-3/7 activity and excitation at 499nm, the rhodamine 110 leaving group becomes intensely fluorescent (Figure 20). The emission maximum is 521nm. The amount of fluorescent product generated is proportional to the amount of caspase-3/7 cleavage activity present in the sample.

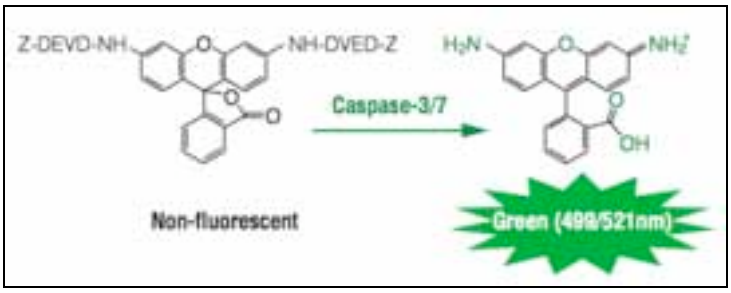

Figure 20. Cleavage of the non-fluorescent Caspase Substrate Z-DEVD-R110 by Caspase-3/7 to obtain the fluorescent Rhodamine 110.

Briefly, 10^3 cells were seeded on 96-well plates and transfected with 200 ng of s-ODN3; as a positive control of apoptotic induction, cells were incubated with 100 nM Staurosporine (Sigma). Absorbance was measured every 24 h, after treatment with 1 volume of Apo-ONE Reagent and 12 h incubation at room temperature.

4.13 Statistical analysis.

Statistical analyses were performed using Anova-one way test. All *P* values less than 0.05 were considered statistically significant.

5. Results

5.1 Silencing of PrPC expression by antisense oligonucleotides transfection induces cell death in different glioma cell lines

Three different antisense phosphorothioate oligonucleotides (hereafter called s-ODN1,2,3) targeting different portions of the prion gene (*PRNP*) transcript were designed and transfected into different human glioma (T98G, IPDDC-A2, PRT-HU2, U373-MG, D384-MG, U87-MG), and non-glial tumor cell lines (HeLa, HL60, SHSY5Y), as well as into normal human primary fibroblasts (C3PV) and rat adult astrocytes (T4). Cell viability was monitored through careful microscopic observations and was evaluated at 24, 48 (data not shown) and 72 h post transfection (p.t.) using a MTT-based colorimetric assay (i.e. Cell Titer 96 One Aqueous Solution Proliferation Assay). As reported in Figure 21A, cell viability was differentially affected depending on the cell line and on the type of s-ODN employed. While s-ODN2 did not alter tumor cells viability, s-ODN1 transfection significantly decreased the viability of glioma cells without affecting non-glial tumor cells. On the contrary, s-ODN3 treatment induced a decrease in the viability of both glial and non-glial tumor cell lines. In particular, T98G, D384-MG, U373-MG and IPDDC-A2 glial tumor cells viability was reduced by 80% after s-ODN3 transfection. A comparative phase contrast microscopy analysis of the morphological effects induced by s-ODN3 treatment in the investigated glioma cells is reported in Figure 21B. Importantly, as summarized in Figure 21C, s-ODN3 was the most selective in reducing the viability of tumor cells, showing a lesser effect on normal human fibroblasts and rat adult astrocytes. Since all s-ODNs have the same lenght and a similar G+C content, it was decided to use as a negative control a single scrambled s-ODN, corresponding to s-ODN3 random sequence. Control scrambled s-ODN3 (s-ODN3scr) did not significantly affect the viability of any of the cell lines tested (Fig. 21A and C).

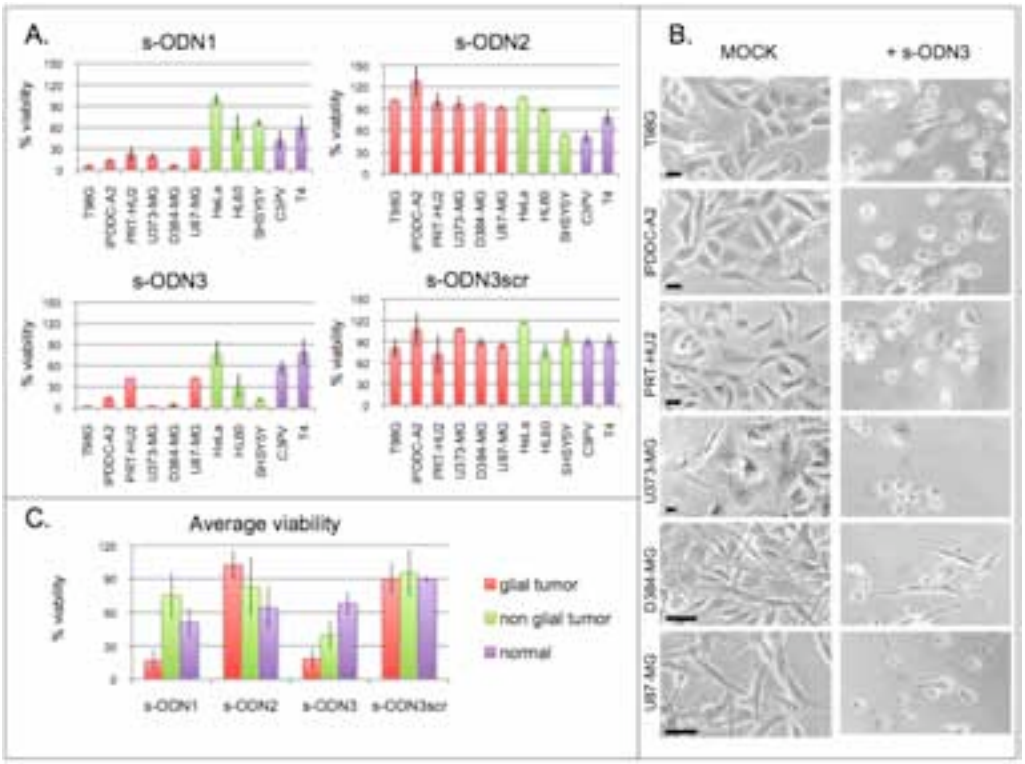

Figure 21. Cell viability and morphology are affected by s-ODN1 and s-ODN3 antisense treatments. (A) s-ODN1 and s-ODN3 decreased glioma cell viability. Human glioma (red bars), and non glial tumor (green bars) cell lines, as well as human normal fibroblasts (C3PV) and normal rat astrocytes (T4) (violet bars), were transfected with s-ODN1,2,3 and with the same amount of scrambled s-ODN3 (s-ODN3scr). Cell viability was measured at 72 h p.t.. Y-axes report percentage of cell viability after normalization with the corresponding mock controls. Each value is the average±standard deviations of three independent replicas. (B) s-ODN3 altered cellular morphology. Phase contrast light microscopy images of s-ODN3 treated cells were collected in live cells 72 h p.t. using an inverted Nikon Eclipse TS100 microscope with a 40 X objective. Micrometric bars (10 μm) are indicated. (C) s-ODN3 was the most selective in specifically reducing tumor cells viability. Average of glioma, non-glial tumor, and normal cells viability at 72 h p.t. Y-axes report percentage of cell viability after normalization with the corresponding mock controls. Black bars indicate standard deviations.

To evaluate if the different sensitivity to s-ODN3 treatment between normal and tumor cells was related to differences in the cellular uptake of the antisense oligonucleotide, an Alexa Fluor 488 5'-conjugated s-ODN3 molecule was transfected in T98G and C3PV cells, respectively as sensitive- and resistant to s-ODN3 treatment. The transfection efficiency and the intracellular localization of the anti-*PRNP* antisense molecules was time-monitored and visualised by fluorescence microscopy at

488 nm. At 24 h p.t. both cell types exhibited high transfection efficiency (>75%) and a cytoplasmic and perinuclear punctuate staining that was maintained within the cells even at longer time intervals (48 to 72 h p.t.) (data not shown).

To assess whether the diversity of effects exerted on cellular viability by the different s-ODNs correlated with differences in their ability to silence *PRNP*, a Real-time PCR analysis was performed at 48 h p.t. on the cDNAs of the previously investigated cell lines. As shown in Figure 22A, s-ODN3 and s-ODN1 treatments induced the most effective *PRNP* mRNA reduction both in tumor and normal cells. On the contrary, s-ODN2 induced a null or less efficient decrease in *PRNP* expression in the majority of the cells, with the exception of HeLa and C3PV where s-ODN1 and s-ODN2 mediated *PRNP* silencing were similar.

Among the cell lines tested, T98G glioma cells displayed major sensitivity to s-ODN1 and s-ODN3 mediated *PRNP* down-regulation and cell death. Being one of the most employed glioma cell lines, T98G cells were therefore selected for subsequent experiments.

Immunoblotting analysis of PrPC protein expression after s-ODNs transfections in T98G cells is reported in Figure 22B. While s-ODN2 and s-ODN3scr did not alter PrPC levels, a marked decrease in cellular prion protein expression was observed at 24-48 h p.t. after s-ODN1 and s-ODN3 transfection. PrPC expression was generally rescued at 72 h p.t

To investigate whether the rescue of PrPC levels at 72 h p.t. could lead to a recovery of cellular viability, the long term effects of the different antisense oligonucleotides on glial tumor cells survival were assessed by a clonogenic replating assay. While s-ODN1 and s-ODN3 significantly reduced the colony forming ability of T98G cells, s-ODN2 and s-ODN3scr treatments did not alter the cellular ability to proliferate and form colonies (Fig. 22C).

Being the most effective in down-regulating prion expression both at the mRNA and protein level, and in selectively decreasing tumor cells viability without affecting normal cells (Fig. 21), s-ODN3 was selected for subsequent experiments.

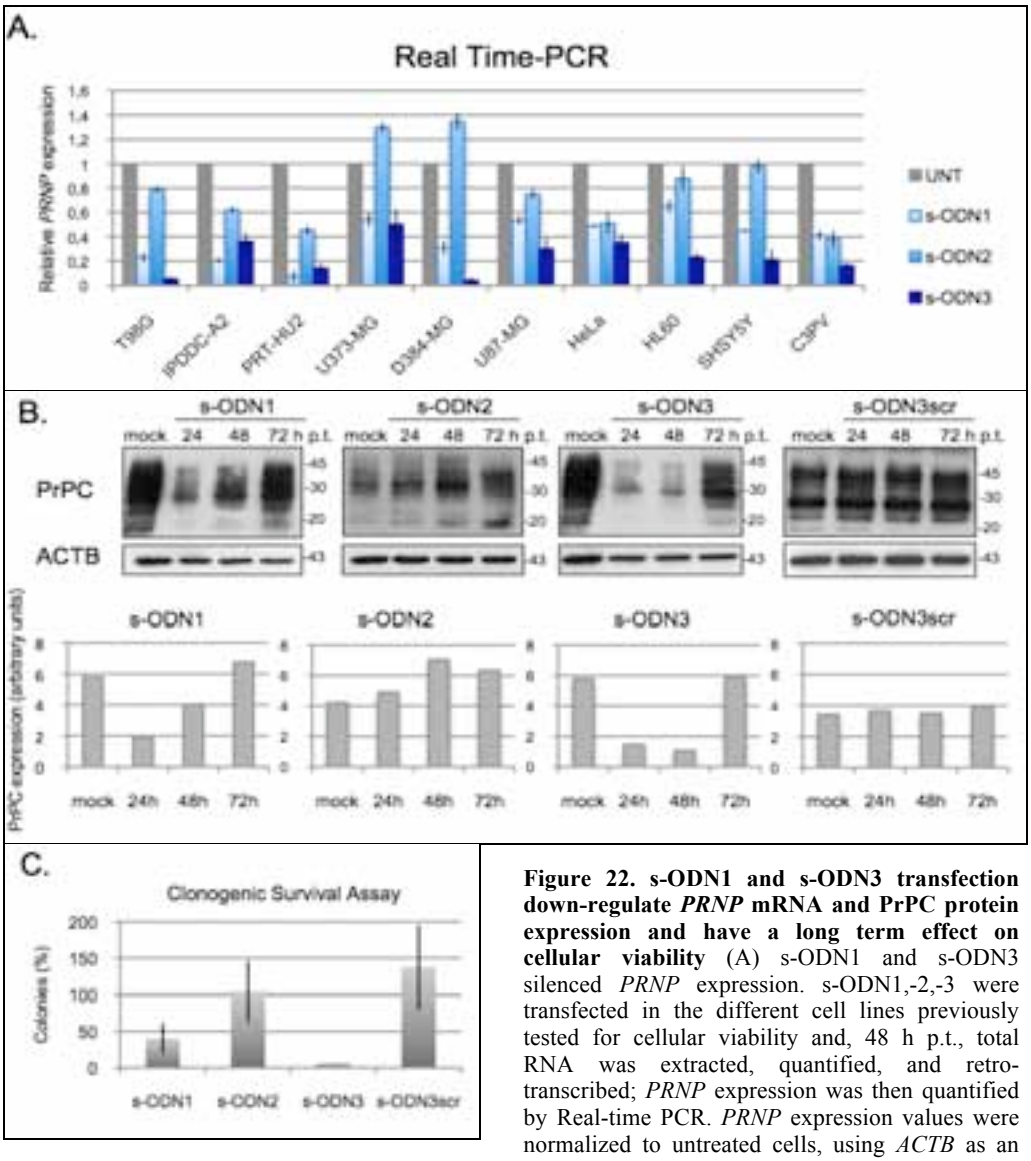

Figure 22. s-ODN1 and s-ODN3 transfection down-regulate *PRNP* mRNA and PrPC protein expression and have a long term effect on cellular viability (A) s-ODN1 and s-ODN3 silenced *PRNP* expression. s-ODN1,-2,-3 were transfected in the different cell lines previously tested for cellular viability and, 48 h p.t., total RNA was extracted, quantified, and retro-transcribed; *PRNP* expression was then quantified by Real-time PCR. *PRNP* expression values were normalized to untreated cells, using *ACTB* as an internal housekeeping calibrator. Results are expressed as mean±standard deviations (vertical bars). (B) s-ODN1 and s-ODN3 down-regulated PrPC levels. T98G cells were transfected with the three *PRNP*-specific s-ODNs and with the scrambled control and were harvested at 24 h p.t. intervals. Total proteins were then extracted, quantified and separated by SDS-PAGE. Mock indicates Lipofectamine 2000 treated cells pooled at 24-48-72 h. Molecular weights are expressed in kDa. Histograms report the densitometric analysis of PrPC expression normalized to ACTB levels (ImageJ software). C) s-ODN1 and s-ODN3 significantly reduced the colony forming ability of T98G cells. Clonogenic replating assay was performed in T98G cells after transfection with s-ODN1,2,3 and s-ODN3scr: percentage of colonies, normalized to the mock sample, are reported on Y-axis. Values are expressed as mean±SEM of three independent experiments.

5.2 s-ODN3 induces autophagy in T98G cells

A transmission electron microscopy comparative analysis of the ultrastructural features of s-ODN3 transfected T98G cells performed at 48 h p.t., revealed an unaltered nuclear morphology and the presence of large cytoplasmic vacuoles containing residual digested material. These vesicles were nearly absent in mock treated cells and in cells transfected with an equal amount of scrambled s-ODN3 and, importantly, they were similar to those observed in cells treated for 72 hours with the autophagy inducer Rapamycin (100 nM) (Fig. 23A).

Autophagy was therefore investigated to elucidate the mechanism of cell death induced by s-ODN3-mediated PrPC down-regulation.

Autolysosome formation in s-ODN3 treated T98G cells was investigated using acridine orange staining, as described by Paglin and collaborators (Paglin et al., 2001). At 48 h p.t., fluorescence microscopy observations and flow cytometry analysis revealed the development of red fluorescent acidic vesicular organelles (AVOs) and a significant increase in the red/green (FL3/FL1) fluorescence ratio in acridine orange stained s-ODN3 transfected cells, as compared to scrambled and mock controls (Fig. 23B).

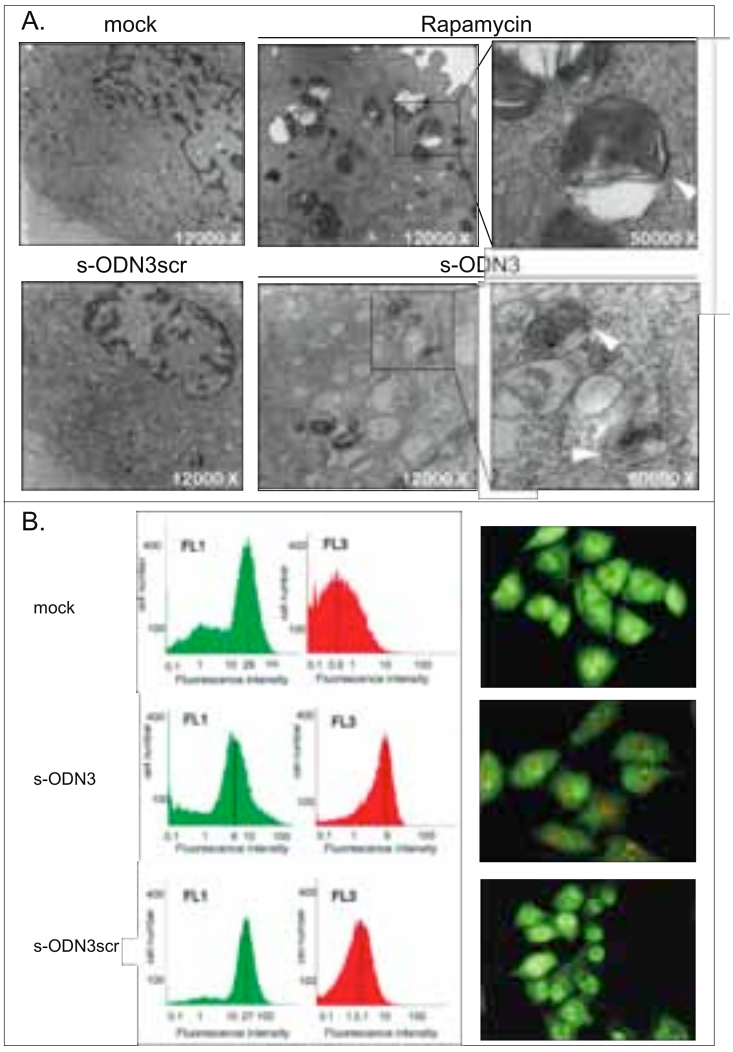

Figure 23. Ultrastructural and flow cytometry analysis indicate autophagy induction in T98G cells after s-ODN3 treatment. (A) s-ODN3 induced the formation of autophagy-like vescicles. For electron microscopy analysis, T98G cells were treated with the autophagy-inducer Rapamycin (100 nM) or transfected with s-ODN3 or s-ODN3scr antisense molecules. Cells were harvested at 48 h p.t. and 72 h after Rapamycin treatment, fixed and stained for ultrastructural visualization. Specimens were then observed with a Zeiss EM900 electron microscope. Arrows indicate large intracellular vesicles, likely autophagosomes. Magnifications are reported. (B) Flow cytometry revealed an increase in acridine orange stained autolysosomes in s-ODN3 treated cells. The presence of autophagic vesicles was examined at 48 h p.t. in acridine orange-stained cells by fluorescence microscopy (on the right) and flow cytometry analysis (on the left) in mock, s-ODN3 and s-ODN3scr transfected cells by comparing green and red (FL1, FL3) fluorescence distributions.

To confirm the induction of autophagy by s-ODN3 transfection, the expression of typical autophagic markers was analyzed.

The microtubule associated-protein 1 light chain 3 (LC3) localization and expression were initially evaluated. LC3 exists in two forms: LC3-I, localized in the cytosol, and LC3-II, localized in autophagosomal membranes. The conversion of LC3-I (16 kDa) to LC3-II (14 kDa) is a strong biochemical marker for the induction of autophagy (Mizushima and Yoshimori, 2007).

LC3-I to LC3-II conversion was initially analyzed using a GFP-LC3 fusion protein: 24 h after transfection with a pEGFP-LC3 expression vector, T98G cells were transfected with s-ODN3 or s-ODN3scr and, 48 h later, GFP-LC3 cellular distribution was evaluated by fluorescence microscopy. While mock and s-ODN3scr transfected cells showed a diffuse distribution, s-ODN3 treated cells presented a punctuate pattern, suggesting GFP-LC3-II protein accumulation in autophagosomes (Fig. 24A).

LC3-I to LC3-II conversion was also evaluated by immunoblotting in a time course study within 72 h p.t.. An increase in LC3-II levels was readily observable at 48 h p.t. in s-ODN3, as compared to s-ODN3scr treated T98G cells. To discern whether the increase in LC3-II levels after s-ODN3 treatment was due to autophagy stimulation or inhibition of LC3-II degradation, the lysosomal inhibitor Bafilomycin A1 (BafA1, 10 nM) was added in the last 4 h of each time point. As reported in the upper panel of Figure 24B, BafA1 treatment induced an increase in LC3-II levels at each time point as compared to s-ODN3 and s-ODN3scr treated cells in which the lysosomal activity was not inhibited. In particular, in the presence of BafA1, at 48 and 72 h p.t., LC3-II levels of s-ODN3 transfected cells were significantly higher compared with the s-ODN3scr BafA1-treated control, indicating that s-ODN3 treatment induced an enhancement of the autophagic flux starting at 48 h p.t..

An alternative method for detecting the autophagic flux is measuring the levels of p62 (SQSTM1), a protein specifically degraded by the autophagy—lysosome system. p62 levels were investigated by western blot in T98G cells at 24 and 48 h after s-ODN3 and s-ODN3scr transfection, in the presence or absence of BafA1. At 48 h p.t., p62 levels decreased by 70% in s-ODN3 transfected cells compared with the s-ODN3scr treated control. This decrease was rescued by BafA1 treatment, consistently with a blockage of the autophagy process (Fig. 24B lower panel).

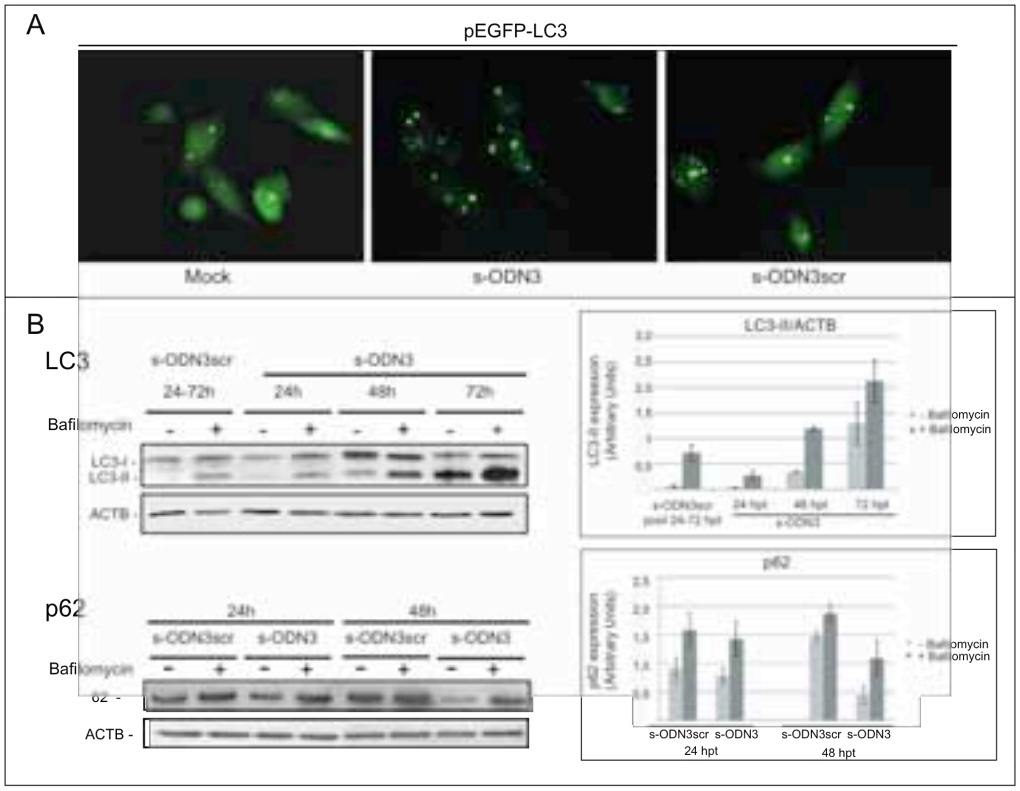

Figure 24. s-ODN3 induces autophagy in T98G cells. (A) s-ODN3 treated cells presented a punctuate distribution of GFP-LC3. T98G cells transiently expressing GFP-LC3 were transfected with s-ODN3 or s-ODN3scr and analysed for GFP-LC3 distribution by fluorescence microscopy. (B) s-ODN3 induced autophagic flux. The expression of LC3 and p62 proteins was investigated in T98G cells transfected with s-ODN3 and s-ODN3scr, in presence/absence of Bafilomycin A1 lysosomal inhibitor. On the right, densitometric analysis using ImageJ software (http://rbsweb.nih:gov/ij/) of LC3-II and p62 expression after normalization with ACTB is reported in arbitrary units: values are mean±standard deviation of three independent experiments.

5.3 ODN3 induces autophagy through inhibition of PI3K/Akt/mTOR pathway and activation of Beclin-1/Vps34

In order to assess the mechanims by which s-ODN3 treatment induces autophagy, the activation status of the two autophagy regulators mTOR and Beclin-1 was investigated by assessing the phosphorylation status of two downstream targets of mTOR – i.e. p70S6K and the eukaryotic initiation factor 4E binding protein 1 (4E-BP1) - and the expression levels of Beclin-1. As reported in Figure 25A, both Phospho-p70S6K/p70S6K and Phospho-4E-BP1/4E-BP1 ratios significantly decreased in s-ODN3 treated cells (P<0.01), as compared to s-ODN3scr transfected cells, indicating an inhibition of mTOR kinase activity following PrPC silencing. On the contrary Beclin-1 levels increased following s-ODN3 transfection as compared to controls. S-ODN3 treatment therefore induces an inhibition of the autophagy negative regulator mTOR and an increase in the levels of the autophagy positive regulator Beclin-1.

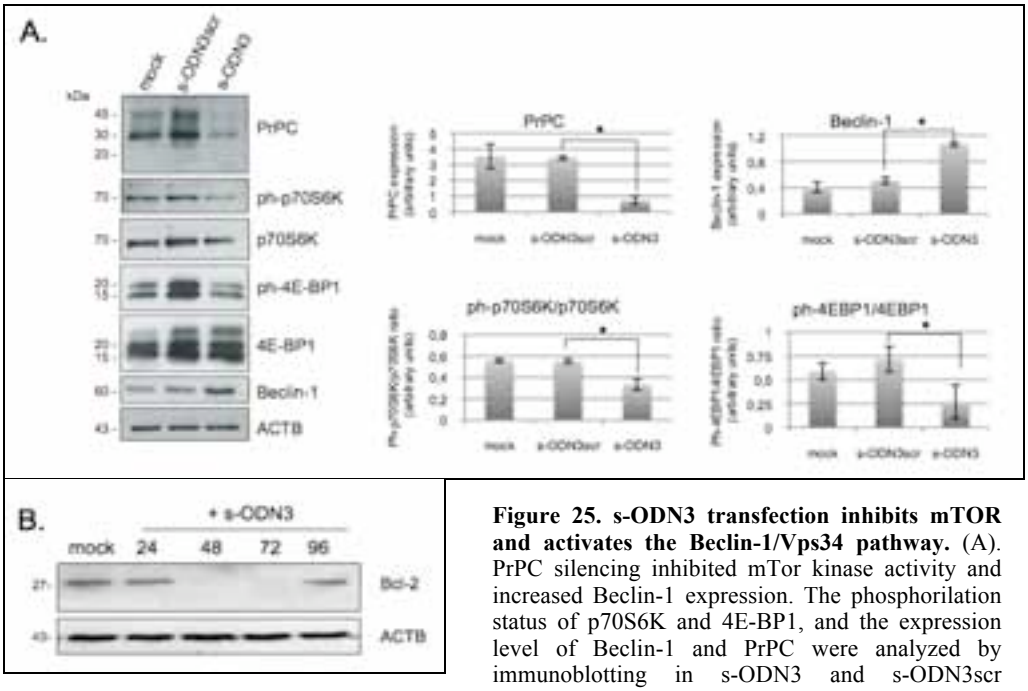

Figure 25. s-ODN3 transfection inhibits mTOR and activates the Beclin-1/Vps34 pathway. (A). PrPC silencing inhibited mTor kinase activity and increased Beclin-1 expression. The phosphorilation status of p70S6K and 4E-BP1, and the expression level of Beclin-1 and PrPC were analyzed by immunoblotting in s-ODN3 and s-ODN3scr transfected cells 72 h.p.t. PrPC and Beclin-1 expression and ph-p70S6K/p70SK and ph-4E-BP1/4E-BP1 ratios is reported in arbitrary units after normalization with ACTB. Values are expressed as means±standard deviations of threee independent experiments. Asterisks indicate P<0.01, Anova one way (B) s-ODN3 transfection induced Bcl-2 down-regulation at 48 and 72 hours post transfection. Time course analysis (24-96 h p.t.) of Bcl-2 expression in s-ODN3 transfected T98G.

Bcl-2, a well known antiapoptotic protein, was recently shown to negatively regulate autophagy by binding to Beclin-1. To investigate whether the cell death pathway induced by s-ODN3 transfection involved the modulation of Bcl-2, its protein levels were analyzed by immunoblotting in a time course study within 96h after s-ODN3 transfection in T98G cells. Bcl-2 resulted to be down-regulated at 48 and 72 h p.t. and to return to control levels at 96 h p.t (Fig. 25B). These finding suggest that one of the mechanisms by which autophagy is induced after s-ODN3 treatment could involve the down-regulation of Bcl-2.

5.4 Inhibition of Atg genes suppresses s-ODN3- induced autophagy

To test whether autophagy is required for PrPC-silencing induced cell death, the autophagic process was inhibited by Beclin-1 or Atg7 knockdown with specific siRNAs. Cell viability was evaluated at 72 h after s-ODN3 and s-ODN3scr transfection. As shown in Figure 26A, the viability of T98G cells treated with s-ODN3 was increased from 53 to 74% and from 57% to 91% by Beclin-1 and Atg7 silencing respectively; in addition, both Beclin-1 and Atg7 knocking down reduced LC3-I to LC3-II conversion in s-ODN3 treated cells (Fig. 26B). On the contrary, Beclin-1 and Atg7 silencing *per se* or in combination with s-ODN3 and s-ODN3scr treatments did not alter Phospho-4E-BP1/4E-BP1 ratios as compared to Beclin-1 and Atg7 expressing cells.

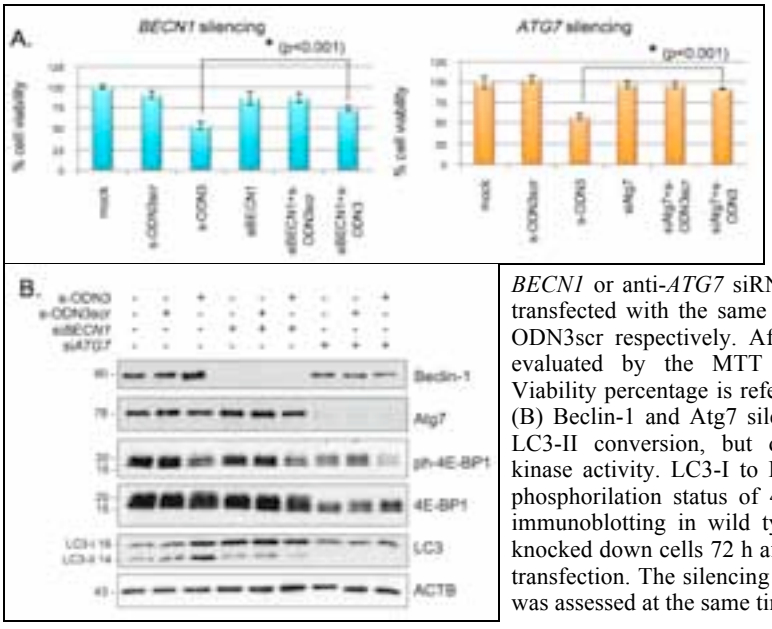

Figure 26. Silencing of Beclin-1 and Atg7 exerts a cyto-protective role against s-ODN3 treatment. (A) Beclin-1 and Atg7 silencing increased the viability of s-ODN3 treated T98G cells. T98G cells were transfected with anti-*BECN1* or anti-*ATG7* siRNA and 48h later were co-transfected with the same siRNA and s-ODN3 or s-ODN3scr respectively. After 72h cell viability was evaluated by the MTT based Cell titer Assay. Viability percentage is referred to mock treated cells. (B) Beclin-1 and Atg7 silencing decreased LC3-I to LC3-II conversion, but did not influence mTOR kinase activity. LC3-I to LC3-II conversion and the phosphorilation status of 4E-BP1 were analyzed by immunoblotting in wild type and Beclin-1 or Atg7 knocked down cells 72 h after s-ODN3 or s-ODN3scr transfection. The silencing of the respective Atg gene was assessed at the same time. MW are in kDa.

5.5 s-ODN3 treatment does not induce apoptosis

To address whether s-ODN3 mediated PrPC down-regulation in T98G cells was additionally associated with apoptotic events, caspases activation was investigated by performing the Apo-ONE Homogeneous Caspase-3/7 assay (Promega): as reported in Figure 27A, the analysis of the caspase-induced fluorescence did not evidence significant differences between untreated and s-ODN3 treated cells, while, on the contrary, caspases activity was significantly induced in Staurosporine-treated cells at 72 h p.t. (P<0.05, Anova one-way). This result was confirmed by immunoblotting, showing marked caspase-3, -7 and PARP-1 cleavage only after Staurosporine induction, compared to mock and s-ODN3 treated cells (Fig. 27B and C). In agreement with these observations, other typical apoptotic features, i.e. nuclear fragmentation, chromatin condensation and apoptotic-bodies formation, were mostly absent following s-ODN3 treatment, comparing with staurosporine treated cells (Fig. 27D).

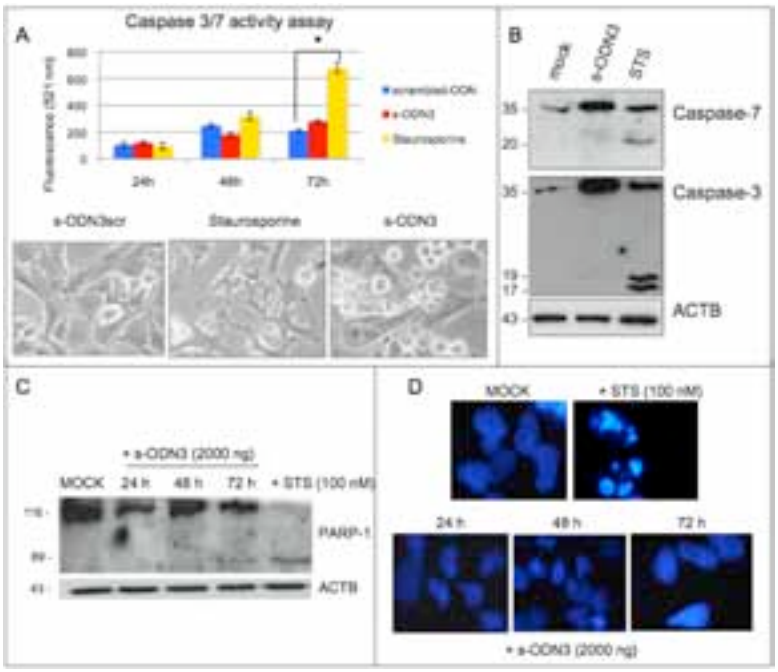

Figure 27. s-ODN3 treatment does not induce apoptosis. (A-B) s-ODN3 transfection did not activate caspase-3 and -7. (A) Caspase-3/-7 activation was monitored in T98G cells at 24-72 h after s-ODN3 and s-ODN3scr transfection using the Apo-One Caspase 3/7 Apoptosis Assay. STS: Staurosporine-treated cells (100 nM). Below, light microscopy examinations are reported (40 X) after 48 h p.t. Asterisk (*) indicates P<0.05, Anova-one way. (B) Immunoblotting analysis of caspase-7 and -3 in T98G cells at 72 h p.t.. Molecular weights are reported in kDa. (C) s-ODN3 transfection did not induce PARP-1 cleavage. PARP-1 immunoblotting 24-72 h after s-ODN3 transfection. Molecular Weights are reported in kDa. (D) s-ODN3 treatment did not induce alterations in nuclear morphology. DAPI nuclear fluorescence staining after s-ODN3 transfection and STS (100 nM) treatments was monitored at 24-48-72 h.

5.6 Bcl-2 silencing *per se* has a minor effect on s-ODN3 induced cell death

As reported in Figure 25B, s-ODN3 treatment induced a down-regulation of Bcl-2 expression at 48 and 72 h p.t.. To investigate the contribution of Bcl-2 down-regulation to s-ODN3 induced cell death, *BCL-2* expression was silenced using a validated 18-mer anti-*BCL-2* antisense phosphorothioate oligonucleotide targeting the first 6 codons of the *BCL-2* open reading frame (Oblimersen G3139/Genasense™ hereafter indicated as s-ODN-*BCL-2*). As evidenced by Real-Time PCR and western blot analysis, s-ODN-*BCL-2* transfection induced a decrease in *BCL-2* expression both at mRNA and protein level (Fig. 28A).

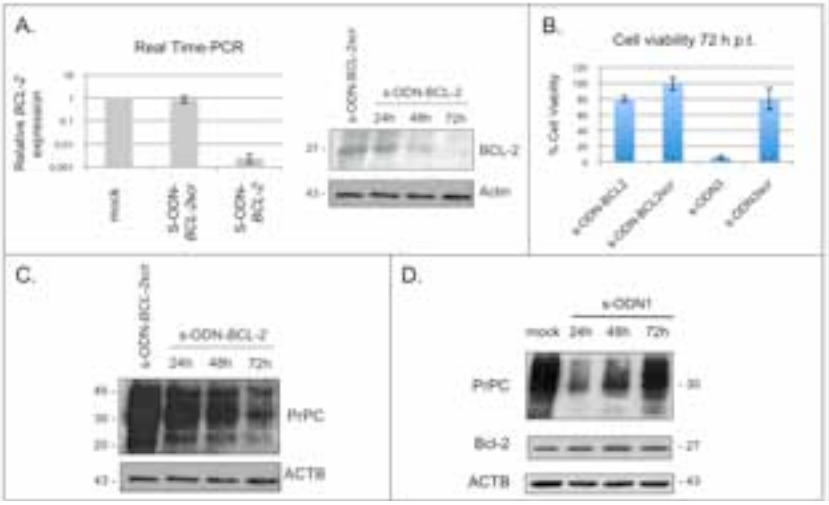

Figure 28. Bcl-2 silencing has a minor effect on s-ODN3 induced cell death. (A). s-ODN-*BCL-2* transfection decreased *BCL-2* transcript and protein levels. s-ODN-*BCL-2* and the corresponding scrambled control were transfected in T98G cells. (Left panel) 48 h p.t. total RNA was extracted, quantified, and retro-transcribed; *BCL-2* expression was then quantified by Real-time PCR. *BCL-2* expression values were normalized to untreated cells, using *ACTB* as an internal housekeeping calibrator. Results are expressed as means±standard deviations (vertical bars). (Right panel) Immunoblotting analysis of Bcl-2 expression was performed on total proteins extracted at 24 h intervals 24 to 72 h p.t.. (B). s-ODN-*BCL-2* decreased cell viability of T98G cells. s-ODN-*BCL-2*, s-ODN3 and their relative scrambled controls were transfected in T98G cells and cell viability was measured 72 h p.t. Y-axes report percentage of cell viability after normalization with the corresponding mock controls. Value are mean±standard deviations of three independent replicas. (C). s-ODN-*BCL-2* transfection induced a decrease in PrPC levels. Immunoblotting analysis of PrPC expression was performed on total proteins extracted at 24 h intervals after transfection with s-ODN-*BCL-2*. S-ODN-*BCL-2*scr indicates scrambled transfected cells pooled at 24-48-72 h (D) PrPC silencing induced cell death independently of Bcl-2 expression. Bcl-2 expression was evaluated by immunoblotting at 24 hours interval within 72h after -ODN1 transfection. Mock indicates Lipofectamine 2000 treated cells pooled at 24-48-72 h

Cell viability after s-ODN-*BCL-2* or s-ODN3 transfection was evaluated at 72 h p.t. using the Cell Titer 96 One Aqueous Solution Proliferation Assay. As reported in Figure 28B, *BCL-2* silencing had a minor effect on cell viability as compared to s-ODN3. Since *BCL-2* silencing *per se* induced a 20% reduction in cell viability, it is possible to argue that the down-regulation of Bcl-2 in s-ODN3 treated cells has a minor contribution to s-ODN3 induced cell death. Interestingly, immunoblotting analysis of PrPC expression in s-ODN-*BCL-2* treated cells highlighted a slight decrease in prion protein levels at 72 h p.t. (Fig. 28C)

To investigate whether it played a role also in s-ODN1 induced cell death, Bcl-2 protein expression was evaluated in s-ODN1 transfected cells. While inducing a >90% decrease in cell viability (Figure 21A), s-ODN1 transfection did not affect Bcl-2 levels (Fig. 28D).

It is therefore possible to conclude that PrPC silencing is sufficient to induce a significant cell death in T98G glioma cells.

5.7 Bcl-2 silencing *per se* induces apoptosis in T98G glioma cells

To determine the type of cell death induced by s-ODN-*BCL-2* in T98G, the expression of typical autophagic and apoptotic markers was investigated.

Western blot analysis of Beclin-1 expression and LC3-I to LC3-II conversion did not evidence any alteration in the status of these two autophagic markers (Fig. 29A). On the contrary, s-ODN-*BCL-2* treatment caused the cleavage of both caspase-3 and PARP-1, suggesting the activation of apoptosis (Fig. 29B).

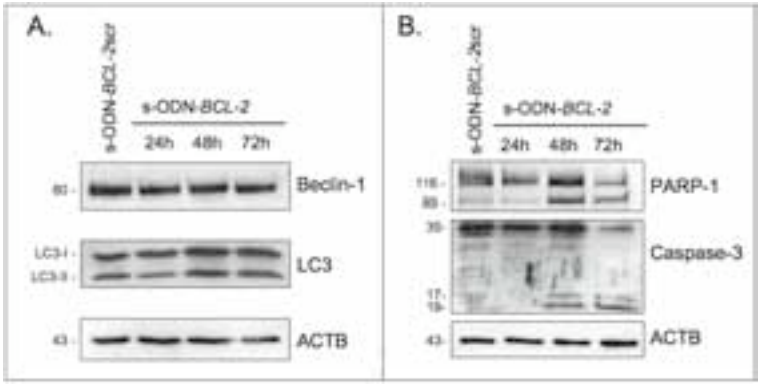

Figure 29. Bcl-2 silencing induces apoptosis but not autophagy in T98G cells. (A). Autophagic markers were not affected by Bcl-2 silencing. Immunoblotting analysis of Beclin-1 and LC3 was performed at 24h intervals within 72h after s-ODN-*BCL-2* transfection. (B). Bcl-2 silencing induced apoptosis. PARP-1 and caspase-3 cleavage were assessed by immunoblotting in T98G s-ODN-*BCL-2* transfected cells. S-ODN-*BCL-2*scr indicates scrambled transfected cells pooled at 24-48-72 h. Molecular weights are expressed in kDa.

6. Discussion

Although the physiological function of PrPC is still unknown, a currently growing literature indicates its increasing importance in cellular protection from internal and external stimuli. The survival-promoting effect of PrPC on neuronal and non-neuronal cells has been observed *in vitro* as well as in *in vivo* studies (Aguzzi et al., 2008a) (see 2.2.6-7): immortalized hippocampal neurons from *Prnp*$^{-/-}$ mice are more susceptible to apoptotic and oxidative stresses independently of Doppel expression (Kim et al., 2004; Kuwahara et al., 1999); ectopic expression of PrPC protects primary human neurons against Bax-mediated cell death (Bounhar et al., 2001); over-expression of PrPC reduces infarct size in rat brain and improves neurological behavior after cerebral ischemia (Shyu et al., 2005); finally, PrPC is able to protect the brain from neurodegeneration induced by the expression of Doppel or by PrPC deletion mutants (Nishida et al., 1999; Shmerling et al., 1998). In addition to these evidences, PrPC over-expression has recently been reported to be associated with the development of tumor resistance to cell death (Antonacopoulou et al., 2008; Diarra-Mehrpour et al., 2004; Du et al., 2005; Han et al., 2002) (see 2.3).

With the aim to assess whether the cellular prion protein exerts a protective role in glioma cells, this thesis has focused on the analysis of the cellular and molecular effects exerted by a *PRNP* targeted antisense phosphorothioate oligonucleotide, named s-ODN3, on T98G glioma cell line.

Many different preclinical and clinical studies have indicated a role for antisense nucleotides as therapeutics for malignant diseases and, in particular for astrocytomas (Caruso et al., 2010; Yao et al., 2009). An antisense oligonucleotide is a single-stranded deoxyribonucleotide (usually 18-20 nucleotides in length) that sequence-specifically hybridizes to the target RNA through Watson-Crick base pairing thus resulting in specific inhibition of gene expression. The mechanism of action of the currently most potent and clinically most advanced antisense oligonucleotides, is based on activation of RNase H, a ubiquitously expressed endonuclease which hydrolyses the RNA strand of the heteroduplex (Jansen and Zangemeister-Wittke, 2002). In addition, gene expression can be inhibited by translational arrest through steric hindrance of ribosomal activity, interference with mRNA maturation by inhibiting splicing and destabilization of pre-mRNA in the nucleus (Kurreck, 2003). Antisense oligonucleotides are not only a useful tool for studies of loss-of-gene function and target validation, but are also highly valuable as a novel therapeutic strategy. Reported targets for antisense ODNs therapy in malignant glioma include those encoding bFGF, c-myc, c-sis, c-erb, c-myb, CD44, platelet-derived growth factor, transforming growth factor-beta, IGF-1, PKC-alpha, tumor necrosis factor,

urokinase, S100 beta protein, Bcl-2, MMP9, telomerase RNA component. Some of them have been approved for Phase I/II clinical brain tumor trials (Tamm and Wagner, 2006). Since oligodeoxynucleotides are vulnerable to nucleases and are rapidly degraded *in vivo*, functionally improved antisense oligonucleotides have been developed by replacing the phosphodiester backbone with a nuclease resistant phosphorothioate backbone. All antisense oligonucleotides currently in clinical trials contain this improved chemistry and combine serum stability, reasonable RNA binding affinity and the ability to activate RNase H (Stahel and Zangemeister-Wittke, 2003).

In this study, three antisense molecules against *PRNP* were employed. s-ODN3 was specifically designed against a portion coding for the octapteptide repeated motif of PrPC (see 2.1.3): in the different employed cells, this region is repeated five times, in a manner similar to human genomic DNA (data not shown). In particular, the repeated motives should improve the stability and efficiency of the specific interaction between the antisense and the target *PRNP* mRNA molecules, thus increasing the probability of the DNA/RNA cleavage by RNAse-H or the better steric interference with PrPC synthesis. As a control of effectiveness of the antisense strategy, s-ODN1 was canonically designed against the beginning of the *PRNP* coding sequence, while s-ODN2 recognized the basic residues (28-34) of the human cellular prion protein. Since s-ODN1,2 and 3 had the same length and a similar G+C content, as a negative control, it was possible to use a single scrambled s-ODN, corresponding to s-ODN3 random sequence. s-ODN3scr did not show any complementarity with the human genome and its transfection did not produce apparent phenotypic effects, even considering different tumor and control cells. The analysis of the effects of s-ODNs transfection in different human glial-tumor, non glial-tumor and normal cells evidenced the ability of s-ODN1 and s-ODN3 to induce a significant decrease in the viability of different glial and non glial-tumor cell lines. This effect was associated with their ability to silence PrPC expression. On the contrary, the lack of phenotype in s-ODN2 transfected cells was associated with the inability of this antisense oligonucleotide to silence PrPC expression.

Being the most effective in PrPC silencing, and the most specific in inducing tumor cell death while having minor effects on normal cells, s-ODN3 was selected for further experiments. In order to analyze the effects of PrPC silencing in the context of gliomas, it was decided to continue the study using the well known and widely employed glial tumor cell line T98G which, in addition, resulted to be one of the most sensitive to s-ODN3 treatment.

In this work it has been demonstrated that s-ODN3 induces an autophagy dependent cell death in T98G cells.

s-ODN3 induced autophagy was initially detected by the appearance of characteristic autophagosomes on transmission electron microscopy, and by the

increase in the number of acidic vesicular organelles as measured by acridine orange staining and FACS analysis. The focal degradation of cytoplasmic areas sequestered by a specialized type of smooth, ribosome free double membrane vesicle, the phagophore, which matures into the prelysosomal autophagosome, is the hallmark of autophagy and can be qualitatively and quantitatively monitored by electron microscopy analysis. The fusion of an autophagosome with an endosome or a lysosome generates an amphisome or an autolysosome, respectively. The early autophagosome is not an acidic compartment, whereas amphisomes and autolysosomes are acidic (Klionsky et al., 2008) and can therefore be detected by vital staining with acidotrophic dyes. In acridine orange stained cells, the acidic compartments in the cell fluoresce bright red, whereas the nucleus and cytoplasm fluoresce bright green and dim red, respectively. Since the intensity of the red fluorescence is proportional to the degree of acidity or the volume of the cellular acidic compartments, or both (Paglin et al., 2001), acridine orange staining allows to monitor the development of acidic vesicular organelles during autophagy (Ito et al., 2006; Iwamaru et al., 2007; Jiang et al., 2007; Kanzawa et al., 2004). However, acidotropic dyes can also be retained in other intracellular acidic compartments, such as lysosomes, endocytic vesicles, portions of the trans-Golgi apparatus, and certain secretory vesicles. Therefore, the intensity of the red fluorescence is not exclusively an indication of autophagic vacuoles and thus this methodology should be used with other autophagic markers (Klionsky et al., 2008).

The involvement of PrPC expression in autophagy regulation was deeply investigated using different autophagic markers. The microtubule associated-protein 1 light chain 3 (LC3) expression was initially evaluated: it exists in two forms: LC3-I, localized in the cytosol, and LC3-II, localized in autophagosomal membranes. During autophagy induction, LC3-I is C-terminally lipidated with phosphatidylethanolamine to form LC3-II, which is essential for the formation of the autophagosome. Although the molecular weight of LC3-II is larger than that of LC3-I, LC3-II migrates faster than LC3-I in SDS-PAGE probably because of its extreme hydrophobicity. Since the amount and localization of LC3-II is closely correlated with the number of autophagosomes, the conversion of LC3-I to LC3-II is a strong biochemical marker for the induction of autophagy (Mizushima, 2004). Using a GFP-LC3 fusion protein it has been observed that s-ODN3 transfection induces the redistribution of LC3 from a cytosolic diffuse pattern to a punctate staining in vacuolar membranes. In addition, immunoblotting analysis of LC3 has highlighted a significant increase in LC3-II isoform as compared to controls. It's important to note that the increase in LC3-II simply indicates the accumulation of autophagosomes but does not guarantee autophagic degradation. Increased LC3-II levels can in fact be associated with either enhanced autophagosome synthesis or reduced autophagosome turnover, perhaps due to delayed trafficking to the lysosomes, reduced fusion between compartments, or impaired lysosomal proteolytic activity. To discern between these two possibilities it is necessary to evaluate LC3 conversion in the presence of lysosomal protease

inhibitors (such as E64d and pepstatin A) or inhibitors of the autophagosome-lysosome fusion (Bafilomycin A1). If the amount of LC3-II further accumulates in the presence of Bafilomycin A1, this would indicate enhancement of the autophagic flux. Importantly, s-ODN3 mediated increase in LC3-II isoform was confirmed after blockage of the fusion of autophagosomes with lysosomes by treatment with BafA1.

The existence of an induced autophagic flux was also confirmed through the analysis of p62 levels. This protein, also called sequestosome 1 (SQSTM1), is an ubiquitin-binding scaffold protein localized to the autophagosome via LC3-interaction and it is therefore specifically degraded by the autophagy–lysosome system. Ablation of autophagy leads to marked accumulation of p62 (Komatsu and Ichimura, 2010). Concordantly, we have reported that after transfection of T98G cells with s-ODN3, p62 levels were significantly decreased compared with s-ODN3scr treatment, thus suggesting a possible s-ODN3-mediated activation of autophagy. As a counterpart, BafA1-mediated blockage of the autophagy process restored p62 levels in s-ODN3 treated cells, indicating that the degradation was lysosomal in nature, consistent with p62 proteolysis in autolysosomes.

Autophagy is known to be regulated by at least two pathways: the class I and class III phopshoinositide 3-kinase (PI3K) pathways. In mammalian cells mTOR complex 1 of the class I PI3K pathway is a negative regulator of autophagy playing an important role upstream of Atg1 complex, which regulates different steps in autophagosome formation; on the contrary, the Beclin-1/Vps34 complex of the class III PI3K is essential for initiating the nucleation of the pre-autophagosome. Beclin-1 interactors include UVRAG, Ambra1 and Bif-1, all indispensable for the activation of autophagy. In addition, in mice and humans, Beclin-1 has been reported to constitutively interact with the anti-apoptotic proteins of the Bcl-2 family (Bcl-2, Bcl-xL, Bcl- w and Mcl-1) (Fimia et al., 2007; Liang et al., 2006a; Takahashi et al., 2007). In contrast to the previously mentioned proteins contained in the Beclin-1 interactome that activate autophagy, Bcl-2 and Bcl-xL act as inhibitors of the autophagic process: induction of autophagy by a variety of different inducers is accompanied by the dissociation of Beclin-1 from Bcl-2 or Bcl-xL (Levine et al., 2008) (see 2.5.1).

One of the hallmark biological aberrations in glioma is the alteration of the PI3K/Akt/mTor pathway (Furnari et al., 2007) whose inhibition has been shown to induce autophagy in human malignant glioma cells (Iwamaru et al., 2007). PrPC silencing through s-ODN3 treatment resulted in an inhibition of mTOR kinase activity, as indicated by the decreased Phospho-4E-BP1/4E-BP1 and Phospho-p70S6K/p70S6K ratios as compared to controls. As expected, blocking autophagy downstream of mTOR, i.e. silencing Beclin-1 and Atg7, did not rescue the phosphorylation status of Phospho-4E-BP1 in s-ODN3 treated cells.

The expression of Beclin-1 was shown to be upregulated in s-ODN3 treated cells suggesting a role for the Beclin-1/Vps34 complex in s-ODN3 induced autophagy.

In order to investigate whether s-ODN3 induced cell death was Beclin-1, or more generally, autophagy dependent, the autophagic pathway was inhibited by Beclin-1 and Atg7 silencing. While Beclin-1 knocking down only partially restored the cell viability of s-ODN3 treated cells, Atg7 silencing inhibited s-ODN3 mediated cell death. These results indicate that autophagy is required for s-ODN3 induced cell death. The minor effect of Beclin-1 silencing as compared to Atg7 could be related to the fact that, being located at the crossroad of autophagy and apoptosis, modulation of Beclin-1 expression could influence not only the autophagic but also the apoptotic pathway. However, both Beclin-1 and Atg7 silencing inhibited autophagy, as demonstrated by the reduction in LC3-I to LC3-II conversion following s-ODN3 treatment.

As reported, PrPC silencing and the increase in Beclin-1 expression were concomitant with a down-regulation of Bcl-2. As mentioned above, by binding to Beclin-1, anti-apoptotic Bcl-2 proteins are able to negatively regulate autophagy. Bcl-2 down-regulation could therefore represent the mechanism by which Beclin-1 can initiate autophagy in s-ODN3 treated cells. A decrease in Bcl-2 levels following PrPC silencing was previously reported by Meslin and collaborators (Meslin et al., 2007b). In this study siRNA mediated down-regulation of PrPC in two breast carcinoma cell lines resistant to TRAIL proapoptotic activity, correlated with a change in Bax localization and a large decrease in the amount of Bcl-2 such that the Bax/Bcl-2 ratio increased (Meslin et al., 2007b). The observed decline in Bcl-2 levels following PrPC silencing is also consistent with previous findings indicating that PrPC acts through Bcl-2. Indeed, the octapeptide repeats in the N-terminal region of PrPC shares a limited similarity with the Bcl-2 homology domain (BH2) of the Bcl-2 protein family members and is essential for the neuroprotective function of PrPC against Bax (Roucou et al., 2005); in addition, PrPC interacts with Bcl-2 in the yeast two-hybrid system (Kurschner and Morgan, 1996), like Bcl-2, PrPC prevents Bax conformational change (Roucou et al., 2005; Roucou et al., 2003) and Bax-mediated cell death (Bounhar et al., 2001), and finally, both PrPC and Bcl-2 expression protect against cell death associated with serum deprivation (Kuwahara et al., 1999) and oxidative stress (Brown et al., 2002).

Since, given its anti-apoptotic protective role, there is evidence that specific inhibition of Bcl-2 may alone be sufficient to sensitize various types of cancers to chemotherapy (Kögel et al., 2010), in order to evaluate the contribution of Bcl-2 down-regulation in s-ODN3 induced cell death, the effects of Bcl-2 silencing were investigated. To this purpose, a validated *BCL-2* targeted antisense phosphorothioate oligonucleotide (Oblimersen – Genasense) was employed. Oblimersen has been extensively studied in clinical trials, none of which investigated its impact on glioma. In a recent phase III study, Oblimersen combined with fludarabine/cyclophosphamide was shown to prolong survival of a subset of patients with refractory or relapsed chronic lymphocytic leukemia (CLL) (O'Brien et al., 2009). Oblimersen also holds

promise for the treatment of malignant melanoma (Di Cresce and Koropatnick, 2010).

The evidences that s-ODN-*BCL-2* transfection induced a minor decrease in cellular viability as compared to s-ODN3, and that s-ODN1 treatment decreases cell viability without affecting Bcl-2 levels, suggest that the silencing of Bcl-2 in s-ODN3 treated cells is not indispensable for PrPC silencing mediated cell death but is rather a consequence of s-ODN3 mediated prion down-regulation. The lack of Bcl-2 down-regulation following s-ODN1 treatment in T98G cells could be related to the lower PrPC silencing ability of this antisense as compared to s-ODN3 in this cell line.

Worthy of note is the fact that, despite down-regulating both Bcl-2 and PrPC, s-ODN-*BCL-2* treatment induces apoptosis rather than autophagy in T98G cells. This evidence could be explained by the fact that autophagy/apoptosis control may be dictated by distinct thresholds: activation of BH3-only proteins at a low, sub-apoptotic level (that fails to engage the activation of pro-apopotic multidomain proteins such as Bax and Bak) would induce autophagy. Only when the buffering capacity of anti-apoptotic Bcl-2 proteins is exhausted would the activation of BH3-only proteins succeed in stimulating Bax or Bak and thereby induce apoptotic cell death (Levine et al., 2008). S-ODN-*BCL-2* could therefore be more efficient in moving the equilibrium between anti- and pro-apoptotic proteins of the Bcl-2 family toward the latter thus inducing apoptosis rather than autophagy. In addition, the minor extent of PrPC down-regulation mediated by Oblimersen may contribute to the preference of activating apoptosis and not autophagy.

In conclusion, the results here presented evidence that PrPC silencing induces autophagy dependent cell death in malignant glial tumor cells thus suggesting a cytoprotective role of the cellular prion protein in the context of glial tumor. The mechanism by which PrPC is able to modulate autophagy induction is still to be determined but it involves inhibition of the PI3K/Akt/mTOR pathway and the activation of the Beclin-1/Vps34 complex both by decreasing the level of its negative regulator Bcl-2 and by increasing Beclin-1 levels. Since both the activation of PI3K/Akt/mTOR pathway and the over-expression of Bcl-2 are hallmarks of glial tumors, the ability of PrPC silencing to revert these conditions and therefore sensitize glioma cells to autophagy induction is noteworthy. Even if the role of autophagy in cancer is still controversial, some neoplasms, including glioblastoma, are known to benefit from autophagy enhancement. Anti-prion antisense molecules may therefore represent a relatively selective strategy for the treatment of glioblastoma multiforme through the activation of autophagy-dependent processes that might lead to tumor cell death.

7. Conclusions and perspectives

The work here presented shows for the first time that the cellular prion protein exerts a cytoprotective role in the context of glial tumor cells.

PrPC silencing by antisense phosphorothioate oligonucleotides has been demonstrated to induce cell death in different human glial-tumor and non glial-tumor cell lines. Among the three different s-ODNs employed, s-ODN3 was identified as the most effective in PrPC silencing and the most selective in inducing tumor cell death without significantly affecting normal cells.

s-ODN3 mediated cell death was not associated with apoptotic events but was dependent on autophagy activation, as revealed by the observation of typical autophagic features, such as detection of autophagosome by electron microscopy and AVOs by acridine orange staining, and the alteration in specific autophagic biochemical markers such as LC3 localization and conversion from isoform I to isoform II, and p62 degradation.

s-ODN3 induced autophagy was found to be activated through inhibition of PI3K/Akt/mTOR pathway - as revealed by the alteration of the phosphorilation status of two targets of mTOR kinase activity i.e. p70S6K and 4E-BP1- and activation of Beclin-1/Vps34 complex. This latter effect is exerted by up-regulation of Beclin-1 expression and concomitant down-regulation of the Beclin-1 negative regulatior Bcl-2.

Beclin-1 plays a significant role in the activation of the autophagic process following PrPC silencing: knocking down of Beclin-1 by specific siRNAs inhibits autophagy and significantly reduces the ability of s-ODN3 to induce cell death in T98G cells. A more efficient inhibition of autophagy by Atg7 silencing almost inhibits s-ODN3 mediated cell death thus demonstrating the autophagy dependent nature of PrPC silencing induced cell death.

The existence of a possible functional link between PrPC and Bcl-2 was also proposed: not only, as previously observed by Meslin and collaborators (Meslin et al., 2007b), PrPC silencing induced Bcl-2 down-regulation but, in addition, here it has been shown that antisense mediated Bcl-2 silencing induced apoptotic cell death in T98G cells and decreased PrPC levels.

Although PrPC and Bcl-2 interaction was demonstrated in 1996 (Kurschner and Morgan, 1996), the functional link between these two proteins is still to be explored. To further investigate this subject, future work might analyze the effects of Bcl-2 over-expression on s-ODN3 mediated cell death. It would be interesting to investigate whether an increase in Bcl-2 levels could counteract PrPC down-regulation

mediated cell death. In addition, since Bcl-2–PrPC interaction has been demonstrated only by yeast two hybrid screen, additional methods are required to confirm this interaction and to investigate its localization within the cell.

Finally, having demonstrated that PrPC exerts a cytoprotective activity in T98G glioma cells, further work might be directed toward the analysis of prion protein expression in bioptic specimens of human gliomas from different tumoral grades, to eventually correlate PrPC expression profiles with the malignancy grading and with clinical data.

References

Abounader R, Laterra J. 2005. Scatter factor/hepatocyte growth factor in brain tumor growth and angiogenesis. Neuro Oncol 7:436-451.

Aguzzi A, Baumann F, Bremer J. 2008a. The prion's elusive reason for being. Annu Rev Neurosci 31:439-477.

Aguzzi A, Calella A. 2009. Prions: protein aggregation and infectious diseases. Physiol Rev 89:1105-1152.

Aguzzi A, Polymenidou M. 2004. Mammalian prion biology: one century of evolving concepts. Cell 116:313-327.

Aguzzi A, Sigurdson C, Heikenwaelder M. 2008b. Molecular mechanisms of prion pathogenesis. Annu Rev Pathol 3:11-40.

Anantharam V, Kanthasamy A, Choi C, Martin D, Latchoumycandane C, Richt J, Kanthasamy A. 2008. Opposing roles of prion protein in oxidative stress- and ER stress-induced apoptotic signaling. Free Radic Biol Med 45:1530-1541.

Andre F, Pusztai L. 2006. Molecular classification of breast cancer: implications for selection of adjuvant chemotherapy. Nat Clin Pract Oncol 3:621-632.

Antonacopoulou A, Grivas P, Skarlas L, Kalofonos M, Scopa C, Kalofonos H. 2008. POLR2F, ATP6V0A1 and PRNP expression in colorectal cancer: new molecules with prognostic significance? Anticancer Res 28:1221-1227.

Antonacopoulou A, Palli M, Marousi S, Dimitrakopoulos F, Kyriakopoulou U, Tsamandas A, Scopa C, Papavassiliou A, Kalofonos H. 2010. Prion protein expression and the M129V polymorphism of the PRNP gene in patients with colorectal cancer. Mol Carcinog 49:693-699.

Arantes C, Nomizo R, Lopes M, Hajj G, Lima F, Martins V. 2009. Prion protein and its ligand stress inducible protein 1 regulate astrocyte development. Glia 57:1439-1449.

Argyriou AA, Kalofonos HP. 2009. Molecularly targeted therapies for malignant gliomas. Mol Med 15:115-122.

Armendariz A, Gonzalez M, Loguinov A, Vulpe C. 2004. Gene expression profiling in chronic copper overload reveals upregulation of Prnp and App. Physiol Genomics 20:45-54.

Assanah M, Lochhead R, Ogden A, Bruce J, Goldman J, Canoll P. 2006. Glial progenitors in adult white matter are driven to form malignant gliomas by platelet-derived growth factor-expressing retroviruses. J Neurosci 26:6781-6790.

Atarashi R, Nishida N, Shigematsu K, Goto S, Kondo T, Sakaguchi S, Katamine S. 2003. Deletion of N-terminal residues 23-88 from prion protein (PrP) abrogates the potential to rescue PrP-deficient mice from PrP-like protein/doppel-induced Neurodegeneration. J Biol Chem 278:28944-28949.

Azzalin A, Sbalchiero E, Barbieri G, Palumbo S, Muzzini C, Comincini S. 2008. The doppel (Dpl) protein influences in vitro migration capability in astrocytoma-derived cells. Cell Oncol 30:491-501.

Bacciocchi G, Gibelli N, Zibera C, Pedrazzoli P, Bergamaschi G, De Piceis Polver P, Danova M, Mazzini G, Palomba L, Tupler R. 1992. Establishment and characterization of two cell lines derived from human glioblastoma multiforme. Anticancer Res 12:853-861.

Barbashina V, Salazar P, Holland E, Rosenblum M, Ladanyi M. 2005. Allelic losses at 1p36 and 19q13 in gliomas: correlation with histologic classification, definition of a 150-kb minimal deleted region on 1p36, and evaluation of CAMTA1 as a candidate tumor suppressor gene. Clin Cancer Res 11:1119-1128.

Barrow P, Holmgren C, Tapper A, Jefferys J. 1999. Intrinsic physiological and morphological properties of principal cells of the hippocampus and neocortex in hamsters infected with scrapie. Neurobiol Dis 6:406-423.

Berens M, Giese A. 1999. "...those left behind." Biology and oncology of invasive glioma cells. Neoplasia 1:208-219.

Beringue V, Mallinson G, Kaisar M, Tayebi M, Sattar Z, Jackson G, Anstee D, Collinge J, Hawke S. 2003. Regional heterogeneity of cellular prion protein isoforms in the mouse brain. Brain 126:2065-2073.

Bessen R, Marsh R. 1994. Distinct PrP properties suggest the molecular basis of strain variation in transmissible mink encephalopathy. J Virol 68:7859-7868.

Bessen R, Raymond G, Caughey B. 1997. In situ formation of protease-resistant prion protein in transmissible spongiform encephalopathy-infected brain slices. J Biol Chem 272:15227-15231.

Bjornsti MA, Houghton PJ. 2004. The TOR pathway: a target for cancer therapy. Nat Rev Cancer 4:335-348.

Bobo R, Laske D, Akbasak A, Morrison P, Dedrick R, Oldfield E. 1994. Convection-enhanced delivery of macromolecules in the brain. Proc Natl Acad Sci U S A 91:2076-2080.

Bonnet S, Archer S, Allalunis-Turner J, Haromy A, Beaulieu C, Thompson R, Lee C, Lopaschuk G, Puttagunta L, Harry G, Hashimoto K, Porter C, Andrade M, Thebaud B, Michelakis E. 2007. A mitochondria-K+ channel axis is suppressed in cancer and its normalization promotes apoptosis and inhibits cancer growth. Cancer Cell 11:37-51.

Bouillet P, Strasser A. 2002. Bax and Bak: back-bone of T cell death. Nat Immunol 3:893-894.

Bounhar Y, Zhang Y, Goodyer C, LeBlanc A. 2001. Prion protein protects human neurons against Bax-mediated apoptosis. J Biol Chem 276:39145-39149.

Brandner S, Raeber A, Sailer A, Blättler T, Fischer M, Weissmann C, Aguzzi A. 1996. Normal host prion protein (PrPC) is required for scrapie spread within the central nervous system. Proc Natl Acad Sci U S A 93:13148-13151.

Brandsma D, Dorlo T, Haanen J, Beijnen J, Boogerd W. 2010. Severe encephalopathy and polyneuropathy induced by dichloroacetate. J Neurol.

Bredel M, Scholtens D, Harsh G, Bredel C, Chandler J, Renfrow J, Yadav A, Vogel H, Scheck A, Tibshirani R, Sikic B. 2009. A network model of a cooperative genetic landscape in brain tumors. JAMA 302:261-275.

Bredesen D, Rao R, Mehlen P. 2006. Cell death in the nervous system. Nature 443:796-802.

Brenner D, Mak T. 2009. Mitochondrial cell death effectors. Curr Opin Cell Biol 21:871-877.

Breuleux M, Klopfenstein M, Stephan C, Doughty C, Barys L, Maira S, Kwiatkowski D, Lane H. 2009. Increased AKT S473 phosphorylation after mTORC1 inhibition is rictor dependent and does not predict tumor cell response to PI3K/mTOR inhibition. Mol Cancer Ther 8:742-753.

Brown D, Nicholas R, Canevari L. 2002. Lack of prion protein expression results in a neuronal phenotype sensitive to stress. J Neurosci Res 67:211-224.

Brown D, Schulz-Schaeffer W, Schmidt B, Kretzschmar H. 1997. Prion protein-deficient cells show altered response to oxidative stress due to decreased SOD-1 activity. Exp Neurol 146:104-112.

Brown D, Wong B, Hafiz F, Clive C, Haswell S, Jones I. 1999. Normal prion protein has an activity like that of superoxide dismutase. Biochem J 344 Pt 1:1-5.

Büeler H, Aguzzi A, Sailer A, Greiner R, Autenried P, Aguet M, Weissmann C. 1993. Mice devoid of PrP are resistant to scrapie. Cell 73:1339-1347.

Büeler H, Fischer M, Lang Y, Bluethmann H, Lipp H, DeArmond S, Prusiner S, Aguet M, Weissmann C. 1992. Normal development and behaviour of mice lacking the neuronal cell-surface PrP protein. Nature 356:577-582.

Cabral A, Lee K, Martins V. 2002. Regulation of the cellular prion protein gene expression depends on chromatin conformation. J Biol Chem 277:5675-5682.

Campana V, Sarnataro D, Zurzolo C. 2005. The highways and byways of prion protein trafficking. Trends Cell Biol 15:102-111.

Carleton A, Tremblay P, Vincent J, Lledo P. 2001. Dose-dependent, prion protein (PrP)-mediated facilitation of excitatory synaptic transmission in the mouse hippocampus. Pflugers Arch 442:223-229.

Caruso G, Caffo M, Raudino G, Alafaci C, Salpietro F, Tomasello F. 2010. Antisense oligonucleotides as innovative therapeutic strategy in the treatment of high-grade gliomas. Recent Pat CNS Drug Discov 5:53-69.

Castedo M, Ferri K, Kroemer G. 2002. Mammalian target of rapamycin (mTOR): pro- and anti-apoptotic. Cell Death Differ 9:99-100.

Caughey B, Raymond G, Bessen R. 1998. Strain-dependent differences in beta-sheet conformations of abnormal prion protein. J Biol Chem 273:32230-32235.

Chakravarti A, Zhai G, Suzuki Y, Sarkesh S, Black P, Muzikansky A, Loeffler J. 2004. The prognostic significance of phosphatidylinositol 3-kinase pathway activation in human gliomas. J Clin Oncol 22:1926-1933.

Chen R, Knez J, Merrick W, Medof M. 2001. Comparative efficiencies of C-terminal signals of native glycophosphatidylinositol (GPI)-anchored proproteins in conferring GPI-anchoring. J Cell Biochem 84:68-83.

Chen S, Mangé A, Dong L, Lehmann S, Schachner M. 2003. Prion protein as trans-interacting partner for neurons is involved in neurite outgrowth and neuronal survival. Mol Cell Neurosci 22:227-233.

Chesebro B, Trifilo M, Race R, Meade-White K, Teng C, LaCasse R, Raymond L, Favara C, Baron G, Priola S, Caughey B, Masliah E, Oldstone M. 2005. Anchorless prion protein results in infectious amyloid disease without clinical scrapie. Science 308:1435-1439.

Chiarini L, Freitas A, Zanata S, Brentani R, Martins V, Linden R. 2002. Cellular prion protein transduces neuroprotective signals. EMBO J 21:3317-3326.

Chonghaile T, Letai A. 2008. Mimicking the BH3 domain to kill cancer cells. Oncogene 27 Suppl 1:S149-157.

Clinton J, Forsyth C, Royston M, Roberts G. 1993. Synaptic degeneration is the primary neuropathological feature in prion disease: a preliminary study. Neuroreport 4:65-68.

Colling S, Collinge J, Jefferys J. 1996. Hippocampal slices from prion protein null mice: disrupted Ca(2+)-activated K+ currents. Neurosci Lett 209:49-52.

Colling S, Khana M, Collinge J, Jefferys J. 1997. Mossy fibre reorganization in the hippocampus of prion protein null mice. Brain Res 755:28-35.

Collinge J, Whittington M, Sidle K, Smith C, Palmer M, Clarke A, Jefferys J. 1994. Prion protein is necessary for normal synaptic function. Nature 370:295-297.

Comincini S, Chiarelli LR, Zelini P, Del Vecchio I, Azzalin A, Arias A, Ferrara V, Rognoni P, Dipoto A, Nano R, Valentini G, Ferretti L. 2006. Nuclear mRNA retention and aberrant doppel protein expression in human astrocytic tumor cells. Oncol Rep 16:1325-1332.

Comincini S, Facoetti A, Del Vecchio I, Peoc'h K, Laplanche JL, Magrassi L, Ceroni M, Ferretti L, Nano R. 2004. Differential expression of the prion-like protein doppel gene (PRND) in astrocytomas: a new molecular marker potentially involved in tumor progression. Anticancer Res 24:1507-1517.

Comincini S, Ferrara V, Arias A, Malovini A, Azzalin A, Ferretti L, Benericetti E, Cardarelli M, Gerosa M, Passarin M, Turazzi S, Bellazzi R. 2007. Diagnostic value of PRND gene expression profiles in astrocytomas: relationship to tumor grades of malignancy. Oncol Rep 17:989-996.

Criado J, Sánchez-Alavez M, Conti B, Giacchino J, Wills D, Henriksen S, Race R, Manson J, Chesebro B, Oldstone M. 2005. Mice devoid of prion protein have cognitive deficits that are rescued by reconstitution of PrP in neurons. Neurobiol Dis 19:255-265.

Cuneo K, Tu T, Geng L, Fu A, Hallahan D, Willey C. 2007. HIV protease inhibitors enhance the efficacy of irradiation. Cancer Res 67:4886-4893.

Daido S, Kanzawa T, Yamamoto A, Takeuchi H, Kondo Y, Kondo S. 2004. Pivotal role of the cell death factor BNIP3 in ceramide-induced autophagic cell death in malignant glioma cells. Cancer Res 64:4286-4293.

Dalby K, Tekedereli I, Lopez-Berestein G, Ozpolat B. 2010. Targeting the prodeath and prosurvival functions of autophagy as novel therapeutic strategies in cancer. Autophagy 6:322-329.

Daniel F, Legrand A, Pessayre D, Borrega-Pires F, Mbida L, Lardeux B, Degott C, van Nhieu J, Bernuau D. 2007. Beclin 1 mRNA strongly correlates with Bcl-XLmRNA expression in human hepatocellular carcinoma. Cancer Invest 25:226-231.

Dash R, Richards J, Su Z, Bhutia S, Azab B, Rahmani M, Dasmahapatra G, Yacoub A, Dent P, Dmitriev I, Curiel D, Grant S, Pellecchia M, Reed J, Sarkar D, Fisher P. 2010. Mechanism by which Mcl-1 regulates cancer-specific apoptosis triggered by mda-7/IL-24, an IL-10-related cytokine. Cancer Res 70:5034-5045.

Demuth T, Berens M. 2004. Molecular mechanisms of glioma cell migration and invasion. J Neurooncol 70:217-228.

Dent P, Yacoub A, Park M, Sarkar D, Shah K, Curiel D, Grant S, Fisher P. 2008. Searching for a cure: gene therapy for glioblastoma. Cancer Biol Ther 7:1335-1340.

Devary Y, Gottlieb R, Smeal T, Karin M. 1992. The mammalian ultraviolet response is triggered by activation of Src tyrosine kinases. Cell 71:1081-1091.

Deveraux Q, Reed J. 1999. IAP family proteins--suppressors of apoptosis. Genes Dev 13:239-252.

Di Cresce C, Koropatnick J. 2010. Antisense Treatment in Human Prostate Cancer and Melanoma. Curr Cancer Drug Targets.

Diarra-Mehrpour M, Arrabal S, Jalil A, Pinson X, Gaudin C, Piétu G, Pitaval A, Ripoche H, Eloit M, Dormont D, Chouaib S. 2004. Prion protein prevents human breast carcinoma cell line from tumor necrosis factor alpha-induced cell death. Cancer Res 64:719-727.

Drisaldi B, Coomaraswamy J, Mastrangelo P, Strome B, Yang J, Watts J, Chishti M, Marvi M, Windl O, Ahrens R, Major F, Sy M, Kretzschmar H, Fraser P, Mount H, Westaway D. 2004. Genetic mapping of activity determinants within cellular prion proteins: N-terminal modules in PrPC offset pro-apoptotic activity of the Doppel helix B/B' region. J Biol Chem 279:55443-55454.

Drisaldi B, Stewart R, Adles C, Stewart L, Quaglio E, Biasini E, Fioriti L, Chiesa R, Harris D. 2003. Mutant PrP is delayed in its exit from the endoplasmic reticulum, but neither wild-type nor mutant PrP undergoes retrotranslocation prior to proteasomal degradation. J Biol Chem 278:21732-21743.

Du C, Fang M, Li Y, Li L, Wang X. 2000. Smac, a mitochondrial protein that promotes cytochrome c-dependent caspase activation by eliminating IAP inhibition. Cell 102:33-42.

Du J, Pan Y, Shi Y, Guo C, Jin X, Sun L, Liu N, Qiao T, Fan D. 2005. Overexpression and significance of prion protein in gastric cancer and multidrug-resistant gastric carcinoma cell line SGC7901/ADR. Int J Cancer 113:213-220.

Eisenberg-Lerner A, Kimchi A. 2009. The paradox of autophagy and its implication in cancer etiology and therapy. Apoptosis 14:376-391.

Fallaux F, Kranenburg O, Cramer S, Houweling A, Van Ormondt H, Hoeben R, Van Der Eb A. 1996. Characterization of 911: a new helper cell line for the titration and propagation of early region 1-deleted adenoviral vectors. Hum Gene Ther 7:215-222.

Fan Q, Cheng C, Nicolaides T, Hackett C, Knight Z, Shokat K, Weiss W. 2007. A dual phosphoinositide-3-kinase alpha/mTOR inhibitor cooperates with blockade of epidermal growth factor receptor in PTEN-mutant glioma. Cancer Res 67:7960-7965.

Favre-Krey L, Theodoridou M, Boukouvala E, Panagiotidis C, Papadopoulos A, Sklaviadis T, Krey G. 2007. Molecular characterization of a cDNA from the gilthead sea bream (Sparus aurata) encoding a fish prion protein. Comp Biochem Physiol B Biochem Mol Biol 147:566-573.

Ferrer I, Rivera R, Blanco R, Martí E. 1999. Expression of proteins linked to exocytosis and neurotransmission in patients with Creutzfeldt-Jakob disease. Neurobiol Dis 6:92-100.

Fimia G, Stoykova A, Romagnoli A, Giunta L, Di Bartolomeo S, Nardacci R, Corazzari M, Fuoco C, Ucar A, Schwartz P, Gruss P, Piacentini M, Chowdhury K, Cecconi F. 2007. Ambra1 regulates autophagy and development of the nervous system. Nature 447:1121-1125.

Frederick L, Wang X, Eley G, James C. 2000. Diversity and frequency of epidermal growth factor receptor mutations in human glioblastomas. Cancer Res 60:1383-1387.

Fulda S, Wick W, Weller M, Debatin K. 2002. Smac agonists sensitize for Apo2L/TRAIL- or anticancer drug-induced apoptosis and induce regression of malignant glioma in vivo. Nat Med 8:808-815.

Furnari F, Fenton T, Bachoo R, Mukasa A, Stommel J, Stegh A, Hahn W, Ligon K, Louis D, Brennan C, Chin L, DePinho R, Cavenee W. 2007. Malignant astrocytic glioma: genetics, biology, and paths to treatment. Genes Dev 21:2683-2710.

Gabriel J, Oesch B, Kretzschmar H, Scott M, Prusiner S. 1992. Molecular cloning of a candidate chicken prion protein. Proc Natl Acad Sci U S A 89:9097-9101.

García-Arencibia M, Hochfeld W, Toh P, Rubinsztein D. 2010. Autophagy, a guardian against neurodegeneration. Semin Cell Dev Biol 21:691-698.

Gauczynski S, Peyrin J, Haïk S, Leucht C, Hundt C, Rieger R, Krasemann S, Deslys J, Dormont D, Lasmézas C, Weiss S. 2001. The 37-kDa/67-kDa laminin receptor acts as the cell-surface receptor for the cellular prion protein. EMBO J 20:5863-5875.

Gladson C, Prayson R, Liu W. 2010. The pathobiology of glioma tumors. Annu Rev Pathol 5:33-50.

Gohel C, Grigoriev V, Escaig-Haye F, Lasmézas C, Deslys J, Langeveld J, Akaaboune M, Hantaï D, Fournier J. 1999. Ultrastructural localization of cellular prion protein (PrPc) at the neuromuscular junction. J Neurosci Res 55:261-267.

Goudar R, Shi Q, Hjelmeland M, Keir S, McLendon R, Wikstrand C, Reese E, Conrad C, Traxler P, Lane H, Reardon D, Cavenee W, Wang X, Bigner D, Friedman H, Rich J. 2005. Combination therapy of inhibitors of epidermal growth factor receptor/vascular endothelial growth factor receptor 2 (AEE788) and the mammalian target of rapamycin (RAD001) offers improved glioblastoma tumor growth inhibition. Mol Cancer Ther 4:101-112.

Gozuacik D, Kimchi A. 2007. Autophagy and cell death. Curr Top Dev Biol 78:217-245.

Graner E, Mercadante A, Zanata S, Forlenza O, Cabral A, Veiga S, Juliano M, Roesler R, Walz R, Minetti A, Izquierdo I, Martins V, Brentani R. 2000. Cellular prion protein binds laminin and mediates neuritogenesis. Brain Res Mol Brain Res 76:85-92.

Green D. 2006. At the gates of death. Cancer Cell 9:328-330.

Green DR, Evan GI. 2002. A matter of life and death. Cancer Cell 1:19-30.

Halliwell B. 2006. Oxidative stress and neurodegeneration: where are we now? J Neurochem 97:1634-1658.

Han H, Bearss D, Browne L, Calaluce R, Nagle R, Von Hoff D. 2002. Identification of differentially expressed genes in pancreatic cancer cells using cDNA microarray. Cancer Res 62:2890-2896.

Hanahan D, Weinberg RA. 2000. The hallmarks of cancer. Cell 100:57-70.

Hao C, Beguinot F, Condorelli G, Trencia A, Van Meir E, Yong V, Parney I, Roa W, Petruk K. 2001. Induction and intracellular regulation of tumor necrosis factor-related apoptosis-inducing ligand (TRAIL) mediated apotosis in human malignant glioma cells. Cancer Res 61:1162-1170.

He C, Klionsky D. 2009. Regulation mechanisms and signaling pathways of autophagy. Annu Rev Genet 43:67-93.

Hegde R, Mastrianni J, Scott M, DeFea K, Tremblay P, Torchia M, DeArmond S, Prusiner S, Lingappa V. 1998. A transmembrane form of the prion protein in neurodegenerative disease. Science 279:827-834.

Hengartner MO. 2000. The biochemistry of apoptosis. Nature 407:770-776.

Henson J, Schnitker B, Correa K, von Deimling A, Fassbender F, Xu H, Benedict W, Yandell D, Louis D. 1994. The retinoblastoma gene is involved in malignant progression of astrocytomas. Ann Neurol 36:714-721.

Herlyn M. 2006. Molecular targets in melanoma: strategies and challenges for diagnosis and therapy. Int J Cancer 118:523-526.

Hetschko H, Voss V, Horn S, Seifert V, Prehn J, Kögel D. 2008. Pharmacological inhibition of Bcl-2 family members reactivates TRAIL-induced apoptosis in malignant glioma. J Neurooncol 86:265-272.

Hjelmeland A, Lattimore K, Fee B, Shi Q, Wickman S, Keir S, Hjelmeland M, Batt D, Bigner D, Friedman H, Rich J. 2007. The combination of novel low molecular weight inhibitors of RAF (LBT613) and target of rapamycin (RAD001) decreases glioma proliferation and invasion. Mol Cancer Ther 6:2449-2457.

Hsiao K, Dlouhy S, Farlow M, Cass C, Da Costa M, Conneally P, Hodes M, Ghetti B, Prusiner S. 1992. Mutant prion proteins in Gerstmann-Sträussler-Scheinker disease with neurofibrillary tangles. Nat Genet 1:68-71.

Huse J, Holland E. 2010. Targeting brain cancer: advances in the molecular pathology of malignant glioma and medulloblastoma. Nat Rev Cancer 10:319-331.

Hutter G, Heppner F, Aguzzi A. 2003. No superoxide dismutase activity of cellular prion protein in vivo. Biol Chem 384:1279-1285.

Inoki K, Ouyang H, Zhu T, Lindvall C, Wang Y, Zhang X, Yang Q, Bennett C, Harada Y, Stankunas K, Wang C, He X, MacDougald O, You M, Williams B, Guan K. 2006. TSC2 integrates Wnt and energy signals via a coordinated phosphorylation by AMPK and GSK3 to regulate cell growth. Cell 126:955-968.

Itakura E, Kishi C, Inoue K, Mizushima N. 2008. Beclin 1 forms two distinct phosphatidylinositol 3-kinase complexes with mammalian Atg14 and UVRAG. Mol Biol Cell 19:5360-5372.

Ito H, Aoki H, Kühnel F, Kondo Y, Kubicka S, Wirth T, Iwado E, Iwamaru A, Fujiwara K, Hess K, Lang F, Sawaya R, Kondo S. 2006. Autophagic cell death of malignant glioma cells induced by a conditionally replicating adenovirus. J Natl Cancer Inst 98:625-636.

Iwamaru A, Kondo Y, Iwado E, Aoki H, Fujiwara K, Yokoyama T, Mills G, Kondo S. 2007. Silencing mammalian target of rapamycin signaling by small interfering RNA enhances rapamycin-induced autophagy in malignant glioma cells. Oncogene 26:1840-1851.

Jahreiss L, Menzies F, Rubinsztein D. 2008. The itinerary of autophagosomes: from peripheral formation to kiss-and-run fusion with lysosomes. Traffic 9:574-587.

Jansen B, Zangemeister-Wittke U. 2002. Antisense therapy for cancer--the time of truth. Lancet Oncol 3:672-683.

Jeffrey M, Halliday W, Bell J, Johnston A, MacLeod N, Ingham C, Sayers A, Brown D, Fraser J. 2000. Synapse loss associated with abnormal PrP precedes neuronal degeneration in the scrapie-infected murine hippocampus. Neuropathol Appl Neurobiol 26:41-54.

Jemal A, Siegel R, Ward E, Murray T, Xu J, Thun M. 2007. Cancer statistics, 2007. CA Cancer J Clin 57:43-66.

Jiang H, Gomez-Manzano C, Aoki H, Alonso M, Kondo S, McCormick F, Xu J, Kondo Y, Bekele B, Colman H, Lang F, Fueyo J. 2007. Examination of the therapeutic potential of Delta-24-RGD in brain tumor stem cells: role of autophagic cell death. J Natl Cancer Inst 99:1410-1414.

Jones C, Klewpatinond M, Abdelraheim S, Brown D, Viles J. 2005a. Probing copper2+ binding to the prion protein using diamagnetic nickel2+ and 1H NMR: the unstructured N terminus facilitates the coordination of six copper2+ ions at physiological concentrations. J Mol Biol 346:1393-1407.

Jones S, Batchelor M, Bhelt D, Clarke A, Collinge J, Jackson G. 2005b. Recombinant prion protein does not possess SOD-1 activity. Biochem J 392:309-312.

Juanes M, Elvira G, García-Grande A, Calero M, Gasset M. 2009. Biosynthesis of prion protein nucleocytoplasmic isoforms by alternative initiation of translation. J Biol Chem 284:2787-2794.

Kaiser S, Park Y, Franklin J, Halberg R, Yu M, Jessen W, Freudenberg J, Chen X, Haigis K, Jegga A, Kong S, Sakthivel B, Xu H, Reichling T, Azhar M et al. 2007. Transcriptional recapitulation and subversion of embryonic colon development by mouse colon tumor models and human colon cancer. Genome Biol 8:R131.

Kanaani J, Prusiner S, Diacovo J, Baekkeskov S, Legname G. 2005. Recombinant prion protein induces rapid polarization and development of synapses in embryonic rat hippocampal neurons in vitro. J Neurochem 95:1373-1386.

Kang M, Reynolds C. 2009. Bcl-2 inhibitors: targeting mitochondrial apoptotic pathways in cancer therapy. Clin Cancer Res 15:1126-1132.

Kanzawa T, Germano I, Komata T, Ito H, Kondo Y, Kondo S. 2004. Role of autophagy in temozolomide-induced cytotoxicity for malignant glioma cells. Cell Death Differ 11:448-457.

Kanzawa T, Zhang L, Xiao L, Germano I, Kondo Y, Kondo S. 2005. Arsenic trioxide induces autophagic cell death in malignant glioma cells by upregulation of mitochondrial cell death protein BNIP3. Oncogene 24:980-991.

Karantza-Wadsworth V, Patel S, Kravchuk O, Chen G, Mathew R, Jin S, White E. 2007. Autophagy mitigates metabolic stress and genome damage in mammary tumorigenesis. Genes Dev 21:1621-1635.

Karin M, Cao Y, Greten F, Li Z. 2002. NF-kappaB in cancer: from innocent bystander to major culprit. Nat Rev Cancer 2:301-310.

Katayama M, Kawaguchi T, Berger M, Pieper R. 2007. DNA damaging agent-induced autophagy produces a cytoprotective adenosine triphosphate surge in malignant glioma cells. Cell Death Differ 14:548-558.

Key T. 2001. Glycemic index, hyperinsulinemia, and breast cancer risk. Ann Oncol 12:1507-1509.

Kim B, Lee H, Choi J, Kim J, Choi E, Carp R, Kim Y. 2004. The cellular prion protein (PrPC) prevents apoptotic neuronal cell death and mitochondrial dysfunction induced by serum deprivation. Brain Res Mol Brain Res 124:40-50.

Kim H, Huang W, Jiang X, Pennicooke B, Park P, Johnson M. 2010. Integrative genome analysis reveals an oncomir/oncogene cluster regulating glioblastoma survivorship. Proc Natl Acad Sci U S A 107:2183-2188.

Klionsky D, Abeliovich H, Agostinis P, Agrawal D, Aliev G, Askew D, Baba M, Baehrecke E, Bahr B, Ballabio A, Bamber B, Bassham D, Bergamini E, Bi X, Biard-Piechaczyk M et al. 2008. Guidelines for the use and interpretation of assays for monitoring autophagy in higher eukaryotes. Autophagy 4:151-175.

Knaus K, Morillas M, Swietnicki W, Malone M, Surewicz W, Yee V. 2001. Crystal structure of the human prion protein reveals a mechanism for oligomerization. Nat Struct Biol 8:770-774.

Kocisko D, Come J, Priola S, Chesebro B, Raymond G, Lansbury P, Caughey B. 1994. Cell-free formation of protease-resistant prion protein. Nature 370:471-474.

Komatsu M, Ichimura Y. 2010. Physiological significance of selective degradation of p62 by autophagy. FEBS Lett 584:1374-1378.

Koneri K, Goi T, Hirono Y, Katayama K, Yamaguchi A. 2007. Beclin 1 gene inhibits tumor growth in colon cancer cell lines. Anticancer Res 27:1453-1457.

Krakstad C, Chekenya M. 2010. Survival signalling and apoptosis resistance in glioblastomas: opportunities for targeted therapeutics. Mol Cancer 9:135.

Kretzschmar H, Stowring L, Westaway D, Stubblebine W, Prusiner S, Dearmond S. 1986. Molecular cloning of a human prion protein cDNA. DNA 5:315-324.

Kurreck J. 2003. Antisense technologies. Improvement through novel chemical modifications. Eur J Biochem 270:1628-1644.

Kurschner C, Morgan J. 1996. Analysis of interaction sites in homo- and heteromeric complexes containing Bcl-2 family members and the cellular prion protein. Brain Res Mol Brain Res 37:249-258.

Kuwahara C, Takeuchi A, Nishimura T, Haraguchi K, Kubosaki A, Matsumoto Y, Saeki K, Yokoyama T, Itohara S, Onodera T. 1999. Prions prevent neuronal cell-line death. Nature 400:225-226.

Kögel D, Fulda S, Mittelbronn M. 2010. Therapeutic exploitation of apoptosis and autophagy for glioblastoma. Anticancer Agents Med Chem 10:438-449.

Lamszus K, Schmidt N, Jin L, Laterra J, Zagzag D, Way D, Witte M, Weinand M, Goldberg I, Westphal M, Rosen E. 1998. Scatter factor promotes motility of human glioma and neuromicrovascular endothelial cells. Int J Cancer 75:19-28.

Lazarini F, Castelnau P, Chermann J, Deslys J, Dormont D. 1994. Modulation of prion protein gene expression by growth factors in cultured mouse astrocytes and PC-12 cells. Brain Res Mol Brain Res 22:268-274.

Le Pichon C, Valley M, Polymenidou M, Chesler A, Sagdullaev B, Aguzzi A, Firestein S. 2009. Olfactory behavior and physiology are disrupted in prion protein knockout mice. Nat Neurosci 12:60-69.

Lee I, Westaway D, Smit A, Wang K, Seto J, Chen L, Acharya C, Ankener M, Baskin D, Cooper C, Yao H, Prusiner S, Hood L. 1998. Complete genomic sequence and analysis of the prion protein gene region from three mammalian species. Genome Res 8:1022-1037.

Lee T, Jung E, Lee J, Kim S, Park J, Choi K, Kwon T. 2006. Mithramycin A sensitizes cancer cells to TRAIL-mediated apoptosis by down-regulation of XIAP gene promoter through Sp1 sites. Mol Cancer Ther 5:2737-2746.

Lefranc F, Facchini V, Kiss R. 2007. Proautophagic drugs: a novel means to combat apoptosis-resistant cancers, with a special emphasis on glioblastomas. Oncologist 12:1395-1403.

Lefranc F, Rynkowski M, DeWitte O, Kiss R. 2009. Present and potential future adjuvant issues in high-grade astrocytic glioma treatment. Adv Tech Stand Neurosurg 34:3-35.

Leist M, Jäättelä M. 2001. Four deaths and a funeral: from caspases to alternative mechanisms. Nat Rev Mol Cell Biol 2:589-598.

Lessene G, Czabotar P, Colman P. 2008. BCL-2 family antagonists for cancer therapy. Nat Rev Drug Discov 7:989-1000.

Levine B, Klionsky DJ. 2004. Development by self-digestion: molecular mechanisms and biological functions of autophagy. Dev Cell 6:463-477.

Levine B, Kroemer G. 2008. Autophagy in the pathogenesis of disease. Cell 132:27-42.

Levine B, Sinha S, Kroemer G. 2008. Bcl-2 family members: dual regulators of apoptosis and autophagy. Autophagy 4:600-606.

Li A, Harris D. 2005. Mammalian prion protein suppresses Bax-induced cell death in yeast. J Biol Chem 280:17430-17434.

Li C, Xin W, Sy M. 2010. Binding of pro-prion to filamin A: by design or an unfortunate blunder. Oncogene 29:5329-5345.

Li C, Yu S, Nakamura F, Yin S, Xu J, Petrolla A, Singh N, Tartakoff A, Abbott D, Xin W, Sy M. 2009. Binding of pro-prion to filamin A disrupts cytoskeleton and correlates with poor prognosis in pancreatic cancer. J Clin Invest 119:2725-2736.

Liang C, Feng P, Ku B, Dotan I, Canaani D, Oh B, Jung J. 2006a. Autophagic and tumour suppressor activity of a novel Beclin1-binding protein UVRAG. Nat Cell Biol 8:688-699.

Liang G, Zhou H, Wang Y, Gurley E, Feng B, Chen L, Xiao J, Yang S, Li X. 2009a. Inhibition of LPS-induced production of inflammatory factors in the macrophages by mono-carbonyl analogues of curcumin. J Cell Mol Med 13:3370-3379.

Liang J, Ge F, Guo C, Luo G, Wang X, Han G, Zhang D, Wang J, Li K, Pan Y, Yao L, Yin Z, Guo X, Wu K, Ding J, Fan D. 2009b. Inhibition of PI3K/Akt partially leads to the inhibition of PrP(C)-induced drug resistance in gastric cancer cells. FEBS J 276:685-694.

Liang J, Pan Y, Zhang D, Guo C, Shi Y, Wang J, Chen Y, Wang X, Liu J, Guo X, Chen Z, Qiao T, Fan D. 2007. Cellular prion protein promotes proliferation and G1/S transition of human gastric cancer cells SGC7901 and AGS. FASEB J 21:2247-2256.

Liang J, Wang J, Pan Y, Wang J, Liu L, Guo X, Sun L, Lin T, Han S, Xie H, Yin F, Guo X, Fan D. 2006b. High frequency occurrence of 1-OPRD variant of PRNP gene in gastric cancer cell lines and Chinese population with gastric cancer. Cell Biol Int 30:920-923.

Liang X, Jackson S, Seaman M, Brown K, Kempkes B, Hibshoosh H, Levine B. 1999. Induction of autophagy and inhibition of tumorigenesis by beclin 1. Nature 402:672-676.

Linden R, Martins V, Prado M, Cammarota M, Izquierdo I, Brentani R. 2008. Physiology of the prion protein. Physiol Rev 88:673-728.

Liu E. 2008. Functional genomics of cancer. Curr Opin Genet Dev 18:251-256.

Livak KJ, Schmittgen TD. 2001. Analysis of relative gene expression data using real-time quantitative PCR and the 2(-Delta Delta C(T)) Method. Methods 25:402-408.

Lledo P, Tremblay P, DeArmond S, Prusiner S, Nicoll R. 1996. Mice deficient for prion protein exhibit normal neuronal excitability and synaptic transmission in the hippocampus. Proc Natl Acad Sci U S A 93:2403-2407.

Loewith R, Jacinto E, Wullschleger S, Lorberg A, Crespo J, Bonenfant D, Oppliger W, Jenoe P, Hall M. 2002. Two TOR complexes, only one of which is rapamycin sensitive, have distinct roles in cell growth control. Mol Cell 10:457-468.

Lomonaco S, Finniss S, Xiang C, Decarvalho A, Umansky F, Kalkanis S, Mikkelsen T, Brodie C. 2009. The induction of autophagy by gamma-radiation contributes to the radioresistance of glioma stem cells. Int J Cancer 125:717-722.

Lopes M, Hajj G, Muras A, Mancini G, Castro R, Ribeiro K, Brentani R, Linden R, Martins V. 2005. Interaction of cellular prion and stress-inducible protein 1 promotes neuritogenesis and neuroprotection by distinct signaling pathways. J Neurosci 25:11330-11339.

Louis D. 1994. The p53 gene and protein in human brain tumors. J Neuropathol Exp Neurol 53:11-21.

Louis D, Ohgaki H, Wiestler O, Cavenee W, Burger P, Jouvet A, Scheithauer B, Kleihues P. 2007. The 2007 WHO classification of tumours of the central nervous system. Acta Neuropathol 114:97-109.

Lund-Johansen M, Bjerkvig R, Humphrey P, Bigner S, Bigner D, Laerum O. 1990. Effect of epidermal growth factor on glioma cell growth, migration, and invasion in vitro. Cancer Res 50:6039-6044.

Ma J, Lindquist S. 2002. Conversion of PrP to a self-perpetuating PrPSc-like conformation in the cytosol. Science 298:1785-1788.

Ma J, Wollmann R, Lindquist S. 2002. Neurotoxicity and neurodegeneration when PrP accumulates in the cytosol. Science 298:1781-1785.

Mabbott N, Turner M. 2005. Prions and the blood and immune systems. Haematologica 90:542-548.

Maehama T, Dixon J. 1999. PTEN: a tumour suppressor that functions as a phospholipid phosphatase. Trends Cell Biol 9:125-128.

Mahal S, Asante E, Antoniou M, Collinge J. 2001. Isolation and functional characterisation of the promoter region of the human prion protein gene. Gene 268:105-114.

Maher E, Brennan C, Wen P, Durso L, Ligon K, Richardson A, Khatry D, Feng B, Sinha R, Louis D, Quackenbush J, Black P, Chin L, DePinho R. 2006. Marked genomic differences characterize primary and secondary glioblastoma subtypes and identify two distinct molecular and clinical secondary glioblastoma entities. Cancer Res 66:11502-11513.

Maiuri M, Le Toumelin G, Criollo A, Rain J, Gautier F, Juin P, Tasdemir E, Pierron G, Troulinaki K, Tavernarakis N, Hickman J, Geneste O, Kroemer G. 2007. Functional and physical interaction between Bcl-X(L) and a BH3-like domain in Beclin-1. EMBO J 26:2527-2539.

Makrinou E, Collinge J, Antoniou M. 2002. Genomic characterization of the human prion protein (PrP) gene locus. Mamm Genome 13:696-703.

Mallucci G, Dickinson A, Linehan J, Klöhn P, Brandner S, Collinge J. 2003. Depleting neuronal PrP in prion infection prevents disease and reverses spongiosis. Science 302:871-874.

Mallucci G, Ratté S, Asante E, Linehan J, Gowland I, Jefferys J, Collinge J. 2002. Post-natal knockout of prion protein alters hippocampal CA1 properties, but does not result in neurodegeneration. EMBO J 21:202-210.

Mangé A, Béranger F, Peoc'h K, Onodera T, Frobert Y, Lehmann S. 2004. Alpha- and beta-cleavages of the amino-terminus of the cellular prion protein. Biol Cell 96:125-132.

Manning B, Cantley L. 2003. Rheb fills a GAP between TSC and TOR. Trends Biochem Sci 28:573-576.

Manson J, Clarke A, Hooper M, Aitchison L, McConnell I, Hope J. 1994. 129/Ola mice carrying a null mutation in PrP that abolishes mRNA production are developmentally normal. Mol Neurobiol 8:121-127.

Mason W, Cairncross J. 2008. Invited article: the expanding impact of molecular biology on the diagnosis and treatment of gliomas. Neurology 71:365-373.

Mathew R, Karantza-Wadsworth V, White E. 2007. Role of autophagy in cancer. Nat Rev Cancer 7:961-967.

McEwan J, Windsor M, Cullis-Hill S. 2009. Antibodies to prion protein inhibit human colon cancer cell growth. Tumour Biol 30:141-147.

McLennan N, Brennan P, McNeill A, Davies I, Fotheringham A, Rennison K, Ritchie D, Brannan F, Head M, Ironside J, Williams A, Bell J. 2004. Prion protein accumulation and neuroprotection in hypoxic brain damage. Am J Pathol 165:227-235.

Mehrpour M, Codogno P. 2010. Prion protein: From physiology to cancer biology. Cancer Lett 290:1-23.

Meng Y, Tang W, Dai Y, Wu X, Liu M, Ji Q, Ji M, Pienta K, Lawrence T, Xu L. 2008. Natural BH3 mimetic (-)-gossypol chemosensitizes human prostate cancer via Bcl-xL inhibition accompanied by increase of Puma and Noxa. Mol Cancer Ther 7:2192-2202.

Meslin F, Conforti R, Mazouni C, Morel N, Tomasic G, Drusch F, Yacoub M, Sabourin J, Grassi J, Delaloge S, Mathieu M, Chouaib S, Andre F, Mehrpour M. 2007a. Efficacy of adjuvant chemotherapy according to Prion protein expression in patients with estrogen receptor-negative breast cancer. Ann Oncol 18:1793-1798.

Meslin F, Hamaï A, Gao P, Jalil A, Cahuzac N, Chouaib S, Mehrpour M. 2007b. Silencing of prion protein sensitizes breast adriamycin-resistant carcinoma cells to TRAIL-mediated cell death. Cancer Res 67:10910-10919.

Miracco C, Cosci E, Oliveri G, Luzi P, Pacenti L, Monciatti I, Mannucci S, De Nisi M, Toscano M, Malagnino V, Falzarano S, Pirtoli L, Tosi P. 2007. Protein and mRNA expression of autophagy gene Beclin 1 in human brain tumours. Int J Oncol 30:429-436.

Mizushima N. 2004. Methods for monitoring autophagy. Int J Biochem Cell Biol 36:2491-2502.

Mizushima N. 2010. Autophagy. FEBS Lett 584:1279.

Mizushima N, Levine B, Cuervo AM, Klionsky DJ. 2008. Autophagy fights disease through cellular self-digestion. Nature 451:1069-1075.

Mizushima N, Yoshimori T. 2007. How to interpret LC3 immunoblotting. Autophagy 3:542-545.

Mobley W, Neve R, Prusiner S, McKinley M. 1988. Nerve growth factor increases mRNA levels for the prion protein and the beta-amyloid protein precursor in developing hamster brain. Proc Natl Acad Sci U S A 85:9811-9815.

Momota H, Nerio E, Holland E. 2005. Perifosine inhibits multiple signaling pathways in glial progenitors and cooperates with temozolomide to arrest cell proliferation in gliomas in vivo. Cancer Res 65:7429-7435.

Moore R, Lee I, Silverman G, Harrison P, Strome R, Heinrich C, Karunaratne A, Pasternak S, Chishti M, Liang Y, Mastrangelo P, Wang K, Smit A, Katamine S, Carlson G et al. 1999. Ataxia in prion protein (PrP)-deficient mice is associated with upregulation of the novel PrP-like protein doppel. J Mol Biol 292:797-817.

Mouillet-Richard S, Ermonval M, Chebassier C, Laplanche J, Lehmann S, Launay J, Kellermann O. 2000. Signal transduction through prion protein. Science 289:1925-1928.

Mouillet-Richard S, Pietri M, Schneider B, Vidal C, Mutel V, Launay J, Kellermann O. 2005. Modulation of serotonergic receptor signaling and cross-talk by prion protein. J Biol Chem 280:4592-4601.

Nakada M, Drake KL, Nakada S, Niska JA, Berens ME. 2006. Ephrin-B3 ligand promotes glioma invasion through activation of Rac1. Cancer Res 66:8492-8500.

Natarajan M, Stewart J, Golemis E, Pugacheva E, Alexandropoulos K, Cox B, Wang W, Grammer J, Gladson C. 2006. HEF1 is a necessary and specific downstream effector of FAK that promotes the migration of glioblastoma cells. Oncogene 25:1721-1732.

Nishida N, Tremblay P, Sugimoto T, Shigematsu K, Shirabe S, Petromilli C, Erpel S, Nakaoke R, Atarashi R, Houtani T, Torchia M, Sakaguchi S, DeArmond S, Prusiner S, Katamine S. 1999. A mouse prion protein transgene rescues mice deficient for the prion protein gene from purkinje cell degeneration and demyelination. Lab Invest 79:689-697.

Nishimura T, Sakudo A, Hashiyama Y, Yachi A, Saeki K, Matsumoto Y, Ogawa M, Sakaguchi S, Itohara S, Onodera T. 2007. Serum withdrawal-induced apoptosis in ZrchI prion protein (PrP) gene-deficient neuronal cell line is suppressed by PrP, independent of Doppel. Microbiol Immunol 51:457-466.

Niyazi M, Niyazi I, Belka C. 2007. Counting colonies of clonogenic assays by using densitometric software. Radiat Oncol 2:4.

Noda T, Fujita N, Yoshimori T. 2009. The late stages of autophagy: how does the end begin? Cell Death Differ 16:984-990.

Novakova J, Slaby O, Vyzula R, Michalek J. 2009. MicroRNA involvement in glioblastoma pathogenesis. Biochem Biophys Res Commun 386:1-5.

Nutt C. 2005. Molecular genetics of oligodendrogliomas: a model for improved clinical management in the field of neurooncology. Neurosurg Focus 19:E2.

O'Brien S, Moore J, Boyd T, Larratt L, Skotnicki A, Koziner B, Chanan-Khan A, Seymour J, Gribben J, Itri L, Rai K. 2009. 5-year survival in patients with relapsed or refractory chronic lymphocytic leukemia in a randomized, phase III trial of fludarabine plus cyclophosphamide with or without oblimersen. J Clin Oncol 27:5208-5212.

O'Reilly K, Rojo F, She Q, Solit D, Mills G, Smith D, Lane H, Hofmann F, Hicklin D, Ludwig D, Baselga J, Rosen N. 2006. mTOR inhibition induces upstream receptor tyrosine kinase signaling and activates Akt. Cancer Res 66:1500-1508.

Oesch B, Westaway D, Wälchli M, McKinley M, Kent S, Aebersold R, Barry R, Tempst P, Teplow D, Hood L. 1985. A cellular gene encodes scrapie PrP 27-30 protein. Cell 40:735-746.

Ohgaki H, Kleihues P. 2005. Epidemiology and etiology of gliomas. Acta Neuropathol 109:93-108.

Opipari AJ, Tan L, Boitano A, Sorenson D, Aurora A, Liu J. 2004. Resveratrol-induced autophagocytosis in ovarian cancer cells. Cancer Res 64:696-703.

Paglin S, Hollister T, Delohery T, Hackett N, McMahill M, Sphicas E, Domingo D, Yahalom J. 2001. A novel response of cancer cells to radiation involves autophagy and formation of acidic vesicles. Cancer Res 61:439-444.

Pammer J, Cross H, Frobert Y, Tschachler E, Oberhuber G. 2000. The pattern of prion-related protein expression in the gastrointestinal tract. Virchows Arch 436:466-472.

Pammer J, Weninger W, Tschachler E. 1998. Human keratinocytes express cellular prion-related protein in vitro and during inflammatory skin diseases. Am J Pathol 153:1353-1358.

Pan K, Baldwin M, Nguyen J, Gasset M, Serban A, Groth D, Mehlhorn I, Huang Z, Fletterick R, Cohen F. 1993. Conversion of alpha-helices into beta-sheets features in the formation of the scrapie prion proteins. Proc Natl Acad Sci U S A 90:10962-10966.

Pan Y, Zhao L, Liang J, Liu J, Shi Y, Liu N, Zhang G, Jin H, Gao J, Xie H, Wang J, Liu Z, Fan D. 2006. Cellular prion protein promotes invasion and metastasis of gastric cancer. FASEB J 20:1886-1888.

Parkyn C, Vermeulen E, Mootoosamy R, Sunyach C, Jacobsen C, Oxvig C, Moestrup S, Liu Q, Bu G, Jen A, Morris R. 2008. LRP1 controls biosynthetic and endocytic trafficking of neuronal prion protein. J Cell Sci 121:773-783.

Parsons D, Jones S, Zhang X, Lin J, Leary R, Angenendt P, Mankoo P, Carter H, Siu I, Gallia G, Olivi A, McLendon R, Rasheed B, Keir S, Nikolskaya T et al. 2008. An integrated genomic analysis of human glioblastoma multiforme. Science 321:1807-1812.

Pattingre S, Tassa A, Qu X, Garuti R, Liang X, Mizushima N, Packer M, Schneider M, Levine B. 2005. Bcl-2 antiapoptotic proteins inhibit Beclin 1-dependent autophagy. Cell 122:927-939.

Pauly P, Harris D. 1998. Copper stimulates endocytosis of the prion protein. J Biol Chem 273:33107-33110.

Peretz D, Williamson R, Legname G, Matsunaga Y, Vergara J, Burton D, DeArmond S, Prusiner S, Scott M. 2002. A change in the conformation of prions accompanies the emergence of a new prion strain. Neuron 34:921-932.

Pike L. 2006. Rafts defined: a report on the Keystone Symposium on Lipid Rafts and Cell Function. J Lipid Res 47:1597-1598.

Pozsgai E, Schally A, Zarandi M, Varga J, Vidaurre I, Bellyei S. 2010. The effect of GHRH antagonists on human glioblastomas and their mechanism of action. Int J Cancer 127:2313-2322.

Prado M, Alves-Silva J, Magalhães A, Prado V, Linden R, Martins V, Brentani R. 2004. PrPc on the road: trafficking of the cellular prion protein. J Neurochem 88:769-781.

Prusiner S. 1998. Prions. Proc Natl Acad Sci U S A 95:13363-13383.

Pucer A, Castino R, Mirković B, Falnoga I, Slejkovec Z, Isidoro C, Lah T. 2010. Differential role of cathepsins B and L in autophagy-associated cell death induced by arsenic trioxide in U87 human glioblastoma cells. Biol Chem 391:519-531.

Puckett C, Concannon P, Casey C, Hood L. 1991. Genomic structure of the human prion protein gene. Am J Hum Genet 49:320-329.

Puduvalli V, Sampath D, Bruner J, Nangia J, Xu R, Kyritsis A. 2005. TRAIL-induced apoptosis in gliomas is enhanced by Akt-inhibition and is independent of JNK activation. Apoptosis 10:233-243.

Qin K, Zhao L, Ash R, McDonough W, Zhao R. 2009. ATM-mediated transcriptional elevation of prion in response to copper-induced oxidative stress. J Biol Chem 284:4582-4593.

Qin K, Zhao L, Tang Y, Bhatta S, Simard J, Zhao R. 2006. Doppel-induced apoptosis and counteraction by cellular prion protein in neuroblastoma and astrocytes. Neuroscience 141:1375-1388.

Qu X, Yu J, Bhagat G, Furuya N, Hibshoosh H, Troxel A, Rosen J, Eskelinen E, Mizushima N, Ohsumi Y, Cattoretti G, Levine B. 2003. Promotion of tumorigenesis by heterozygous disruption of the beclin 1 autophagy gene. J Clin Invest 112:1809-1820.

Quaglio E, Chiesa R, Harris D. 2001. Copper converts the cellular prion protein into a protease-resistant species that is distinct from the scrapie isoform. J Biol Chem 276:11432-11438.

Radotra B, McCormick D. 1997. Glioma invasion in vitro is mediated by CD44-hyaluronan interactions. J Pathol 181:434-438.

Rambold A, Miesbauer M, Rapaport D, Bartke T, Baier M, Winklhofer K, Tatzelt J. 2006. Association of Bcl-2 with misfolded prion protein is linked to the toxic potential of cytosolic PrP. Mol Biol Cell 17:3356-3368.

Rascher G, Fischmann A, Kröger S, Duffner F, Grote E, Wolburg H. 2002. Extracellular matrix and the blood-brain barrier in glioblastoma multiforme: spatial segregation of tenascin and agrin. Acta Neuropathol 104:85-91.

Re L, Rossini F, Re F, Bordicchia M, Mercanti A, Fernandez O, Barocci S. 2006. Prion protein potentiates acetylcholine release at the neuromuscular junction. Pharmacol Res 53:62-68.

Reardon DA, Rich JN, Friedman HS, Bigner DD. 2006. Recent advances in the treatment of malignant astrocytoma. J Clin Oncol 24:1253-1265.

Reddy K, Nabha S, Atanaskova N. 2003. Role of MAP kinase in tumor progression and invasion. Cancer Metastasis Rev 22:395-403.

Rieger R, Edenhofer F, Lasmézas C, Weiss S. 1997. The human 37-kDa laminin receptor precursor interacts with the prion protein in eukaryotic cells. Nat Med 3:1383-1388.

Riek R, Hornemann S, Wider G, Billeter M, Glockshuber R, Wüthrich K. 1996. NMR structure of the mouse prion protein domain PrP(121-321). Nature 382:180-182.

Robertson S. 2005. Filamin A: phenotypic diversity. Curr Opin Genet Dev 15:301-307.

Rossi D, Cozzio A, Flechsig E, Klein M, Rülicke T, Aguzzi A, Weissmann C. 2001. Onset of ataxia and Purkinje cell loss in PrP null mice inversely correlated with Dpl level in brain. EMBO J 20:694-702.

Roucou X, Giannopoulos P, Zhang Y, Jodoin J, Goodyer C, LeBlanc A. 2005. Cellular prion protein inhibits proapoptotic Bax conformational change in human neurons and in breast carcinoma MCF-7 cells. Cell Death Differ 12:783-795.

Roucou X, Guo Q, Zhang Y, Goodyer C, LeBlanc A. 2003. Cytosolic prion protein is not toxic and protects against Bax-mediated cell death in human primary neurons. J Biol Chem 278:40877-40881.

Roucou X, LeBlanc A. 2005. Cellular prion protein neuroprotective function: implications in prion diseases. J Mol Med 83:3-11.

Ruano Y, Mollejo M, Camacho F, Rodríguez de Lope A, Fiaño C, Ribalta T, Martínez P, Hernández-Moneo J, Meléndez B. 2008. Identification of survival-related genes of the phosphatidylinositol 3'-kinase signaling pathway in glioblastoma multiforme. Cancer 112:1575-1584.

Rubinsztein DC, Gestwicki JE, Murphy LO, Klionsky DJ. 2007. Potential therapeutic applications of autophagy. Nat Rev Drug Discov 6:304-312.

Rusten T, Vaccari T, Lindmo K, Rodahl L, Nezis I, Sem-Jacobsen C, Wendler F, Vincent J, Brech A, Bilder D, Stenmark H. 2007. ESCRTs and Fab1 regulate distinct steps of autophagy. Curr Biol 17:1817-1825.

Safar J, Roller P, Gajdusek D, Gibbs CJ. 1993. Thermal stability and conformational transitions of scrapie amyloid (prion) protein correlate with infectivity. Protein Sci 2:2206-2216.

Sailer A, Büeler H, Fischer M, Aguzzi A, Weissmann C. 1994. No propagation of prions in mice devoid of PrP. Cell 77:967-968.

Saito R, Bringas J, Panner A, Tamas M, Pieper R, Berger M, Bankiewicz K. 2004. Convection-enhanced delivery of tumor necrosis factor-related apoptosis-inducing ligand with systemic administration of temozolomide prolongs survival in an intracranial glioblastoma xenograft model. Cancer Res 64:6858-6862.

Sakaguchi S. 2007. Molecular biology of prion protein and its first homologous protein. J Med Invest 54:211-223.

Sakaguchi S, Katamine S, Nishida N, Moriuchi R, Shigematsu K, Sugimoto T, Nakatani A, Kataoka Y, Houtani T, Shirabe S, Okada H, Hasegawa S, Miyamoto T, Noda T. 1996. Loss of cerebellar Purkinje cells in aged mice homozygous for a disrupted PrP gene. Nature 380:528-531.

Sakudo A, Lee D, Nishimura T, Li S, Tsuji S, Nakamura T, Matsumoto Y, Saeki K, Itohara S, Ikuta K, Onodera T. 2005. Octapeptide repeat region and N-terminal half of hydrophobic region of prion protein (PrP) mediate PrP-dependent activation of superoxide dismutase. Biochem Biophys Res Commun 326:600-606.

Sakudo A, Xue G, Kawashita N, Ano Y, Takagi T, Shintani H, Tanaka Y, Onodera T, Ikuta K. 2010. Structure of the prion protein and its gene: an analysis using bioinformatics and computer simulation. Curr Protein Pept Sci 11:166-179.

Sanson M, Marie Y, Paris S, Idbaih A, Laffaire J, Ducray F, El Hallani S, Boisselier B, Mokhtari K, Hoang-Xuan K, Delattre J. 2009. Isocitrate dehydrogenase 1 codon 132 mutation is an important prognostic biomarker in gliomas. J Clin Oncol 27:4150-4154.

Santuccione A, Sytnyk V, Leshchyns'ka I, Schachner M. 2005. Prion protein recruits its neuronal receptor NCAM to lipid rafts to activate p59fyn and to enhance neurite outgrowth. J Cell Biol 169:341-354.

Sarnataro D, Campana V, Paladino S, Stornaiuolo M, Nitsch L, Zurzolo C. 2004. PrP(C) association with lipid rafts in the early secretory pathway stabilizes its cellular conformation. Mol Biol Cell 15:4031-4042.

Sbalchiero E, Azzalin A, Palumbo S, Barbieri G, Arias A, Simonelli L, Ferretti L, Comincini S. 2008. Altered cellular distribution and sub-cellular sorting of doppel (Dpl) protein in human astrocytoma cell lines. Cell Oncol 30:337-347.

Schimmer A, Estey E, Borthakur G, Carter B, Schiller G, Tallman M, Altman J, Karp J, Kassis J, Hedley D, Brandwein J, Xu W, Mak D, LaCasse E et al. Phase I/II trial of AEG35156 X-linked inhibitor of apoptosis protein antisense oligonucleotide combined with idarubicin and cytarabine in patients with relapsed or primary refractory acute myeloid leukemia. J Clin Oncol 27:4741-4746.

Schmitt-Ulms G, Legname G, Baldwin M, Ball H, Bradon N, Bosque P, Crossin K, Edelman G, DeArmond S, Cohen F, Prusiner S. 2001. Binding of neural cell adhesion molecules (N-CAMs) to the cellular prion protein. J Mol Biol 314:1209-1225.

Schneider B, Mutel V, Pietri M, Ermonval M, Mouillet-Richard S, Kellermann O. 2003. NADPH oxidase and extracellular regulated kinases 1/2 are targets of prion protein signaling in neuronal and nonneuronal cells. Proc Natl Acad Sci U S A 100:13326-13331.

Senator A, Rachidi W, Lehmann S, Favier A, Benboubetra M. 2004. Prion protein protects against DNA damage induced by paraquat in cultured cells. Free Radic Biol Med 37:1224-1230.

Seznec J, Silkenstedt B, Naumann U. 2010. Therapeutic effects of the Sp1 inhibitor mithramycin A in glioblastoma. J Neurooncol.

Shimizu S, Kanaseki T, Mizushima N, Mizuta T, Arakawa-Kobayashi S, Thompson C, Tsujimoto Y. 2004. Role of Bcl-2 family proteins in a non-apoptotic programmed cell death dependent on autophagy genes. Nat Cell Biol 6:1221-1228.

Shmerling D, Hegyi I, Fischer M, Blättler T, Brandner S, Götz J, Rülicke T, Flechsig E, Cozzio A, von Mering C, Hangartner C, Aguzzi A, Weissmann C. 1998. Expression of amino-terminally truncated PrP in the mouse leading to ataxia and specific cerebellar lesions. Cell 93:203-214.

Shyu W, Harn H, Saeki K, Kubosaki A, Matsumoto Y, Onodera T, Chen C, Hsu Y, Chiang Y. 2002. Molecular modulation of expression of prion protein by heat shock. Mol Neurobiol 26:1-12.

Shyu W, Lin S, Chiang M, Ding D, Li K, Chen S, Yang H, Li H. 2005. Overexpression of PrPC by adenovirus-mediated gene targeting reduces ischemic injury in a stroke rat model. J Neurosci 25:8967-8977.

Simonic T, Duga S, Strumbo B, Asselta R, Ceciliani F, Ronchi S. 2000. cDNA cloning of turtle prion protein. FEBS Lett 469:33-38.

Sinha S, Levine B. 2008. The autophagy effector Beclin 1: a novel BH3-only protein. Oncogene 27 Suppl 1:S137-148.

Soni D, King J, Kaye A, Hovens C. 2005. Genetics of glioblastoma multiforme: mitogenic signaling and cell cycle pathways converge. J Clin Neurosci 12:1-5.

Sonnemann J, Kumar K, Heesch S, Müller C, Hartwig C, Maass M, Bader P, Beck J. 2006. Histone deacetylase inhibitors induce cell death and enhance the susceptibility to ionizing radiation, etoposide, and TRAIL in medulloblastoma cells. Int J Oncol 28:755-766.

Sotiriou C, Neo S, McShane L, Korn E, Long P, Jazaeri A, Martiat P, Fox S, Harris A, Liu E. 2003. Breast cancer classification and prognosis based on gene expression profiles from a population-based study. Proc Natl Acad Sci U S A 100:10393-10398.

Sparkes R, Simon M, Cohn V, Fournier R, Lem J, Klisak I, Heinzmann C, Blatt C, Lucero M, Mohandas T. 1986. Assignment of the human and mouse prion protein genes to homologous chromosomes. Proc Natl Acad Sci U S A 83:7358-7362.

Spudich A, Frigg R, Kilic E, Kilic U, Oesch B, Raeber A, Bassetti C, Hermann D. 2005. Aggravation of ischemic brain injury by prion protein deficiency: role of ERK-1/-2 and STAT-1. Neurobiol Dis 20:442-449.

Stahel RA, Zangemeister-Wittke U. 2003. Antisense oligonucleotides for cancer therapy-an overview. Lung Cancer 41 Suppl 1:S81-88.

Steele A, Emsley J, Ozdinler P, Lindquist S, Macklis J. 2006. Prion protein (PrPc) positively regulates neural precursor proliferation during developmental and adult mammalian neurogenesis. Proc Natl Acad Sci U S A 103:3416-3421.

Steele A, Lindquist S, Aguzzi A. 2007. The prion protein knockout mouse: a phenotype under challenge. Prion 1:83-93.

Stegh A, Kesari S, Mahoney J, Jenq H, Forloney K, Protopopov A, Louis D, Chin L, DePinho R. 2008. Bcl2L12-mediated inhibition of effector caspase-3 and caspase-7 via distinct mechanisms in glioblastoma. Proc Natl Acad Sci U S A 105:10703-10708.

Stegh A, Kim H, Bachoo R, Forloney K, Zhang J, Schulze H, Park K, Hannon G, Yuan J, Louis D, DePinho R, Chin L. 2007. Bcl2L12 inhibits post-mitochondrial apoptosis signaling in glioblastoma. Genes Dev 21:98-111.

Stettner M, Wang W, Nabors L, Bharara S, Flynn D, Grammer J, Gillespie G, Gladson C. 2005. Lyn kinase activity is the predominant cellular SRC kinase activity in glioblastoma tumor cells. Cancer Res 65:5535-5543.

Stewart R, Piccardo P, Ghetti B, Harris D. 2005. Neurodegenerative illness in transgenic mice expressing a transmembrane form of the prion protein. J Neurosci 25:3469-3477.

Stommel J, Kimmelman A, Ying H, Nabioullin R, Ponugoti A, Wiedemeyer R, Stegh A, Bradner J, Ligon K, Brennan C, Chin L, DePinho R. 2007. Coactivation of receptor tyrosine kinases affects the response of tumor cells to targeted therapies. Science 318:287-290.

Strumbo B, Ronchi S, Bolis L, Simonic T. 2001. Molecular cloning of the cDNA coding for Xenopus laevis prion protein. FEBS Lett 508:170-174.

Sunyach C, Jen A, Deng J, Fitzgerald K, Frobert Y, Grassi J, McCaffrey M, Morris R. 2003. The mechanism of internalization of glycosylphosphatidylinositol-anchored prion protein. EMBO J 22:3591-3601.

Suzuki K, Ohsumi Y. 2007. Molecular machinery of autophagosome formation in yeast, Saccharomyces cerevisiae. FEBS Lett 581:2156-2161.

Takahashi Y, Coppola D, Matsushita N, Cualing H, Sun M, Sato Y, Liang C, Jung J, Cheng J, Mulé J, Pledger W, Wang H. 2007. Bif-1 interacts with Beclin 1 through UVRAG and regulates autophagy and tumorigenesis. Nat Cell Biol 9:1142-1151.

Tamm I, Wagner M. 2006. Antisense therapy in clinical oncology: preclinical and clinical experiences. Mol Biotechnol 33:221-238.

Tamura M, Gu J, Takino T, Yamada K. 1999. Tumor suppressor PTEN inhibition of cell invasion, migration, and growth: differential involvement of focal adhesion kinase and p130Cas. Cancer Res 59:442-449.

Tanida I, Ueno T, Kominami E. 2004a. Human light chain 3/MAP1LC3B is cleaved at its carboxyl-terminal Met121 to expose Gly120 for lipidation and targeting to autophagosomal membranes. J Biol Chem 279:47704-47710.

Tanida I, Ueno T, Kominami E. 2004b. LC3 conjugation system in mammalian autophagy. Int J Biochem Cell Biol 36:2503-2518.

Taylor D, Hooper N. 2006. The prion protein and lipid rafts. Mol Membr Biol 23:89-99.

Taylor D, Watt N, Perera W, Hooper N. 2005. Assigning functions to distinct regions of the N-terminus of the prion protein that are involved in its copper-stimulated, clathrin-dependent endocytosis. J Cell Sci 118:5141-5153.

Tobler I, Deboer T, Fischer M. 1997. Sleep and sleep regulation in normal and prion protein-deficient mice. J Neurosci 17:1869-1879.

Tobler I, Gaus S, Deboer T, Achermann P, Fischer M, Rülicke T, Moser M, Oesch B, McBride P, Manson J. 1996. Altered circadian activity rhythms and sleep in mice devoid of prion protein. Nature 380:639-642.

Tse C, Shoemaker A, Adickes J, Anderson M, Chen J, Jin S, Johnson E, Marsh K, Mitten M, Nimmer P, Roberts L, Tahir S, Xiao Y, Yang X, Zhang H et al. 2008. ABT-263: a potent and orally bioavailable Bcl-2 family inhibitor. Cancer Res 68:3421-3428.

Uhlén M, Björling E, Agaton C, Szigyarto C, Amini B, Andersen E, Andersson A, Angelidou P, Asplund A, Asplund C, Berglund L, Bergström K, Brumer H, Cerjan D, Ekström M et al. 2005. A human protein atlas for normal and cancer tissues based on antibody proteomics. Mol Cell Proteomics 4:1920-1932.

Vassallo N, Herms J. 2003. Cellular prion protein function in copper homeostasis and redox signalling at the synapse. J Neurochem 86:538-544.

Viegas P, Chaverot N, Enslen H, Perrière N, Couraud P, Cazaubon S. 2006. Junctional expression of the prion protein PrPC by brain endothelial cells: a role in trans-endothelial migration of human monocytes. J Cell Sci 119:4634-4643.

Viles J, Cohen F, Prusiner S, Goodin D, Wright P, Dyson H. 1999. Copper binding to the prion protein: structural implications of four identical cooperative binding sites. Proc Natl Acad Sci U S A 96:2042-2047.

Vincent B, Paitel E, Saftig P, Frobert Y, Hartmann D, De Strooper B, Grassi J, Lopez-Perez E, Checler F. 2001. The disintegrins ADAM10 and TACE contribute to the constitutive and phorbol ester-regulated normal cleavage of the cellular prion protein. J Biol Chem 276:37743-37746.

Voss V, Senft C, Lang V, Ronellenfitsch M, Steinbach J, Seifert V, Kögel D. 2010. The pan-Bcl-2 inhibitor (-)-gossypol triggers autophagic cell death in malignant glioma. Mol Cancer Res 8:1002-1016.

Wagenknecht B, Glaser T, Naumann U, Kügler S, Isenmann S, Bähr M, Korneluk R, Liston P, Weller M. 1999. Expression and biological activity of X-linked inhibitor of apoptosis (XIAP) in human malignant glioma. Cell Death Differ 6:370-376.

Walmsley A, Zeng F, Hooper N. 2003. The N-terminal region of the prion protein ectodomain contains a lipid raft targeting determinant. J Biol Chem 278:37241-37248.

Walter E, Chattopadhyay M, Millhauser G. 2006. The affinity of copper binding to the prion protein octarepeat domain: evidence for negative cooperativity. Biochemistry 45:13083-13092.

Walz R, Amaral O, Rockenbach I, Roesler R, Izquierdo I, Cavalheiro E, Martins V, Brentani R. 1999. Increased sensitivity to seizures in mice lacking cellular prion protein. Epilepsia 40:1679-1682.

Wang H, Zhang W, Huang H, Liao W, Fuller G. 2004. Analysis of the activation status of Akt, NFkappaB, and Stat3 in human diffuse gliomas. Lab Invest 84:941-951.

Wang Z, Peng Z, Duan Z, Liu H. 2006. [Expression and clinical significance of autophagy gene Beclin 1 in cervical squamous cell carcinoma]. Sichuan Da Xue Xue Bao Yi Xue Ban 37:860-863.

Watt N, Hooper N. 2003. The prion protein and neuronal zinc homeostasis. Trends Biochem Sci 28:406-410.

Watt N, Taylor D, Gillott A, Thomas D, Perera W, Hooper N. 2005. Reactive oxygen species-mediated beta-cleavage of the prion protein in the cellular response to oxidative stress. J Biol Chem 280:35914-35921.

Watts J, Westaway D. 2007. The prion protein family: diversity, rivalry, and dysfunction. Biochim Biophys Acta 1772:654-672.

Wei Y, Pattingre S, Sinha S, Bassik M, Levine B. 2008. JNK1-mediated phosphorylation of Bcl-2 regulates starvation-induced autophagy. Mol Cell 30:678-688.

Wen P, Kesari S. 2008. Malignant gliomas in adults. N Engl J Med 359:492-507.

Westaway D, Cooper C, Turner S, Da Costa M, Carlson G, Prusiner S. 1994. Structure and polymorphism of the mouse prion protein gene. Proc Natl Acad Sci U S A 91:6418-6422.

Westergard L, Christensen H, Harris D. 2007. The cellular prion protein (PrP(C)): its physiological function and role in disease. Biochim Biophys Acta 1772:629-644.

Westermark B, Heldin C, Nistér M. 1995. Platelet-derived growth factor in human glioma. Glia 15:257-263.

White M, Farmer M, Mirabile I, Brandner S, Collinge J, Mallucci G. 2008. Single treatment with RNAi against prion protein rescues early neuronal dysfunction and prolongs survival in mice with prion disease. Proc Natl Acad Sci U S A 105:10238-10243.

Wick W, Wagner S, Kerkau S, Dichgans J, Tonn J, Weller M. 1998. BCL-2 promotes migration and invasiveness of human glioma cells. FEBS Lett 440:419-424.

Wolter K, Wang S, Henson B, Wang S, Griffith K, Kumar B, Chen J, Carey T, Bradford C, D'Silva N. 2006. (-)-gossypol inhibits growth and promotes apoptosis of human head and neck squamous cell carcinoma in vivo. Neoplasia 8:163-172.

Wong B, Liu T, Li R, Pan T, Petersen R, Smith M, Gambetti P, Perry G, Manson J, Brown D, Sy M. 2001. Increased levels of oxidative stress markers detected in the brains of mice devoid of prion protein. J Neurochem 76:565-572.

Xue L, Fletcher G, Tolkovsky A. 1999. Autophagy is activated by apoptotic signalling in sympathetic neurons: an alternative mechanism of death execution. Mol Cell Neurosci 14:180-198.

Yacoub A, Hamed H, Emdad L, Dos Santos W, Gupta P, Broaddus W, Ramakrishnan V, Sarkar D, Shah K, Curiel D, Grant S, Fisher P, Dent P. 2008. MDA-7/IL-24 plus radiation enhance survival in animals with intracranial primary human GBM tumors. Cancer Biol Ther 7:917-933.

Yan H, Parsons D, Jin G, McLendon R, Rasheed B, Yuan W, Kos I, Batinic-Haberle I, Jones S, Riggins G, Friedman H, Friedman A, Reardon D, Herndon J et al. 2009. IDH1 and IDH2 mutations in gliomas. N Engl J Med 360:765-773.

Yang Z, Klionsky DJ. 2010. Eaten alive: a history of macroautophagy. Nat Cell Biol 12:814-822.

Yao Y, Wang C, Varshney R, Wang D. 2009. Antisense makes sense in engineered regenerative medicine. Pharm Res 26:263-275.

Yue Z, Jin S, Yang C, Levine A, Heintz N. 2003. Beclin 1, an autophagy gene essential for early embryonic development, is a haploinsufficient tumor suppressor. Proc Natl Acad Sci U S A 100:15077-15082.

Zahn R, Liu A, Lührs T, Riek R, von Schroetter C, López García F, Billeter M, Calzolai L, Wider G, Wüthrich K. 2000. NMR solution structure of the human prion protein. Proc Natl Acad Sci U S A 97:145-150.

Zanata S, Lopes M, Mercadante A, Hajj G, Chiarini L, Nomizo R, Freitas A, Cabral A, Lee K, Juliano M, de Oliveira E, Jachieri S, Burlingame A, Huang L, Linden R et al. 2002. Stress-inducible protein 1 is a cell surface ligand for cellular prion that triggers neuroprotection. EMBO J 21:3307-3316.

Zhang C, Steele A, Lindquist S, Lodish H. 2006. Prion protein is expressed on long-term repopulating hematopoietic stem cells and is important for their self-renewal. Proc Natl Acad Sci U S A 103:2184-2189.

Zhao Y, You H, Liu F, An H, Shi Y, Yu Q, Fan D. 2002. Differentially expressed gene profiles between multidrug resistant gastric adenocarcinoma cells and their parental cells. Cancer Lett 185:211-218.

Zhen H, Zhang X, Hu P, Yang T, Fei Z, Zhang J, Fu L, He X, Ma F, Wang X. 2005. Survivin expression and its relation with proliferation, apoptosis, and angiogenesis in brain gliomas. Cancer 104:2775-2783.

List of original manuscripts

Sbalchiero E, Azzalin A, Palumbo S, **Barbieri G**, Arias A, Simonelli L, Ferretti L, Comincini S. 2008. Altered cellular distribution and sub-cellular sorting of doppel (Dpl) protein in human astrocytoma cell lines. 30:337-347.

Azzalin A, Sbalchiero E, **Barbieri G**, Palumbo S, Muzzini C, Comincini S. 2008. The doppel (Dpl) protein influences in vitro migration capability in astrocytoma-derived cells. Cell Oncol 30:491-501.

Comincini S, Paolillo M, **Barbieri G**, Palumbo S, Sbalchiero E, Azzalin A, Russo MA, Schinelli S. 2009. Gene expression analysis of an EGFR indirectly related pathway identified PTEN and MMP9 as reliable diagnostic markers for human glial tumor specimens. J Biomed Biotechnol 2009:924565.

Barbieri G, Palumbo S, Gabrusiewicz K, Sbalchiero E, Marchesi N, Muzzini C, Spedito A, Biggiogera M, Azzalin A, Miracco C, Pirtoli L, Kaminska B, Cominicini S. 2010. Silencing of cellular prion protein (PrPC) expression by DNA-antisense oligonucleotides induces autophagic death in glioma cells. *Submitted to Autophagy*

Cellular Oncology 30 (2008) 337–347
DOI 10.3233/CLO-2008-0429
IOS Press

Altered cellular distribution and sub-cellular sorting of doppel (Dpl) protein in human astrocytoma cell lines

Elena Sbalchiero *, Alberto Azzalin *, Silvia Palumbo, Giulia Barbieri, Agustina Arias, Luca Simonelli, Luca Ferretti and Sergio Comincini **
Dipartimento di Genetica e Microbiologia, Università di Pavia, Pavia, Italy

Abstract. Doppel, a prion-like protein, is a GPI-membrane anchored protein generally not expressed in the Central Nervous System (CNS) of different mammalian species, including human. Nevertheless, in astrocytomas, a particular kind of glial tumors, the doppel encoding gene (*PRND*) is over-expressed and the corresponding protein product (Dpl) is ectopically localized in the cytoplasm of the tumor cells. In this study we have analysed the sub-cellular localization of Dpl using double-immunofluorescence staining and confocal microscopy examinations in two astrocytoma-derived human cell lines (IPDDC-A2 and D384-MG). Our results confirmed that Dpl is localized in the cytoplasm of the astrocytoma cells and indicated that it is mostly associated with Lamp-1 and Limp-2 positive lysosomal vesicles and, marginally, to the Golgi apparatus and other cellular organelles. Noticeably, none of the examined tumor cells showed a membrane-Dpl localization. The membrane-associated Dpl expression was restored after the transfection of the astrocytoma cells with mutated Dpl-expression vectors in its glycosylation sites. Additionally, Dpl showed altered expression and traffic using the acidotropic agent ammonium chloride, leading to the accumulation of Dpl in nascent exocytic vesicles. Altogether, these results indicated that in the astrocytic tumor cells Dpl has an altered biosynthetic trafficking, likely derived from abnormal post-translational processes: these modifications do not permit the localization of Dpl in correspondence of the plasma membrane and lead to its intracellular accumulation in the lysosomes. In these proteolytic compartments, the astrocytic tumor cells might provide to the degradation of the excess of a potentially cytotoxic Dpl product.

Keywords: Glioma, immunofluorescence, prion-like protein, lysosome

1. Introduction

The first prion paralogue gene, doppel, has been recently discovered [25], leading to the hypothesis that ancestral gene-duplication events might have originated a prion-related gene family [7]. On the course of evolution, functional divergences have contributed to the different expression profile patterns of the cellular prion (PrP^C) and doppel (Dpl) proteins, with the former widely expressed in different tissues, particularly in the CNS [23] and the latter localized mainly in the testicular tissue of different mammalian species [13, 34]. Additionally, functional divergence has related PrP^C to the occurence and propagation of prion diseases in humans and animals, as originally proposed by Prusiner [29], while Dpl has been demonstrated to be not associated with the onset and development of these neurodegenerative diseases [10,36]. Doppel, similarly to the cellular prion protein, is in fact a GPI-anchored molecule but its expression is restricted to the plasma membrane of adluminal pole of human Sertoli cells and in correspondence of the flagella of mature ejaculated spermatozoa [28]; since Sertoli cells communicate with the germ ones either directly (cell–cell interaction) or indirectly (paracrine interaction) throughout gametogenesis, Dpl was proposed to be involved in spermiogenesis [28]; different authors have discovered that mice deficient for Dpl exhibited male sterility [5] and cellular models for Dpl functions in fertilization were suggested in mediating sperm–egg interaction [14]. On the other hand, other contributions have investigated Dpl cellular functions through protein-interaction studies. Unfortunately, these contributions did not address to clear physiological functions of Dpl, even considering different biological and cellular contexts [3,17]. Otherwise, we have investi-

*These authors contributed equally to the work.
**Corresponding author: Fax: +39 0382 528496; E-mail: sergio.c@ipvgen.unipv.it.

gated if Dpl might interact with some prion-interacting proteins, Grb2, GFAP and PrP itself, in astrocytoma cell line models, suggesting that Dpl was likely not involved in these protein partnerships [2]. Furthermore, during the past years, we have observed that the doppel encoding gene (*PRND*) was over-expressed in human astrocytic [11] and in haematological tumors [35]; additionally, *PRND* transcript was shown to be retained in the nucleus of the astrocytic tumor cells and its protein product was ectopically expressed in the cytoplasm of the neoplastic cells; additionally, Dpl was also hyper-glycosylated and it failed to be detected at the cell membranes [9].

Consequently, in this study we deeper investigated the unusual Dpl cellular localization in astrocytoma cell lines in order to gain a better understanding of some of the molecular events that accomplish the neoplastic cell transformation.

2. Material and methods

2.1. Cell lines

Human established glioblastoma cell lines IPDDC-A2 (ECACC, Salisbury, UK) and D384-MG (provided by Dr. Mauro Ceroni, University of Pavia, Italy) were used in the present study. IPDDC-A2 was derived from a Grade II mixed astrocytoma, while D384-MG is a clone isolated from a human glioblastoma (WHO grade IV) cell line, previously described [4]. IPDDC-A2 cells were cultivated in D-MEM medium supplemented with 10% FBS, 100 units/ml penicillin, 0.1 mg/ml streptomycin and 1% L-glutamine (GIBCO, Paisley, UK). D384-MG was maintained with D-MEM F12 medium (GIBCO) supplemented with 10% FBS, 100 units/ml penicillin, 0.1 mg/ml streptomycin and 1% L-glutamine.

Glioma (T98G and U373-MG) and human cervix tumor (HeLa) established cell lines were purchased from ECACC (UK). The human astrocytic tumor established PRT-HU2 cell line, previously described in [9] was isolated from a glioblastoma multiforme 61-years old female patient. These tumor cell lines were maintained in D-MEM medium supplemented with 10% FBS, 100 units/ml penicillin, 0.1 mg/ml streptomycin and 1% L-glutamine (GIBCO).

The tumor tissue for a glioma primary cell line was kindly provided by the Department of Neurosurgery, Monza (Italy), shortly after surgery of a 29-year-old male patient diagnosed with glioblastoma multiforme of the right temporal parietal lobe. Histological examination revealed a grade IV astrocytoma according to the WHO classification, and expressing GFAP immunohistochemically. The tumor tissue was washed with Hanks' balanced salt solution (HBSS; Sigma) and minced to 1–2 mm fragments with scissors. The fragments were dissociated by mechanical means and placed into 25 cm tissue culture flasks with D-MEM F12 supplemented 10% inactivated fetal calf serum (FBS) containing 100 units/ml penicillin and 0.1 mg/ml streptomycin. The culture was incubated at 37°C in a humidified atmosphere of 5% CO_2.

Normal human astrocytes (NHA) were purchased from Cambrex (UK) and cultivated in the specific astrocyte AGM medium (Cambrex) according to the manufacturer's specifications.

Glioma primary and NHA cells were maintained and fixed on coverslips at their second culture passages for immunofluorescent analysis.

2.2. Immunofluorescence microscopy

For immunofluorescence, different monoclonal and polyclonal antibodies were adopted. Species-specific Alexa Fluor 488 and Alexa Fluor 633 secondary conjugated antibodies (Invitrogen, Carlsbad, CA, USA) were coupled with primary antibodies and used as specified in Table 1. Cells cultured on coverslips were rinsed with phosphate-buffered saline (PBS), fixed immediately in 4% paraformaldehyde-PBS, pH 7.4, for 15 min at room temperature. Cells on coverslips were treated with 100 μl of Image-If Enhancer (Invitrogen) for 30 min at room temperature, according to the supplier's specifications. Cells were then incubated for 1 hour with primary antibodies diluted in PBS + 5% fat milk powder (w/v), using the dilutions reported in Table 1. Cells were washed with PBS and incubated for 1 hour with secondary antibodies (species-specific Alexa Fluor 488 or Alexa Fluor 633), diluted in PBS + 5% fat milk powder. Coverslips were then washed three times with PBS and treated with ProLong Gold antifade reagent with DAPI (Invitrogen) according to the manufacturer's instructions; finally, coverslips were mounted onto glass slides. Fluorescence was viewed using a fluorescence light inverted microscope (Nikon Eclipse TS100, Japan) with a 100× oil immersion objective. Confocal and Normanski interference contrast analysis were performed by laser scanning microscopy using a Leica TCS SPII microscopy equipped with the confocal inverted microscopy system Leica DM IRBE, using a 63× NA 1.32 oil immersion objective.

Table 1
Antibodies employed in immunofluorescence detection

Primary					Secondary		
Name	Target	Source	Provenience	Dil.	Name	Source	Dil.
H4A3	Lamp-1	Mouse monoclonal	Abcam	1:30	Alexa Fluor 488	Rabbit anti-mouse	1:100
G-20	Dpl	Goat polyclonal	Santa Cruz Biotechnologies	1:30	Alexa Fluor 633	Donkey anti-goat	1:100
N-18	Limp-2	Goat polyclonal	Santa Cruz Biotechnologies	1:30	Alexa Fluor 488	Donkey anti-goat	1:100
D7C7	Dpl	Mouse monoclonal	Dr. Man-Su Sy	1:30	Alexa Fluor 633	Rabbit anti-mouse	1:100
H4A3	Lamp-1	Mouse monoclonal	Abcam	1:30	Alexa Fluor 488	Rabbit anti-mouse	1:100
N-18	Limp-2	Goat polyclonal	Santa Cruz Biotechnologies	1:30	Alexa Fluor 633	Donkey anti-goat	1:100
RL90	PDI	Mouse monoclonal	Abcam	1:200	Alexa Fluor 488	Rabbit anti-mouse	1:200
G-20	Dpl	Goat polyclonal	Santa Cruz Biotechnologies	1:40	Alexa Fluor 633	Donkey anti-goat	1:200
CDF4	Golgin97	Mouse monoclonal	Invitrogen	1:30	Alexa Fluor 488	Rabbit anti-mouse	1:100
G-20	Dpl	Goat polyclonal	Santa Cruz Biotechnologies	1:30	Alexa Fluor 633	Donkey anti-goat	1:200
Ab1877	Catalase	Rabbit polyclonal	Abcam	1:100	Alexa Fluor 488	Donkey anti-goat	1:200
G-20	Dpl	Goat polyclonal	Santa Cruz Biotechnologies	1:30	Alexa Fluor 633	Donkey anti-goat	1:50

Antibodies were diluted (dil.) in PBS + 5% fat milk powder. Alexa Fluor 488 and 633 antibodies were provided by Invitrogen (USA).

2.3. Construction of wild-type and glycosylation mutant human Dpl expression plasmids

Both the *wild-type* and the glycosylation mutant Dpl proteins were cloned into two types of expression plasmids, containing or not-*EGFP*.

The non-fluorescent human *wild-type* Dpl expression vector, namely p-Dpl, was produced as follows: *PRND* coding sequence was amplified from 20 ng of human genomic DNA using Dpl-U and Dpl-L primers containing *XhoI* and *NotI* restriction sites (underlined), respectively: Dpl-U 5′-CCG CTC GAG CGG ATG AGG AAG CAC CTG AGC TG-3′ and Dpl-L 5′-ATT TGC GGC CGC TTA TTA TTT CAC CAT GAG CCA GAT CA-3′. After *XhoI/NotI* digestion, PCR products were cloned into the pEGFP-N1 expression plasmid (Clontech, Palo Alto, CA, USA), *XhoI/NotI* digested in order to delete *EGFP*.

The p-Dpl^{mut} vector, expressing Dpl with mutated glycosylation sites, was produced as follows. Mutagenesis was performed on p-Dpl to specifically introduce the threonine to alanine (at position 43) and asparagine to serine (at 98 and 110) substitutions into the amino acid sequence of Dpl, according to the QuickChange® mutagenesis kit guidelines (Stratagene, La Jolla, CA, USA). In particular, the following mutagenic primers (N98S-U, N98S-L; N110S-U, N110S-L; T43A-U, T43A-L) were adopted (mutated codons are underlined): N98S-U 5′-TGC TCT GAG GCT AGT GTG ACC AAG GAG GCA-3′ and N98S-L 5′-TGC CTC CTT GGT CAC ACT AGC CTC AGA GCA-3′, N110S-U 5′-TTT GTC ACC GGC TGC ATC AGT GCC ACC CAG G-3′ and N110S-L 5′-CCT GGG TGG CAC TGA TGC AGC CGG TGA CAA A-3′, O43A-U 5′-AAG GCC CTG CCC AGC GCT GCC CAG ATC ACT-3′ and O43A-L 5′-AGT GAT CTG GGC AGC GCT GGG CAG GGC CTT-3′. To obtain p-Dpl^{mut}, three serial mutagenesis experiments were performed. For each mutagenesis step a long PCR was performed as follows: 50 μl reaction containing 20 ng of p-Dpl plasmid, 100 ng of each primer, 0.2 mM dNTPs, 2.5 U of AccuTaq™ LA DNA Polymerase (Sigma, St. Louis, MO, USA) was amplified for 18 cycles consisting of 30 s denaturation at 95°C, 1 min annealing step at 60°C, followed by a 6 min extension step at 68°C. After PCR-based site-specific mutagenesis, the plasmid was digested with *Dpn*I and transformed into *E. coli* DH5α competent cells. Colonies were screened by PCR and the positive clones were sequenced.

The *EGFP*-fluorescent human *wild-type* Dpl construct, namely pEGFP-N1/Dpl, was made as described in Comincini et al. [9]. Briefly, the pEGFP-N1 plasmid (Clontech) was mutagenized by PCR using the primers 5′-CCG GAA TTC CCA CCA TGG TGA GCA AGG GCG AG-3′ and 5′-GTC GCG GCC GCT TTC TTG TAC AGC TCG TCC ATG-3′, to remove the stop codon at the end of *EGFP*. The pEGFP-N1/Dpl construct was produced amplifying the *PRND* amino terminal signal peptide coding region (from 1 to 25 Dpl residues) with the primers 5′-CCG CTC GAG CGG ATG AGG AAG CAC CTC AGC TG-3′ and 5′-CCG AAT TCG CTG GAC CGC AGA GAG GT-3′. This *PRND* portion was then cloned into the pEGFP-N1 mutagenized plasmid, 5′ of *EGFP,* in the *Xho*I

and *Eco*RI restriction sites. The remaining *PRND* peptide coding region (26–176 Dpl residues) was amplified using the primers 5′-GCG GCC GCT ACG AGG GGC ATC AAG CAC A-3′ and 5′-TGC GGC CGC TTA TTT CAC CAT GAG CCA GAT CA-3′. The product was then cloned downstream of *EGFP* in the modified pEGFP-N1 plasmid, using the *Not*I restriction site, thus obtaining pEGFP-N1/Dpl. The pEGFP-N1/Dpl^{mut}, expressing the Dpl protein with mutated glycosylation sites, was obtained amplifying the Dpl 26–176 peptide coding region from p-Dpl^{mut}, using the primers 5′-GCG GCC GCT ACG AGG GGC ATC AAG CAC A-3′ and 5′-TGC GGC CGC TTA TTT CAC CAT GAG CCA GAT CA-3′, and cloning the *Not*I digested PCR purified product into the mutagenized pEGFP-N1 plasmid. Each construct, i.e. p-Dpl and p-Dpl^{mut}, pEGFP-N1/Dpl and pEGFP-N1/Dpl^{mut} were confirmed by DNA sequencing.

2.4. Astrocytoma cells transfections and immunofluorescence

Highly purified p-Dpl or p-Dpl^{mut}, pEGFP-N1/Dpl or pEGFP-N1/Dpl^{mut} plasmids (1 μg) were mixed with 0.1 ml of transfection medium (D-MEM supplemented with 10% FBS and 1% L-glutamine). The mixture was incubated at room temperature for 5 min. Then, 2.5 μl of Lipofectamine 2000 reagent (Invitrogen) was added to the mixture, mixed for 10 s and finally incubated at room temperature for 20 min. IPDDC-A2 and D384-MG cells (plated one day before transfection at 5×10^5 into 30 mm culture dishes) were washed with PBS and trypsinized before adding the transfection mixture. The cells were then plated on glass coverslips and incubated for additional 24 h at 37°C and 5% CO_2. Dpl protein was visualised using anti-Dpl goat polyclonal G-20 (Santa Cruz Biotechnology, Santa Cruz, CA, USA) and Alexa Fluor 488 (Invitrogen) antibodies, as indicated in Table 1, by means of confocal and Normanski interference contrast microscopic examinations, as previously described.

2.5. Lysosomal pathway investigations

IPDDC-A2 and D384-MG astrocytoma cell lines (1.5×10^5 cells) were seeded onto coverslips glasses the day before the treatment, as above described. The cells were then treated with 10 mM ammonium chloride (Sigma) and incubated for 24–48–72 h in culture medium. After each treatment, the cells were fixed in 4% paraformaldehyde-PBS (pH 7.4) and incubated with G-20 anti-Dpl and Alexa Fluor 488 donkey anti-goat antibodies, as indicated in Table 1. Immunofluorescence was performed using DIC interference contrast microscopic examinations.

2.6. Western blot analysis

For immunoblot analysis of IPDDC-A2 and D384-MG cell extracts, 50 μg of total protein lysates were quantified using the Qubit instrument, according to the Quant-iT Protein Assay kit (Invitrogen), boiled for 5 min in Laemmli sample buffer (2% SDS (w/v), 6% Glycerol (v/v), 150 mM β-mercaptoethanol, 0.2% bromophenol blue (w/v), 62.5 mM Tris–HCl pH 6.8) and electrophoresed by SDS-PAGE (12% gel). Proteins were transferred onto a nitro-cellulose membrane Hybond™-C Extra (Amersham Biosciences, Little Chalfont, Buckinghamshire, UK). Membranes were blocked with 2% non-fat milk in PBS containing 0.1% Tween™ 20. The primary and secondary antibodies (Table 1) employed for immunodetection were used at 1:10000 dilution. As a control, an anti-GAPDH mouse monoclonal antibody (Ambion) was adopted at 1:20000. Blots were treated with specific peroxidase-coupled secondary antibodies (1:10000 dilution) and protein signals were revealed by the "ECL Advance™ Western Blotting Detection Kit" (Amersham Biosciences).

3. Results

Previous studies showed that Dpl was over-expressed in glioma specimens [11] and in astrocytoma cell lines [9]. In these studies, Dpl showed a diffuse and granular staining, suggesting a cytoplasmic accumulation of the protein within glial tumor cells.

In the present study, confocal microscopy was used to examine in further detail the Dpl sub-cellular localization in astrocytomas. We have therefore performed immunofluorescence localization of Dpl in two established tumor astrocytic cell lines, namely IPDDC-A2 and D384-MG, using different anti-Dpl and organelle-specific antibodies, reported in Table 1. Generally, these astrocytoma cells predominantly exhibited overlapping multi-punctate patterns of Dpl cytoplasmic localization, suggesting the presence of protein aggregates. These Dpl mass-like conglomerates were mainly identified in peri-nuclear proximal regions. Differently, no Dpl signal was highlighted in correspondence of the cellular membranes (Fig. 1, panels c

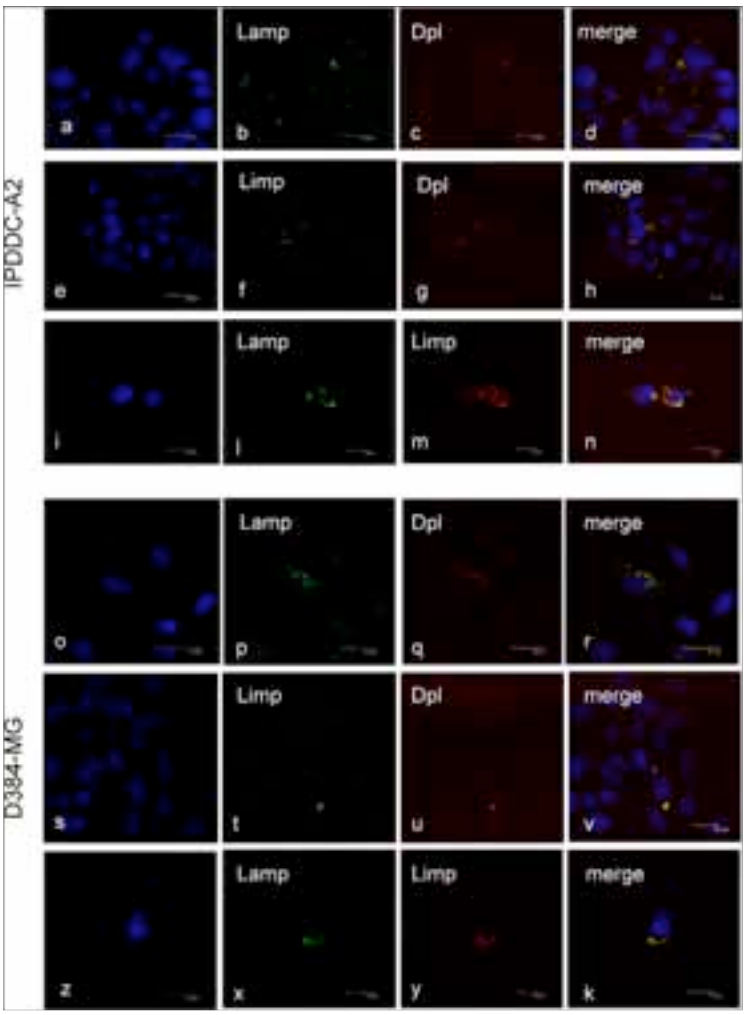

Fig. 1. Sub-cellular localization of Dpl in IPDDC-A2 and D384-MG astrocytoma cells. Cells were grown on glass slides as described in Materials and methods. At 48 hours, cells were fixed and incubated with primary antibodies, specifically mouse monoclonal Lamp-1 (Abcam) and G-20 (Santa Cruz Biotechnologies), anti-Dpl goat polyclonal or goat polyclonal Limp-2 (Santa Cruz Biotechnologies) and mouse monoclonal D7C7 antibodies. Species-specific Alexa Fluor 488 and Alexa Fluor 633 secondary antibodies (Invitrogen) were finally employed, as illustrated in Table 1. Panels i–n (IPDDC-A2) and z–k (D384-MG) indicated co-localization of the lysosomal membrane protein markers, i.e. Lamp-1 and Limp-2. Slides were incubated with ProLong Gold antifade reagent with DAPI (Invitrogen) to stain nuclei (blue). The cell morphology and fluorescence were observed with a confocal fluorescence microscope (Leica, original magnification, 63×). The scale bars are reported.

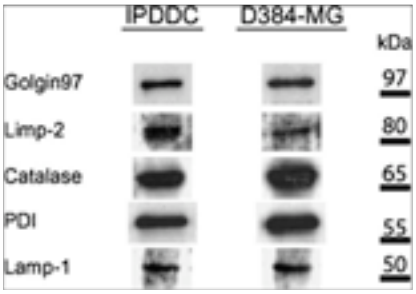

Fig. 2. Expression of organelle specific markers in IPDDC-A2 and D384-MG cells. Immunoblotting of Lamp-1 and Limp-2 for lysosomes, PDI for ER, Golgin97 for Golgi and Catalase for peroxisomes, was produced using the antibodies described in Table 1. Molecular weights, in kDa, was reported. Immunodetection was performed on the following amount of total extracted proteins: Golgin97 (20 μg), Limp-2, Lamp-1 and Catalase (50 μg) and PDI (2.5 μg).

and g for IPDDC-A2; q and u for D384-MG cells). Consequently, a panel of organelle specific markers, namely Lamp-1 and Limp-2 for lysosomes, PDI for ER, Golgin97 for Golgi and Catalase for peroxisomes, were employed for Dpl co-localization: the endogenous expression of the markers was primary assayed by Western blot in IPDDC-A2 and D384-MG cell lysates (Fig. 2). In these cells, Dpl was extensively co-localized with lysosomal membrane proteins, Lamp-1 and Limp-2, demonstrated by the yellow patches in the merged images (Fig. 1, panels d, h, r, v); additionally, Lamp-1 and Limp-2 showed nearly identical localization signals in the investigated cells (Fig. 1, panels n, k). Similar results in Dpl-lysosome co-localization were obtained using different monoclonal (D7C7) and polyclonal (DplVal, N-20 and FL176) anti-Dpl antibodies, as well as adopting additional astrocytoma cell lines (T98G, PRT-HU2 and U373-MG); differently, a predominant nuclear Dpl immunoreactivity was detected in the U87-MG astrocytoma cell line (data not shown).

Furthermore, differently from lysosomes, Dpl was barely detected in the other organelles, with the majority of the signals in correspondence of the Golgi apparatus (data available upon request). At last, co-immunoprecipitation experiments failed to detect Dpl–Limp 2 or Dpl–Lamp 1 interactions.

Dpl endogenous expression was investigated in a primary glioma cell line, isolated from a WHO IV patient and in normal human astrocytes (NHA): as reported in Fig. 3, Dpl was expressed in the primary glioma cells (panel a), with, however, a lesser extent of lysosome co-localization signals (c) compared to continuous glioma cell lines; differently, Dpl has a very faint expression in few NHA cells, with punctuate signals in the cytoplasm (d) and absence of Dpl-lysosome co-localization (f).

As previously reported, Dpl exhibited abnormal glycosylation patterns in several astrocytoma cell lines, including the investigated IPDDC-A2 and D384-MG ones [9]. In order to address if such abnormal post-translational modifications might influence the topology of Dpl in astrocytoma cells, we have therefore constructed a Dpl expression mutagenized plasmid (p-Dpl^{mut}), specifically in correspondence of O-(Thr 43) and N-glycosylation (Asn 98 and Asn 110) sites. Through site specific mutagenesis, these positions were substituted by the amino acids alanine (at position 43) and serine (98 and 110). Similarly, a chimaeric mutagenized Dpl vector (pEGFP-N1/Dpl^{mut}) expressing *EGFP* was constructed. As controls, *wild-type* Dpl expression vector, i.e. p-Dpl, and pEGFP-N1/Dpl vector expressing both Dpl and EGFP, were produced (see Section 2). These plasmids were sequenced, transfected and transiently expressed in IPDDC-A2 and D384-MG cells. Then, the cells were subjected to immunofluorescence reactions, followed by confocal and Normanski contrast interference microscopy examinations, using G-20 goat polyclonal anti-Dpl primary antibody and followed by incubation with Alexa Fluor 488 secondary antibody (Table 1). The results, reported in Fig. 4, indicated that p-Dpl and pEGFP-N1/Dpl expression gave cytoplasmic immunoreactive signals, similar to the endogenous Dpl ones (panels a and b in IPDDC-A2; f and g in D384-MG cells); differently, Dpl-membrane localization signals were shown in few cells after p-Dpl^{mut} expression (c, d; h, i). Similar membrane staining were obtained using the pEGFP-N1/Dpl^{mut} mutated plasmid (e, l). Western blot analysis after the isolation of membrane and whole total proteins of IPDDC-A2 and D384-MG cells, transfected with p-Dpl^{mut} vector, failed to reveal differences in Dpl expression compared to non-transfected cells. On the contrary, HeLa transfected cells with the p-Dpl^{mut} vector highlighted a Dpl unglycosylated band at 17–18 kDa by Western blot analysis (data not shown).

To further investigate on the Dpl lysosomal localization in the astrocytoma, IPDDC-A2 and D384-MG cells were treated with ammonium chloride, a known lysosomal inhibitor. The cells at different densities (from 10^4 to 1.5×10^5 cells, cultivated onto stan-

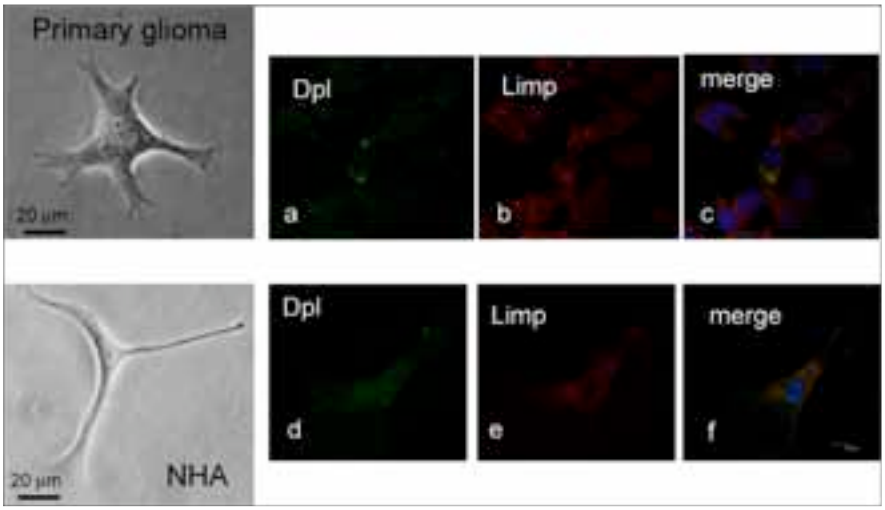

Fig. 3. Dpl expression in a primary glioma and in normal human astrocytic cells. At their second culture-passages, cells were fixed and incubated with primary antibodies, specifically goat polyclonal Limp-2 (Abcam) and mouse monoclonal anti-Dpl D7C7 antibodies. Species-specific Alexa Fluor 488 and Alexa Fluor 633 secondary antibodies (Invitrogen) were employed, as illustrated in Table 1. Slides were incubated with ProLong Gold antifade reagent with DAPI (Invitrogen) to stain nuclei (blue). The cell morphology and fluorescence were observed with a confocal fluorescence microscope (Leica, original magnification, 63×). The scale bars are reported.

dard microscopic glass coverslips) were subjected to different concentrations of the inhibitor (10–30 mM) and their viability was evaluated through microscopic examinations. In particular, using high concentration of ammonium chloride (30 mM), a high percentage (about 80%) of cells death was reported. Therefore, to investigate the effect of the lysosomal inhibition on the Dpl expression, we adopted a low concentration of ammonium chloride (10 mM) in presence of a high density of cells (1.5×10^5 cells *per* coverslip). Generally, after 48 hours of the treatment, a cytoplasmic increase of vacuolization compared to the control was observed (Fig. 5, panels a and b for IPDDC-A2; g and h for D384-MG cells, respectively); finally, at 72 hours the cells exhibited difference in morphology with large budding vesicles that de-touched from the plasma membrane (c, i). Dpl immunofluorescence studies showed after 48 hours a more diffuse cytoplasmic localization, and, additionally, some cells showed an intense staining in correspondence of the inner plasma membranes (d, l); noticeably, the Dpl staining in the vesicles significantly increased after 72 hours of the treatment, even through the release of Dpl-positive exocytic vesicles in the medium (e, f; m, n). Following this treatment, immunoblotting analysis was employed to investigate Dpl expression in IPDDC-A2 and D384-MG cells. As reported in Fig. 5, comparing to the untreated samples, a significant increase in Dpl expression was observed in IPDDC-A2 cells after 48 and 72 hours p.t., while a lesser variation in Dpl expression was observed in D384-MG cells.

4. Discussion

Recently, a novel protein, named doppel (Dpl), was identified which shares significant biochemical and structural homology with PrP^C [25,33]. Differently from PrP^C, Dpl is dispensable for prion diseases progression, but Dpl appears to have an essential function in male spermatogenesis (reviewed in [6]). Doppel gene (*PRND*) expression is highly tissue-specific and developmental stage-dependent, normally quiescent in adult brain but highly active in testis. However, abnormal and high levels of Dpl protein has been observed in human astrocytoma and in other non-glial tu-

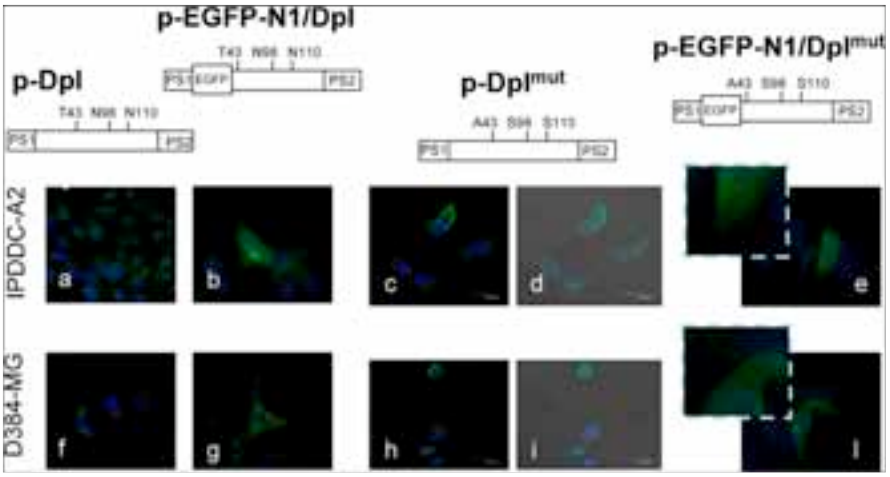

Fig. 4. Dpl transfection in astrocytoma cells. IPDDC-A2 and D384-MG cells (5×10^5 onto 30 mm dishes) were transfected with 1 μg of p-Dpl, pEGFP-N1/Dpl, p-Dpl^{mut} or pEGFP-N1/Dpl^{mut} expression vectors, combined with 2.5 μl of Lipofectamine 2000 (Invitrogen) as a transfection agent. After 24 hours post-transfection the medium was changed and the following day the cells were fixed on glass slides. Single immunofluorescence reactions were performed using G-20 anti-Dpl goat polyclonal (Santa Cruz Biotechnologies) and Alexa Fluor 488 (Invitrogen) antibodies. In pEGFP-N1/Dpl and pEGFP-N1/Dpl^{mut} transfected cells, EGFP was excited at 488 nm wavelength. IPDDC-A2 and D384-MG cells showed a diffuse cytoplasmic Dpl expression after p-Dpl and pEGFP-N1/Dpl transfection (respectively, panels a, b; f, g) while a plasma membrane Dpl localization was highlighted in p-Dpl^{mut} and pEGFP-N1/Dpl^{mut} transfected cells, after confocal or Normanski interference contrast examinations (c, d, e; h, i, l). Cells were visualized with a confocal fluorescence microscope (Leica, original magnification, 63×). The scale bars are reported.

mor specimens [8]. These findings suggest that *PRND* is activated under tumorigenic conditions that might be associated with the tumor progression [8]. In the astrocytic tumors that we have recently studied, Dpl is ectopically expressed in the cell cytoplasm [9]. In this context we have therefore deeper investigated the sub-cellular localization of Dpl in astrocytoma, reporting that Dpl-positive signals were localized in the lysosomes, through immunoreactivity to Limp-2 and Lamp-1 lysosome specific markers.

Lysosomes are acidic membrane-bound organelles involved in degradation of extracellular materials internalized by endocytosis and intracellular materials derived from autophagic processes [12,18]. The formation of lysosomes requires protein transport from the biosynthetic and the endocytic pathway. Proteins destined to be targeted to lysosomes are delivered to an acidic endosomal compartment either from the trans-Golgi network or from the plasma membrane via endocytosis. This system therefore contributes to the maintenance of homeostasis via numerous functions, including the supply of nutrients, the turnover of cellular proteins, the elimination of defective or unfavourable molecules and the down-regulation of surface receptors [37].

The sub-cellular localization of Dpl observed in astrocytoma cells (this study) is markedly different from the Dpl outer membrane attachment to neuro-2a (N2a) cells through its GPI anchor, as previously reported [33]. Furthermore, Massimino and colleagues [24] expressed human Dpl and PrP^C in neuroblastoma cells and demonstrated that the two proteins co-patched extensively at the cell membrane; additionally, when the two proteins were internalized by cross-linking to the cholera toxin, Dpl and PrP^C were together endocytosed within the Golgi complex [24]. Differently, our results pointed that Dpl was not detected on the cell membranes and that its internalization pathway is different from that previously described in neuroblastoma cells; in fact, Dpl is barely detected in both Golgi and ER apparatus, showing a predominant accumulation within lysosomal vesicles. The most parsimonious explanation to this observation might be that the tumor cells may overproduce Dpl and its internalization into

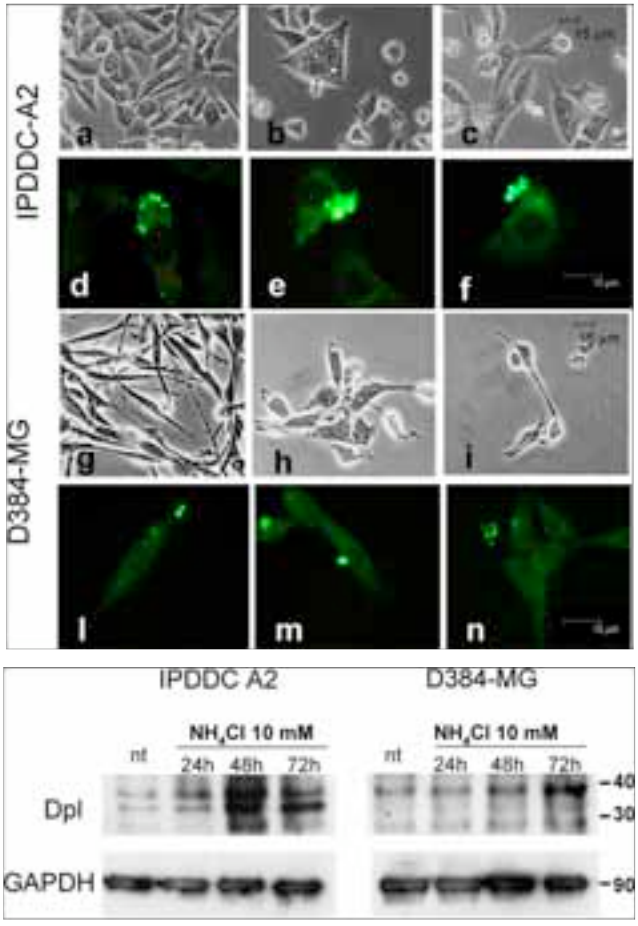

Fig. 5. Effect of ammonium chloride treatment on the Dpl traffic and expression in IPDDC-A2 and D384-MG cells. IPDDC-A2 cells were treated with 10 mM ammonium chloride, analysed in their morphology and in Dpl immunofluorescence after 24, 48 and 72 h, and finally compared to untreated control cells (a); extensive vacuolization was observed at 48 h (b) and several budding vesicles after 72 h (c). Dpl immunolocalization showed strong signals after 48 h in correspondence of the inner layer of the plasma membrane (d); Dpl was significantly accumulated in nascent budding and exocytic vesicles at 72 h (e and f). In D384-MG cells, treated as above, changes in morphology compared to the controls (g) were observed after 48 h (h), while several rounded and shrunken cells appeared after 72 h (i). Dpl immunolocalization showed strong signals after 48 hours in correspondence of the apical portion of the cells (l); as above described, Dpl was significantly accumulated in nascent budding and exocytic vesicles at 72 h (m and n). The morphology of the cells and Dpl immunofluorescence reactivity were DIC visualised with an inverted fluorescence microscope (Eclipse TS100, Nikon, original magnifications, 10, 40 and 100×). The scale bars are reported. Dpl expression in IPDDC-A2 and D384-MG cells was analysed by immunoblotting using the D7C7 anti-Dpl monoclonal antibody. Controls (NT) were compared to ammonium chloride treated cells after 24, 48 and 72 h. Control GAPDH protein expression was reported. Molecular weights (kDa) are indicated.

lysosomes could serve to eliminate the excess of protein. This concept could be reinforced by the fact that Dpl has a cellular toxic effect that could be directly counteracted by the expression of PrP^C and possibly through a direct interaction of the two proteins [32]. In a different cellular context, i.e. healthy adult rat astrocytes, Dpl shared co-localization with PrP^C on cell membrane: additionally, Dpl was shown to directly interact with PrP^C [30]. These differences in Dpl localization between tumoral glial and nervous cells might reflect a complex recycling machinery of the astrocytomas membrane proteins where GPI-linked proteins have remarkably different traffic and half-life within the cells, as previously reported [21,22].

In astrocytic tumor cells, Dpl is a highly glycosylated protein and it is ectopically expressed in the cell cytoplasm, as we previously reported [9]. We have therefore investigated if glycosylation *per se* could be involved in differences in the topology of Dpl in these glial tumor cells. As highlighted in the microscopic examination of p-Dpl^{mut} and pEGFP–N1/Dpl^{mut} transfected cells, the absence of glycosylation sites targeted Dpl to the membrane of a limited number of astrocytoma cells. Additionally, Normanski interference contrast examinations showed that some Dpl-membrane positive transfected cells became round and shrunken. Due to the limited number of the Dpl-membrane positive cells, Western blot failed to reveal differences in Dpl expression. Differently, immunoblotting analysis of protein lysates from HeLa transfected cells with the mutated Dpl expression vector p-Dpl^{mut} evidenced a band of 17–18 kDa, likely represented by the unglycosylated Dpl isoform (data not shown).

As a comment of our results, glycosylation might therefore be involved in the traffic and in the cytoplasmic localization of the Dpl protein in astrocytic tumor cells: our experiments indicated that a plasma membrane localization of Dpl needs at least post-translational modifications of the protein and that this cellular localization seems not well efficient and tolerated by the tumor cells. In fact, it is known that protein linked oligosaccharide moieties are considered to serve diverse functions. They stabilize the proteins against denaturation and proteolysis, enhance solubility, modulate immune responses, facilitate orientation of proteins relative to a membrane, confer structural rigidity to proteins and regulate their turnover [16]. Furthermore, it has long been predicted that the carbohydrate moieties of glycoproteins play important roles in the physical function and structural stability of the cell surface proteins [15].

According to our results, the most parsimonious explanation of Dpl localization in lysosomes, could be that the excess of a potentially cytotoxic Dpl product was targeted to these organelles for degradation. We therefore interfered with the lysosomal degradation pathway, treating the astrocytoma cells with ammonium chloride, a known lysosomotropic compound, resulting in alkalinization of the acidic compartments [26]. Our results suggest that the lysosomal compartments may be important for the cellular traffic and the expression of Dpl in astrocytoma cells: the raising of the pH of lysosomes by means of ammonium chloride might contribute to the mis-sorting of Dpl and its accumulation within the cells and finally in the exocytic vesicles. Additionally, as previously reported, the defective acidification of intracellular organelles in cancer cells results in aberrant secretion of different cytoplasmic proteins [19]. Nevertheless, we cannot exclude the possibility that the delivery of Dpl to lysosomes serves additional functions apart from those discussed. In particular, the absence of expression or the rapid turnover of some membrane proteins within astrocytoma cells might also contribute to a complex reassortment of plasma membrane proteins likely plausible in such cancers [1]. Further studies on the alteration of the traffic of plasma membrane proteins in cancer cells – as documented for Dpl in this study – should be required to increase our knowledge on the molecular processes involved in malignant cell transformation.

Acknowledgements

This work was supported by a grant from the Italian Ministry for Education, University and Research (MIUR), “Progetti di Ricerca di Interesse Nazionale (2005)”. A.A. is granted by “Fondo Sociale Europeo”. The authors are grateful to Dr. Patrizia Vaghi (Centro Grandi Strumenti, University of Pavia, Italy) for technical support in confocal microscopy examinations, to Prof. Giovanna Valentini (University of Pavia) and Dr. Man-Sun Sy (Case Western Reserve University, USA) for providing DplVal and D7C7 anti-Dpl antibodies, respectively.

References

[1] M.M. Aloysius, R.A. Robins, J.M. Eremin et al., Vaccination therapy in malignant disease, *Surgeon* **4** (2006), 309–320.

[2] A. Azzalin, I. Del Vecchio, L.R. Chiarelli et al., Absence of interaction between doppel and GFAP, Grb2, PrPc proteins in human tumor astrocytic cells, *Anticancer Res.* **25** (2005), 4369–4374.

[3] A. Azzalin, I. Del Vecchio, L. Ferretti and S. Comincini, The prion-like protein Doppel (Dpl) interacts with the human receptor for activated C-kinase 1 (RACK1) protein, *Anticancer Res.* **26** (2006), 4539–4547.

[4] A.J. Balmfort, S.G. Ball, R.I. Freshney et al., D-1 dopaminergic and b-adrenergic stimulation of adenylate cyclase in a clone derived from the human astrocytoma cell line G-CCM, *J. Neurochem.* **47** (1986), 715–719.

[5] A. Behrens, N. Genoud, H. Naumann et al., Absence of the prion protein homologue Doppel causes male sterility, *EMBO J.* **21** (2002), 3652–3658.

[6] A. Behrens, Physiological and pathological functions of the prion protein homologue Dpl, *Br. Med. Bull.* **66** (2003), 35–42.

[7] S. Comincini, M.G. Foti, M.A. Tranusis et al., Genomic organization, comparative analysis, and genetic polymorphisms of the bovine and ovine prion Doppel genes (PRND), *Mamm. Genome* **12** (2001), 729–733.

[8] S. Comincini, A. Facoetti, I. Del Vecchio et al., Differential expression of the prion-like protein doppel gene (PRND) in astrocytomas: a new molecular marker potentially involved in tumor progression, *Anticancer Res.* **24** (2004), 1507–1517.

[9] S. Comincini, L.R. Chiarelli, P. Zelini et al., Nuclear mRNA retention and aberrant doppel protein expression in human astrocytic tumor cells, *Oncol. Rep.* **16** (2006), 1325–1332.

[10] S. Comincini, I. Del Vecchio and A. Azzalin, The doppel gene biology: a scientific journey from brain to testis, and return, *Centr. Eur. J. Biol.* **1** (2006), 494–505.

[11] S. Comincini, V. Ferrara, A. Arias et al., Diagnostic value of PRND gene expression profiles in astrocytomas: relationship to tumor grades of malignancy, *Oncol. Rep.* **17** (2007), 989–996.

[12] C. de Duve, Lysosomes revisited, *Eur. J. Biochem.* **137** (1983), 391–397.

[13] A. Espenes, I. Harbitz, S. Skogtvedt et al., Dynamic expression of the prion-like protein Doppel in ovine testicular tissue, *Int. J. Androl.* **29** (2006), 400–408.

[14] N. Genoud, A. Behrens, I. Arrighi et al., Prion proteins and infertility: insight from mouse models, *Cytogenet. Genome Res.* **103** (2003), 285–289.

[15] R.S. Haltiwanger and J.B. Lowe, Role of glycosylation in development, *Ann. Rev. Biochem.* **73** (2004), 491–537.

[16] A. Helenius and M. Aebi, Roles of N-linked glycans in the endoplasmic reticulum, *Ann. Rev. Biochem.* **73** (2004), 1019–1049.

[17] C. Hundt and S. Weiss, The prion-like protein Doppel fails to interact with itself, the prion protein and the 37 kDa/67 kDa laminin receptor in the yeast two-hybrid system, *Biochim. Biophys. Acta* **1689** (2004), 1–5.

[18] W. Hunziker and H.J. Geuze, Intracellular trafficking of lysosomal membrane proteins, *Bioessays* **18** (1996), 379–389.

[19] N. Kokkonen, A. Rivinoja, A. Kauppila et al., Defective acidification of intracellular organelles results in aberrant secretion of cathepsin D in cancer cells, *J. Biol. Chem.* **279** (2004), 39982–39988.

[20] S. Kornfeld and I. Mellman, The biogenesis of lysosomes, *Ann. Rev. Cell. Biol.* **5** (1989), 483–525.

[21] P. Lemansky, S.H. Fatemi, B. Gorican et al., Dynamics and longevity of the glycolipid-anchored membrane protein, Thy-1, *J. Cell Biol.* **110** (1990), 1525–1531.

[22] N. Madore, K.L. Smith, C.H. Graham et al., Functionally different GPI proteins are organized in different domains on the neuronal surface, *EMBO J.* **18** (1999), 6917–6926.

[23] E. Makrinou, J. Collinge and M. Antoniou, Genomic characterization of the human prion protein (PrP) gene locus, *Mamm. Genome* **13** (2002), 696–703.

[24] M.L. Massimino, C. Ballarin, A. Bertoli et al., Human Doppel and prion protein share common membrane microdomains and internalization pathways, *Int. J. Biochem. Cell Biol.* **36** (2004), 2016–2031.

[25] R.C. Moore, I.Y. Lee, G.L. Silverman et al., Ataxia in prion protein (PrP)-deficient mice is associated with upregulation of the novel PrP-like protein doppel, *J. Mol. Biol.* **292** (1999), 797–817.

[26] C.R. Morales, Q. Zhao and S. Lefrancoise, Biogenesis of the lysosomes by endocytic flow of plasma membrane, *Biocell* **23** (1999), 149–160.

[27] D. Paisley, S. Banks, J. Selfridge et al., Male infertility and DNA damage in Doppel knockout and prion protein/Doppel double-knockout mice, *Am. J. Pathol.* **164** (2004), 2279–2288.

[28] K. Peoc'h, C. Serres, Y. Frobert et al., The human "prion-like" protein Doppel is expressed in both Sertoli cells and spermatozoa, *J. Biol. Chem.* **277** (2002), 43071–43078.

[29] S.B. Prusiner, Novel proteinaceous infectious particles cause scrapie, *Science* **216** (1982), 136–144.

[30] K. Qin, L. Zhao, Y. Tang et al., Doppel-induced apoptosis and counteraction by cellular prion protein in neuroblastoma and astrocytes, *Neuroscience* **141** (2006), 1375–1388.

[31] M. Rondena, F. Ceciliani, S. Comazzi et al., Identification of bovine doppel protein in testis, ovary and ejaculated spermatozoa, *Theriogenology* **63** (2005), 1195–1206.

[32] D. Rossi, A. Cozzio, E. Flechsig et al., Onset of ataxia and Purkinje cell loss in PrP null mice inversely correlated with Dpl level in brain, *EMBO J.* **20** (2001), 694–702.

[33] G.L. Silverman, K. Qin, R.C. Moore et al., Doppel is an N-glycosylated, glycosylphosphatidylinositol-anchored protein, *J. Biol. Chem.* **275** (2000), 26834–26841.

[34] M.A. Tranulis, A. Espenes, S. Comincini et al., The PrP-like protein Doppel gene in sheep and cattle: cDNA sequence and expression, *Mamm. Genome* **12** (2001), 376–379.

[35] E. Travaglino, S. Comincini, C. Benatti et al., Overexpression of the Doppel protein in acute myeloid leukaemias and myelodysplastic syndromes, *Br. J. Haematol.* **128** (2005), 877–884.

[36] N.L. Tuzi, E. Gall, D. Melton et al., Expression of doppel in the CNS of mice does not modulate transmissible spongiform encephalopathy disease, *J. Gen. Virol.* **83** (2002), 705–711.

[37] A. Vellodi, Lysosomal storage disorders, *Br. J. Haematol.* **128** (2004), 413–431.

Cellular Oncology 30 (2008) 491–501
DOI 10.3233/CLO-2008-0437
IOS Press

The doppel (Dpl) protein influences *in vitro* migration capability in astrocytoma-derived cells

Alberto Azzalin, Elena Sbalchiero, Giulia Barbieri, Silvia Palumbo, Cristina Muzzini and Sergio Comincini *
Dipartimento di Genetica e Microbiologia, Università di Pavia, Pavia, Italy

Abstract. Doppel (Dpl) protein is the paralogue of the cellular prion (PrP^C) protein. In humans, Dpl is expressed almost exclusively in testis where it is involved in spermatogenesis. Recently, the protein has been described to be ectopically expressed in astrocytomas and its potential association to the brain tumor malignancy progression has been advanced. In this study, we aimed to investigate *in vitro* the potential involvement of Dpl in the tumor cell migration: to this purpose, Dpl expression was reduced in the IPDDC-A2 astrocytoma-derived cell line, by means of antisense and siRNA approaches; migration rates were then evaluated by means of a scratch wound healing assay. As a result, the cellular migration was sensibly reduced after Dpl silencing. Following a complementary approach, in HeLa cells, showing very low endogenous Dpl expression, the protein expression was induced by transfection and stabilization of an eukaryotic expression vector containing the doppel gene coding sequence. These stably Dpl-overexpressing cells revealed a significant increase in the migration rate, compared to untreated and control cells. In addition, Dpl-forced expression induced substantial changes in the cell morphology. Of note, in these cells, viability examination by means of tetrazolium-based assay did not reveal differences in the proliferation; on the contrary, a variation in density-dependent growth, leading to an increase of cell contact inhibition was highlighted. These results, in conclusion, might suggest a potential and functional role for Dpl in tumor cells migratory and morphological behaviours and address to future gene-targeted therapeutic interventions.

Keywords: Prion-like proteins, glial tumor, IPDDC-A2, HeLa, siRNA, antisense oligonucleotide, gene-silencing, migration scratch assay

Abbreviations

CNS:	Central nervous system,
D-MEM:	Dulbecco's modified eagle's medium,
GPI:	Glycosyl-phosphatidyl-inositol,
IRES:	Internal ribosome entry site,
MTS:	3-(4,5-dimethylthiazol-2-yl)-5-(3-carboxymethoxyphenyl)-2-(4-sulphofenyl)-2H-tetrazolium,
NMR:	Nuclear magnetic resonance,
S-ODN:	Phosphothioate-oligonucleotide,
PBS:	Phosphate buffered saline,
SD:	Standard deviation,
SDS-PAGE:	Sodium dodecyl sulphate-polyacrilamide gel electrophoresis,
siRNA:	Short interfering RNA,
WHO:	World health organization.

*Corresponding author: Sergio Comincini, Dipartimento di Genetica e Microbiologia, Università di Pavia, via Ferrata, 1, 27100 Pavia, Italy. Tel.: +39 0382 985539; Fax: +39 0382 528496; E-mail: sergio.c@ipvgen.unipv.it.

1. Introduction

The majority of malignant brain tumors is derived from glial cells and most of them display an astrocytic component, but the high degree of heterogeneity often makes it difficult to determine the cell of origin [23,24]. Four malignancy grades are accepted by the WHO, from grade I, the biologically least aggressive, to the grade IV tumors (glioblastoma), the most aggressive [30]. Despite advances in clinical and molecular fields, high grade astrocytomas remain fatal, particularly because of striking rates of *de novo* and acquired resistance to therapeutic intervention [7]. Up to date, no therapy has been able to give tangi-

ble improvements in the prognosis and the survival of patients with this pathology is often less than one year [44,46]. Malignant astrocytomas, like most aggressive cancers, present aberrant proliferation, diminished apoptosis, escaping from both growth control and immuno-regulation [23]. Moreover, these tumors exhibit a characteristic ability to infiltrate healthy brain tissue and form satellite tumors. To this regard, many genes have been identified to be associated with astrocytic tumors migration [15,40]. This migration capacity makes these tumors exceedingly difficult to treat and even after resection, invasive cells can give rise to tumors within centimeters of the resection site [15].

In the recent past, the first prion-like protein gene, doppel (*PRND*), was described in rodents, cattle, sheep, goat and human [28,36,38,51,53]. In 2004, we first reported an altered expression of this gene in brain tumors, and we hypothesized that doppel might be considered as an astrocytic tumors progression marker [10]. Doppel gene product, Dpl, is a paralogue of the cellular prion protein (PrP^C), the main causative agent of spongiform encephalopathies, but it seems not be involved in these diseases [52]. Human Dpl protein is composed of 126 aminoacids, GPI-anchored to the cytoplasmic membrane, highly glycosylated and NMR analysis confirmed a carboxy-terminal domain composed of three α-helices and two β-sheets [31]. Dpl, differently from PrP^C that is widely expressed in different tissues, is described only in adult testis where it is involved in spermatogenesis and fertilization capability [6,33,41]. As we recently documented, Dpl is ectopically expressed in brain tumors; additionally, *PRND* mRNA expression was associated with the glial tumor malignant transformation [11]. Furthermore, in these tumors, the transcript showed a nuclear retention and the protein product was subjected to an unusual glycosylation; finally, Dpl failed to be GPI-anchored at the astrocytic tumor cellular membrane and it was mainly localized in the cellular cytoplasm [8].

In this work, an *in vitro* functional analysis was performed to clarify the role of the doppel gene product in regulating cell migration in human brain tumors.

2. Materials and methods

2.1. Cell lines and culture reagents

Human astrocytoma-derived IPDDC-A2 and cervical carcinoma HeLa cell lines (ECACC, Salisbury, UK) were employed. Cells were maintained at 37°C, 5% CO_2 in D-MEM supplied with 10% fetal bovine serum, 1% L-glutamine, 100 U/ml penicillin and 100 μg/ml streptomycin. Cell culture media and supplements were provided by Invitrogen (Carlsbad, CA, USA). For transfectants selection, puromycin (Sigma-Aldrich, St. Louis, MO, USA) was employed.

2.2. siRNA, antisense DNA oligonucleotides and treatments

Three *PRND*-specific siRNA molecules were purchased from Ambion (Austin, TX, USA). Their sequences were: *Silencer*® siRNA ID# 133939-sense 5′-GCA AAU CCU GGC AAG UGA Ctt-3′ and 133939-antisense 5′-GUC ACU UGC CAG GAU UUG Ctc-3′, ID# 133940-sense 5′-GCC UAA UGA AGG CCA UCA Utt-3′ and 133940-antisense 5′-AUG AUG GCC UUC AUU AGG CTG-3′, ID# 133941-sense 5′-CCA CCU UAU UAG CUA AAA Att-3′ and 133941-antisense 5′-UUU UUA GCU AAU AAG GUG Gtg-3′. A *GAPDH*-specific *Silencer*® siRNA was employed as control (ID# 4624).

Two antisense DNA oligonucleotides (ODN), fully phosphorothioated and HPLC-purified, were provide by Sigma®-Genosys. *PRND*-specific antisense S-ODN sequence was 5′-ATG AGG AAG CAC CTG AGC TG-3′ and *GAPDH*-specific antisense S-ODN sequence was 5′-CCG ACC TTC ACC TTC CCC AT-3′, both complementary to the first twenty nucleotides of their respectively gene coding sequences.

Transfection reactions were carried out using Lipofectamine™ 2000 reagent (Invitrogen) on a cells monolayer of about 70% confluence previously plated on 30 mm Petri dishes (Corning, New York, NY, USA) and, after respectively 18 and 24 h, migration assay and western blot analysis were performed. Briefly, the *PRND*-specific siRNAs were co-transfected, each one at the final concentration of 0.10 μM, in presence of 5.0 μl of transfection reagent; antisense S-ODNs were transfected at the final concentration of 1.57 μM with 2.5 μl of liposome reagent. Antibiotics-free medium was employed.

2.3. Plasmids construction

For overexpression experiments, pIRESpuro3 plasmid (Clontech Laboratories Inc., Palo Alto, CA, USA) was employed. The human doppel protein coding sequence was amplified from genomic DNA (Clontech Laboratories Inc.) using the following primers: Dpl(EcoRI)-U, 5′-CCG GAA TTC ATG AGG AAG CAC CTG AGC TG-3′ and Dpl(NotI)-L, 5′-TGC GGC

CGC TTA TTT CAC CAT GAG CCA GAT CA-3′; the PCR product was then *Eco*RI/*Not*I-cloned into the plasmid, thus originating the pIRESpuro3-*PRND* construct. As control, the pIRESpuro3-*PRNP* construct was prepared as follow: the human prion protein coding sequence was amplified from genomic DNA (Clontech Laboratories Inc.) employing the following primers: PrP(*Eco*RI)-U, 5′-CCG GAA TTC ATG GCG AAC CTT GGC TGC-3′ and PrP(*Not*I)-L, 5′-ATT TGC GGC CGC TTA TCA TCC CAC TAT CAG GAA GAT GA-3′. The PCR product was then *Eco*RI/*Not*I-digested and cloned into the pIRESpuro3. PCR thermal profile was: 31 cycles at 94°C × 15 s, 62°C × 30 s and 72°C × 60 s.

2.4. Generation of stably transfected HeLa cells

HeLa cells were transfected using Lipofectamine™ 2000 reagent (Invitrogen), as described in the manufacturer's protocol, with, respectively, pIRESpuro3 empty vector, pIRESpuro3-*PRND*, pIRESpuro3-*PRNP* and both constructs pIRESpuro3-*PRND* and pIRESpuro3-*PRNP*. Briefly, 10^5 cells were plated in 24-wells plate; 24 h later, 1 μg of the construct of interest was transfected with 2 μl of Lipofectamine™ 2000 and, after a 24 h-incubation time, puromycin (Sigma-Aldrich) at a final concentration of 1 μg/ml was added. Transfection efficiency was evaluated by means of the pEGFP-N1 plasmid (Clontech Laboratories Inc.), transfected independently, and evaluating the originated green-fluorescent cells. The stable cell lines were isolated, by sub-culturing and selecting with 1 μg/ml of puromycin for 1 month, prior of performing the experiments.

2.5. Western blot analysis and antibodies employed

For immuno-blot analysis, cells monolayer was washed twice with 37°C pre-warmed phosphate-buffered saline (PBS), trypsinized and the pellet was lysed with ice-cold RIPA buffer (150 mM NaCl, 50 mM Tris-HCl pH 8.0, 0.5% sodium deoxycholate, 1% Nonidet P-40 (Roche, Basel, Switzerland), 0.1% sodium dodecyl sulphate) by a 30-min incubation on ice; cell debris was removed by centrifugation at 13,000 rpm for 12 min at 4°C and supernantant was recovered and supplemented with Complete™ Mini protease inhibitor cocktail (Roche). Protein samples were quantified by Qubit™ fluorometer (Invitrogen) following manufacturer's instructions. 100 μg of total protein extract was boiled in Laemmli sample buffer (2% SDS (w/v), 6% glycerol (v/v), 150 mM β-mercaptoethanol, 0.02% bromophenol blue (w/v) and 62.5 mM Tris-HCl pH 6.8). Proteins were blotted onto nitro-cellulose membrane Hybond™-C Extra (Amersham Biosciences, Little Chalfont, Buckinghamshire, UK). Membranes were blocked with 2% non-fat milk in PBS containing 0.1% Tween® 20 (v/v). The following antibodies were employed for immuno-detection: rabbit polyclonal anti-human Dpl (kindly provided by Prof. Valentini), mouse monoclonal anti-human PrP^C (3F4, Sigma-Aldrich) and mouse monoclonal anti-*GAPDH* (Ambion), used at 1:10,000 dilution. The blots were then treated with species-specific peroxidase-coupled secondary antibodies (1:10,000, Amersham Biosciences) and protein signals were revealed by the "ECL Advance™ Western Blotting Detection Kit" (Amersham Biosciences).

2.6. In vitro scratch wound healing assay

The ability of cells to migrate in monolayer cultures was assessed by a scratch assay on 30-mm Petri dishes (Corning). For transient transfection experiments in IPDDC-A2 cells, eighteen hours after siRNA or S-ODN treatments, the assay was performed as follows. Cells, at a confluence of about 95%, were rinsed once with PBS and replaced with new complete medium. At the same time, three parallel lines were drawn with a permanent marker on the bottom of the dishes as reference and three parallel wounds were scraped, perpendicularly to these lines on the cells monolayer, by a sterile plastic micropipette tip: to measure the migratory capacity of the cells into the scrape wounds, nine points of reference were taken for each sample for each interval time (0–2–4–6–8 h). Microscopic photographs were taken where each wound crossed a marker line, first immediately after scrapings and then at the indicated time intervals. The migration distances were then deduced from the comparison of the t_0 (0 h) and the next intervals photographs and expressed in arbitrary units.

For the stably transfected cell lines, the day before, cells were plated in order to obtain approximately a 95% confluence at the start point of the assay. Cells were then rinsed once with PBS to remove cellular debris and replaced with new medium supplemented with 1 μg/ml puromycin and the scratch assay was performed as described above. For each plasmid construct, two different stable cell lines were tested.

For the transient transfection of S-ODN molecules in stably Dpl-expressing HeLa cells, seventeen hours after the treatment at a confluence of about 95% in

antibiotics-free medium (except 1 µg/ml of puromycin), the scratch assay was performed as previously described.

Morphology analysis and photographs were made using the inverted microscope Nikon Eclipse TS100 (Nikon, Tokyo, Japan).

2.7. Cell viability and cell growth assays

To test the cellular viability, an MTS-based assay, the "CellTiter 96® Aqueous One Solution Cell Proliferation Assay" (Promega, Madison, WI, USA) was employed. Cells were plated into 96-wells flat-bottom plate in triplicate at a density of 10^4 cells per well. First readouts were measured 24 h after plating and then at intervals of 24 h, following the manufacturer's instructions. Readouts were measures with a microplate reader (Titertek Multiskan, Huntsville, AL, USA) at 492 nm wavelength.

Growth curves were made employing a 96-wells plate: similarly, stably Dpl-expressing HeLa cells were plated at a density of 10^4 per well in triplicates. The cells were incubated up to 8 days: at intervals of 24 h, cells were trypsinized and counted by a hemocytometer.

2.8. Software employed and statistical analysis

The software employed for densitometric analysis was the GelixOne version 1.2.1 (Biostep GmbH, Jahnsdorf, Germany). Statistical analysis and graphs design were performed with Office Excel (Microsoft, Redmond, WA, USA); figures were processed with Illustrator® 10.0 (Adobe Systems Inc., San Jose, CA, USA). Data are expressed as mean $\pm$ SD of two independent experiments. The results were analyzed using the Student's t test; p value inferior to 0.05 was considered significant.

3. Results

Astrocytoma-derived cell line IPDDC-A2 (previously characterized for doppel expression in [8,14]) was transiently transfected with *PRND*-specific siRNA and antisense S-ODN molecules at a final concentration of 0.30 and 1.57 µM, respectively; immunoblotting analysis, carried out 24 h after transfection, showed a decreased Dpl protein expression of the previously described Dpl isoforms (Fig. 1(a)). Specifically, a more defined Dpl knockdown effect at this interval was obtained after S-ODN-treatment. A densitometrical analysis of the 30 kDa Dpl electrophoretic band, widely conserved in protein extracts from different tumor cells, in S-ODN- and siRNA-treated samples reported, respectively, an intensity of 35% and 49%, compared to the untreated sample (Fig. 1(a)).

To verify whether the doppel expression disruption was able to influence cell migration *in vitro*, we performed a scratch assay in IPDDC-A2 cells subjected or not to a *PRND* silencing. Since a strong reduction of Dpl was observed at 24 h after transfection with siRNA and S-ODN molecules, experiments addressing cellular migratory capacity were carried out accordingly. As shown in Fig. 1(b), both silencing techniques induced a sensitive decrease in the cell motility. As a negative control, validated *GAPDH*-specific siRNA and *GAPDH*-antisense S-ODN molecules were assayed: these interfering treatments did not influence cells migration ability. In particular, siRNA treatment showed the phenotipic effect earlier than S-ODN treatment, as shown in Fig. 1(c). The average migration rate varied from about 60 µm/h, in untreated and *GAPDH*-transfected cells, to approximately 40 µm/h, in Dpl-silenced cells. Finally, Fig. 1(b) shows some snapshots of the cells treated with the Dpl-silencing molecules respect to the not treated cells.

To extend the Dpl specific effect on the migrating phenotype, a different tumor cell line was assayed. HeLa cells, that showed a very low Dpl protein expression as reported in Fig. 2(a), have been stably transfected with the eukaryotic expression vector pIRESpuro3 (Clontech Laboratories Inc.) containing the *PRND* gene coding sequence. As shown in Fig. 2(a), Dpl protein displayed a heterodisperse intense band respects to the cell line stably selected for pIRESpuro3 plasmid alone and to the untreated cells. In addition, the *PRNP* gene coding sequence was cloned into the pIRESpuro3 plasmid and stably transfected HeLa cells overexpressing PrP^C protein, as shown in Fig. 2(a), were then assayed for migration capability. As reported in Fig. 2(c), the graph indicated an increase migration rate for Dpl-expressing cells (about 17 µm/h), while untreated cells, empty plasmid-selected cells and PrP^C-expressing cells exhibited a similar migration capability, significantly lower than Dpl-expressing cells (7 µm/h). Interestingly, stably expressing PrP^C and Dpl proteins cells, showed a migration rate similar to the Dpl transfectants (Fig. 2(c)). Finally, Fig. 2(b) showed photographs of Dpl-expressing and untreated cells, 24 h after performing the scratch.

Furthermore, stable Dpl transfectants were subjected to a treatment with the *PRND*-specific S-ODN

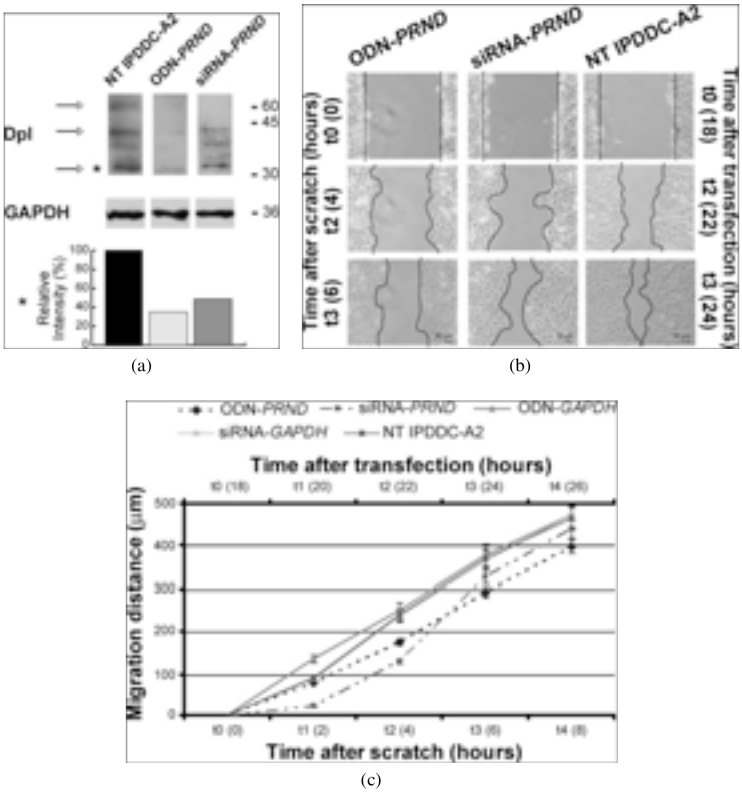

Fig. 1. IPDDC-A2 cells treatment with Dpl-silencing molecules and migration rate curves. (a) Doppel (Dpl) and GAPDH immuno-blot analysis of Dpl-silenced cell lysates, 24 h after transfection with *PRND*-specific S-ODN (ODN-*PRND*) and siRNA (siRNA-*PRND*), revealed an expression decrement of the three Dpl major isoforms (indicated by the arrows). The histogram reports the percentage relative intensities of the 30 kDa band (*), taken as representative band, normalized to the untreated sample (NT IPDDC-A2). Bands molecular weights are indicated in kDa. (b) The snapshots of the cell monolayer scratches indicate the higher migration rate of the untreated cells respects to the Dpl-silenced cells, respectively, at 4 h after scrape (i.e. 22 h after transfection) and at 6 h after scrape (i.e. 24 h after transfection). Scale bars are reported (50 µm). (c) The graphical representations of the migration curves show that both S-ODN (ODN-*PRND*) and siRNA (siRNA-*PRND*) treatment influences the migratory behaviour of IPDDC-A2 cells reducing the migration capability, while *GAPDH*-specific silencing treatment (ODN-*GAPDH* and siRNA-*GAPDH*) does not affect migration, being similar to the untreated control (NT IPDDC-A2). In particular, siRNA-*PRND* treatment shows the phenotypic effect earlier than ODN-*PRND* treatment, while an inverted trend is observed 5 h after scratch (i.e. 23 h after transfection). Statistical analysis was performed by Student's t test ($p < 0.05$).

molecules: a partial rescue of the migration rate of these cells was observed, respect to the untreated and to the *GAPDH*-specific S-ODN treated cells (Fig. 3).

Of note, average migration rate of untreated IPDDC-A2 cells on the Petri plastic support was much more higher than untreated HeLa, respectively 43 ± 0.1 µm/h and 7 ± 0.1 µm/h.

Dpl stably expressing HeLa cells were analyzed for cellular parameters such as viability, growth and morphology. As reported in Fig. 4(a), the viability assay

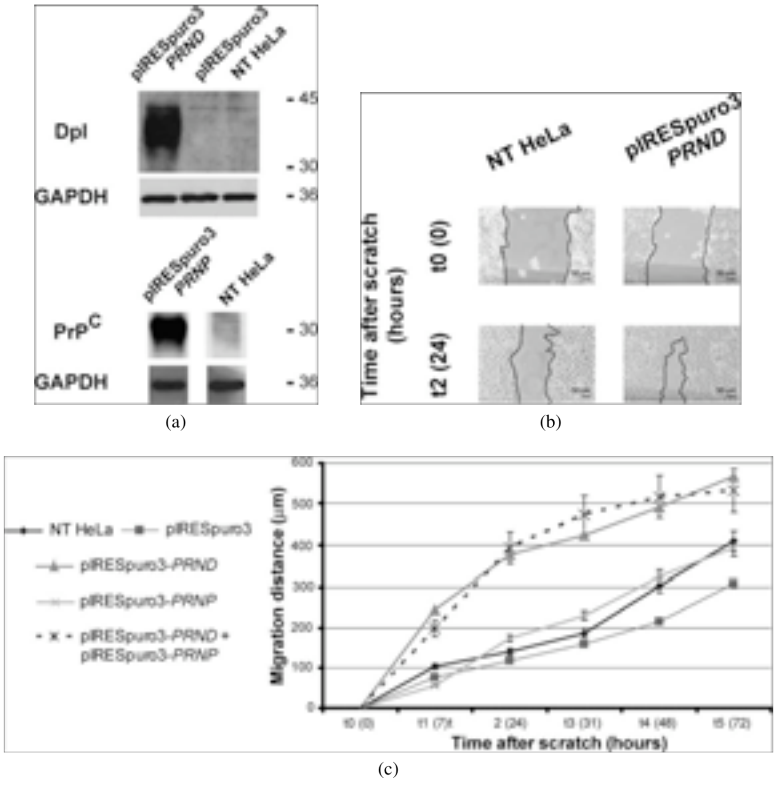

Fig. 2. Stably selected HeLa cells and migratory behaviour analysis. (a) Western blot analysis of HeLa cells overexpressing Dpl (pIRESpuro3-*PRND*) and PrP^C (pIRESpuro3-*PRNP*) respects to the empty-vector transfectants (pIRESpuro3) and the not-transfected (NT HeLa) controls. (b) The snapshots of the cell monolayer scratches indicate the increased migration rate for the overexpressing HeLa (pIRESpuro3-*PRND*) respects to the untreated cells (NT HeLa), observed at 24 h after scratch. Scale bars are reported (50 μm). (c) The migration rate curves of the stably transfected HeLa cells expressing Dpl (pIRESpuro3-*PRND*) or co-expressing both Dpl and PrP^C (pIRESpuro3-*PRND* + pIRESpuro3-*PRNP*) proteins show a higher value respect to, respectively, untreated (NT HeLa), empty vector transfectants (pIRESpuro3) and PrP^C expressing cells (pIRESpuro3-*PRNP*). Statistical analysis was performed by Student's t test ($p < 0.05$).

carried out with a tetrazolium-based method, showed similar curves for all the samples (correlation coefficients average $r = 0.99 \pm 0.012$), within the first 72 h. Figure 4(b) reported HeLa growth curves that were similar for untreated, for empty vector-transfectants and for stably expressing PrP^C cells. On the contrary, Dpl overexpressing cells showed a modified growth curve, particularly at the plateau phase, measurably lower than expected. Cells expressing both Dpl and PrP^C proteins showed a growth curve similar to the control. With regard to morphological aspects reported in Fig. 4(c), Dpl- and Dpl/PrP^C-expressing cells showed relevant alterations in the cellular shape: the typical squared shape of HeLa cells, resulting after empty vector and *PRNP* transfection, changed towards a lengthened and flattened forms in Dpl- and Dpl/PrP^C-expressing cells. In particular, the average length of Dpl-expressing cells varied from 75 to 175 μm com-

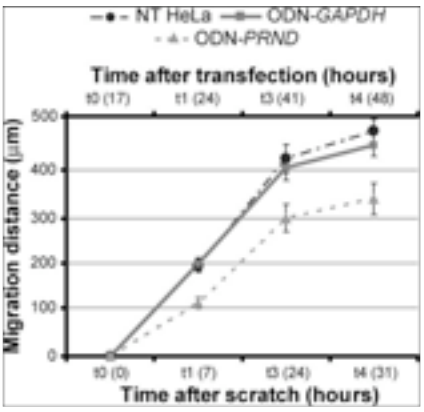

Fig. 3. Migration rate rescue in Dpl-expressing HeLa cells. The *PRND*-specific S-ODN treatment of the stably Dpl-expressing HeLa cells reduced their migration capability respects to untreated (NT HeLa) and to *GAPDH*-specific S-ODN treated cells (ODN-*GAPDH*). Statistical analysis was performed by Student's t test ($p < 0.05$).

pared to the controls (50–75 µm length); moreover, the nuclei underwent a significant dimension increase from about 25–30 µm to 37.5–40 µm in diameter, respectively.

4. Discussion

Astrocytomas are the most common CNS neoplasms; the accepted tumor grading is composed by four classes (WHO I–IV) according to the histological characteristics, but many efforts are performed, at the molecular level, to improve this classification [37]. We have recently proposed a potential novel marker, the doppel gene, *PRND*, the expression of which correlates with the astrocytoma malignancy [10,11]. *PRND* encodes for the Dpl protein, the first discovered paralogue of the cellular prion protein, PrP^C, the agent involved in spongiform encephalopathy diseases [38,43]. Dpl is expressed almost entirely in adult testis where it plays a role in spermatogenesis and in male fertilization but, as we described, it was ectopically and consistently up-regulated in brain tumors [6,9,41]. In this pathological context, some biological variations occurred respects to the physiological conditions: its transcript was retained in the nucleus, underwent an alternative splicing event and might be subjected to post-transcriptional modifications similarly to other genes involved in glioma progression [29]; moreover, the gene product failed to be GPI-anchored to the cytoplasmic membrane and it finally localized in the cytoplasm, undergoing a heavy and unexpected glycosylation [8].

Up to now, our investigations about doppel in the tumor context failed to trace a hypothetical functional role [1,2]. In this work, we analyzed the involvement of Dpl into one of the typical hallmarks of cancer, cell migration. Cells movement is a complex mechanism that is subjected to a rigid control by several genes during various stages of embryonic and adult developmental processes; during carcinogenesis, the motile behaviour reappears without usual cellular controls and this causes tumor cells spreading throughout the healthy tissue [45]; moreover, cancer cells motility plays a primary role in tumor invasion and metastasis formation [57]. In particular, in astrocytomas, infiltration ability of tumor cells constitutes one of the main causes of the unfortunate prognosis for these malignancies and it explains the intensive efforts in aiming the development of novel therapies [27,44]. Several key proteins are described as effectors of migratory ability of astrocytoma cells and several analysis of the transcriptomes are carried out to discovery novel targets [15,16,21,39].

The *in vitro* cellular assay to investigate the role of Dpl in tumor cells migration was performed in an astrocytoma established cell line, i.e. IPDDC-A2, showing detectable levels of Dpl expression, and in HeLa cells, as a Dpl-low expressing cell system. Among several available astrocytoma-derived cell lines (Hu-2 [3], D384-MG [4], U-87 MG and U-373 MG [42]), IPDDC-A2 was employed for the more substantial Dpl expression level and for its highest viability and transfection efficiency of nucleic acids. The migration behaviour was analyzed, respectively, in Dpl-silenced IPDDC-A2 and in stable Dpl-expressing HeLa cells, using an *in vitro* scratch wound healing assay on a cell monolayer, a widely used method to test the migration efficiency of a cell line, as reviewed in [54]. Dpl silencing was performed using two complementary approaches, namely antisense oligonucleotides-based technology and siRNA. These approaches share some similarities in the length molecules and in inducing target degradation after a complementary mRNA hybridization. On the other side, while siRNA adopt a specific cellular machinery (i.e. the RNA induced silencing complex, RISC), antisense technology is mainly based on RNA–DNA duplexes, that obstruct the ribosome processing and induce RNase H-mediated degradation. However, impor-

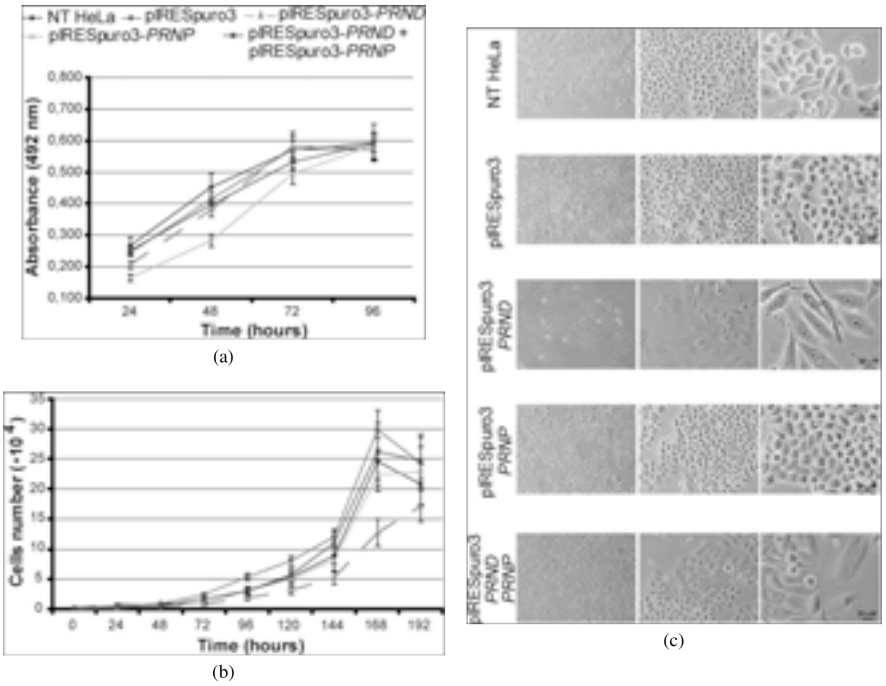

(a)

(b)

(c)

Fig. 4. Growth, viability assays and morphology evaluations. (a) An MTS-based assay was performed to evaluate the cellular viability. Absorbance readouts at 492 nm, evaluated at 24, 48, 72 and 96 h time intervals, revealed a similar behaviour among overexpressing Dpl (pIRESpuro3-*PRND*), PrP^C (pIRESpuro3-*PRNP*), both Dpl and PrP^C (pIRESpuro3-*PRND* + pIRESpuro3-*PRNP*), empty vector transfectants (pIRESpuro3) and untreated cells (NT HeLa). (b) The growth curves of the cells (evaluated for a 192 h time course) were analyzed; Dpl overexpressing cells show a lower plateau threshold compared to other cells. (c) Morphological analysis of HeLa cells, at 10×, 20× and 40× magnifications respectively, show relevant alterations in the cellular shape: the typical squared shape of HeLa cells changes towards a lengthened forms in Dpl- and Dpl/PrP^C-expressing cells. Scale bars are reported (30 μm).

tantly, the *in vitro* or *in vivo* efficacy of antisense *versus* siRNA technology is not theoretically predictable [12]. For the antisense technology, a fully phosphothioate DNA oligonucleotide (S-ODN), widely employed in cancer research [25,35,50], was designed against the first twenty nucleotides of the *PRND* coding sequence. As reported, after transfection, an earlier phenotypic effect on the cell migration after siRNA treatment respect to S-ODNs was detected; however, as immunoblotting revealed, S-ODN molecules showed a more efficient silencing on doppel protein expression than pre-designed siRNA molecules at twenty-four hours after transfection. This phenomenon might be related to an enhanced cellular stability of S-ODN compared to siRNA molecules and, conversely, to an earlier and more transient effect of *PRND*-specific siRNA on cellular migration [49].

To better evaluate the contribution of the doppel gene product in tumor cell migration, stably expressing-Dpl HeLa cells were produced. HeLa cells, that showed a very low endogenous Dpl expression as revealed by real time PCR analysis (data not shown) and western blot analysis (this work), were transfected and stabilized with the eukaryotic expression plasmid pIRESpuro3 containing the *PRND* coding sequence.

Transfected HeLa cells were selected for the stable overexpression of Dpl and the scratch wound healing assay was carried out. Western blot analysis re-

vealed a Dpl diffuse band of about 30–45 kDa, similar to that generally observed in the normal human testis tissue [41]. The migration rate of the Dpl-expressing HeLa cells was sensibly increased, more than two-fold higher, respects to the untreated cells and to the cells stably selected for the empty vector alone, proving that the effect of Dpl on migration capability of the cells was cell-type specific and due to the expression of Dpl. In addition, we treated these transfectants with the *PRND*-decoy ODNs previously tested with IPDDC-A2 cells instead of siRNA whose targets are located outside the *PRND* coding sequence and this make the mRNA transcript derived from the pIRESpuro3-*PRND* construct an "off-target" for our siRNA molecules: the treatment partially restored the migration rate similar to the untreated HeLa, while *GAPDH*-specific S-ODN did not affect this behaviour. Furthermore, we transfected and stably selected HeLa cells with the plasmid containing cellular prion protein coding gene sequence and, as we reported, cells overexpressing PrP^C did not show variations in migratory behaviour neither in morphology. The rationale of using this construct was because PrP^C and Dpl are homologue proteins that display a strong structural similarity [34]. Interestingly, when we examined the HeLa cells stably selected for both the plasmids containing *PRND* and *PRNP* coding sequences, the migration rate became similar to the Dpl-expressing cells. To this regard, our data showed that Dpl and PrP^C might exhibit different functions, following the hypothesis that two paralogue genes, after the duplication from their ancestor, are subjected to mutations that originate two functionally different genes with dissimilar expression patterns [32]. Furthermore, under our experimental conditions that consider cellular migratory behaviour, Dpl and PrP^C did not display any antagonizing role; differently, as previously described, in prion knock-out animal models and cell lines, Dpl neurotoxic effects were counteracted by *PRNP* transgene reintroduction [5,56]. However, in our cellular system, i.e. HeLa cells, the potentially toxic effect determined by the overexpression of doppel was not observed.

To discern the increased migration in Dpl-silenced cells from differences in viability rates, proliferation assays were performed in HeLa cells in a ninety-six growing time interval. Untreated HeLa and Dpl-stable expressing cells had a similar growing behaviour with, however, a significant difference of cell density in Dpl-overexpressing ones: these, differently from HeLa or other tumor cells, failed to reach a complete plate growth density, probably because of an augmented contact inhibition. This phenomenon might be also sustained by the documented differences in cell morphology after Dpl-expression stabilization, possibly explained by the interfering with unknown networks of genes involved in density-dependent cell growth [17, 18,20,22]. An inverted correlation between migration and growth rates, the "go or grow" dichotomy, was already described in tumor cells; however, the molecular and cellular mechanisms involved in these mutually exclusive phenotypes, are up to now not completely elucidated [18,19]. In the case of human astrocytomas, it might be hypothesized that Dpl is expressed mostly in the highly migratory cells of the external edge of the tumor area (work in progress). It is possible to hypothesized that doppel influence cell migration by means of its physiological cellular membrane localization that might be involved in cell-to-cell contacts; however, our knowledge about doppel localization in a tumor scenario could not sustain this speculation since we reported a cytoplasmic ectopic localization of the protein in astrocytoma [8,47]. An additional possibility is that doppel could take part to an up to now unknown signaling network that might influence migration. To this regard, we recently documented RACK1 (Receptor for Activated C-Kinase) as a Dpl interacting protein [2]. RACK1 is an adaptor protein that regulates signaling via Src- and PKC (protein kinase C)-dependent pathways and in particular it has been described to modulate the integrin-mediated cellular adhesion and migration [13,26,48].

Furthermore, as we reported, a forced-Dpl expression induced an irreversible morphological change in HeLa cells. This phenotype was Dpl-specific, since prion and empty expression vector did not induce differences in their cellular shape. Variations in cell motility is often associated with morphological changes and differences in actin expression [55]: to this regard, however, HeLa-treated cells did not exhibit differences in actin expression (data not shown), suggesting that other cyto-architectural proteins might be involved. Finally, neither siRNA nor ODNs treatment of IPDDC-A2 cells showed morphological changes, probably due the transient mechanism of action of these molecules.

In summary, our study highlighted for the first time a functional role of the doppel gene product in inducing differences in astrocytic tumor cell migration and morphology, suggesting a potential antisense therapy against this target protein with the aim of interfering with the described phenotypes.

Acknowledgements

This study was supported by a grant from the Italian MIUR, "Progetti di Ricerca di Rilevante Interesse Nazionale (2005)"; A.A. is granted by Fondo Sociale Europeo (F.S.E.); the authors are grateful to: Prof. Valentini (University of Pavia) for providing the anti-human Dpl antibody; Prof. Ferretti and Prof. Ranzani (University of Pavia) for the cell culture facilities; Prof. Giulotto (University of Pavia) for providing eukaryotic expression vector.

References

[1] A. Azzalin, I. Del Vecchio, L.R. Chiarelli et al., Absence of interaction between doppel and GFAP, Grb2, PrP^C proteins in human tumor astrocytic cells, *Anticancer Research* **25** (2005), 4369–4374.

[2] A. Azzalin, I. Del Vecchio, L. Ferretti et al., The prion-like protein doppel (Dpl) interacts with the human receptor for activated C-kinase 1 (RACK1) protein, *Anticancer Research* **26** (2006), 4539–4548.

[3] G. Bacciocchi, N. Gibelli, C. Zibera et al., Establishment and characterization of two cell lines derived from human glioblastoma multiforme, *Anticancer Research* **12** (1992), 853–861.

[4] A.J. Balmfort, S.G. Ball, R.I. Freshney et al., D-1 dopaminergic and β-adrenergic stimulation of adenylate cyclase in a clone derived from the human astrocytoma cell line G-CCM, *Journal Neurochemistry* **47** (1986), 715–719.

[5] A. Behrens and A. Aguzzi, Small is not beautiful: antagonizing functions for the prion protein PrP(C) and its homologue Dpl, *Trends in Neuroscience* **25** (2002), 150–154.

[6] A. Behrens, S. Brandner, N. Genoud et al., Absence of the prion protein homologue doppel causes male sterility, *EMBO Journal* **21** (2002), 3652–3658.

[7] V.P. Collins, Mechanisms of disease: genetic predictors of response to treatment in brain tumors, *Nature Clinical Practice Oncology* **4** (2006), 362–374.

[8] S. Comincini, L.R. Chiarelli, P. Zelini et al., Nuclear mRNA retention and aberrant doppel protein expression in human astrocytic tumor cells, *Oncology Reports* **16** (2006), 1325–1332.

[9] S. Comincini, I. Del Vecchio and A. Azzalin, The doppel gene biology: a scientific journey from brain to testis, and return, *Central European Journal of Biology* **1** (2006), 494–505.

[10] S. Comincini, A. Facoetti, I. Del Vecchio et al., Differential expression of the prion-like protein doppel gene (*PRND*) in astrocytomas: a new molecular marker potentially involved in tumor progression, *Anticancer Research* **24** (2004), 1507–1517.

[11] S. Comincini, V. Ferrara, A. Arias et al., Diagnostic value of *PRND* gene expression profiles in astrocytomas: relationship to tumor grades of malignancy, *Oncology Reports* **17** (2007), 989–996.

[12] D.R. Corey, RNA learns from antisense, *Nature Chemical Biology* **3** (2007), 8–11.

[13] E.A. Cox, D. Bennin, A.T. Doan et al., RACK1 regulates integrin-mediated adhesion, protrusion, and chemotactic cell migration via its Src-binding site, *Molecular Biology of the Cell* **14** (2003), 658–669.

[14] I. Del Vecchio, A. Azzalin, E. Guidi et al., Functional mapping of the bovine doppel gene promoter region, *Gene* **356** (2005), 101–108.

[15] T. Demuth and M.E. Berens, Molecular mechanisms of glioma cell migration and invasion, *Journal of Neuro-Oncology* **70** (2004), 217–228.

[16] T. Demuth, J.L. Rennet, D.B. Hoelzinger et al., Glioma cells on the run – the migratory transcriptome of 10 human glioma cell lines, *BMC Genomics* **29** (2008), 9–54.

[17] F. Fagotto and B.M. Gumbiner, Cell contact-dependent signaling, *Developmental Biology* **180** (1996), 445–454.

[18] A. Giese, R. Bjerkvig, M.E. Berens et al., Cost of migration: invasion of malignant gliomas and implications for treatment, *Journal Clinical Oncology* **21** (2003), 1624–1636.

[19] A. Giese, M.A. Loo, N. Tran et al., Dichotomy of astrocytoma migration and proliferation, *International Journal of Cancer* **67** (1996), 275–282.

[20] B.M. Gumbiner, Cell adhesion: the molecular basis of tissue architecture and morphogenesis, *Cell* **84** (1996), 345–357.

[21] D.B. Hoelzinger, L. Mariani, J. Weis et al., Gene expression profile of glioblastoma multiforme invasive phenotype points to new therapeutic targets, *Neoplasia* **7** (2005), 7–16.

[22] R.O. Hynes, Cell adhesion: old and new questions, *Trends in Genetics* **15** (1999), M33–M37.

[23] K. Ichimura, H. Ohgaki, P. Kleihues et al., Molecular pathogenesis of astrocytic tumours, *Journal of Neuro-Oncology* **70** (2004), 137–160.

[24] K.R. Jessen, Glial cells, *International Journal of Biochemistry & Cell Biology* **36** (2004), 1861–1867.

[25] A. Kalota, Progress in the development of nucleic acid therapeutics for cancer, *Cancer Biology & Therapy* **3** (2004), 4–12.

[26] P.A. Kiely, D. O'Gorman, K. Luong et al., Insulin-like growth factor I controls a mutually exclusive association of RACK1 with protein phosphatase 2A and β1 integrin to promote cell migration, *Molecular and Cellular Biology* **26** (2006), 4041–4051.

[27] F. Lefranc, J. Brotchi and R. Kiss, Possible future issues in the treatment of glioblastomas: special emphasis on cell migration and the resistance of migrating glioblastoma cells to apoptosis, *Journal of Clinical Oncology* **23** (2006), 2411–2422.

[28] A. Li, S. Sakaguchi, R. Atarashi et al., Identification of a novel gene encoding a PrP-like protein expressed as chimeric transcripts fused to PrP exon 1/2 in ataxic mouse line with a disrupted PrP gene, *Cellular and Molecular Neurobiology* **20** (2000), 553–567.

[29] I. Lopez de Silanes, M.P. Quesada and M. Esteller, Aberrant regulation of messenger RNA $3'$-untraslated region in human cancer, *Cellular Oncology* **29** (2007), 1–17.

[30] D.N. Louis, H. Ohgaki, O.D. Wiestler et al., The 2007 WHO classification of tumours of the central nervous system, *Acta Neuropathologica* **114** (2007), 97–109.

[31] T. Lührs, R. Riek, P. Güntert et al., NMR structure of the human doppel protein, *Journal of Molecular Biology* **326** (2003), 1549–1557.

[32] M. Lynch and S. Conery, The evolutionary fate and consequences of duplicate genes, *Science* **290** (2000), 1151–1155.

[33] E. Makrinou, J. Collinge and M. Antoniou, Genomic characterization of the human prion protein (PrP) gene locus, *Mammalian Genome* **13** (2002), 696–703.

[34] P. Mastrangelo and D. Westaway, The prion gene complex encoding PrP^C and Doppel insights from mutational analysis, *Gene* **275** (2001), 1–18.

[35] A. Matsuno and T. Nagashima, Specific gene suppression using antisense strategy for growth suppression of glioma, *Medical Electron Microscopy* **37** (2004), 158–161.

[36] S. Mead, J. Beck, A. Dickinson et al., Examination of the human prion protein-like gene Doppel for genetic susceptibility to sporadic and variant Creutzfeldt–Jakob disease, *Neuroscience Letters* **290** (2000), 117–120.

[37] P.S. Mischel, T.F. Cloughesy and S.F. Nelson, DNA-microarray analysis of brain cancer: molecular classification for therapy, *Nature Review Neuroscience* **5** (2004), 782–792.

[38] R.C. Moore, I.Y. Lee, G.L. Silverman et al., Ataxia in prion protein (PrP)-deficient mice is associated with upregulation of the novel PrP-like protein doppel, *Journal of Molecular Biology* **292** (1999), 797–817.

[39] M. Nakada, S. Nakada, T. Demuth et al., Molecular targets of glioma invasion, *Cellular and Molecular Life Sciences* **64** (2007), 458–478.

[40] H. Ohgaki and P. Kleihues, Genetic pathways to primary and secondary glioblastoma, *American Journal of Pathology* **170** (2007), 1445–1453.

[41] K. Peoc'h, C. Serres, Y. Frobert et al., The human "prion-like" protein Doppel is expressed in both Sertoli cells and spermatozoa, *Journal of Biological Chemistry* **277** (2002), 43071–43078.

[42] J. Pontén and E.H. Macintyre, Long term culture of normal and neoplastic human glia, *Acta Pathologica et Microbiologica Scandinavica* **74** (1968), 465–486.

[43] S.B. Prusiner, Novel proteinaceous infectious particles cause scrapie, *Science* **216** (1982), 136–144.

[44] D.A. Reardon, J.N. Rich, H.S. Friedman et al., Recent advances in the treatment of malignant astrocytoma, *Journal of Clinical Oncology* **24** (2006), 1253–1264.

[45] E. Sahai, Mechanisms of cancer cell invasion, *Current Opinion in Genetics & Development* **15** (2005), 87–96.

[46] S. Sathornsumetee and J.N. Rich, New treatment strategies for malignant gliomas, *Expert Review of Anticancer Therapy* **6** (2006), 1087–1104.

[47] E. Sbalchiero, A. Azzalin, S. Palumbo et al., Altered cellular distribution and sub-cellular sorting of doppel (Dpl) protein in human astrocytoma cell lines, *Cellular Oncology* **30** (2008), 337–347.

[48] D. Schechtman and D. Mochly-Rosen, Adaptor proteins in protein kinase C-mediated signal transduction, *Oncogene* **20** (2001), 6339–6347.

[49] F. Shi and D. Hoekstra, Effective intracellular delivery of oligonucleotides in order to make sense of antisense, *Journal of Controlled Release* **97** (2004), 189–209.

[50] I. Tamm, Antisense therapy in malignant diseases: status quo and quo vadis?, *Clinical Science* **110** (2006), 427–442.

[51] M.A. Tranulis, A. Espenes, S. Comincini et al., The PrP-like protein doppel gene in sheep and cattle: cDNA sequence and expression, *Mammalian Genome* **12** (2001), 376–379.

[52] N.L. Tuzi, E. Gall, D. Melton et al., Expression of doppel in the CNS of mice does not modulate transmissible spongiform encephalopathy disease, *Journal of General Virology* **83** (2002), 705–711.

[53] C. Uboldi, I. Del Vecchio, M.G. Foti et al., Prion-like doppel gene (*PRND*) in the goat: genomic structure, cDNA, and polymorphisms, *Mammalian Genome* **16** (2005), 963–971.

[54] A. Valster, N.L. Tran, M. Nakada et al., Cell migration and invasion assays, *Methods* **37** (2005), 208–215.

[55] M. Vicente-Manzanares, D.J. Webb and A.R. Horwitz, Cell migration at a glance, *Cell Science* **118** (2005), 4917–4919.

[56] C. Weissmann and A. Aguzzi, Perspectives: neurobiology. PrP's double causes trouble, *Science* **286** (1999), 914–915.

[57] H. Yamaguchi, J. Wyckoff and J. Condeelis, Cell migration in tumors, *Current Opinion in Cellular Biology* **17** (2005), 559–564.

Hindawi Publishing Corporation
Journal of Biomedicine and Biotechnology
Volume 2009, Article ID 924565, 12 pages
doi:10.1155/2009/924565

Methodology Report

Gene Expression Analysis of an *EGFR* Indirectly Related Pathway Identified *PTEN* and *MMP9* as Reliable Diagnostic Markers for Human Glial Tumor Specimens

Sergio Comincini,[1] Mayra Paolillo,[2] Giulia Barbieri,[1] Silvia Palumbo,[1] Elena Sbalchiero,[1] Alberto Azzalin,[1] Marika A. Russo,[2] and Sergio Schinelli[2]

[1] *Dipartimento di Genetica e Microbiologia, Università di Pavia, Via Ferrata 1, 27100 Pavia, Italy*
[2] *Dipartimento di Farmacologia Sperimentale ed Applicata, Università di Pavia, Viale Taramelli 14, 27100 Pavia, Italy*

Correspondence should be addressed to Sergio Comincini, sergio.c@ipvgen.unipv.it

Received 9 February 2009; Revised 23 April 2009; Accepted 18 May 2009

Recommended by Zhumur Ghosh

In this study the mRNA levels of five *EGFR* indirectly related genes, *EGFR*, *HB-EGF*, *ADAM17*, *PTEN*, and *MMP9*, have been assessed by Real-time PCR in a panel of 37 glioblastoma multiforme specimens and in 5 normal brain samples; as a result, in glioblastoma, *ADAM17* and *PTEN* expression was significantly lower than in normal brain samples, and, in particular, a statistically significant inverse correlation was found between *PTEN* and *MMP9* mRNA levels. To verify if this correlation was conserved in gliomas, *PTEN* and *MMP9* expression was further investigated in an additional panel of 16 anaplastic astrocytoma specimens and, in parallel, in different human normal and astrocytic tumor cell lines. In anaplastic astrocytomas *PTEN* expression was significantly higher than in glioblastoma multiforme, but no significant correlation was found between *PTEN* and *MMP9* expression. *PTEN* and *MMP9* mRNA levels were also employed to identify subgroups of specimens within the different glioma malignancy grades and to define a gene expression-based diagnostic classification scheme. In conclusion, this gene expression survey highlighted that the combined measurement of *PTEN* and *MMP9* transcripts might represent a novel reliable tool for the differential diagnosis of high-grade gliomas, and it also suggested a functional link involving these genes in glial tumors.

1. Introduction

Glioblastoma multiforme is the most malignant brain tumor among astrocytic gliomas with a typical prognosis of about 12 months in spite of current therapeutic approaches that include neurosurgery followed by combined chemotherapy and radiotherapy [1]. Recently, the development of massive screening genome technologies, such as gene expression profiling, has prompted new attempts to the classification of glioblastoma subgroups on molecular basis in order to identify new diagnostic or prognostic tools. At present the search for potential molecular markers among aberrant signal transduction pathways in glioblastoma is actively exploited for the optimization of existing therapies or the development of innovative drugs [2]. However, the accomplishment of this ambitious task is severely hindered by the extreme heterogeneity of glioblastoma tumor samples and by the subsequent variability of possibly identified molecular markers. One way to overcome this limit could be represented by the concomitant analysis of the mRNA expression of several selected genes, already known to be functionally involved in the cellular malignant transformation. This analysis could highlight differences in gene expression levels among high-grade gliomas, or at the same time it could reveal relationships within glioma subtypes between the genes analyzed in order to improve their reliability as prognostic or diagnostic markers.

The epidermal growth factor (EGF) receptor (EGFR or ErbB1) plays a pivotal role in cancer physiology because its activation, elicited by at least six different endogenous peptidergic EGF-like ligands, leads to the activation of intracellular signalling pathways that modulate cell

Table 1: Age, gender, mRNA expression values (in femptograms), and anatomical location of glioblasytoma multiforme samples.

Age	Sex	*EGFR*	*ADAM17*	*HB-EGF*	*PTEN*	*MMP9*	Location
68	M	2.78	0.31	0.69	1.85	6.39	Parietal
84	F	155.97	0.31	4.43	6.81	31.13	Parietal
23	M	95.25	3.54	19.01	5.15	0.04	Cerebellum
50	M	579.69	0.87	9.28	8.97	43.32	Frontal dx
71	F	7.11	0.08	0.82	2.27	0.21	Frontal dx
58	M	236.18	0.91	8.98	15.05	183.29	Parietal dx
66	M	12.85	0.13	1.38	0.41	0.04	Temporal sx
50	M	150.97	3.08	4.87	1.65	3.09	Temporal dx
38	F	60.10	2.23	9.23	7.01	30.41	Occipital dx
61	F	2.88	0.41	1.75	1.96	0.72	Frontal sx
68	F	4.87	0.63	8.71	0.82	0.82	Occipital dx
70	M	23.38	2.13	2.82	3.92	3.51	Frontal dx
59	M	425.51	1.28	4.32	4.84	8.04	Frontal sx
67	F	1268.24	2.99	13.92	12.68	32.58	Temporal dx
31	M	13.33	1.87	52.08	6.66	13.33	Frontal sx
68	F	0.77	0.59	12.85	0.62	1.04	Parietal dx
39	F	6.87	13.33	0.21	3.14	0.16	Frontoinsular
39	M	2.37	0.42	3.96	4.79	0.21	Parietal sx
45	F	274.74	0.66	7.14	1.25	2.52	Frontal dx
63	M	1284.37	13.33	0.21	3.12	10.62	Temporal dx
71	M	30.11	5.42	10.62	2.92	2.08	Frontal sx
60	M	73.96	17.71	7.54	3.33	4.37	Temporal sx
44	F	2562.92	6.87	18.96	3.33	8.33	Thalamus sx
73	F	38.75	13.12	7.53	3.33	1.04	Paratrigonal sx
47	F	16.88	4.79	7.29	3.13	1.04	Frontal sx
63	M	12.01	12.31	28.22	3.85	3.28	Occipital dx
77	F	239.85	8.72	22.56	2.92	6.31	Cortical anterior
55	F	22.36	2.51	5.38	1.54	0.05	Parietal dx
70	F	13.18	9.18	12.31	3.08	0.16	Parietal dx
60	F	8.92	7.95	16.56	1.54	0.23	Temporal sx
54	M	1071.43	15.49	16.56	2.56	1.64	Temporal sx
55	M	371.49	9.54	19.49	1.54	1.85	Temporal sx
55	F	27.54	9.23	5.13	1.54	0.15	Temporal sx
58	M	21.38	20.87	17.38	3.08	1.23	Temporal sx
53	F	8.1	7.23	9.74	2.05	0.15	Occipital sx
69	F	4.66	12.56	26.69	3.08	1.69	Frontal sx
70	F	29.49	5.23	7.08	7.23	0.61	Parietal dx

proliferation, metastasis, and angiogenesis [3]. About 40%–50% of glioblastoma cases are characterized by *EGFR* gene amplification or overexpression, together with the expression of the mutated and constitutively active EGFR isoform EGFRvIII [3]. Upregulation of the EGFR pathway could also result from an increased availability of EGFR endogenous agonists belonging to the family of EGF-like growth factors.

Heparin-binding epidermal growth factor (HB-EGF) acts as a potent proliferative agent in many different cell types via the activation of EGFR or the other EGF-like receptor ErbB4 [4]. HB-EGF is initially synthesized as the membrane-spanning protein proHB-EGF and then is proteolytically cleaved by "A *D*isintegrin *A*nd *M*etalloproteinase" (ADAM) family members that release the soluble form (sHB-EGF) in the extracellular space. The ADAM isoform responsible for this process appears to be cell type dependent, since in different experimental models ADAM 10, 12, and 17 have been involved in proHB-EGF shedding [3]. The overexpression of ADAM17, also named "tumor necrosis factor-alpha-converting enzyme" (TACE), seems to be involved in the malignant potential of cancer cells [5], and, notably, this metalloprotease modulates HB-EGF shedding and cell proliferation in U373-MG glioblastoma cell line [5].

In the clinical practice only 10%–20% of glioblastoma patients respond to EGFR kinase inhibitors, and this poor response has been ascribed to a combination of EGFR

Table 2: Age, gender, *PTEN*, and *MMP9* expression values (in femtograms), and anatomical location of anaplastic astrocytoma samples.

Age	Sex	*PTEN*	*MMP9*	Location
44	M	1.72	1.25	Temporal sx
68	F	7.66	0.57	Thalamus sx
67	F	2.25	37.06	Frontal dx
60	F	2.44	1.62	Frontal sx
50	M	92.46	0.79	Temporal dx
39	M	79.25	32.92	Parietal dx
64	F	33.82	43.21	Parietal dx
28	F	25.64	26.24	Temporal sx
55	F	12.47	0.32	Temporal sx
31	M	19.81	1.95	Temporal sx
52	F	50.12	4.37	Temporal sx
71	F	17.98	0.28	Frontal cortex
62	M	20.41	0.03	Total cortex
50	M	60.72	0.76	Occipital cortex
52	M	45.11	0.45	Total cortex
68	F	25.30	0.23	Frontal cortex

Table 3: Age, gender, mRNA expression values (in femtograms), and anatomical location of normal brain specimens.

Age	Sex	*EGFR*	*ADAM17*	*HB-EGF*	*PTEN*	*MMP9*	Location
71	F	32.58	10.74	14.84	17.98	0.28	Frontal cortex
62	M	16.70	12.76	10.41	20.41	0.03	Total cortex
50	M	57.94	18.35	30.41	60.72	0.76	Occipital cortex
52	M	25.74	13.87	28.55	45.11	0.45	Total cortex
68	F	46.98	17.20	7.60	25.30	0.23	Frontal cortex

Table 4: *MMP9* and *PTEN* absolute quantitative expression in different human normal (NHA) and glioma (PRT-HU2 and U138-MG) cell lines. Expression is indicated in femptograms.

Cell line	*MMP9*	*PTEN*
NHA	0.59	117.97
PRT-HU2	0.56	45.62
U138-MG	3.09	4.08

overexpression and loss or mutation of the Phosphatase and TEN sin homolog deleted from chromosome 10 (PTEN) tumor suppressor protein [6]. The PTEN phosphatase reduces the levels of the second messenger phosphatidylinositol 3,4,5-triphosphate (PI3K) and regulates the activity of the downstream PI-3K/AKT- and mammalian target of rapamacyn- (mTOR-) dependent pathways [7]. Notably, PTEN functional loss or mutation is present in 60%–70% of high-grade gliomas and is associated with malignant phenotypic changes such as migration capability, probably by modulation of FAK activity [8]. Moreover, since PTEN loss appears to accelerate the formation of high-grade gliomas [6], it could potentially represent a valid candidate gene to discriminate between high- and low-grade gliomas.

One typical feature of glioblastoma is its high ability to disseminate and spread to distant brain areas. Proteases expressed by glioma cells appear to play a significant role in these processes because selective matrix metalloproteinases like MMP2 or MMP9 degrade the extracellular environment in order to facilitate tumor cell growth and migration. Expression of these proteases appears to increase with glioma grade and in vitro studies showed that modifications of their expression levels resulted in altered migratory properties [9]. Although some previous reports have examined the expression of EGFR [3], PTEN [10], HB-EGF [9], ADAM17 [11], and MMP9 [12] in astrocytoma samples, at present the transcriptional expression of these five EGFR pathway-related genes has not yet been simultaneously investigated in glioma.

Therefore, in this study we have evaluated by quantitative Real-time PCR the expression of *ADAM17*, *EGFR*, *HB-EGF*, *PTEN*, and *MMP9* mRNAs in a panel of glioblastoma and anaplastic astrocytomas specimens and cell lines, and we have finally compared them to normal control samples to ascertain whether these expression profiles might provide additional tools in glioma diagnosis and in tumor subtypes identification.

2. Materials and Methods

2.1. Human Biopsy Samples. Biopsy samples, obtained from Azienda Ospedaliera Universitaria di Parma (Parma, Italy) after informed consent of the patients, were placed in ice-cold Trizol reagent (Invitrogen, Paisley, UK) and immediately processed for RNA extraction. Sections of samples were

Table 5: GeneBank accession numbers, PCR primer sequences, and products.

Gene	Accession number	PCR primer sequences (5′-3′)	PCR product (bp)
EGFR	NM_005228	AGGAAGAAGCTTGCTGGTAGC CTCTGGAAGACTTGTGGCTTG	88
ADAM17	NM_003183	CAAGTCATTTGAGGATCTCACG TCTTTGCTGTCAACACGATTCT	96
HB-EGF	NM_001945	GCCTAGGCGATTTTGTCTACC GCCCAACCTCTTCTGAGACTT	119
PTEN	NM_000314	CAGCAGTGGCTCTGTGTGTAA ATGGACATCTGATTGGGATGA	98
MMP9	NM_004994	AAAGCCTATTTCTGCCAGGAC GCACTGCAGGATGTCATAGGT	105

independently histologically and morphologically evaluated by different neuropathologists and classified as grade IV (glioblastoma multiforme) or grade III (anaplastic astrocytoma), according to WHO guidelines [13]. Clinical data of glioblastoma patients are reported in Table 1, and they included 19 females and 18 males (age range 23–84 years, mean 57.8 ± 13.3). The anaplastic astrocytoma patients (Table 2) included 7 males and 9 females (age 28–68, mean 50.7 ± 13.9). Total RNA samples extracted from human postmortem normal brain (NB) cortical regions, as reported in Table 3, were purchased from Ambion (Foster City, Calif, USA): these included 2 females and 3 males (age range 50–71 years, mean 60.6 ± 9.3).

2.2. Cell Lines. Normal human astrocytes (NHAs) were purchased from Cambrex (East Rutherford, NJ, USA) and cultivated in the specific astrocyte AGM medium (Cambrex) according to the manufacturer's specifications. Human glioma cell line U138-MG, derived from a glioblastoma multiforme patient and widely employed, was purchased from ATCC (Rockville, Md, USA); PRT-HU2 cells, previously described [14], were analogously derived from a glioblastoma multiforme patient. U138-MG and PRT-HU2 cells were cultivated in D-MEM medium supplemented with 10% FBS, 100 units/mL penicillin, 0.1 mg/mL streptomycin, and 1% L-glutamine (Invitrogen, Paisley, UK).

2.3. Real Time Quantitative PCR. Total RNA was extracted as previously described [14] and accurately quantified using spectrophotometric and fluorimetric (Quant-it RNA Assay, Invitrogen) approaches. The gene-specific primers were designed using the "Primer3 input" software (http://frodo.wi.mit.edu/primer3/), and their specificity was verified using the Primer-BLAST software (http://www.ncbi.nlm.nih.gov/tools/primer-blast/index.cgi?LINK_LOC=BlastHome/). GeneBank accession numbers of the five genes examined, their respective primer pairs sequences, and PCR products lengths were reported in Table 5. Quantitative Real-time PCR analysis was performed as previously described [14]. For the absolute quantification of specific cDNA, standard curves were derived using different concentrations of *EGFR*, *ADAM17*, *MMP9*, *HB-EGF*, and *PTEN* DNA-sequenced templates, prepared by reamplifying the PCR purified products obtained from Real-time PCR. The second derivative maximum method in the Light Cycler software was used to calculate the crossing point (Cp) value, and the concentrations of each specific cDNA were determined. All results were quantitative expressed in femtograms (fg) of cDNA, normalized to a total RNA input of 1 microgram.

2.4. Statistical and Bioinformatics Analysis. All results were expressed as mean ± standard deviation of each biopsy specimens, assayed in duplicate. The Instat v.3 software (GraphPad Software Inc., Mass, USA) was used for the statistical analysis of differences in gene expression between groups by one-way ANOVA and for the analysis of correlations among gene expression profiles, using the Pearson coefficient *r*. A *P*-value less than .05 was considered statistically significant. The dendrogram and the classification tree analysis were performed using the Orange data mining software (http://www.ailab.si/orange/). In particular, for the hierarchical clustering analysis, an Euclidean distance matrix was adopted. Statistical trends were obtained from the *PTEN* and *MMP9* average quantitative expression within normal control, anaplastic astrocytoma, and glioblastoma multiforme diagnostic classes, using the Excel software with an exponential setting (Microsoft Word Package 2003, Redmond, Wash, USA).

3. Results

The mRNA expression of the investigated genes of glioblastoma multiforme and normal brain specimens were analytically reported in Tables 1 and 2 and depicted in Figures 1 and 2. On the basis of their expression patterns in glioblastoma and using the mean values of normal samples as cut-off, the investigated genes were roughly classified in three different subgroups, the first including *ADAM17, HB-EGF*, and *PTEN*, whose average levels in glioblastoma were below the controls, the second comprising *MMP9,* whose majority of values in glioblastoma specimens were higher than in controls and, finally, the last one constituted by the *EGFR* gene, displaying the widest variation and data dispersion (Figure 1).

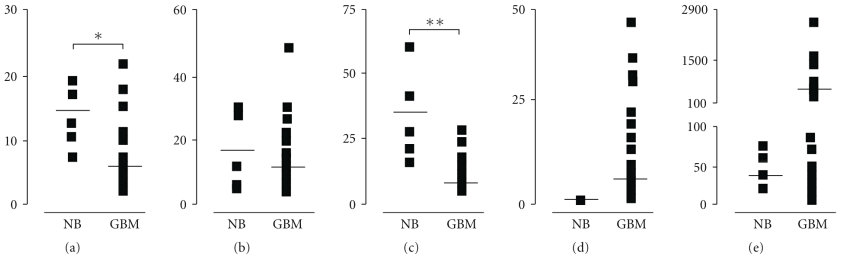

Figure 1: The mRNA expression levels of (a) *ADAM17*, (b) *HB-EGF*, (c) *PTEN*, (d) *MMP9*, and (e) *EGFR* in 37 human glioblastoma samples (GBM) and in five normal brain cortex samples (NB). Horizontal lines represent the mean values. $^{*}P < .002$, $^{**}P < .0001$.

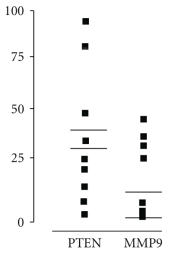

Figure 2: The mRNA expression levels of *PTEN* and *MMP9* in 16 human grade III astrocytoma samples (AA). Bold horizontal lines represent the mean values, and thin lines represent the mean normal brain cortex samples (NB) values.

The mRNA levels of *ADAM17* metallo-protease in glioblastoma (mean 5.88 fg ± 5.71) were significantly lower ($P < .002$) than in controls (14.51 fg ± 3.15). In particular, in 33 out of 37 cases (89.19%), *ADAM17* expression was lower than in control samples. For *HB-EGF* gene, although 31 out of 37 (83.78%) glioblastoma samples displayed mRNA levels lower than controls, statistical analysis revealed that the difference between controls (18.36 fg ± 10.52) and glioblastoma specimens (10.96 fg±10.13) was not statistically significant ($P < .434$).

PTEN expression pattern showed statistically lower mRNA levels in all glioblastoma samples compared to controls. Notably, the highest *PTEN* expression level among all glioblastoma had a quantitative expression (15.05 fg) that was less than 50% of the mean controls values (33.91 fg), with a control normalized ratio ranging from 2.25 to 82.72 fg. As expected, there was a very high statistically significant difference ($P < .0001$) of *PTEN* mRNA expression between glioblastoma (3.86 fg ± 3.15) and controls (33.91 fg ± 18.44).

MMP9 was overexpressed in the majority of glioblastoma specimens (72.22%) and, furthermore, in a subgroup of 24 cases (64.86%) the expression level was at least twofold higher than in controls, with a control normalized ratio within this subgroup ranging from 1.74 to 123.71 fg. However, the mean expression level of *MMP9* mRNA in glioblastoma (5.11 fg ± 8.78) was not significantly different ($P = .238$) from control samples (0.35 fg ± 0.27).

EGFR mRNA transcript levels, due to their amplitude in expression, were arbitrarily divided into two glioblastoma subgroups. The former, ranging from 0.77 to 95.25 fg, included 25 samples (67.63%); the latter, had *EGRF* absolute quantitative values ranging from 150.97 to 2562.92 fg. All control samples showed *EGFR* expression values below 100 fg, with a mean value of 35.98 fg ± 16.51. It was evident that for *EGFR* there was no statistically significant difference ($P < .371$) between glioblastoma (247.60 fg ± 517.45) and control samples (35.98 fg ± 16.52).

Within glioblastoma samples, a highly statistically significant negative correlation ($P < .0001$; Person coefficient $r = -0.776$) was related to the expression of *PTEN* and *MMP9*; in a different manner, a statistically significant positive correlation ($P < .05$; Pearson coefficient, $r = 0.9221$) was scored for the same genes within the control samples. The inverse correlation found between *PTEN* and *MMP9* mRNA expression in glioblastoma compared to control samples, prompted us to investigate whether this correlation was also detectable in other glioma grades of malignancy. Therefore, *PTEN* and *MMP9* expression, reported in Table 2 and illustrated in Figure 2, was investigated in 16 histological confirmed anaplastic astrocytoma specimens, previously classified as WHO grade III. In these samples, *PTEN* mRNA normalized quantitation (29.72 fg ± 31.62) was not significantly different from control ($P = .792$), but this value was significantly higher compared to glioblastoma ($P < .0001$). *MMP9* expression (13.60 fg ± 17.28) was neither significantly different from the control (0.35 fg ± 0.27, $P = .113$) nor from glioblastoma specimens ($P = .103$). Notably, no statistically significant correlation ($P = .709$) was found between the mRNA levels of these two genes in anaplastic astrocytoma samples. Differently from glioblastoma, no inverse correlation in *PTEN* and *MMP9* expression was found comparing anaplastic astrocytoma and control samples (Pearson coefficient, $r = 0.127$).

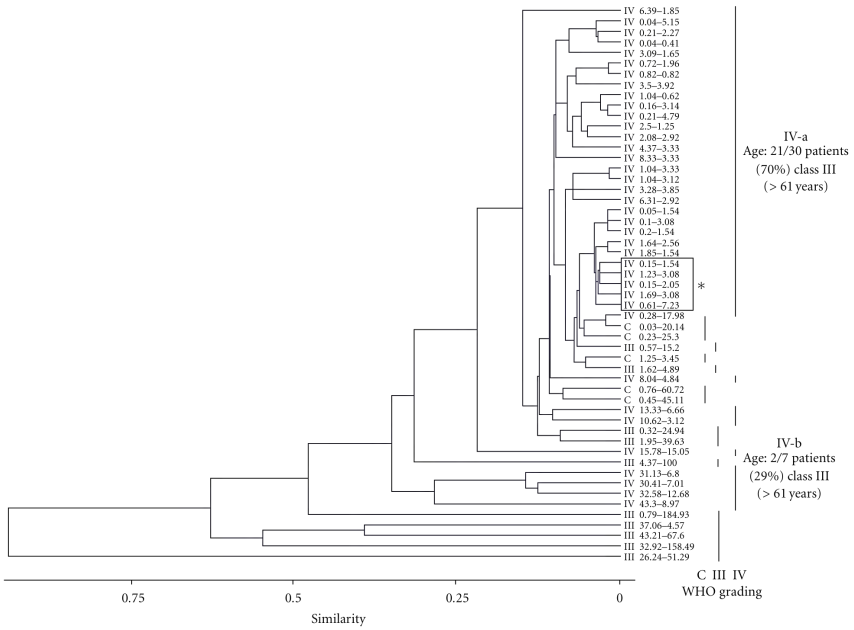

Figure 3: Dendrogram comparing *PTEN* and *MMP9* absolute quantitative expression. Absolute quantifications are expressed in femtograms, as reported in Materials and Methods. WHO grades of malignancy (III, IV) and healthy brain control (C) specimens are indicated. Glioblastoma multiforme subgroups IV-a, including the majority of glioblastoma specimens, and IV-b, described in Results, are highlighted. The box (∗) indicates subgrouping of patients sharing similar tumor anatomical localization (i.e., temporal). Subgroups IV-a and IV-b have a different and significant distribution of age-class III patients (>61 years, $P < .01$ Anova-one way).

Then, *PTEN* and *MMP9* mRNA levels were comparatively examined in two different human established glioblastoma cell lines (PRT-HU2 and U138-MG) and in a primary culture of embryonic normal human astrocytes (NHA), as shown in Table 4. In these cells, *PTEN* mRNA levels were much variable comparing to *MMP9* expression; similarly to the above examined control samples, normal astrocytes exhibited the highest *PTEN* expression.

We next exploited if *PTEN* and *MMP9* expression might be more tightly related to the glioma tumor progression. To this purpose, different bioinformatics analyses were performed using the experimental data set reported in Tables 1, 2, 3, and 4 and considering the WHO grading of the specimens. We therefore performed hierarchical clustering, a standard unsupervised learning method [10] of the tumor specimens. The WHO grading was simultaneously compared to *PTEN* and *MMP9* expression values, to identify homogeneous clusters. As reported in the dendrogram of Figure 3, different groups of samples were created, according to the above mentioned criteria. Using Euclidean distances, WHO grades IV and III and normal control samples were roughly classified into different clusters. Of note, a major subset of the glioblastoma specimens was identified (Figure 3, subgroup IV-a), showing the lowest and almost similar levels of both *PTEN* and *MMP9* transcripts; the remaining glioblastoma samples clustered within subgroup IV-b. The association of tumor anatomical localization and age of the patients with the levels of *PTEN* and *MMP9* expression was also investigated. According to the clinical data (Tables 1–3), ages of the patients were divided into three classes (i.e., I, 20–40; II, 41–60; III, >61 years): as reported in the dendrogram, the age-class III patients exhibited a statistically significant difference in distribution between subgroups IV-a and IV-b ($P < .01$, Anova one-way). Differently, no clear associations between levels of *PTEN* and *MMP9* expression and tumor localization were highlighted, with the exception of a single cluster of four class-III patients with a temporal tumor localization within subgroup IV-a.

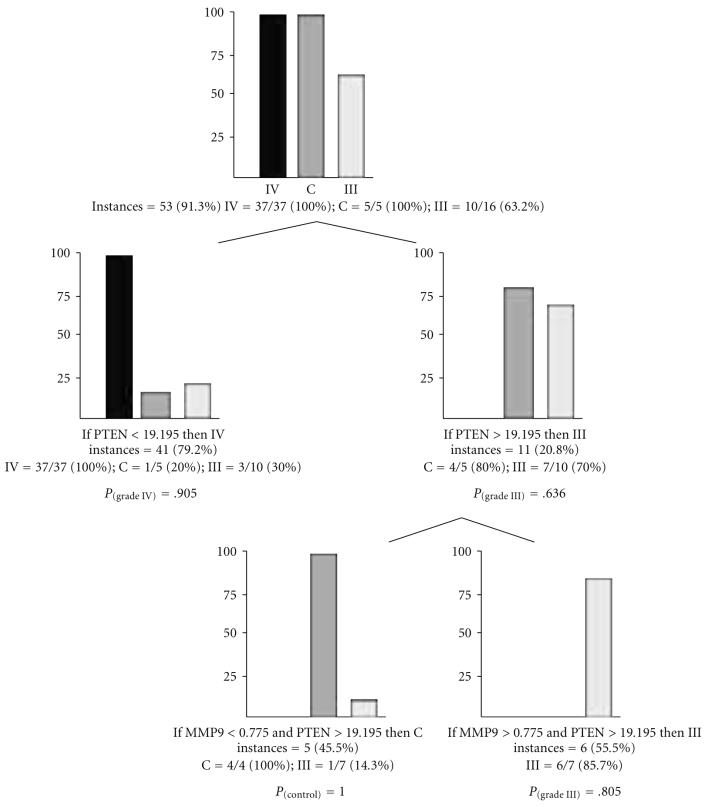

Figure 4: Classification tree derived from the combined measurement of *PTEN* and *MMP9* quantitative expression. At each root, diagnostic classes are divided following the absolute quantification and expressed in femtograms. Probabilities values (P) for the different classes are reported.

Then, a classification tree was produced, evaluating the performance of *PTEN* and *MMP9* expression in predicting roots characterized by different WHO malignant grades; as reported in Figure 4, 53 out of 58 total samples, corresponding to 53 instances (i.e., 91.3%) fitted with the classification tree; in detail, all grade IV samples had *PTEN* normalized expression values below a quantity of 19.195 fg (37/37 instances, $P = .905$), while the large majority of control (80% of the total C instances) and anaplastic astrocytomas samples (70%, $P = .636$) were grouped with *PTEN* > 19.195 fg; in this subgroup, to further differentiate control and anaplastic astrocytomas, *MMP*9 < 0.775 fg clustered all control instances ($P = 1.000$).

Nomogram analysis, performed within the same data set and reported in Figure 5 confirmed that *PTEN* and *MMP9* expression analysis might be particularly helpful in the identification of anaplastic astrocytoma specimens having a 95% of probability ($P_{(\text{grade III})} = .95$) to correctly classify these samples, in correspondence of *MMP9*-normalized expression value of 19.195 fg, independently of *PTEN* expression level. Nomograms analysis with control and glioblastoma as target diagnostic classes showed less statistical significant probabilities ($P_{(\text{control})} = .60$ and $P_{(\text{grade IV})} = .55$).

To further elucidated if *PTEN* and *MMP9* expression had an expression trend that reflected the malignant grade of the specimens (i.e., normal, anaplastic astrocytomas,

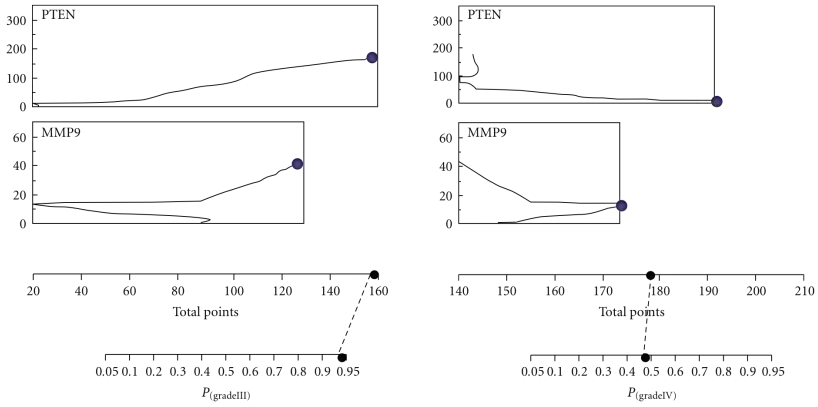

Figure 5: Nomogram analysis of *PTEN* and *MMP9* expression within the different WHO grades of malignancy (III, IV) of the astrocytomas specimens. Points and total points axes indicate the points attributed to each variable value and the sum of the points for each variable, respectively. *P* axes indicate the predicted probability that relates *PTEN* or *MMP9* quantitative expression to each WHO tumor malignancy grade.

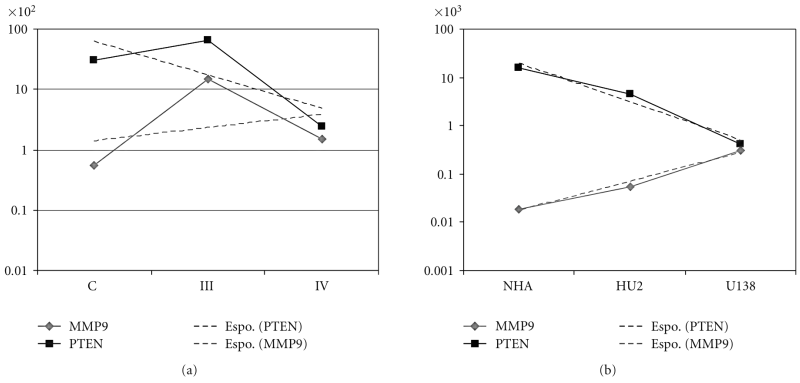

Figure 6: Statistical trends of *PTEN* (black dotted line) and *MMP9* (grey dotted line) expression in control (C), anaplastic astrocytomas (III) and glioblastoma multiforme (IV) specimens (Panel A), and in normal human astrocytes (NHA), glioma PRT-HU2 (HU2), and U138-MG (U138) cells (Panel B). Trends are calculated using average quantitative expression of *PTEN* and *MMP9*, and adopting exponential (Espo) models of prediction as follows: *PTEN* (C, III, IV average expression samples), $y = 2148e^{-1.29x}$; *MMP9* (C, III, IV), $y = 83716e^{0.50x}$; *PTEN* (NHA, HU2, U138), $y = 118596e^{-1.82x}$; *MMP9* (NHA, HU2, U138), $y = 42439e^{1.40x}$.

and glioblastoma multiforme), a statistical trend analysis was performed (Figure 6); the analysis reported in Panel A showed that *PTEN* and *MMP9* differences in their normalized expression clearly decreased following the malignant glioma grading, with the lowest values corresponding to glioblastoma multiforme specimens; similarly, the trend analysis, reported in Figure 6 Panel B, highlighted that, within the investigated cell lines, normal human astrocytes exhibited the largest differences in *PTEN* and *MMP9* expression levels, while, on the contrary, U138-MG cells,

isolated from a glioblastoma multiforme patient, showed nearly coincident *PTEN* and *MMP9* expression values; the glioblastoma derived PRT-HU2 cell line showed values of *PTEN* and *MMP9* expression trends, intermediate between NHA and U138-MG.

4. Discussion

The new challenge in cancer biology is to move from one purely morphological classification of cancer to one that is based on the integration of histological and molecular criteria [15]. Among several cancer specific investigated genes, the epidermal growth factor receptor (*EGFR*) plays a pivotal pathological role through the activation of downstream intracellular signalling pathways that can directly modulate cell proliferation, metastasis, and angiogenesis [8]. Glial tumors, in particular, due to processes of gene-amplification or mutation, showed altered *EGFR*-related functional pathways [3]. Within this context, in order to find clinically relevant correlations between gene expression and tumor malignant progression, a cohort of glioma specimens was analyzed for the expression of several genes, that is, *ADAM-17*, *PTEN*, *MMP9*, *EGFR*, and *HB-EGF*, indirectly involved in the *EGFR*-dependent signaling pathway, In fact, the concurrent measurement of the transcript levels of the different genes could potentially represent a useful tool to identify a dysregulation of receptor activation or of downstream signaling pathways or might also suggest functional links between these genes in pathological conditions [16].

Comparing a cohort of glioblastoma specimens and controls, only two genes, *ADAM-17* and *PTEN*, had expression levels that significantly changed between the two WHO classes; on the contrary, considering the expression of each transcript separately, we did not elucidate any association between clinical status and *EGFR*, *HB-EGF*, and *MMP9* expression profiles. In particular, the wide range of variation for the *EGFR* gene, found in glioblastoma specimens, was in partial agreement with previous studies carried out in glial tumor samples [8]. In general, nearly 50% of glioblastoma multiforme cases express amplified *EGFR*, and about 40% of them also express the constitutively activated mutated EGFRvIII isoform [11]. Since the primers we used in our experiments did not discriminate between *EGFR* and *EGFRvIII*, it is very likely that the *EGFR* mRNA levels found in our samples reflected the combined contribution of both the transcripts.

Since chemotherapic treatments enhance the EGFR-mediated proliferative responses via an increased *HB-EGF* expression and shedding [17], previous studies have suggested a prominent role for *HB-EGF* in tumorigenic processes. In fact, in glioma cell lines, the inducible expression of *EGFRvIII* can enhance *HB-EGF* expression and can activate *EGFR*-dependent pathways via a positive feedback autocrine loop [18]. The only previous published study, based on a semiquantitative assessment by Northern blot analysis, found an increased expression of *HB-EGF* in glioblastoma compared to control samples [9]. On the opposite, our data seemed to suggest that *HB-EGF* is not upregulated in glioblastoma; however, our results agreed with microarray gene expression profiles studies that showed no significant differences in *HB-EGF* expression between glioblastoma and control samples [19].

Recent mounting evidence showed that the expression of *MMP9* might play a critical role in brain neoplastic tissue invasion, metastasis, and angiogenesis [12]. Even if not completely statistically supported, our findings were in good agreement with a previous work showing an upregulation of *MMP9* mRNA levels in glioblastoma compared to controls and suggesting a close relationship between *MMP9* expression and tumor malignant progression [12].

Although *ADAM17* expression has been reported in normal human brain tissue and in cell lines [5], its expression at mRNA level has been poorly investigated in brain tumors. Functional studies in U373-MG glioma cells have demonstrated that cannabinoids induced cell proliferation through a two-step mechanism involving *ADAM17*-mediated shedding of *proHB-EGF* and subsequent *EGFR* stimulation [5]. Our finding that *ADAM17* mRNA levels in glioblastoma are statistically lower compared to controls is in contrast with a previous work that reported an increased expression of *ADAM17* in glioblastoma specimens [20]. This might reflect differences in tumor sampling or a consequence of glioblastoma multiforme cellular and molecular heterogeneity.

Our finding showing that glioblastoma expressed statistically significant lower *PTEN* mRNA levels compared to control samples confirmed previous reports [21], showing that *PTEN* expression variations were detectable only in a low fraction of anaplastic astrocytoma and were almost absent in low-grade brain tumors and controls. Taken together, these observations strengthen the hypothesis that an impairment of *PTEN* expression, together with a consequent aberrant activity of the PI3K-dependent pathway, might represent a typical hallmark of glioblastoma multiforme. A functional confirmation of this hypothesis was that, in a mouse astrocytoma model with genetic inactivation of the *Nf1* and *p53* tumor suppressor genes, the loss of *PTEN* heterozygosity and the Akt activation contributed to the brain tumor malignant progression [6].

Differently from the above mentioned investigated genes, the analysis of *PTEN* and *MMP9* expression, using a combination of unsupervised and supervised algorithms, provided interesting results: firstly, as reported in the dendrogram analysis, the expression profiling derived novel subsets of astrocytomas. This hierarchically clustering analysis clarified that tumor classification based even on a quantization of two genes could generate a patient stratification, clinically relevant and more informative than a single conventional histological classification. The *PTEN* and *MMP9* expression-generated subgroups produced also a different distribution of the patients according to their age: in particular subgroup IV-a, differently from IV-b, was enriched in age-class III patients (i.e., >61 years); this result might suggest that in glioblastoma multiforme tumor specimens *PTEN* and *MMP9* expression levels might be partly related with the elderly of the patients. On the contrary, in anaplastic astrocytoma and in control patients no association between age-related classes and *PTEN*/*MMP9* expression levels was evidenced. Furthermore, the originated dendrogram does

not reflect a classification of samples according to their anatomical tumor localization. However, in the light of the development of new pharmacological treatments, the identification of patient subsets with specific molecular signatures within tumor malignancy grades is becoming more and more relevant [22]. A finer analysis of *PTEN* and *MMP9* expression was also employed to derive a parsimonious classification tree of the investigated samples into their tumor malignancy grades. Specific *PTEN* and *MMP9* expression values significantly addressed the specimens into a specific diagnostic class, that is, glioblastoma or anaplastic astrocytomas. However, the significance and the sensitivity of this classification might be further refined with the increasing of specimens and through the identification of novel tumor-diagnostic markers. Basing on the average expression of *PTEN* and *MMP9*, the observed statistical trends clearly differentiate the control, anaplastic astrocytomas, and glioblastoma multiforme diagnostic classes; a similar expression trend for *PTEN* and *MMP9* genes was documented comparing normal versus astrocytic tumor cell lines. These results, in particular, reinforced the concept that anaplastic astrocytomas were intermediate-grade tumors, showing detectable mitotic activity, absent in low-grade astrocytomas, but not necrosis and prominent vascular proliferation, characteristic of glioblastoma multiforme [23, 24].

An additional interesting finding emerging from our study was the significant negative correlation between *PTEN* and *MMP9* mRNA expression in glioblastoma multiforme. Notably, not only was this negative correlation absent in anaplastic astrocytoma samples, but it was reversed in control samples. It was evident that differences in *PTEN* gene expression mainly account for these correlations because its levels in glioblastoma were significant higher compared to anaplastic astrocytoma samples, whilst no statistical difference was found for *MMP9* mRNA levels. The positive correlation between *PTEN* and *MMP9* in controls is derived essentially from an overexpression of *PTEN* rather than a low expression of *MMP9* compared to glioblastoma. The functional significance of these correlations is currently unknown, and future functional studies aimed at elucidating possible interplays of these genes in glioblastoma are clearly warranted. The negative correlation in glioblastoma between *MMP9* and *PTEN* could imply a functional interplays between these two genes, as already documented. It has been reported that *PTEN* modulates the expression and secretion of MMP2 and MMP9, thereby modifying tumor cell invasiveness [9, 25]. Notably, recent reports have clearly demonstrated that, in glioblastoma, *PTEN* may regulate migration via a PI3K-independent pathway [26]. In this model, the lack or functional loss of *PTEN* not only potentiates the migration induced by EGFR- and beta-integrin-dependent pathways but also enhances cell migration via a still largely unclear mechanism. On this regard, a recent report suggested that integrins could be a converging point in the mechanism supporting tumor invasion and migration of cancer cells with *PTEN* loss and *MMP9* overexpression.

The intrinsic genetic heterogeneity and redundant overlapping aberrant signalling transduction pathways underlie the failure of monotherapies in glioblastoma [8]. Therefore a sensitive and reliable method to measure gene expression, such as Real-time PCR, may greatly ameliorate diagnostic tools and eventually address the pharmacological approach using multitarget kinase inhibitors or combination of therapies based on multiple single-targeted receptor or intracellular kinase inhibitors. Some researchers have proposed that the combination of *PTEN* loss and *EGFR* hyperfunctionality could be predictive of the ineffectiveness of therapies with *EGFR* inhibitors [4] because these two pathways might synergize to enhance glioblastoma malignancy. This hypothesis has been elegantly supported by the recent observation that the pharmacological inhibition of PI3K-alpha and mTOR augments the antiproliferative activity of the EGFR inhibitor erlotinib in glioblastoma cell lines [7]. The inverse correlation between *PTEN* and *MMP9* expression reported here raised the issue whether the concomitant hyperactivation of the PI3K-alpha and MMP9-dependent pathways might be instrumental in devising or refining combined pharmacological therapies in glioblastoma. The modest efficacy of mTOR inhibitors alone in clinical trials was greatly enhanced when these compounds were administered in combination with the EGFR inhibitor Gefitinib [27]. Although monotherapy regimens with MMPs inhibitors in clinical trials have been quite disappointing, the relevance of MMPs as valid target has been reevaluated by the recent finding that the combined use of MMPs, COX2, and EGFR inhibitors reduced human breast cancer tumor growth [11]. We therefore speculate that the pivotal role of MMPs in glioma invasion and angiogenesis deserves future in vitro and in vivo experiments using MMP inhibitors in combination with PI3K inhibitors alone or with these latter compounds plus EGFR inhibitors.

The analyses of gene expression at transcriptional level in biopsy tissue samples are instrumental in delineating abnormal gene expression signature of brain tumors, but it should be mentioned that these studies suffer some pitfalls and limitations: in particular, the use of supervised approaches, based on the assumption that the grouping (i.e., the histological tumor diagnoses) is correct, may not be a valid assumption for all the clinical cases examined; additionally, the intrinsic heterogeneity of glioblastoma, together with the presence of nontumor cells in the samples, probably accounts for the variability found in transcripts levels and may represent a critical factor and a limitation in the interpretation of our results. From a technical point of view, a main difference of our contribution, compared to other reports, deals with the criteria adopted to express transcript levels in the investigated specimens. The majority of clinical gene expression profile studies performed by Real-time PCR normalized data using an internal housekeeping gene as a reference, but great caution in choosing this normalization method is necessary especially when analyzing tumor biopsy samples [28]. The tumorigenic process itself, via genomic mutations or amplifications, could induce modifications of housekeeping genes levels [29], and hence the choice of unreliable housekeeping genes may lead to interpretation errors and bias in experimental results [30]. Our attempts to use *GAPDH*, *ACTB*, and *HPRT* as reference genes were unsuccessful due to the great variations among

all the samples (data not shown); therefore, we decided to express gene expression as absolute amount of femtograms (fg) of transcripts, normalized to the total amount of RNA employed, through accurate quantification using the combination of spectrofotometric and fluorimetric approaches.

In conclusion, the combined analysis of the transcripts of *PTEN* and *MMP9* genes in biopsy specimens could represent a reliable diagnostic and prognostic marker of human glial tumor. Further epidemiological and functional in vitro studies are required to establish the reliability of *PTEN* and *MMP9* genes as possible valid molecular targets in the pharmacological strategies aimed at controlling human glioma malignant progression.

Acknowledgments

This study was supported by grants from the Italian MIUR, "Progetti di Ricerca di Rilevante Interesse Nazionale (2005)." A. A. is granted by Fondo Sociale Europeo (F.S.E.). The authors are particularly grateful to Dr. Eugenio Benericetti (Azienda Ospedaliera di Parma, Italy) for providing WHO graded glioma specimens. Orange Software is released under General Programming License (GPL). The authors are therefore particularly grateful to Orange Program's authors, Demsar J, Zupan B, Leban G: (2004) Orange: From Experimental Machine Learning to Interactive Data Mining, White Paper (http://www.ailab.si/orange/), Faculty of Computer and Information Science, University of Ljubljana (Slovenia).

References

[1] D. N. Louis, "Molecular pathology of malignant gliomas," *Annual Review of Pathology*, vol. 1, pp. 97–117, 2006.

[2] H. Ohgaki and P. Kleihues, "Genetic pathways to primary and secondary glioblastoma," *American Journal of Pathology*, vol. 170, no. 5, pp. 1445–1453, 2007.

[3] S. Higashiyama and D. Nanba, "ADAM-mediated ectodomain shedding of HB-EGF in receptor cross-talk," *Biochimica et Biophysica Acta*, vol. 1751, no. 1, pp. 110–117, 2005.

[4] S. Miyamoto, H. Yagi, F. Yotsumoto, T. Kawarabayashi, and E. Mekada, "Heparin-binding epidermal growth factor-like growth factor as a novel targeting molecule for cancer therapy," *Cancer Science*, vol. 97, no. 5, pp. 341–347, 2006.

[5] S. Hart, O. M. Fischer, and A. Ullrich, "Cannabinoids induce cancer cell proliferation via tumor necrosis factor α-converting enzyme (TACE/ADAM17)-mediated transactivation of the epidermal growth factor receptor," *Cancer Research*, vol. 64, no. 6, pp. 1943–1950, 2004.

[6] C.-H. Kwon, D. Zhao, J. Chen, et al., "Pten haploinsufficiency accelerates formation of high-grade astrocytomas," *Cancer Research*, vol. 68, no. 9, pp. 3286–3294, 2008.

[7] Q.-W. Fan, C. K. Cheng, T. P. Nicolaides, et al., "A dual phosphoinositide-3-kinase α/mTOR inhibitor cooperates with blockade of epidermal growth factor receptor in PTEN-mutant glioma," *Cancer Research*, vol. 67, no. 17, pp. 7960–7965, 2007.

[8] J. B. Johnston, S. Navaratnam, M. W. Pitz, et al., "Targeting the EGFR pathway for cancer therapy," *Current Medicinal Chemistry*, vol. 13, no. 29, pp. 3483–3492, 2006.

[9] M.-S. Kim, M.-J. Park, E.-J. Moon, S.-J. Kim, C.-H. Lee, and H. Yoo, "Hyaluronic acid induces osteopontin via the phosphatidylinositol 3-kinase/Akt pathway to enhance the motility of human glioma cells," *Cancer Research*, vol. 65, no. 3, pp. 686–691, 2005.

[10] T. Hastie, R. Tibshirani, D. Botstein, and P. Brown, "Supervised harvesting of expression trees," *Genome Biology*, vol. 2, no. 1, article research0003.1-0003.12, 2001.

[11] I. K. Mellinghoff, M. Y. Wang, I. Vivanco, et al., "Molecular determinants of the response of glioblastomas to EGFR kinase inhibitors," *The New England Journal of Medicine*, vol. 353, no. 19, pp. 2012–2024, 2005.

[12] K. Komatsu, Y. Nakanishi, N. Nemoto, T. Hori, T. Sawada, and M. Kobayashi, "Expression and quantitative analysis of matrix metalloproteinase-2 and -9 in human gliomas," *Brain Tumor Pathology*, vol. 21, no. 3, pp. 105–112, 2004.

[13] P. Kleihues and W. K. Cavenee, *World Health Organization Classification of Tumors of the Nervous System*, Lyon, France, 2000.

[14] M. Paolillo, A. Barbieri, P. Zanassi, and S. Schinelli, "Expression of endothelins and their receptors in glioblastoma cell lines," *Journal of Neuro-Oncology*, vol. 79, no. 1, pp. 1–7, 2006.

[15] D. N. Louis, E. C. Holland, and J. G. Cairncross, "Glioma classification: a molecular reappraisal," *American Journal of Pathology*, vol. 159, no. 3, pp. 779–786, 2001.

[16] Y. Liang, M. Diehn, N. Watson, et al., "Gene expression profiling reveals molecularly and clinically distinct subtypes of glioblastoma multiforme," *Proceedings of the National Academy of Sciences of the United States of America*, vol. 102, no. 16, pp. 5814–5819, 2005.

[17] F. Wang, R. Liu, S. W. Lee, C. M. Sloss, J. Couget, and J. C. Cusack, "Heparin-binding EGF-like growth factor is an early response gene to chemotherapy and contributes to chemotherapy resistance," *Oncogene*, vol. 26, no. 14, pp. 2006–2016, 2007.

[18] D. B. Ramnarain, S. Park, D. Y. Lee, et al., "Differential gene expression analysis reveals generation of an autocrine loop by a mutant epidermal growth factor receptor in glioma cells," *Cancer Research*, vol. 66, no. 2, pp. 867–874, 2006.

[19] D. S. Rickman, M. P. Bobek, D. E. Misek, et al., "Distinctive molecular profiles of high-grade and low-grade gliomas based on oligonucleotide microarray analysis," *Cancer Research*, vol. 61, no. 18, pp. 6885–6891, 2001.

[20] D. Wildeboer, S. Naus, Q.-X. A. Sang, J. W. Bartsch, and A. Pagenstecher, "Metalloproteinase disintegrins ADAM8 and ADAM19 are highly regulated in human primary brain tumors and their expression levels and activities are associated with invasiveness," *Journal of Neuropathology and Experimental Neurology*, vol. 65, no. 5, pp. 516–527, 2006.

[21] C. B. Knobbe, A. Merlo, and G. Reifenberger, "Pten signalling in gliomas," *Neuro-Oncology*, vol. 4, no. 3, pp. 196–211, 2002.

[22] G. N. Fuller, K. R. Hess, C. H. Rhee, et al., "Molecular classification of human diffuse gliomas by multidimensional scaling analysis of gene expression profiles parallels morphology-based classification, correlates with survival, and reveals clinically-relevant novel glioma subsets," *Brain Pathology*, vol. 12, no. 1, pp. 108–116, 2002.

[23] K. Ichimura, H. Ohgaki, P. Kleihues, and V. P. Collins, "Molecular pathogenesis of astrocytic tumours," *Journal of Neuro-Oncology*, vol. 70, no. 2, pp. 137–160, 2004.

[24] B. K. Ahmed Rasheed, R. N. Wiltshire, S. H. Bigner, and D. D. Bigner, "Molecular pathogenesis of malignant gliomas," *Current Opinion in Oncology*, vol. 11, no. 3, pp. 162–167, 1999.

[25] K. Furukawa, Y. Kumon, H. Harada, et al., "PTEN gene transfer suppresses the invasive potential of human malignant

gliomas by regulating cell invasion-related molecules," *International Journal of Oncology*, vol. 29, no. 1, pp. 73–81, 2006.

[26] M. Raftopoulou, S. Etienne-Manneville, A. Self, S. Nicholls, and A. Hall, "Regulation of cell migration by the C2 domain of the tumor suppressor PTEN," *Science*, vol. 303, no. 5661, pp. 1179–1181, 2004.

[27] S. Sathornsumetee, D. A. Reardon, A. Desjardins, J. A. Quinn, J. J. Vredenburgh, and J. N. Rich, "Molecularly targeted therapy for malignant glioma," *Cancer*, vol. 110, no. 1, pp. 12–24, 2007.

[28] C. Tricarico, P. Pinzani, S. Bianchi, et al., "Quantitative real-time reverse transcription polymerase chain reaction: normalization to rRNA or single housekeeping genes is inappropriate for human tissue biopsies," *Analytical Biochemistry*, vol. 309, no. 2, pp. 293–300, 2002.

[29] S. Waxman and E. Wurmbach, "De-regulation of common housekeeping genes in hepatocellular carcinoma," *BMC Genomics*, vol. 8, pp. 243–250, 2007.

[30] J. L. Aerts, M. I. Gonzales, and S. L. Topalian, "Selection of appropriate control genes to assess expression of tumor antigens using real-time RT-PCR," *BioTechniques*, vol. 36, no. 1, pp. 84–91, 2004.